ISSN 2233-9485(Print)
ISSN 2233-9574(Online)

한국자기학회 2020년도 임시총회 및 하계학술연구발표회

KMS 2020 Summer Conference

논문개요집

일시 2020. 7. 19(일) ~ 21(화)

장소 강릉 세인트존스호텔

주최 한국자기학회

Digests of the KMS 2020 Summer Conference

The Korean Magnetics Society

사단법인 한국자기학회

한국자기학회 2020년도 임시총회 및 하계학술연구발표회

KMS 2020 Summer Conference

논문개요집

일시 2020. 7. 19(일) ~ 21(화)

장소 강릉 세인트존스호텔

주최 한국자기학회

공지사항

1. 포스터발표를 하시는 회원은 아래의 사항을 지켜주시기 바랍니다.

1) 포스터보드 크기는 한 명당 가로 100cm X 세로 200cm 사용할 수 있습니다.

2) 포스터는 7월 19일(일) 18:00 까지 부착하시면 되고, 포스터 Q&A는 7월 20일(월) 13:00~14:00, 17:30~18:30 사이에 대면이 아닌 전화나 이메일 등을 통해 비대면 개별 접촉으로 진행되며, 문자나 이메일로 먼저 질문해 주시고 답변은 가능하면 전화로 하시는 것을 추천해 드립니다.

2. 일정

7월 19일(일)	13:00~	참가자 등록				
	14:00~17:50	강습회 프로그램				
7월 20일(월)	08:30~	참가자 등록				
	09:00~18:00	포스터발표 (로비)				
	09:00~12:30	Special Session I (Antigua1)	Special Session II (Antigua2)	Special Session III (Barbuda1+2)	Special Session IV (Barbuda3+4)	
	12:30~14:00	Lunch				
	13:00~14:00	포스터 Q&A (비대면 진행)				
	14:00~17:30	Special Session V (Antigua1)	Special Session VI (Antigua2)	Special Session VII (Barbuda1+2)		
	17:30~18:00	한국자기학회 임시총회 및 시상식 (Antigua1)				
		Dinner (취소)				
	17:30~	포스터 Q&A (비대면 진행)				
7월 21일(화)	08:30~	참가자 등록				
	09:00~12:00	Special Session VIII (Barbuda3+4)	Special Session IX (Antigua2)	Special Session X (Barbuda1+2)	09:00 ~ 12:30	Special Session XI (Antigua1)
	12:30~	폐회 (Antigua1)				

3. 7월 20일(월) 저녁 만찬은 코로나19 확산에 따른 영향으로 부득이하게 취소되었습니다.

7월 19일[일]

시간	프로그램	
13:00 ~	참가자 등록	
	강습회 프로그램	좌장 : 임성현(울산대)
14:00 ~ 14:50	T-1. Topological Defects in Magnetism I	문은국(KAIST)
14:50 ~ 15:00	Coffee Break	
15:00 ~ 15:50	T-1. Topological Defects in Magnetism II	문은국(KAIST)
15:50 ~ 16:00	Coffee Break	
16:00 ~ 16:50	T-2. 딥러닝을 이용한 소재기술 개발	손기선(세종대)
16:50 ~ 17:00	Coffee Break	
17:00 ~ 17:50	T-3. Introduction to electric vehicle development history and technology trends	최윤용(드라이브텍)

7월 20일[월]

시간	프로그램					
08:30 ~	참가자 등록					
09:00 ~ 18:00	포스터발표 (로비) [1] Magnetic theory and calculation [2] Magnetization dynamics [3] Hard-magnetic Materials [4] Soft-magnetic Materials [5] Semiconductor spintronics [6] Spin orbit coupling and related phenomena [7] Nano-structured materials [8] Spin transfer torque for magnetic memory [9] Nanoscale Magnetism [10] Magnetic Oxides and Multiferroics [11] Bio Magnetics [12] Medical Magnetics [13] Sensor and Applications [14] 회원 참여 스페셜 세션 (양자컴퓨팅, 산화물 자성체, 의료 장비 및 소재 등) [15] Others					
09:00 ~ 12:30	Special Session I (Antigua1) 'Magnetic For IOT' 좌장 : 윤석수(안동대)/손대락(한남대)		Special Session II (Antigua2) 'Theory' 좌장 : 임성현(울산대)		Special Session III (Barbuda1+2) 'Medical Magnetics' 좌장 : 한만석(강원대) 안우상(울산대)	Special Session IV (Barbuda3+4) '산화물 자성체 세션' 좌장 : 문은국(KAIST)
	09:00 ~ 09:25	초S-I-1. 해저 매설 자기 센서의 해수 유동 영향 분석 배기웅(국방과학연구소)	09:00 ~ 09:30	초S-II-1. Lattice dynamics study on charge density wave and superconductivity in low-dimensional systems; CuTe and MgC_2 김수란(경북대)	초S-III-1. Brain segmentation analysis using brain magnetic resonance imaging (MRI) measurements for comparison between normal controls and Alzheimer's disease (AD) patients 박상원(강원대)	초S-IV-1. Magnetic skyrmions 한정훈(성균관대)
	09:25 ~ 09:50	초S-I-2. The RPM measurement techniques of the shell using by the magnetic sensor 한동필(㈜한화종합연구소)				
	09:50 ~ 10:15	초S-I-3. 알칼리 원자 – 버퍼가스 셀을 이용한 센서 김태현(국방과학연구소)	09:30 ~ 10:00	초S-II-2. Mimicking superconductivity of Sr2RuO4 using SrRuO3-SrTiO3 superlattice 김봉재(군산대)	초S-III-2. MRI 시스템에 따른 GBCA의 신호 변화 Signal change of GBCA according to MRI System 정현근(HK리서치센터)	초S-IV-2. Spin Liquid State and Topological Structural Defects in Hexagonal $TbInO_3$ 김재욱(한국원자력연구원)
	10:15 ~ 10:40	초S-I-4. UXO 탐지용 자력계의 무인기 적용에 관한 연구 손대락(한남대)	10:00 ~ 10:30	초S-II-3. 브릴루앙 산란으로 연구된 Co_xGd_{1-x}준강자성체의 스핀파 특성 김창수(KRISS)	초S-III-3. Rotatable LYSO-GAPD DEXA Detector Providing Normal-Resolution- and High-Resolution-mode 허희선(전남대)	초S-IV-3. Interplay between spin-orbit coupling and van Hove singularity in Sr_2RuO_4 김충현(서울대)
	10:40 ~ 10:50	Coffee Break	10:30 ~ 11:00	초S-II-4. Self-Generated Spin-Orbit Torque and Spin Pumping by Spin-Orbit Coupled Ferromagnets 김경환(KIST)	초S-III-4. Optimization of variable collimator Thickness for disaster environmental monitoring 원종훈(강원대)	초S-IV-4. Magnetic excitations in $d^7 j_{eff}$=1/2Kitaevhoneycombmaterials,$Na_3Co_2SbO_6$and$Na_2Co_2TeO_6$ 정재홍(서울대)
	10:50 ~ 11:15	초S-I-5. 자기센서용 연자성 코어의 자화곡선 모델링 신광호(경성대)				
	11:15 ~ 11:40	초S-I-6. 자기장을 활용한 콘크리트 보강재 비파괴평가 조창빈(한국건설기술연구원)	11:00 ~ 11:30	초S-II-5. Exotic electronic structures of the superconducting nickelate 이관우(고려대)	초S-III-5. A Feasibility Study on the Clinical Application of alanine/ESR Dosimetry 한기택(KARA)	초S-IV-5. High-velocity spin waves in the Sr_2IrO_4/$Sr_3Ir_2O_7$heterostructure 김범준(포항공대)

7월 20일[월]

시간	프로그램					
09:00 ~ 12:30	11:40 ~ 12:05	초S-I-7. Evaluation of Railway Track Safety using Magnetic Barkhausen Noise method 임남형(충남대)	11:30 ~ 12:00	초S-II-6. Torque generation by orbital current: Orbital torque 이현우(포항공대)	초S-III-6. Magnetic Modulated Radiation Therapy, a simple new idea 정누리현(강원대병원)	
	12:05 ~ 12:30	초S-I-8. 펄스와전류 기술의 소개와 적용 분야 박덕근(한국원자력연구원)	12:00 ~ 12:30	초S-II-7. 수직자성박막에 스커미온을 형성하는 방법 문경웅(KRISS)	초S-III-7. Interplay Effect in Proton Scanning Therapy by Magnetic Scanner 서정민(부산카톨릭대)	
12:30 ~ 14:00	Lunch					
14:00 ~ 17:30	Special Session V (Antigua1) 'Magnetization Dynamics' 좌장 : 최석봉(서울대)		Special Session VI (Antigua2) 'Magnetism in reduced dimension' 좌장 : 유정우(UNIST)		Special Session VII (Barbuda1+2) 'Mossbauer & Nano' 좌장 : 엄영랑(한국원자력연구원)	
	14:00 ~ 14:30	초S-V-1. The Systematic Investigation of Dzyaloshinskii-Moriya Interaction by using Brillouin Light Scattering Spectroscopy 김준서(DGIST)		초S-VI-1. Time-dependent density functional theory calculations of spin-phonon dynamics and band topology of two-dimensional materials 박노정(UNIST)		초S-VII-1. Mössbauer spectroscopic study about firing conditions and coloring mechanism of the ancient Baekje black burnished potteries 문동혁(NRICH)
	14:30 ~ 15:00	초S-V-2. Coupled Spin-Charge Transport in Doped-Graphene 박정민(한국기초과학지원연구원)		초S-VI-2. First principles studies of two dimensional ferromagnetic materials 홍지상(부경대)		초S-VII-2. Activation Study of Nanocrystalline Ferrihydrite-Based Catalysts forFischer-TropschSynthesisusingMössbauerSpectroscopy 천동현(한국에너지기술연구원)
	15:00 ~ 15:30	초S-V-3. Introduction to probabilistic computing based on random MTJs 이억재(KIST)		초S-VI-3. Electron Spin Resonance on Individual Atoms and Molecules on Surfaces 최태영(이화여대)		초S-VII-3. Study on the hyperthermia and magnetic properties of MNPs using Mössbauer spectroscopy 최현경(국민대)
	15:30 ~ 16:00	초S-V-4. Controlled Writing and Deleting of Magnetic Skyrmions in 2- TerminalDevice 제승근(전남대)		초S-VI-4. Molecule-based magnetic thin film for spin-thermoelectrics 오인선(UNIST)	15:30 ~ 15:40	Coffee Break
	16:00 ~ 16:30	초S-V-5. The Exchange Stiffness Constant and Its Applications 조재훈(DGIST)		초S-VI-5. Coupled spin-charge transport in oxide interface 유정우(UNIST)	15:40 ~ 16:10	초S-VII-4. Study of Archeological Heritages using Mössbauer Spectroscopy 엄영랑(한국원자력연구원)
	16:30 ~ 17:00	초S-V-6. The dynamics of magnetic droplet soliton driven by spin transfer torque 정선재(한국교원대)				
	17:00 ~ 17:30	초S-V-7. Energy optimized switching condition for STT-MRAM 유천열(DGIST)				
17:30 ~ 18:00	한국자기학회 임시총회 및 시상식 (Antigua1)					
	Dinner (코로나19 확산에 따른 영향으로 취소되었습니다.)					
17:30 ~	포스터 Q&A (비대면 진행)					

7월 21일[화]

시간	프로그램					
08:30 ~	참가자 등록					
09:00 ~ 12:30	Special Session VIII (Barbuda3+4) 'Electro-Magnetic Energy Convergence' 좌장 :이정종(전자부품연구원)		Special Session IX (Antigua2) 'Hard & Soft Magnetic Materials: Motor' 좌장 : 이우영(연세대)	Special Session X (Barbuda1+2) 'Bio-Convergence Magnetics' 좌장 : 김철기(DGIST)		Special Session XI (Antigua1) 'Spintronics' 좌장 : 이경진(고려대)
	09:00 ~ 09:25	초S-VIII-1. Electrical Parameter Comparison of 8-pole 6-slot and 8-pole 12-slot using Equivalent Magnetic Circuit for Servo motor 박진철(한양대)	초S-IX-1. Development of High Performance (L)RE-Fe-B Permanent Magnets by Grain Boundary Engineering 김수민(연세대)	09:00 ~ 09:30	초S-X-1. Is there any method to overcome conventional magnetic hyperthermia? 김상국(서울대)	초S-XI-1. Spin-orbit torque engineering by orbital current in Cr-based magnetic heterostructures 이수길(KAIST)
	09:25 ~ 09:50	초S-VIII-2. A Study on the Design Technology of Synchronous Motors Related to the Improvement of Permanent Magnet Material Properties 강동우(계명대)	초S-IX-2. Non-trivial Giant Magnetic Anisotropy in 3d Ferromagnetic Materials 박재훈(MPK)	09:30 ~ 10:00	초S-X-2. Role of lactate in metabolism of skeletal muscle 도경오(영남대)	초S-XI-2. 준강자성체에서 전류에 의한 위상 스핀 구조체 운동 김덕호(KIST)
	09:50 ~ 10:15	초S-VIII-3. The Simulation Process of Electromagnetic Field, Thermal and NVH for EV/HEV Traction Motor 한은실(태성에스엔이)	초S-IX-3. Magnetic Field-induced Linear Clustering of Spherical Particles for Thermally Conductive Polymer Composites 김영국(재료연구소)			
	10:15 ~ 10:40	초S-VIII-4. Study on Reduction of Cogging Torque and Torque Ripple of Permanent Magnet Electric Motor Considering Magnetization Pattern Using Magnetization Yoke 이성구(동아대)	초S-IX-4. 입계확산형 희토자석 기술 개발 현황과 향후 과제 김동환(성림첨단산업)	10:00 ~ 10:30	초S-X-3. Single molecular dynamics of Plasmalemmal Vesicle Associated Protein-1 (PV-1) in live vascular cell 서대하(DGIST)	초S-XI-3. Nontrivial Topology induced by Magnon-Phonon Hybridization 고경춘(고려대)
	10:40 ~ 11:05	초S-VIII-5. A Study for motor requirement of electrical airplanes 김성찬(한국항공우주연구원)	초S-IX-5. Properties of soft and hard magnetic materials based on amorphous alloy system 임혜인(숙명여대)	10:30 ~ 11:00	초S-X-4. High resolution magnetic sensor to analyze physical properties of blood vessels through pulse wave pattern detection technology 김철기(DGIST)	초S-XI-4. Effect of broken inversion symmetry in magnetic multilayers 한동수(KIST)
	11:05 ~ 11:10	Coffee Break				
	11:10 ~ 11:35	초S-VIII-6. Vibration Analysis on IPMSM According to Types of Eccentricity 김대기(한양대)	초S-IX-6. Current status and prospect of ceramic permanent magnets 유상임(서울대)	11:00 ~ 11:30	초S-X-5. 자성기반 압력센서를 이용한 맥박 패턴 측정 기술 오선종(한국기계연구원)	초S-XI-5. Spin transport in ferrimagnet 김갑진(KAIST)

7월 21일[화]

<table>
<tr><th>시간</th><th colspan="6">프로그램</th></tr>
<tr><td rowspan="2">09:00
~
12:30</td><td rowspan="2">11:35
~
12:00</td><td>초S-VIII-7.
Design of Four-Layer Winding Method for the Vibration Reduction of Electrical Motor
윤명환(전자부품연구원)</td><td>초S-IX-7.
Mass Production Technologies of Amorphous Fibers and Strips
박언병(포항산업과학연구원)</td><td rowspan="2">11:30
~
12:00</td><td>초S-X-6.
Highly soluble magnetic nanoclusters for biomedical applications
이재종(한국기계연구원)</td><td colspan="2">초S-XI-6.
Topological Spin Transport in 2D Quantum Magnets
김세권(KAIST)</td></tr>
<tr><td>12:00
~
12:30</td><td>초S-XI-7.
Contorl of Half-skyrmion Hall Effect and its Neuromorphic Computing Application
양승모(KRISS)</td></tr>
<tr><td>12:30
~</td><td colspan="6">폐회 (Antigua1)</td></tr>
</table>

CONTENTS

○ Session MD [Magnetization dynamics]

○ **Session HM [Hard-magnetic Materials]**

○ Session SM [Soft-magnetic Materials]

○ Session SS [Semiconductor spintronics]

○ Session SO [Spin orbit coupling and related phenomena]

7월 20일(월) 09:00~12:30
Special Session Ⅰ 'Magnetic For IOT'

Antigua1

좌 장 : 윤석수(안동대) / 손대락(한남대)

7월 20일(월) 09:00~12:30
Special Session Ⅱ 'Theory'

Antigua2

좌 장 : 임성현(울산대)

7월 20일(월) 09:00~12:30
Special Session Ⅲ 'Medical Magnetics'
Barbuda1+2

❀ 좌 장 : 한만석(강원대) / 안우상(울산대)

7월 20일(월) 09:00~11:30
Special Session Ⅳ '산화물 자성체 세션'
Barbuda3+4

❀ 좌 장 : 문은국(KAIST)

7월 20일(월) 14:00~17:30 Special Session Ⅴ 'Magnetization Dynamics' — Antigua1

✿ 좌 장 : 최석봉(서울대)

7월 20일(월) 14:00~16:30 Special Session Ⅵ 'Magnetism in reduced dimension' — Antigua2

✿ 좌 장 : 유정우(UNIST)

7월 20일(월) 15:00~16:10
Special Session Ⅶ 'Mossbauer & Nano'

Barbuda1+2

❀ 좌 장 : 엄영랑(한국원자력연구원)

7월 21일(화) 09:00~12:00
Special Session Ⅷ 'Electro-Magnetic Energy Convergence'

Barbuda3+4

❀ 좌 장 : 이정종(전자부품연구원)

7월 21일(화) 09:00~12:00
Special Session IX 'Hard & Soft Magnetic Materials: Motor'

Antigua2

❀ 좌 장 : 이우영(연세대)

7월 21일(화) 09:00~12:00
Special Session X 'Bio-Convergence Magnetics'

Barbuda1+2

❀ 좌 장 : 김철기(DGIST)

7월 21일(화) 09:00~12:30
Special Session XI 'Spintronics'

Antigua1

좌 장 : 이경진(고려대)

KMS 2020 Summer Conference

강습회 프로그램

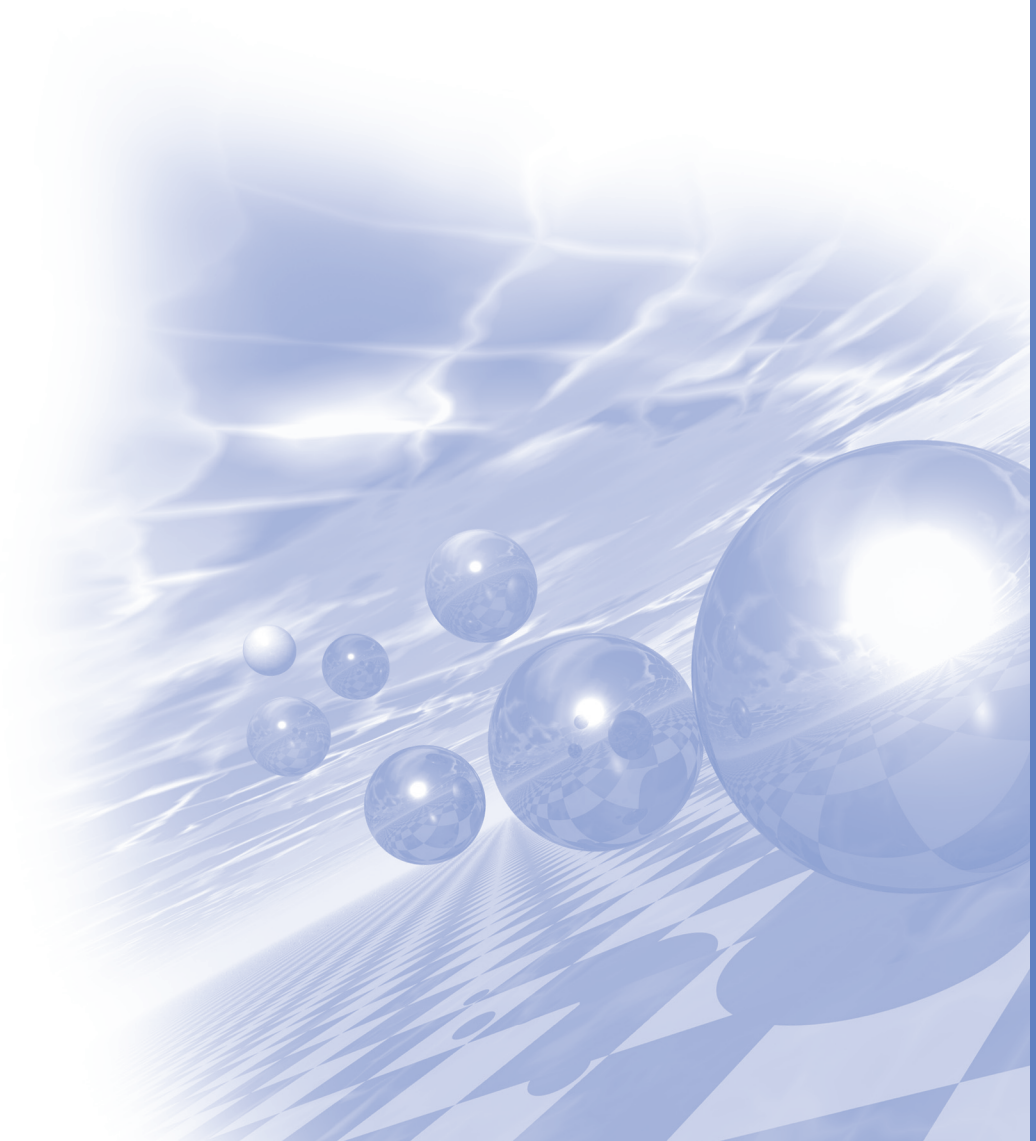

Topological Defects in Magnetism

Eun-Gook Moon*
Department of Physics, Korea Advanced Institute of Science and Technology (KAIST), Daejeon 34141, Korea

Topological defects are important to understand magnetic phenomena. For example, in two spatial dimensions, XY spin systems host topological defects, so-called vortices, and they play a central role in thermal excitations and transports. Even, the topological defects may become an impetus of the celebrated Kosterlitz-Thouless transition. Remarkable advances in recent experiments even visualize topological defects in magnetic systems, and, in this tutorial, we discuss how to understand and apply topological defects to magnetism with examples.

T-2

딥러닝을 이용한 소재기술 개발

손기선*
세종대학교

최근 인공지능을 이용한 소재개발이 매우 중요한 이슈로 부각됨에 따라 소재연구 분야에서도 많은 관심을 받고 있으며, 동시에 논란도 일으키고 있다. 인공지능이란 그 범위가 매우 방대하며, 그 정의도 비전문가들 사이에서 제 각각으로 왜곡되고 있는 실정이라 한마디로 설명할 수는 없으나, 최근 각광을 받고 있는 알파고의 개발자인 데이비드 실버 교수의 정의에 따르면 인공지능이란 딥러닝과 강화학습의 합체를 말한다. 본 발표의 구성은 이러한 인공지능 기술을 기반으로 소재공학 전반에 걸쳐 우리가 연구실 또는 산업현장에서 매일 마주치는 일반적인 문제이며, 가장 골치 아픈 난제인 소재개발에 초점을 맞추고자 한다.

우선 본 발표의 서두에서는 이러한 인공지능 기술의 핵심인 딥러닝 이론을 대략적으로 설명하고, 이를 소재공학 전반에서 이용한 사례를 소개하고자 한다. 특히 딥러닝을 이용하여 XRD 결과를 분석할 수 있는 새로운 개념의 소재 분석 기술을 설명하고, 중반부에서는 딥러닝과 강화학습을 기반으로 하는 인공지능형기술을 금속합금설계 기술에 적용하여 성공한 실례를 바탕으로, 인공지능형 소재 개발 및 조성 최적화 설계에 대해 자세히 소개하고, 공학일반에 걸쳐 가장 중요한 이슈인 최적화에 인공지능이 이용될 수 있는 실례를 소개하고, 더 나아가 기존의 메타휴리스틱스 최적화 기법과의 비교 고찰을 소개한다. 또한 최근 인공지능계에서 가장 큰 주목을 받고 있는 확률적생성모델인 VAE(Variational Auto Encoder)와 GAN(Generative adversarial network)을 소재개발에 이용하고자 하는 새로운 접근을 소개한다. 결론적으로 본 발표에서는 인공지능이 소재공학 전반에 걸쳐 미래기술로 자리매김할 수 있음을 실례를 통해 입증한다.

Introduction to electric vehicle development history and technology trends

Yun-yong Choi*
Electro-Magnetic Energy Convergence of Korean Magnetics Society

지구를 둘러싼 기후변화의 영향으로 인간의 생존권에 위협이 되는 많은 환경 변화가 전세계으로 일어나고 있으며, 그 대책의 중심에 위치한 자동차산업은 현재의 인프라를 유지시키기 위한 각종 환경 규제 대응책 마련과 미래를 위한 최종 대안으로 탄소 배출을 획기적으로 줄이는 전동기술을 활용한 ICT기반의 친환경 이동 수단으로 빠르게 변모해 가고 있다. 이러한 시대적 변화에 가장 화두가 되고 있으며, 현존하는 기술의 집합체라 불리우는 것이 전기자동차 분야이다.

본 강습회에서는 미래 전동화시대의 핵심 산업인 전기자동차 산업이 직면하고 있는 시대적인 요구가 무엇인지, 미래 기술을 위해 무엇을 해야 할지를 같이 생각해 보는 시간을 공유하고자 한다.

기후변화와 자동차산업은 무슨 연관관계가 있는 것인가?
왜 전기자동차로 모두 가야만 한다고 하는 것인가?
전기자동차는 현재 우리의 주변에 얼마나 와 있으며, 미래는 어떤 모습으로 다가올 것인가?
미래 전동화 시대와 전기자동차 시대를 맞이하는 우리는 무엇을 준비해야만 할 것인가?

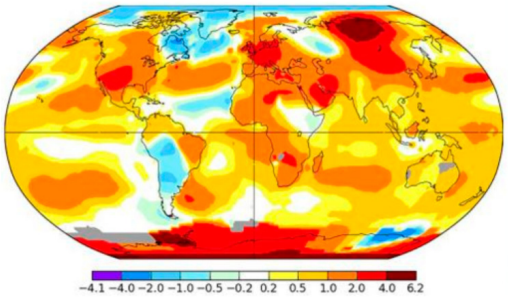

2018년의 지구 표면 온도를 색으로 표현한 그림. 붉을수록 열선이 강함을 뜻한다. / NASA


1800년도 전기자동차 회사의 광고

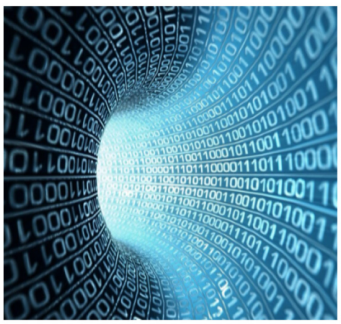

KMS 2020 Summer Conference

포스터발표

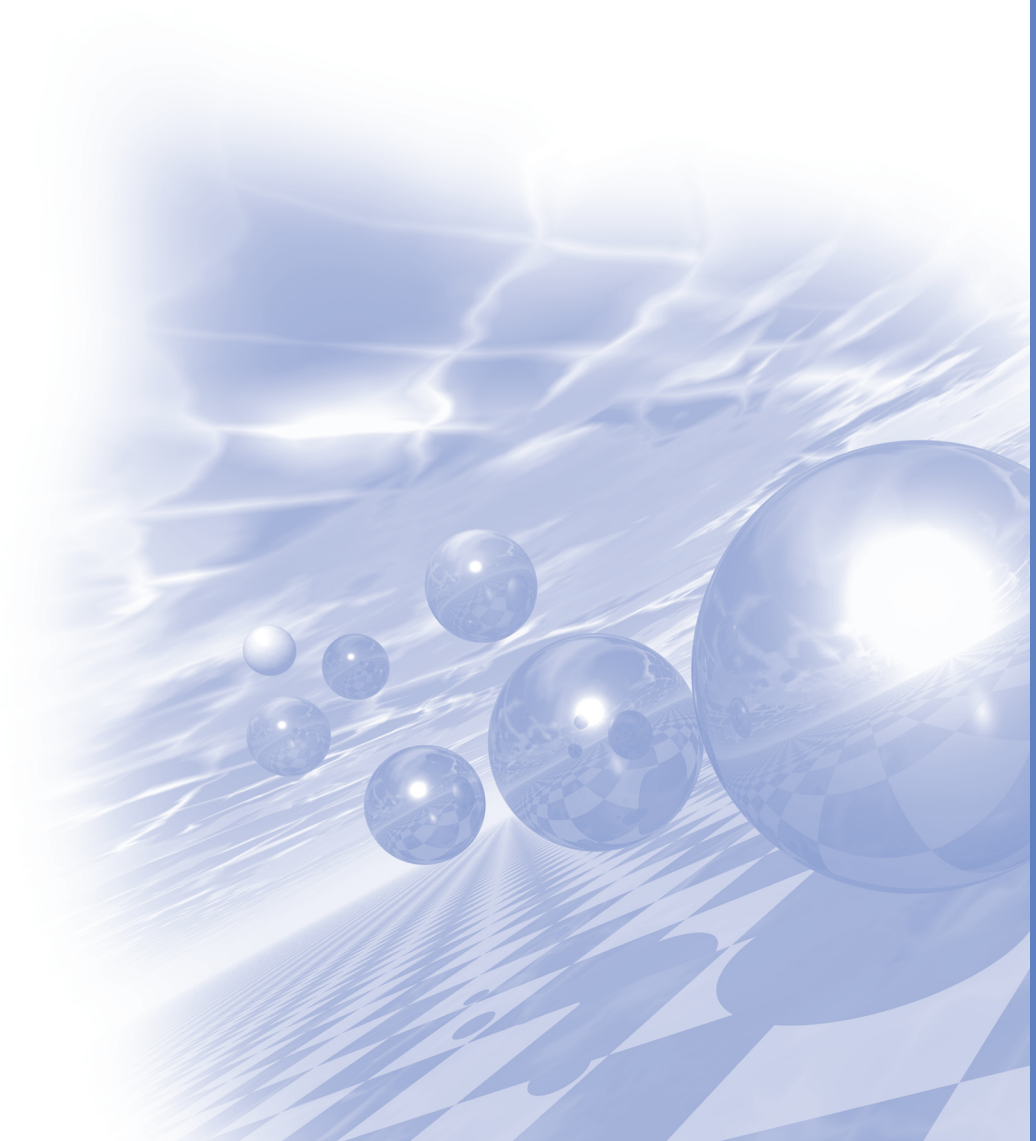

Optical method of determining spin diffusion length of ferromagnetic metals

Kyung-Hun Ko[1*], Gyung-Min Choi[1,2†]
[1]Department of Energy Science, Sungkyunkwan University, Suwon 16419, South Korea
[2]Center for Integrated Nanostructure Physics, Institute for Basic Science (IBS), Suwon 16419, South Korea

We determine the spin diffusion length of ferromagnetic metals by optical method. We induced the spin transport from ferromagnetic metal to nonmagnetic metal via ultrafast demagnetization of the ferromagnetic metal. The spin accumulation on nonmagnetic metal is measured by magneto-optical Kerr effect. The ultrafast demagnetization and the spin transport are analyzed based on the electron-magnon scattering in the bulk of ferromagnetic metal and diffusion of the spin. We analyze the spin diffusion length in two different methods: the quantitative analysis and the relative analysis of the spin accumulation. First, we quantitatively compare the Kerr rotation and the spin accumulation on nonmagnetic metal. Second, we measured ferromagnetic metal thickness dependent spin accumulation on nonmagnetic metal. Both methods give consistent results. We also compare our results with electrical measurements that has been done to confirm the reliability of our technique. From our optical methods, we determine the spin diffusion length of 7.0, 4.6, and 3.3 nm for the ferromagnetic metal of Fe, Co, Ni, respectively.

Skyrmion logic circuit using boundary annihilation

Moojune Song*, San Ko and Kab-Jin Kim†
Department of Physics, Korea Advanced Institute of Science and Technology, Daejeon 34141, Republic of Korea
E-mail: kabjin@kaist.ac.kr.

Magnetic skyrmion is believed to be suitable for new-type magnetic memory/computing devices because of its extraordinary stability due to topological protection. However, many researchers revealed that the skyrmion in real system is not necessarily robust, but can be easily annihilated due to the physical edge effect [1,2]. So the major research efforts have been devoted to avoid the skyrmion annihilation by, e.g., reducing the skyrmion Hall effect [3], introducing magnetic anisotropy step [4], or magnetic domain wall boundary[5]. Contrary to this approach, here we report that the skyrmion annihilation can be utilized for improving the quality of skyrmion logic devices. Using micromagnetic simulation (MUMAX3), we demonstrated that the operation of combinational logic device is possible by utilizing skyrmion annihilation. We present a half adder and a full adder as well as an arbitrary n-bit adder circuit by directly cascading each device. Our skyrmion logic device shows better performance than previously suggested skyrmion logic devices [6], in particular, in cell density due to its simplicity. Our results therefore imply that the skyrmion annihilation at physical edge is not a detrimental effect but is a beneficial for skyrmion logic devices.

References

[1] W. Jiang *et al.* Nat. Phys. **13**, 162 (2016)
[2] D. Ortuno *et al.* Sci. Rep. **7**, 4060 (2017)
[3] Y. Hirata *et al*. Nat. Nanotechnol. **14**, 232 (2019)
[4] P. Lai *et al.* Sci. Rep. **7**, 45330 (2017)
[5] M. Song *et al.* Appl. Phys. Express **13**, 063002 (2020)
[6] M. Chauwin *et al.* Phys. Rev. Appl. **12**, 064053 (2019)

Spin orbit torque efficiency of novel W_3Ta heavy metal layer grown by RF sputtering approach

Jeongwoo Seo[1*], Jeonghun Shin[2], Jungyup Yang[3], Jinpyo Hong[1,2]

[1]Department of Physics, Hanyang University, Seoul 133-791, South Korea

[2]Division of Nanoscale Semiconductor Engineering, Hanyang University, Seoul 133-791, South Korea

[3]Department of physics, Kunsan national University, South Korea 54150

Magnetization manipulation by a Spin Orbit Torque (SOT) phenomena has intense focus on the efficient operation of spintronic devices at extremely lower powers. Recent theoretical work suggests that a W_3Ta layer may have a large spin hall angle in a heavy metal (HM)/ ferromagnet (FM) / Oxide (O) hetero-structure, when compared with the well-known W Heavy Metal. Here, we address the SOT Efficiency of a new W_3Ta layer which are prepared by a RF sputtering approach. The growth key parameters, such as working pressure and annealing temperature are systematically adjusted in our work. Comprehensive structural analyses supported the growth of particular A15 phase(β-phase) in an extremely narrow ranges of growth parameters, thus providing the higher SOT efficiency, as shown in fig 1. We conducted the DC and AC approaches to identify spin orbit torque-driven effective fields and enhanced spin orbit torque efficiency in a W_3Ta-based heterostructure.

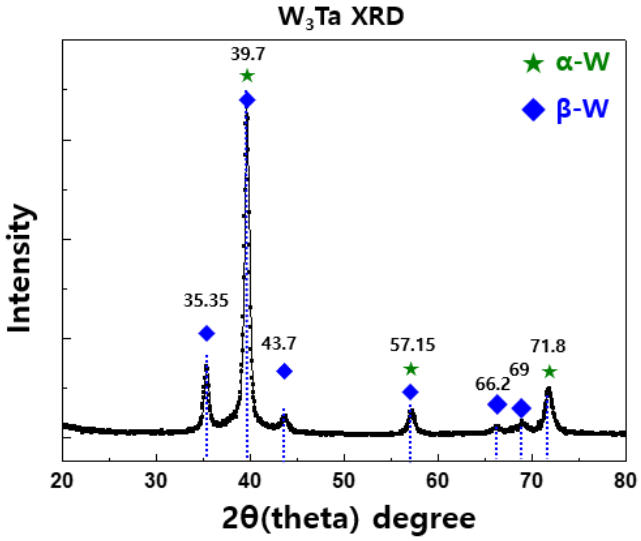

Fig. 1. W_3Ta XRD data with α-phase and β-phase(A15 phase) tungsten

First-principles study on magnetic properties of 1T-VX_2 (X=S, Te)

Jee-Ahn Jung* and Hanchul Kim†
Department of Physics, Sookmyung Women's University, Seoul 04310, Korea
hanchul@sookmyung.ac.kr

Since the discovery of graphene, two-dimensional layered materials such as transition metal dichalcogenides (TMDCs) have attracted researchers due to their potential applicability to next-generation electronic and spintronic devices [1-3]. With the reduced dimensionality, TMDCs show remarkable changes in their properties, for instance, the indirect-to-direct transition of band gap, the charge density wave enhancement, and the emergence of ferromagnetism [4-7]. Recently, as for 1T-VX_2 (X=S, Te), the observation of ferromagnetism in the two-dimensional limit has been reported [8-10]. On the contrary, several studies refute the ferromagnetism in 1T-VX_2 [11-13]. We performed density functional theory calculations using Vienna *ab initio* simulation package to elucidate the magnetic properties of 1T-VX_2. We used the Perdew-Burke-Ernzerh of generalized gradient approximation for the exchange-correlation interaction and the projector-augmented-wave potentials for the electron-ion interaction. For bulk phases, we employed Grimme's dispersion correction methods (DFT-D2 and DFT-D3) to describe the van der Waals interaction between layers. We will address the stable magnetic orderings of bulk and monolayer 1T-VX_2 as well as their electronic structures.

References

[1] B. Radisavljevic *et al.*, Nat. Nanotechnol. **6**, 147 (2011).
[2] X. Xi *et al.*, Nat. Phys. **10**, 343 (2014).
[3] Q. H. Wang *et al.*, Nat. Nanotechnol. **7**, 699 (2012).
[4] Y. Zhang *et al.*, Nat. Nanothechnol. **9**, 111 (2014).
[5] X. Xi *et al.*, Nat. Nanotechnol. **10**, 765 (2015).
[6] K. Xu *et al.*, Angew. Chem. **52**, 10477 (2013).
[7] W. Yu *et al.*, Adv. Mater. **31**, 1903779 (2019).
[8] D. Gao *et al.*, J. Mater. Chem. C **1**, 2909 (2013).
[9] Y. Guo *et al.*, Adv. Mater. **29**, 1700715 (2017).
[10] J. Li *et al.*, Adv. Mater. **30**, 1801043 (2018).
[11] Y. Wang *et al.*, Phys. Rev. B **100**, 241404 (2019).
[12] P. K. J. Wong *et al.*, ACS Nano **13**, 12894 (2019).
[13] H. Liu *et al.*, Nano Lett. **19**, 8572 (2019).

Spin-wave Multiplets Localized in Magnonic Crystal Fractals

Gyu-young Park*, Jaehak Yang and Sang-Koog Kim†
National Creative Research Initiative Center for Spin Dynamics and Spin-Wave Devices,
Nanospinics Laboratory, Research Institute of Advanced Materials,
Department of Materials Science and Engineering, Seoul National University, Seoul 151-744, Republic of Korea
†Correspondence and requests for materials should be addressed to S.-K. K. (sangkoog@snu.ac.kr)

Magnonic crystals enlarge a basic understanding of quantized spin-wave modes. In this regard, we model magnetic antidot-lattice fractals (ALFs) which are constructed using deterministic iterations based on ordinary antidot-lattices (ADLs). A series of earlier studies reported major spin-wave localizations inside the ADL: i.e., center mode versus edge mode [1-4]. We found within the AFLs the major modes split into multiplets according to Fibonacci sequences, caused by inhomogeneity induced from fractal geometries in the Fibonacci sequence. Active controls of spin-wave modes using bias magnetic fields as well as magnonic crystal geometry enable reunion or crossover of the major spin-wave modes.

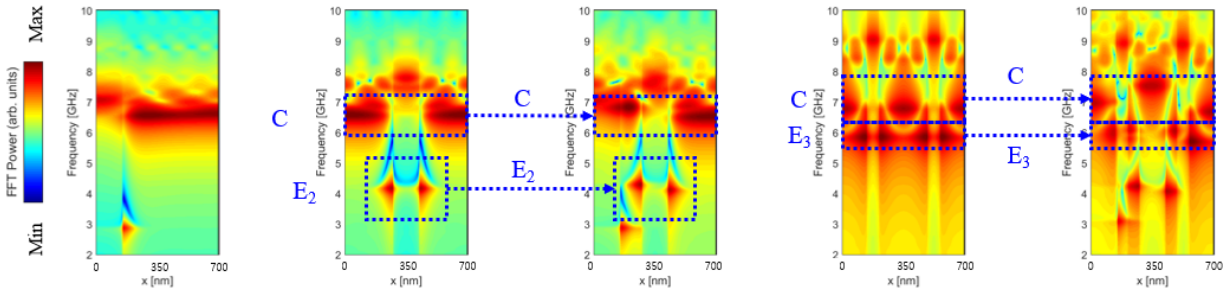

Fig. 1. The quantized spin-wave spectra along a longitudinal direction of each magnonic crystal motif

References

[1] C. Bayer, J. Jorzick, B. Hillebrands, S.O. Demokritov, R.Kouba, R. Bozinoski, A. N. Slavin, K. Y. Guslienko, D. V. Berkov, N. L. Gorn, and M. P. Kostylev, Phys. Rev. B **72**, 064427 (2005).

[2] O. N. Martyanov, V. F. Yudanov, R. N. Lee, S. A. Nepijko, H. J. Elmers, R. Hertel, C. M. Schneider, and G. Schönhense, Phys. Rev. B 75, 174429 (2007).

[3] S. Neusser, B. Botters, and D. Grundler, Phys. Rev. B **78**, 054406 (2008).

[4] C. Swoboda, M, Martens, and G. Meier, Phys. Rev. B **91**, 064416 (2015).

Emergent Geometric Confinement of Magnetic Skyrmion by Spatially Modulated Dzyaloshinskii-Moriya Interaction

Dae-Han Jung*, Hee-Sung Han, Namkyu Kim and Ki-Suk Lee†
School of Materials Science and Engineering, Ulsan National Institute of Science and Technology, Ulsan 44919, Republic of Korea

Magnetic skyrmions, nanometer-sized spin textures, are envisaged to be used as information carrier in the future spintronic devices since their unique dynamic and topological characteristics [1-3]. Unlike theoretically predicted, however, their topological robustness does not seem to be well maintained in a confined geometry [4,5]. To realize such skyrmion-based information devices, it is essential to suppress the annihilation of the skyrmion at the boundaries of a nanostructure and guide the movement of the skyrmion. Several methods to resolve them have been presented using curbed nanowire structures [6] or electric-field-controlled magnetic anisotropy [7]. However, there are many practical difficulties to utilize in integrated circuit devices. Here, we propose a novel type of simple planar track-based structure by spatial modulations of Dzyaloshinskii-Moriya interaction (DMI). The boundaries to geometrically confine the skyrmion are located between high-DMI and low-DMI region. Since the profile of individual skyrmions can extend beyond the boundary in the designed structure, it strongly suppresses the skyrmion annihilation at the boundary and leads to stable propagation along with the reduced size of the skyrmion as show in Fig.1(a). The compressed skyrmion, in turn, results in the significant enhancement of the skyrmion speed as show in Fig.1(b) and thus, we can expect fast signal processing as well as high data storage density. Consequently, our results open a new vista for realizing skyrmion-based integrated composite circuitry.

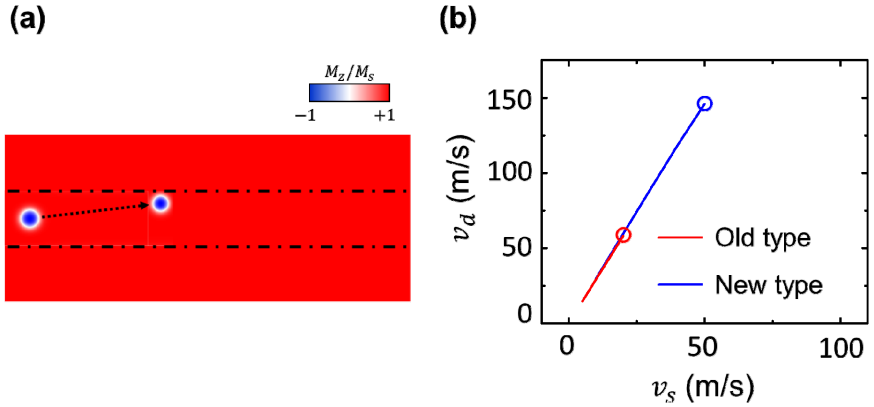

Fig. 1. (a) A nanostrip model for micromagnetic simulation where the color indicates m_z configuration in which a skyrmion is driven by spin transfer torque. The black dash-dotted lines indicate boundaries of the nanostrip. (b) Plot showing the relation between the skyrmion speed and the applied conduction electron velocity (ν_s). The circle symbols indicate the skyrmion annihilation.

References

[1] [1] N. S. Kiselev, A. Bogdanov, R. Schäfer, and U. K. Rößler, *J. Phys. D* **44**, 392001 (2011).

[2] A. Fert, V. Cros, and J. Sampaio, *Nat. Nanotech.* **8**, 152 (2013).

[3] N. Nagaosa and Y. Tokura, *Nat. Nanotech.* **8**, 899–911 (2013).

[4] Xichao Zhang, G. P. Zhao, Hans Fangohr, J. Ping Liu, W. X. Xia, J. Xia, and F. J. Morvan, *Sci. Rep.* **5**, 7643 (2015).

[5] M. W. Yoo, V. Cros, and J. V. Kim, *Phys. Rev. B* **95**, 184423. (2017).

[6] I. Purnama, W. L. Gan, D. W. Wong, and W. S. Lew, *Sci. Rep.* **5**, 10620 (2015).

[7] P. Upadhyaya, G. Yu, P. K. Amiri, and K. L. Wang, *Phys. Rev. B* **92**, 134411 (2015).

Manipulation of Magnetic Skyrmion Motion for Unidirectional Transmission by Tuning the Asymmetry of Potential Energy Surfaces

Dae-Han Jung*, Hee-Sung Han, Namkyu Kim and Ki-Suk Lee†
School of Materials Science and Engineering, Ulsan National Institute of Science and Technology, Ulsan 44919, Republic of Korea

Magnetic skyrmions are topologically stable spin configurations which have recently gained momentum due to these prominence as up-and-coming candidates for next-generation information storage and processing applications. [1-3]. To obtain fully functional and competitive skyrmion-based devices, it is crucial to manipulate skyrmions by electrical means in device-compatible materials with geometrically confined boundaries. Here, we demonstrate that a current-induced skyrmion propagation can be unidirectionally manipulated (see FIG. 1) by forming an asymmetric shape of device. The physical origin of the control of the skyrmion propagation direction of a skyrmion is addressed by micromagnetic numerical and analytical calculations. The dynamic transitions that a skyrmion can undergo are estimated by analyzing the multidimensional surface describing the energy of the system as a function of the skyrmion position and the current density. Out results could provide a fundamental insight on the skyrmion dynamics and manipulation to design skyrmion-based logic device such as a diode element.

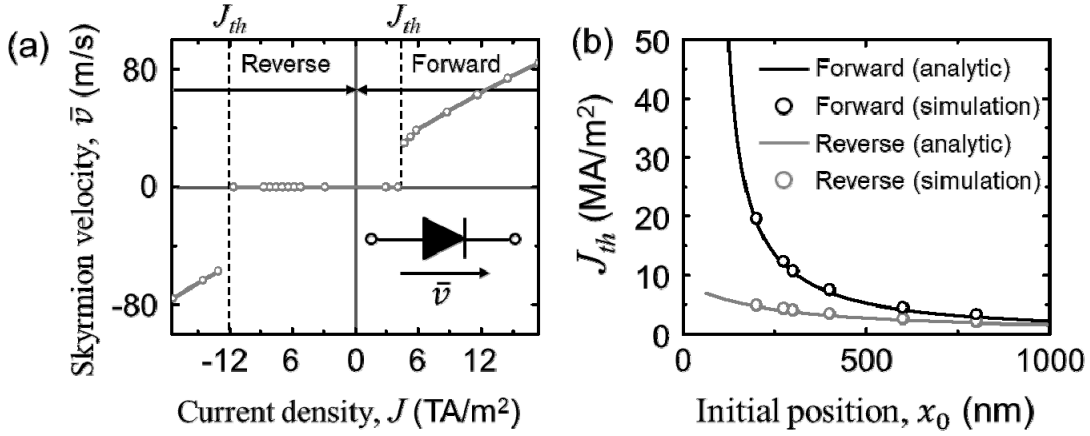

Fig. 1. (a) Diode characteristics of skyrmion propagation manipulated by asymmetrical modulation of potential energy. (b) analytical calculations for dynamic transitions compared to micromagnetic simulations.

References

[1] N. S. Kiselev, A. Bogdanov, R. Schäfer, and U. K. Rößler, J. Phys. D **44**, 392001 (2011).

[2] A. Fert, V. Cros, and J. Sampaio, Nat. Nanotechnol. **8**, 152 (2013).

[3] N. Nagaosa and Y. Tokura, Nat. Nanotechnol. **8**, 899–911 (2013).

Chirality dependence on the dynamical deformation of three-dimensional magnetic vortex structure

Hee-Sung Han*, Sooseok Lee, Dae-Han Jung, Myeonghwan Kang, Ki-Suk Lee
School of Materials Science and Engineering,
Ulsan National Institute of Science and Technology (UNIST), Ulsan, Korea

In magnetic textures, chirality is crucial in the dynamics of magnetic textures [1,2]. In magnetic vortices, the clockwise or counterclockwise curling direction of the in-plane magnetization determines chirality [3,4]. It is reported that the chirality of a magnetic vortex structure influences only phase of vortex core position during dynamic motion [1,2]. In this works, we reported that the harmonic excitation of a three-dimensional (3D) magnetic vortex structure show novel chirality dependence by performing micromagnetic simulation. During a gyrotropic motion, the 3D vortex core structure is tilted and elongated along the direction of the vortex core motion. Furthermore, the tilting direction relative to the motion of the vortex core depends on the chirality of the vortex structure due to the 3D distribution of the gyrotropic field. We confirmed that the 3D distribution of gyrotropic field is dependent on the chirality. These results can provide understanding on the unique 3D characteristics of magnetic vortex structures and open up technological possibilities to harness them in magnetic vortex-based spintronic devices.

References

[1] S.-B. Choe. et al. Science **304** (5669), 420-422 (2004).
[2] K.-S. Lee and S.-K. Kim, Phys. Rev. B **78** (1) (2008).
[3] R. P. Cowburn, Nat. Mat. **6**, 255 (2007).
[4] A. Hubert and R. Schäfer, Magnetic Domains: The Analysis of Magnetic Microstructures (2008).

Practical Energy Product of Magnetic Materials

Namkyu Kim*, Hee-Sung Han, Soo Seok Lee and Ki-Suk Lee†
School of Materials Science and Engineering, Ulsan National Institute of Science and Technology,
Ulsan 44919, Republic of Korea

Devices such as electric vehicles and wind power generators utilize the magnetic energy of permanent magnet. To meet the increasing demand for such devices, researchers have actively developed permanent magnets with higher efficiencies and lower cost. Magnetic energy is represented by the energy product BH, which is twice the energy stored in the stray field outside the magnet. It can be obtained from the volume integral of the square of the stray field outside the magnet, or from the volume integral of the dot product between the demagnetizing field $\boldsymbol{H}_\mathrm{d}$ and the internal magnetic flux density $\boldsymbol{B}$. The maximum energy product, $(BH)_{\max}$ is widely used as a figure of merit for evaluating the performance of hard-magnetic materials. As noted by Skomski and Coey et al, $(BH)_{\max}$ should be evaluated rigorously from the hysteresis loop by considering the exact working point, which is determined by the shape of the magnet. However, many researchers still use $(BH)_{\max}$ obtained from the hysteresis loop of a certain shape as a representation of the material, even though the only information BH from a certain shape of the magnet is an energy product at the remanent state. Thus, we compared correctly calculated $(BH)_{\max}$ with that of obtained from conventional way through several models by using micromagnetic simulation.

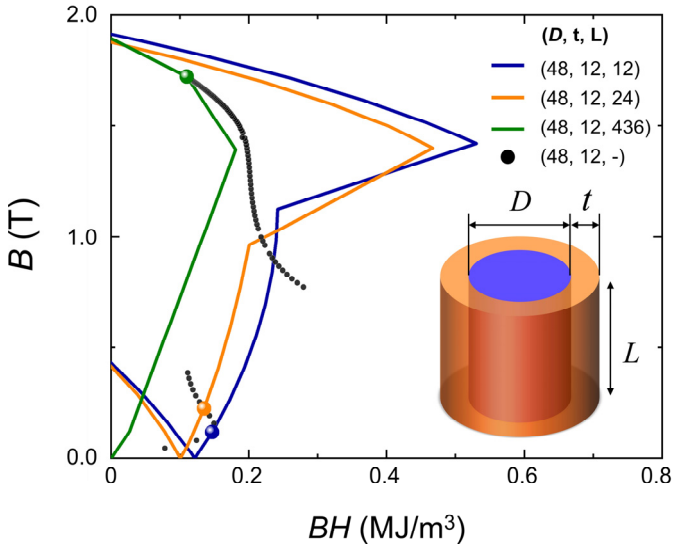

Fig. 1. Energy product of cylindrical core/shell structures. Each line means the energy product from full hysteresis loops. The spherical markers indicate the magnetic flux considering the demagnetization field when the external field is zero. The black dots indicate working points at remanent state of (D, t) = (48, 12) for different lengths

The effects of Y doping on magnetic and microwave absorption properties of $Ba_3Co_2Fe_{24}O_{41}$ hexaferrites

H. J. Woo, N. Tran, S. H. Kong*, T. L. Phan and B. W. Lee†
Department of Physics and Oxide Research Center, Hankuk University of Foreign Studies,
Yongin 17035, South Korea (*E-mail: bwlee@hufs.ac.kr)

$Ba_{3-x}Y_xCo_2Fe_{24}O_{41}$ (Y-Co_2Z, x = 0–0.5) polycrystalline samples were prepared by solid state reaction method. Structural and magnetic properties studied by using X-ray diffractometer (XRD) and vibrating sample magnetometer (VSM). The XRD patterns indicated that samples with x < 0.3 crystallized in Z-type hexaferrite phase while others had an impurity phase of Y-type hexaferrite. This can be attributed to the charge imbalance when the large amount of Ba ions (2+) had replaced by higher valence of Y ions (3+). From the $M(H)$ loops recorded at room temperature, both saturation magnetization M_S and coercivity H_C increased with the increasing of x. In detail, M_s increased from

45.25 emu/g to 50.69 emu/g, and H_C increased from 56.1 Oe to 108.5 Oe when x increased from 0 0.5.

For microwave absorption properties, three typical samples with x = 0, 0.2, and 0.4 were selected then mixed with 7%wt. epoxy. The mixtures were pressed into the toroidal shapes (with outer and inner diameters were 7 mm and 3 mm, respectively) before drying at 170 °C for 0.5 h. Electromagnetic wave absorption properties of the samples were studied by a PNA-X network analyzer in the frequency range of f = 0.1–18 GHz for sample thickness of t = 2.25–1.25 mm (Δt = 0.25 mm). Complex permittivity and permeability were remarkably changed by Y-doping as well as thickness changing. Using transmission line theory, reflection loss (RL) of samples were calculated, which was strongly dependent on x and t. All of three samples showed low RL, especially with the thin samples thickness with t = 1.50 and 1.75 mm. The minimum RLwas –54.4 dB (represent for> 99.9% of incident wave being absorbed) which could be found at f = 16.4 GHz for sample x = 0.2 with t = 1.50 mm. While, the largest effective bandwidth (RL < – 10 dB, represent for ~90% of incident wave being absorbed) could be found in the frequency range f = 12.3–16.9 GHz for x = 0 with t = 1.75 mm. These results suggest that Y-Co_2Z samples are potential candidates for microwave absorption.

Anomalous Hall effects without net magnetization

Minkyu Park[1*], Guihyun Han[2] and S. H. Rhim[2]

[1]Research Institute of Basic Sciences, University of Ulsan, Ulsan, 44610, Republic of Korea

[2]Department of Physics and EHSRC, University of Ulsan, Ulsan, 44610, Republic of Korea

It has long been believed that anomalous Hall effects are supposedly related to net magnetization. However, it has been pointed out recently that the anomalous Hall effect can be observed with vanishing magnetization in non-collinear antiferromagnet [1]. In this work, we extend investigation to collinear magnetic material, Mn_3Al, which is nearly compensated ferrimagnet with magnetization axis along z direction. We found that only σ_{xy} component of anomalous Hall conductivity survives under the constraint of symmetry and explicit firstprinciples calculations reveal that σ_{xy} is about $350(\Omega\cdot cm)^{-1}$.

Reference

[1] H. Chen, Q. Niu and A. H. MacDonald, *Anomalous Hall effect arising from noncollinear antiferromagnetism*, Phys. Rev. Lett. *112* **(2014) 017205,** [1309.4041].

Magnetism of Mn_4C: First-Principles Calculations

Jun Gyu Lee*, S. H. Rhim and S. C. Hong†
Department of Physics and EHSRC, University of Ulsan, Ulsan 44610, Republic of Korea
E-mail: schong@ulasn.ac.kr

A recently synthesized new magnetic compound of Mn_4C has been reported for the first time [1]. According to the report, the saturation magnetization of Mn_4C increases as temperature increases, which is quite different from the behavior of normal magnetic materials. In this talk, we report some basic physical properties of the new Mn_4C compound, using the first-principles calculational method of Vienna Ab-initio Simulation Package. For the self-consistent calculations 14 x 14 x 14 Monkhorst-Pack k-point mesh and cutoff energy of 500 eV are employed. First, we determine the stable structure of Mn_4C from total energy calculations: A cubic phase of a=3.782 Å shown in Fig.1 is found to be most stable; the crystal structure is quite similar to that of Mn_4N [2]. The calculated stable magnetic structure is ferrimagnetic. The calculated magnetic moments of Mn_I and Mn_{II} are 3.383 μ_B and 1.274 μ_B, respectively. Since their magnetizations are antiparallel to each other, the total magnetic moment gets 0.239 μ_B/unit-cell. The calculated results are quite consistent with the experimental values of 3.868 Å and 0.26 μ_B/unit-cell [1]. We will discuss further the origin of increasing magnetic moment as temperature increases.

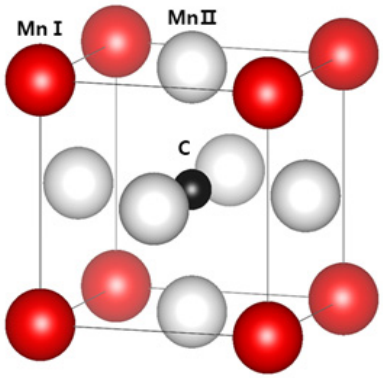

Fig. 1. Crystal Structure of Mn_4C

References

[1] Ping-Zhan Si, Hui-Dong Qian, Hong-Liang Ge, Jihoon Park, and Chul-jin Choi, Appl. Phys. Lett. **113**, 049903 (2018).

[2] W. J. Takei, R. R. Heikes, and G. Shirane, Phys. Rev. **125**, 1893 (1962).

First-Principles Calculations of Intrinsic Spin Hall Conductivity of β-W Based Alloys

Do Duc Cuong*, Soon Cheol Hong† and S. H. Rhim†
Department of Physics and Energy Harvest Storage Research Center, University of Ulsan, Ulsan 44610, South Korea
E-mail: schong@ulsan.ac.kr, sonny@ulsan.ac.kr

Spin Hall effect (SHE) is the conversion of charge current to spin current. Non-magnetic heavy transition metals (TMs) are expected to give large spin Hall conductivity (SHC) for their large spin-orbit coupling. Among transition metals, β-W, in A15 structure, has been reported to have large SHC [1-3], and alloys of β-W are expected to have even higher SHC [2]. In this work, we present *ab initio* study of β-W alloying with V and Ta for their SHCs. For each alloy composition, possible configurations are investigated, whose relative energetics are used for thermodynamic average of SHCs. While similar band structures are expected for both alloys, considering the same valence electrons of Ta and V, the resulting SHCs exhibit different behavior. More specifically, SHC of the V-W alloy reaches up to –1208 $\hbar/e$S/cm, which is about 48% larger than -817 $\hbar/e$S/cm of β-W, when concentration of V is 25%, while that of Ta-W alloy decreases with Ta concentration.

References

[1] K. Demasius *et al.,* Nat. Commun. **7**, 10644 (2016).
[2] X. Sui *et al.,* Phys. Rev. B **96**, 241105(R) (2017).
[3] E. Derunova *et al.*, Sci. Adv. **5,** eaav8575 (2019).

Magnetism of two-dimensional Fe_3GeTe_2: strain dependent magneto-crystalline anisotropy

G Hye Kim*, Qurat-ul-Ain, Soon Cheol Hong and S. H. Rhim
Department of Physics and Energy Harvest-Storage Research Center, University of Ulsan, Republic of Korea
(schong@ulsan.ac.kr, sonny@ulsan.ac.kr)

In recent years, two-dimensional (2D) materials have received attentions for many intriguing physics and material properties. Fe_3GeTe_2 (FGT) is intensively studied in the context of 2D magnetism [1], whose moment reaches around $1.71\mu_B/Fe$ in ferromagnetic phase. Within collinear magnetism, monolayer is ferromagnetic (FM), and in bilayer (Fig.1) A-type antiferromagnetic (A-AFM) energetically favors over FM. Besides, A-AFM to FM transition occurs at strain (η) of +4.2% (Fig. 2). Using density-functional theory, magneto-crystalline anisotropy (MCA) is studied for $-5\% \leq \eta \leq 5\%$. Monolayer FGT exhibits perpendicular MCA for all η. On the other hand, bilayer shows perpendicular MCA for most of η but does in-plane MCA for η =-5%.

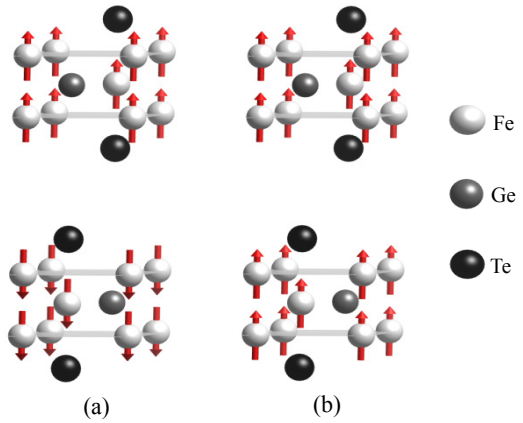

Fig. 1. Structure and spin state of bilayer Fe_3GeTe_2. (a) is AFM, and (b) is FM.

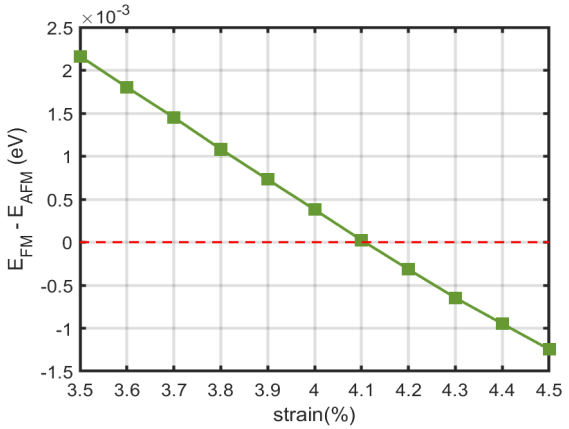

Fig. 2. Energy difference between FM and AFM state of bilayer FGT, $\triangle E = E_{FM} - E_{AFM}$, with respect to strain.

Keywords: 2D magnetic material, density-functional theory, magneto-crystalline anisotropy, strain

Reference

[1] M. Giberini, M. Koperski, A. F. Morpurgo and K. S. Novoselov, Nat. Nanotechnol. **14**, 408 (2019).

Structural and Magnetic Properties of Heusler Compound $Mn_{3-x}Co_xGa$ ($0 \leq x \leq 1$): A First-Principles Study

Quynh Anh T. Nguyen*, Thi H. Ho, S. C. Hong and Sonny H. Rhim
Department of Physics and Energy Harvest Storage Research Center, University of Ulsan,
Ulsan 44610, Republic of Korea

Mn-based Heusler compounds have received attentions for spintronics applications. Two inequivalent Mn sites couple antiparallelly leading to compensated ferrimagnetic state [1,2]. Here, using first-principles calculations, magnetic properties of $Mn_{3-x}Co_xGa$ ($0 \leq x \leq 1$) are investigated in tetragonal and cubic phases, where Co magnetism behaves quite differently. In tetragonal phase, Co moment almost vanishes while in cubic phase is about $1\mu_B$. As a consequence, total moment decreases (increases) with Co concentration in tetragonal (cubic) phase. To elucidate the puzzling Co magnetism, exchange interaction within Heisenberg model is invoked. Interactions between Co and Mn in tetragonal and cubic phases show contrasting behavior. Antiparallel and parallel alignment of Co-Mn(I) and Co-Mn(II) in tetragonal phase are reversed to parallel and antiparallel in cubic phase. Increasing magnetization upon Co concentration is explained by large exchange coefficient of Co-Mn(I) in cubic phase, which is five times larger than tetragonal one.

Keywords: Heusler compound, compensated ferrimagnetic state, magnetic exchange interaction, first-principles calculations

References

[1] B. Balke, G. H. Fecher, J. Winterlik, and C. Felser, Appl. Phys. Lett. **90**, 152504 (2007).

[2] Y. You, G. Xu, F. Hu, Y. Gong, E. Liu, G. Peng, and F. Xu, J. Magn. Magn. Mater. **429**, 40 (2017).

W Thickness Dependence of Perpendicular Magneto-crystalline Anisotropy of Pt/Co/W(111) Superlattices

Thi Huynh Ho*, Sanghoon Kim, S. H. Rhim* and S. C. Hong†
Department of Physics and Energy Harvest Storage Research Center, University of Ulsan,
Ulsan 44610, Republic of Korea
Corresponding authors: *sonny@ulsan.ac.kr, †schong@ulsan.ac.kr

A Pt/Co/W(111) system with reflection asymmetry reveals strong perpendicular magnetocrystalline anisotropy (PMA), which raises great attentions for spintronics applications.[1,2] Despite of its potential, the effects of the W-capping on PMA of Pt/Co have not been fully clarified. In this study, PMA of Pt/Co/W(111) superlattice is investigated by carrying out *ab initio* calculations. Our results show that W thickness dependence of PMA is obvious, and its maximum occurs at three monolayers (Fig. 1). Orbital hybridizations at the interfaces play an important role in PMA, where Co and W exhibit positive contribution while Pt does negative contribution. Particularly, PMA is proportional to orbital magnetic anisotropy ($m^{\perp}_{orb} - m^{\parallel}_{orb}$), which is in good agreement with the so-called Bruno relation.[3] The analysis within the framework of second-order perturbation theory and *k*- and *l*-resolved PMA indicate that most contributions originate from the coupling $\langle |m|=2 \mid L_z \mid |m|=2 \rangle$ at the Γ point.

Keywords: magnetocrystalline anisotropy, superlattices, thickness dependence

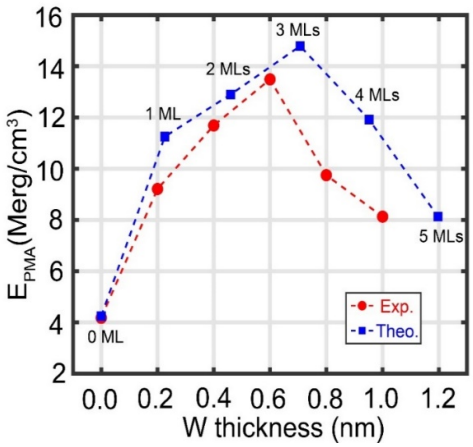

Fig. 1. PMA energy as a function of W thickness. The red circled-dashed line and blue squared-line indicate the experimental and theoretical results, respectively. The number of layers corresponds to the W thickness used in calculations.

References

[1] Z. A. Bekele *et al.*, Solid State Commun. **274**, 41 (2018).
[2] S. Mendisch *et al.*, J. Magn. Magn. Mater. **485, 345 (2019).**
[3] P Bruno, Phys. Rev. B **39**, 865 (1989).

Non-vanishing Anomalous Hall Effect in nearly Compensated Ferrimagnet Mn_3Al

Guihyun Han[1*], Su Yeon An[1], Minkyu Park[2], Soon Cheol Hong[1,3] and S.H. Rhim[1,3]
[1]Department of Physics, University of Ulsan, Republic of Korea
[2]Research Institute of Basic Sciences, University of Ulsan, Ulsan, Republic of Korea
[3]Energy Harvest-Storage Research Center, University of Ulsan, Republic of Korea
(schong@ulsan.ac.kr, sonny@ulsan.ac.kr,)

Anomalous Hall effect (AHE) is believed to accompany non-vanishing magnetization. Recent studies have revealed that AHE emerges in non-collinear antiferromagnets [1,2] and compensated ferrimagnets [3] despite vanishing magnetization. In this work, AHE is studied for Mn_3Al by density functional theory. Total magnetization of Mn_3Al is nearly compensated, where magnetic moments of two inequivalent Mn sites are compensated but Al has small moment. Electronic structure with volume change is investigated for their non-vanishing AHE.

References

[1] Hua Chen, Qian Niu and A. H. MacDonald, Phys. Rev. Lett. **112**, 017205 (2014).
[2] Yang Zhang, Yan Sun, Hao Yang, Jakub Zelezný, Stuart P. P. Parkin, Claudia Felser, and Binghai Yan, Phys. Rev. B **95**, 075128 (2017).
[3] Wujun Shi, Lukas Muechler, Kaustuv Manna, Yang Zhang, Klaus Koepernik, Roberto Car, Jeroen van den Brink, Claudia Felser, and Yan Sun, Phys. Rev. B **97**, 060406(R) (2018).

Structural stability and magnetic anisotropy properties in a Heusler compound Fe_2MnSn

Hoang Thu Thuy*, Qurat-ul-ain, S. H. Rhim and S. C. Hong
Department of Physics and Energy Harvest-Storage Research Center University of Ulsan, Republic of Korea
(sonny@ulsan.ac.kr, schong@ulsan.ac.kr)

Due to limited resource and high cost of rare-earth elements, finding rare-earth-free permanent magnets is important. Among several compounds, tetragonal Fe_2-based Heusler compounds are suggested to be promising candidates[1]. However, experimental efforts have not yet succeeded in synthesizing them[2]. In this work, using *ab-initio* calculation, we find that inverse tetragonal Fe_2MnSn can be stabilized with high perpendicular magnetic anisotropy energy (MAE) (2.23 MJm^{-3}) and large magnetic moment (m_t = 7.40 m_B per formula unit) even without including 4*d or* 5*d heavy elements*. Based on calculated total energies and elastic constants (see Fig. 1), we propose growth of the inverse tetragonal Heusler Fe_2MnSn compound to experimentalists. In this presentation, the role of symmetry will be discussed in achieving high perpendicular MAE of the tetragonal Fe_2MnSn and further possible Heusler compounds also will be addressed.

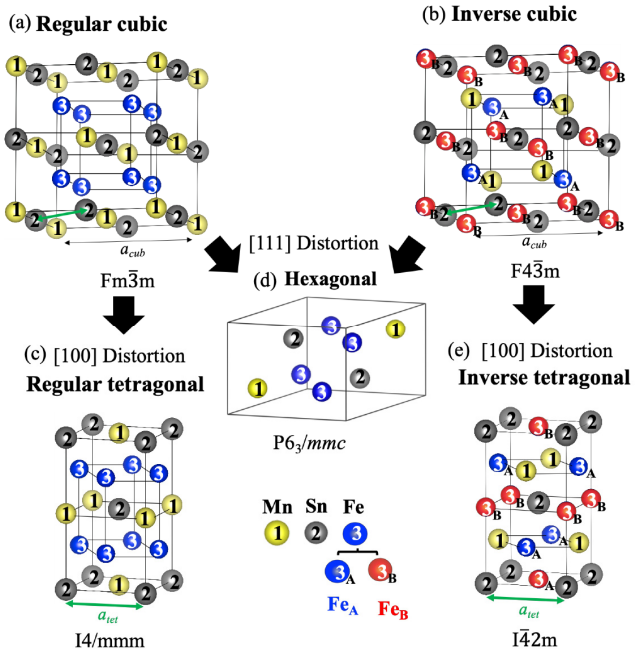

Fig. 1. Different structures of Heusler compounds;
(a) regular cubic, (b) inverse cubic, (c) regular tetragonal, (d) hexagonal, and (e) inverse tetragonal.

References

[1] J. Kiss, S. Chadov, G. H. Fecher, and C. Felser, Phys. Rev. B **87**, 224403 (2013).
[2] T. Gasi et al., Phys. Rev. B **87**, 064411 (2013).

Magnetic anisotropy and uncompensated antiferromagnetic ordering in magnetic van der Waals materials

Muhammad Nauman[1], Sungmin Lee[2], Suhan Son[2], Je-Geun Park[2], Woun Kang[3] and Younjung Jo[1*]

[1]Department of Physics, Kyungpook National University, Daegu 41566, Korea
[2]Center for Correlated Electron Systems, Institute for Basic Science (IBS), Seoul 08826, Korea
[3]Department of Physics, Ewha Womans University, Seoul 03760, Korea

$FePS_3$ is a two-dimensional antiferromagnet with a marked Ising anisotropy that persists down to the monolayer limit. The anisotropy arises from the combined effect of the trigonal distortion from octahedral symmetry and spin-orbit coupling. To determine how the trigonal distortion affects the magnetic anisotropy of $FePS_3$ crystals, we used a torque magnetometer. The temperature-dependent susceptibility and torque showed antiferromagnetic (AFM) ordering below 118 K. By rotating a magnetic field that exerted a torque on the magnetic moments aligned with the field, we precisely determined the out-of-plane and in-plane magnetic anisotropies in both paramagnetic and AFM states. The out-of-plane rotation of the magnetic field shows a slight difference in the magnetization between positive and negative angles relative to the trigonal c*-axis. The field-dependent torque for different crystal orientations provides details of the easy magnetization axis and confirmed the origin of magnetic anisotropy and asymmetry of the torque along the c*-axis. The almost perfect sinusoidal pattern of the angle-dependent torque for the in-plane rotation of the magnetic field signifies extremely small anisotropic behavior in the ab plane. The larger amplitude of the sin2θ fit for the bc rotation compared to that for the ac rotation and the DFT calculations suggest that the b-axis is the easy axis in the ab plane.

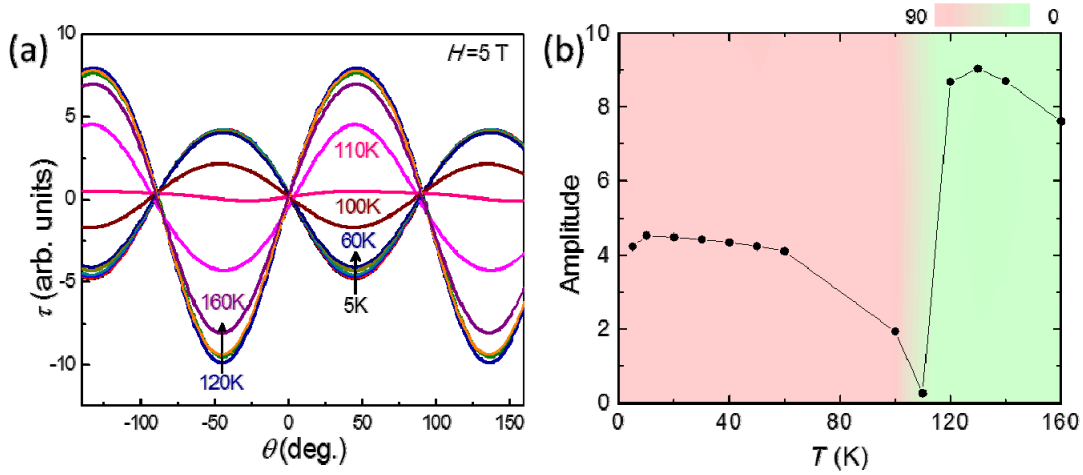

Fig. 1. (a) Angle-dependent torque at different temperatures at 5 T and (b) a plot of amplitude vs. temperature obtained by sine fitting of τ(Θ). In (b), the color indicates the phase.

Tracking the stability and intrinsic magnetic properties of $ThMn_{12}$-ordered $SmFe_{12}$ with metal and metalloid impurities

D. Odkhuu[1*], T. Ochirkhuyag[1] and S. C. Hong[2]
[1]Department of Physics, Incheon National University, Incheon 22012, South Korea
[2]Department of Physics, University of Ulsan, Ulsan 44610, South Korea

Herein we conduct systematic full-potential density functional calculations to reveal possible improvements of the structural stability and magnetic properties of $SmFe_{12}$ with $ThMn_{12}$ structure by replacing Fe with the 3*d* metallic and metalloid elements, Ti−Ge, Al and Si. Among the 13 dopant elements, only two substitutional atoms, Co and Si, are identified to enhance a uniaxial magnetic anisotropy in $SmFe_{12}$ up to 6% and 24%, respectively. Unlike metallic Co, metalloid Si stabilizes otherwise unstable $ThMn_{12}$ structure. In addition to the experimentally known Ti and V, we argue that Ga and Ge dopants can also be applicable to stabilizing the $ThMn_{12}$ phase while preserving the magnetic anisotropy in uniaxial direction.

First-Principles prediction of enhanced magnetic anisotropy of α''-phase $Fe_{16}N_2$ with B and C impurities

Tumentsereg Ochirkhuyag[1*], Chang Geun Park[1], Dorjsuren Tuvshin[1],
Soon Cheol Hong[2*] and Dorj Odkhuu[1†]

[1]Department of Physics, Incheon National University, Incheon 22012, South Korea
[2]Department of Physics and EHSRC, University of Ulsan, Ulsan, South Korea
E-mail: ochirkhuyag.t@inu.ac.kr , *schong@ulsan.ac.kr , †odkhuu@inu.ac.kr

Intrinsic magnetic properties and uniaxial magnetic anisotropy (K_u) of α''-phase ordered $Fe_{16}N_{2-x}B_x$ and $Fe_{16}N_{2-x}C_x$ alloys have been investigated through first-principles calculations. Being in agreement with experimental results, the lattice parameters, magnetic moments, and K_u of α''-$Fe_{16}N_2$ have been determined. Small addition of B or C dopant atoms enhances tetragonal distortion and K_u up to 0.75 MJ·m^{-3} for both $Fe_{16}N_{1.75}B_{0.25}$ and $Fe_{16}N_{1.75}B_{0.25}$ compounds which is more than 20% larger compared with that (0.6 MJ·m^{-3}) of α''-$Fe_{16}N_2$. Furthermore, the presences of B and C reduce magnetic moments of its neighboring Fe atoms at the 4e and 8h sites, resulting in reduced magnetization, due to less electron transfer from Fe to B and C than N. The underlying mechanism is discussed in connection with the Jahn-Teller lattice distortion, atom-decomposed magnetocrystalline anisotropy, and orbital magnetism.

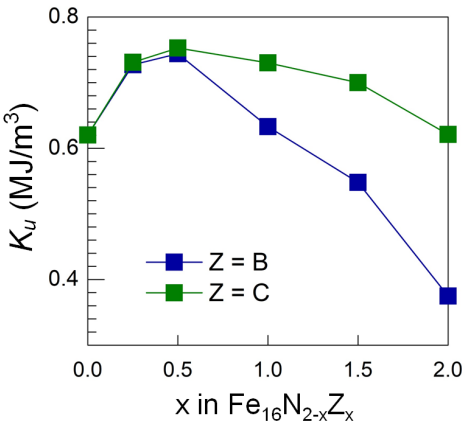

Fig. 1. Uniaxial magnetic anisotropy of $Fe_{16}N_{2-x}Z_x$ as function of Z concentration x for Z = B (blue) and C (green symbols)

Keywords: Rare-earth free permanent magnets, First-principle calculations, Uniaxial magnetic anisotropy

This work is supported by Future Materials Discovery Program through the National Research Foundation of Korea (NRF) funded by the Ministry of Science and ICT (2016M3D1A1027835) and by the Korea Institute of Energy Technology Evaluation and Planning (KETEP) grant funded by the Korean government (MOTIE) (20192010106850, development of magnetic materials for IE4 class motor).

Enhanced Magnetic Anisotropy Predicted in α″-$L1_0$ Transition of $(Fe_{1-x}Ni_x)_{16}N_2$

Tuvshin Dorjsuren[1*], Ochirkhuyag Tumentsereg[1], Chang Geun Park[1],
Soon Cheol Hong[2*] and Dorj Odkhuu[1†]

[1]Department of Physics, Incheon National University, Incheon 22012, South Korea
[2]Department of Physics and EHSRC, University of Ulsan, Ulsan, South Korea
*schong@ulsan.ac.kr, †odkhuu@inu.ac.kr

Due to remarkable success in many uses today including motors in an electric vehicle, there have been intensive research interests recently centered at permanent magnetic materials and various methods to improve their uniaxial magnetic anisotropy (K_u) and saturation magnetization ($\mu_0 M_s$) as well as thermal stability. Rare earth (RE)-free α″-phase $Fe_{16}N_2$ and $L1_0$ ordered FeNi alloys boast with large $\mu_0 M_s$ and also notable K_u owing to their tetragonal structures. Herein, through first-principles electronic structure calculations, we demonstrate that these two phases undergo a transition one to another by controlling amounts of Ni and N elements. More remarkably, we find a significant enhancement in K_u of 1.82 MJ·m^{-3} for $(Fe_{0.5}Ni_{0.5})_{16}N_2$ which is about 3 times larger than α″-phase $Fe_{16}N_2$. The resulting $L1_0$-type structure of $(Fe_{0.5}Ni_{0.5})_{16}N_2$ is further identified to be energetically more favored than α″ -$Fe_{16}N_2$ phase. Furthermore, we reveal that K_u can even reach up to 4 MJ·m^{-3} in $(Fe_{0.5}Ni_{0.5})_{16}N_2$ by adding an interstitial N atom. These results demonstrate the feasibility of possible enhancements on the magnetic anisotropy and energy product of 3*d*-only metals for RE-free permanent magnet applications.

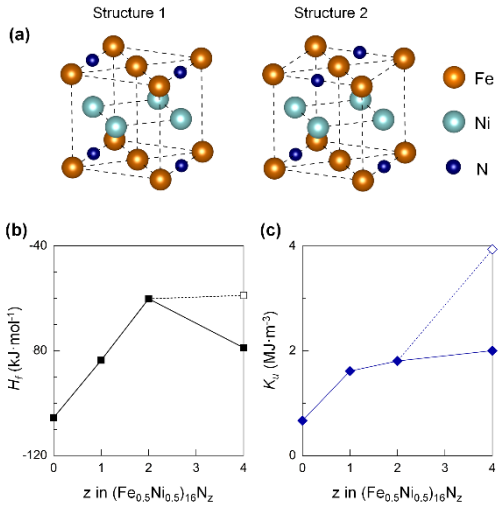

Fig. 1. (a) Possible distribution patterns of the interstitial N atoms, (b) formation enthalpy and (c) uniaxial magnetic anisotropy of structures.

This work is supported by Future Materials Discovery Program through the National Research Foundation of Korea (NRF) funded by the Ministry of Science and ICT (2016M3D1A1027835) and by the Korea Institute of Energy Technology Evaluation and Planning (KETEP) grant funded by the Korean government (MOTIE) (20192010106850, development of magnetic materials for IE4 class motor).

Externally Controllable Damping in Helical-spring Magnet studied by micromagnetic simulations and analytical calculation

Jejun Lee, Jiyeol Yoon*, Jaehak Yang and Sang-Koog Kim†
National Creative Research Initiative Center for Spin Dynamics and Spin-Wave Devices, Nanospinics Laboratory, Research Institute of Advanced Materials, Department of Materials Science and Engineering, Seoul National University, Seoul 151-744, South Korea
†Correspondence and requests for materials should be addressed to S.-K. K. (sangkoog@snu.ac.kr)

Typical mechanical oscillators such as springs made of elastic materials exhibit characteristic oscillation behaviors governed by balance between restoring and damping forces of a given system. The dynamic characteristics of the oscillators are thus determined by material parameters of mass, spring constant, and damping constant. Here we propose a new concept of mechanical oscillators composed of a magnetic material. In this system, magnetic force is another key parameter to determine characteristic oscillation behaviors of mechanical oscillators. In a model system of helical spring magnets (HSMs), we conducted finite-element micromagnetic simulations using FEMME code to examine magnetic interactions of HSMs of different spring dimensions under static magnetic fields applied along the spring axis. We calculated magnetic forces employed in HSMs of Permalloy for various spring-geometry parameters including pitch length, coil and wire diameter, under different strengths of applied magnetic fields. In addition to the numerical simulations, we also derived analytical equations in terms of the spring geometry parameters and the field strength. The analytical derivations reproduce well the simulation results. From both the simulation and analytical calculations, we found that HSMs itself provide magnetically controllable damping to typical mechanical characteristics of mechanical springs. According to the dimensions of a spring magnet and its spring constant, the strength of its mechanical force is variable so that it can be applicable to an active damping of actuators in a wide range of scales from nanometer to centimeter.

References

[1] L. D. Landau and E. M. Lifshitz, On the theory of the dispersion of magnetic permeability in ferromagnetic bodies. Phys. Z Sowjetunion **8**, 153 (1992)
[2] D. Suess, and T. Schrefl, FEMME: Finite Elemant MicroMagnEtics 5.0.9
[3] J. T. Conway, Forces between thin coils with parallel axes using Bessel functions, IEEE Trans. Magn., **49**, 5028–5034 (2013)

On Chip Manipulation of Particles/ Cells on Varied Thickness of the Magnetic Layers for Bio Applications

Keonmok Kim*, Byeonghwa Lim, Jonghwan Yoon, Hyeonseol Kim, Cheol Gi Kim†
Department of Emerging Materials Science, DGIST, Daegu, 711-873, Republic of Korea

In recent years, controlling and transporting micron and sub-micron particles/cells have gained significant interest for myriad biological applications. In comparison with competing strategies based on optical and electrical fields, magnetic fields offer the most scalable and stable method for single cell analysis and separation. The inherent advantage of magnetic manipulation is that it avoids several undesirable side effects associated with optical or electrical field-based manipulation techniques, which are of particular concern for biological materials and living cells.

In this study, we fabricated permalloy micro-magnetic patterns in the form of magnetophoretic circuit, which has the ability to introduce and retrieve single cells from precise locations of the chip to perform with the level of integrated computer circuits and we have observed the particle/cell behavior by varying the distance between the particle and the magnetic pattern, thickness of the micro-magnetic pattern and size of the micro-magnetic particle. In addition, we predict the magnetic potential energy of a particle theoretically and experimentally.

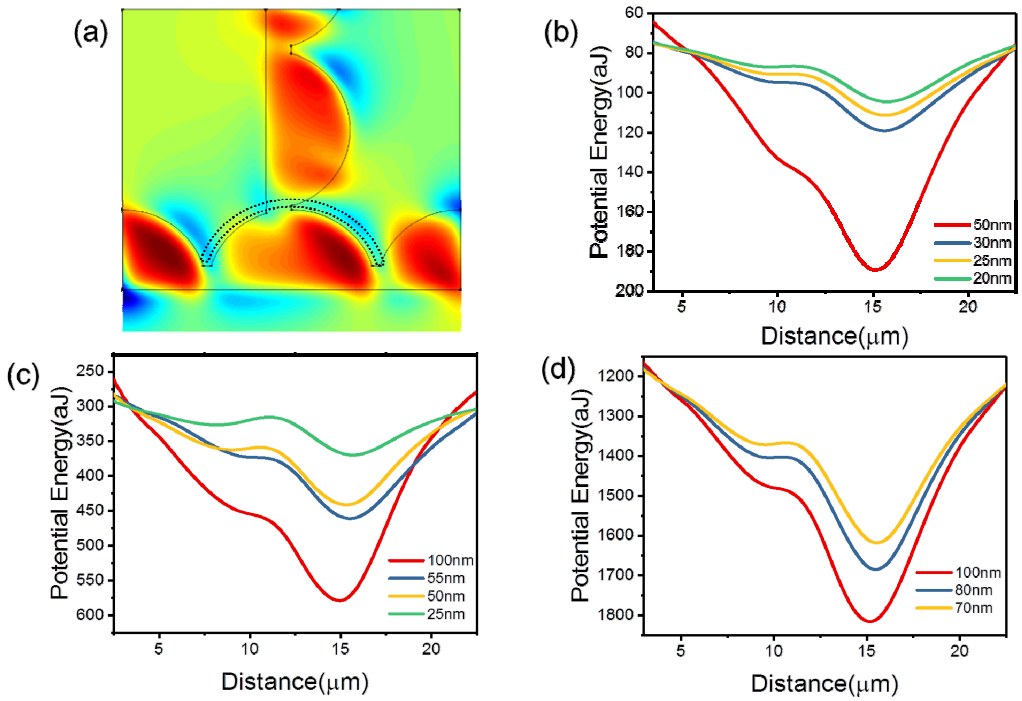

Fig. 1. (a) Energy calculation area Graph 1. (b) Energy distribution of 50 Oe, (c) Energy distribution of 100 Oe, (d) Energy distribution of 200 Oe

Spin-torque majority gate: Interlayer exchange coupling based reconfigurable logic gate

Woo-Yeong Kim[1,2*], Eunchong Baek[2] and Chun-Yeol You[2†]
[1]Department of Materials Science and Engineering, Korea University, Seoul, Republic of Korea
[2]Department of Emerging Materials Science, DGIST, Daegu, Republic of Korea
E-mail: cyyou@dgist.ac.kr

NAND and NOR gates are widely known to be universal logic gates because all logic operations can be implemented with combining these logic gates. Synthesizing of majority gates and inverters is essential for performing any Boolean operation [1]. Spin-Torque Majority Gate (STMG) [2-3] is of considerable interest because of its potential for the application beyond CMOS nonvolatile logic circuits.

We propose a Current-induced domain wall motion (CIDWM) based STMG using interlayer exchange coupling (IEC). The STMG consists of a cross-shaped bottom ferromagnetic (FM) layer and a stripe-shaped top FM layer with perpendicular magnetic anisotropy. Each 'UP' and 'DOWN' domain state represents the logical state '1' and '0'. We use a synthetic antiferromagnet (SyAF) structure by applying a non-magnetic layer such as Ru for IEC working as not only a pinning site but also an inverter. A current is injected in the plane of the free layer in order to move the DW and overcome the IEC. 2D micromagnetic simulation is performed by utilizing Mumax3 [4].

Figure 1 shows an example from the micromagnetic simulation results. When the DWs from the input nodes reach the pinning site, only major signal can overcome the IEC strength, therefore the reversed DW can be propagated to the output node.

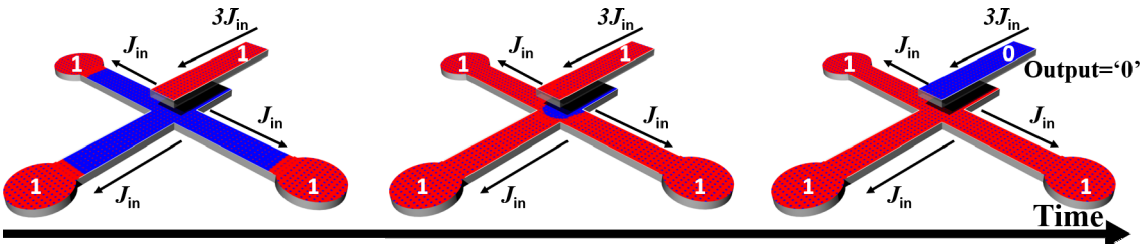

Fig. 1. Micromagnetic simulation of a STMG with a synthetic antiferromagnet structure

References

[1] L. Amaru, P.-E. Gaillardon, and G. De Micheli, IEEE Trans. Comput.-Aided Design Integr. Circuits Syst., **35**, 806-819 (2016).

[2] D. E. Nikonov, G. I. Bourianoff, and T. Ghani, IEEE Elec. Dev. Lett., **32**(8), 1128-1130 (2011).

[3] A. Vaysset, O. Zografos, M. Manfrini, D. Mocuta, and I. P. Radu, API Advances **8**, 055920 (2018).

[4] A. Vansteenkiste, J. Leliaert, M. Dvornik, M. Helsen, F. Garcia-Sanchez, and B. V. Waeyenberge, AIP Advances **4**, 107133 (2014).

Dependence of photon-magnon coupling strength on material parameters of YIG films

Haechan Jeon*, Biswanath Bhoi, Bosung Kim and Sang-Koog Kim†
National Creative Research Initiative Center for Spin Dynamics and Spin-Wave Devices, Nanospinics Laboratory,
Research Institute of Advanced Materials, Department of Materials Science and Engineering,
Seoul National University, Seoul 151-744, South Korea
†Correspondence and requests for materials should be addressed to S.-K. K. (sangkoog@snu.ac.kr)

Photon-magnon (P-M) coupling has been studied as a key for the development of spintronics based quantum information communication technology [1-4]. One of the most important issues in P-M coupling is an accomplishment of strong coupling strength that provides wide bandwidths and high information exchange rates. Therefore, understanding of the strength of P-M interaction is prerequisite for its applications [5,6]. For this reason, ferromagnetic materials with high saturation magnetizations have been used in P-M coupling studies, for example, Yttrium Iron Garnet (YIG) thin film is the promising material owing to its low damping constant ($< 10^{-4}$) and large spin density [7]. However, the effect of other material parameters on the P-M coupling has not been studied so far. In this work, we studied the dependence of the strength of photon-magnon coupling on the material parameters of YIG films in a planar-geometry hybrid structure that consists of stub line resonator (SLR) and an YIG film.

We fabricated the SLR by etching out the metallic portion of the copper/dielectric/copper substrate with the relative dielectric constant ε_r of 10, employing a conventional photolithography technique. Various YIG films with different material parameters (e.g., thickness, anisotropy properties, and damping constant) were prepared by changing fabrication conditions during PLD process. The YIG film was placed on center of the stub line of the resonator terminated with Subminiature version A connectors. The SLR/YIG hybrid sample was connected to calibrated two-port vector network analyzer via coaxial cables with 50 Ω characteristic impedance, then, its transmittance coefficient of S_{21} parameter was measured for characterizing photon-magnon coupling behavior with changing both the external DC magnetic field and the frequency of input AC microwave.

The anti-crossing effect induced by the interaction between the photon mode of the SLR and magnon modes of the YIG film was observed which is similar to that of our previous report [6,8-9]. Interestingly, we found that the strength of the P-M coupling can vary with material parameters of YIG films, such as damping constant, magnetic anisotropy, and saturation magnetization. It means that the coupling strength of P-M coupling can be strongly correlated to total magnetic moment and volume magnetization as well as Gilbert damping constant of the magnets in photon-magnon hybrid systems. This work demonstrates the possibility of modulating P-M coupling strength by magnetic material parameters, which paves the way to design quantum information devices based on light-matter interaction.

References

[1] A. Imamoglu, Phys. Rev. Lett., 102, 083602 (2009).
[2] L. Bai, M. Harder, Y. P. Chen, X. Fan, J. Q. Xiao, and C.-M. Hu, Phys. Rev. Lett., 114, 227201 (2015).

[3] R. Hisatomi, A. Osada, Y. Tabuchi, T. Ishikawa, A. Noguchi, R. Yamazaki, K. Usami, and Y. Nakamura, Phys. Rev. B, 93, 174427 (2016).
[4] L. Kang, Q. Zhao, H. Zhao, and J. Zhou, Opt. Express., 16, 8825 69 (2008).
[5] B. Bhoi, S-K. Kim, Solid State Physics, Volume 70, 2019, Pages 1-77
[6] B. Bhoi, B. Kim, J. Kim, Y-J Cho & S-K Kim, Scientific Reports **volume 7**, Article number: 11930 (2017)
[7] B. Bhoi, B. Kim, Y. Kim, M-K. Kim, J-H. Lee, and S-K. Kim, Journal of Applied Physics **123**, 203902 (2018)
[8] B. Bhoi, B. Kim, S. Jang, J. Kim, J. Yang, Y-J. Cho, and S-K. Kim, Phys. Rev. B 99, 134426
[9] B. Kim, B. Bhoi, and S-K Kim, Journal of Applied Physics **126**, 163902 (2019)

Ultrafast Sagnac Interferometry: tracking Angstrom dynamics of lattice

Yooleemi Shin[1,2] and Ji-Wan Kim[1*]
[1]Department of Physics, Kunsan National University, Kunsan 54150, South Korea
[2]Department of Physics, Chungbuk National University, Cheongju-si 28644, South Korea
E-mail: hwoarang@kunsan.ac.kr

In order to analyze ultrafast spin dynamics, the transient Kerr rotation and reflectivity are generally measured for complementary information. These signals are sensitive to the temperature of the material because the Kerr and the reflectivity dynamics are launched by the change of the effective magnetic field and the refractive index induced by ultrafast heating, respectively. Nevertheless, the dynamics of the lattice thermal expansion, which is induced by heating, has not been considered so far although it is going to be believed to play an important role in driving magnetism and non-magnetism dynamics as well. Since with a standard time-resolved pump-probe technique, it is not possible to extract the information of lattice dynamics, UXRD(ultrafast XRD) and UED (ultrafast electron diffraction) instruments are recently developed and used. They can directly measure the lattice dynamics inside the material with extreme resolutions such as 100 fs in temporal and Angstrom in spatial. However, their facilities are big and the crystallinity of the materials should be single or epitaxial. There are many constraints to use it in a lab size.

Therefore, we set up the ultrafast Sagnac-type interferometry which can track Angstrom vertical motion of the lattice in ultrafast time scale operating on a table top. Twenty years ago, Prof. Oliver Wright group first developed the ultrafast Sagnac interferometry[1], this one has been used only for non-magnetization(reflectivity) dynamics measurement. We modified their setup to measure up to magnetization dynamics at the same time. Here we showed Jones matrix calculation details to explain how properly it works.

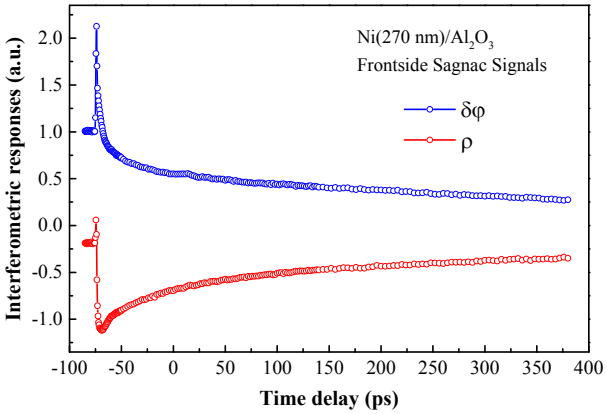

Fig. 1. Measurement of both the lattice expansion(δΦ) and the refractive index(ρ) dynamics using ultrafast Sagnac interferometry

Reference

[1] D. H. Hurley and O. B. Wright, Opt. Lett. **24**, 1305 (1999).

Dynamics of the Bloch point in soft ferromagnetic nanodisk

Hee-Sung Han[1*], Min-Seung Jung[2], Young-Sang Yu[3], Sooseok Lee[1], Seongsoo Yoon[2], Weilun Chao[4], Peter Fischer[5], Jung-Il Hong[2], Mi-Young Im[4], Ki-Suk Lee[1]

[1]School of Materials Science and Engineering,
Ulsan National Institute of Science and Technology (UNIST), Ulsan, Korea
[2]Department of Emerging Materials Science,
Daegu Gyeongbuk Institute of Science and Technology (DGIST), Daegu, Korea
[3]Advanced Light Source, Lawrence Berkeley National Laboratory, Berkeley, CA, USA
[4]Center for X-ray Optics, Lawrence Berkeley National Laboratory, Berkeley, CA, USA
[5]Materials Sciences Division, Lawrence Berkeley National Laboratory, Berkeley, CA, USA

The unique magnetization configurations, called magnetic soliton have been attracted due to their high stability and rich dynamic properties. Among lots of magnetic solitons, a Bloch point is the point where local magnetization vanishes in the ferromagnetic materials [1]. A Bloch point have a novel physical behavior that 2D magnetic solitons does not show. It shows the pinning at the atomic lattice, which is derived from the discrete nature of atomic lattice [2,3]. As well as, it plays a crucial role in the dynamic behavior of 2D magnetic solitons such as vortex core and skyrmion core switching [4]. However, the experimental studies on the physical behavior of the Bloch point are elusive due to the difficulty to stabilize the Bloch point.

Here, we will show the dynamics of the Bloch point embedded in magnetic vortex structures in the patterned permalloy (Ni80Fe20, Py) disk by utilizing the time-resolved magnetic full-field X-ray microscopy (MTXM) with 25 nm-spatial resolution [5,6]. To study the role of Bloch point in the magnetization dynamics, we observed the field pulse-driven magnetization dynamics with and without the Bloch point. The presence of Bloch point makes the vortex gyration be rapidly dissipated, which reveals the testimony to show the existence at the energy barrier at the atomic lattice. We believe that this work contributes to understanding the fundamental studies of the magnetic solitons.

References

[1] E. Feldtkeller. Z. Angew. Phys. **19**, 530-536 (1965).
[2] S.-K. Kim, and O. Tchernyshyov. Phys. Rev. B. **88**, 174402 (2013)
[3] H.-G. Piao. et al. Appl. Phys. Lett. **102**, 112405 (2013)
[4] A, Thiaville. and J, Miltat. Europhys. Lett. **26**, 57 (1994).
[5] M.-Y Im, H.-S. Han, et al. Nature Commun. **10**, 593 (2019)
[6] Fischer, P. et al. Mater. Today **9**, 26-33 (2006).

Probing anisotropic thermal transport in graphite using time-resolved magneto-optical Kerr effect

Ly Pham Ngoc Luu[1*], Gyung-Min Choi[1,2]
[1]Department of Energy Science, Sungkyunkwan University, Suwon 16419, Korea
[2]IBS Center for Integrated Nanostructure Physics, Institute for Basic Science (IBS), Sungkyunkwan University, Suwon 16419, Korea

Highly Ordered Pyrolytic Graphite (HOPG) shows a strong anisotropy of electrical and thermal transport. The in-plane and cross-plane thermal conductivity for HOPG are reported in the range of 1600 – 2000 W/mK and 5-8 W/mK, respectively. In this work, we introduce a thermoreflectance technique to measure thermal conductivity of HOPG. A ferromagnetic metal (FM)/ HOPG structure is prepared, where FM acts as a transducer to detect the thermal transport in HOPG. We measure a time-resolved dynamic of magnetization of FM, which reflects the thermal transport in HOPG. Performing experiment with different modulation frequencies, we determine both in-plane and through-plane thermal conductivity of HOPG.

버퍼층에 따른 코발트 박막의 자성 특성 효과

이광현[1,2*], 이찬강[1,3], 김준우[1], 유천열[3], 조재훈[1], 변명환[2], 김준서[1]
[1]나노융합연구부, DGIST, 대구 42988, 대한민국
[2]재료공학과, 계명대학교, 대구 42601, 대한민국
[3]신물질과학전공, DGIST, 대구 42988, 대한민국

교환 뻣뻣함 상수는 기본적인 자성 물리량 중 하나이며 최인접 자성 원자들의 개수 및 물질의 큐리온도와 연관이 있다[1~3]. 이것은 스핀트로닉스에서 각광받고 있는 자성 스컬미온의 안정적인 형성과 움직임에 결정적인 역할을 한다. 중금속층이 포함된 이종접합 구조에서 중금속층은 자성층과 만나는 계면에서 강한 스핀-궤도 상호작용에 의하여 수직자기이방성 또는 표면 Dzyaloshinskii-Moriya 상호작용과 같은 현상을 일으키는 재료일 뿐만이 아니라, 버퍼층이 사용되는 경우 그 크기가 크게 증가하거나 감소하는 경향을 보인다[4,5]. 한편으로 자성층이 매우 얇을 때의, 교환 뻣뻣함 상수에 대한 체계적인 연구가 진행되지 않아서 얇은 자성 박막에서의 교환 뻣뻣함 상수는 항상 덩어리 시료에서의 교환 뻣뻣함 상수 값을 이용하여 왔다.

본 연구에서는 다양한 버퍼층 (Pt, Pd, Ta)과 코발트 자성 박막의 이종접합 구조에서의 자성 동역학 특성을 브릴루앙 (Billouin) 광 산란 실험을 이용하여 연구하였다. 버퍼층으로 이용된 세 가지 물질 (Pt, Pd, Ta)은 강한 스핀-궤도 상호작용을 가진다고 알려져 있다. 본 연구에서는 DC마그네트론 스퍼터로 제작된, 버퍼층 (Pt, Pd, Ta 5 nm)/Co (25, 30 nm)/Ta (4 nm) 구조의 시료를 이용하였다. 시료는 100 nm 두께의 SiO_x가 증착된 Si 기판 위에 증착되었다. 또한 버퍼층이 없는 시료도 제작하여 버퍼층이 있는 시료들과 함께 비교하였다. 자성동역학 실험의 결과 Pd 버퍼 시료에서 Co박막의 포화자화값이 가장 크게 관측되었고, Ta 버퍼 시료에서는 상대적으로 작은 포화자화값을 관찰하였다. 또한 브릴루앙 광 산란 실험을 통한 결과로 Pd 및 Pt를 버퍼층으로 사용한 시료가 가지는 Co의 교환 뻣뻣함 상수의 값은 Co 덩어리의 교환 뻣뻣함 상수 문헌 값 [6]인 28.5 pJ/m (그림 1.의 회색 선)와 비교하여 조금 낮은 값을 가지고 Ta를 버퍼층으로 사용한 시료가 가지는 Co의 교환 뻣뻣함 상수는 Pd 및 Pt를 버퍼층으로 사용한 시료 보다 12% 감소한 것을 보여주는 반면, 버퍼층이 없는 시료의 경우 브릴루앙 광 산란 실험에서 신호 대 잡음 대비가 불량하여 교환 뻣뻣함 상수 값이 나타나지 않는 것을 그림 1에서 보여주고 있다.

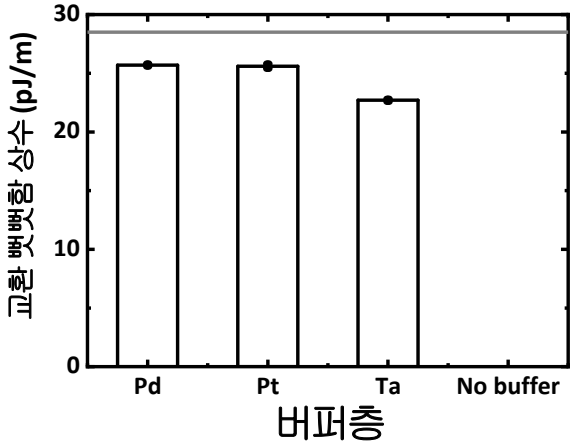

그림 1. 브릴루앙 광산란 장치를 이용하여 측정한다양한 버퍼층 (Pd, Pt, Ta, No buffer)을 가진 Co 박막에서의 교환 뻣뻣함 상수 값

References

[1] S. Chikazumi, Physics of Ferromagnetism, 2nd edition, Oxford, 1997, pp. 129-130.

[2] S.N. Kaul, Phys. Rev. **B 24** (1981) 6550.

[3] A.K. Majumdar, V. Oestreich, D. Weschenfelder, F.E. Luboesky, Phys. Rev. **B 27** (1983) 5618

[4] N.-H. Kim, J. Jung, J. Cho, D.-S. Han, Y. Yin, J.-S. Kim, H.J.M. Swagten, C.-Y. You, Appl. Phys. Lett. **108** (2016) 142406.

[5] N.-H. Kim, D.-S. Han, J. Jung, J. Cho, J.-S. Kim, H.J.M. Swagten, C.-Y. You, Appl. Phys. Lett. **107** (2015) 142408.

[6] B. Hillebrands, G. Guentherodt, Ultrathin Magnetic Structures II, Springer, Berlin, 2005, p. 266

Charge transfer induced anomalous magnetic behavior and thermo-remnant memory effect in β-NiOOH/Graphene 2D system

Shatabda Bhattacharya* and Sang-Koog Kim†

National Creative Research Initiative Center for Spin Dynamics and Spin-Wave Devices, Nanospinics Laboratory, Research Institute of Advanced Materials, Department of Materials Science and Engineering, Seoul National University, Seoul 151-744, South Korea

†Correspondence and requests for materials should be addressed to S.-K. K. (sangkoog@snu.ac.kr).

The interface interaction plays an important role in low dimensional systems because of large surface area. In addition to, literature reports indicate that transition metal (TM) has strong interaction with Graphene surface due to charge transfer effect at the interface and show many intriguing results particularly in the area of magnetism and transport. Combining these two aspects, study of magnetism in low dimensional systems containing TM based oxide/hydroxides and Graphene arising due to strong interface interaction and layer number variation is indeed an interesting area of research. In this case we have synthesized thin β-NiOOH layers grown on Graphene surface. By tuning the thickness of the β-NiOOH layers transition from antiferromagnetic to ferromagnetic ordering along with enhancement of coercivity is achieved. A number of new results viz. giant coercivity, enhancement of exchange bias, increase in both magnetization and coercivity with temperature which appear solely due to interface interaction are observed. With addition to this, temperature based memory effect is also observed i.e. during the relaxation study thermoremnant memory effect is also found which enables for possible application of the system as memory devices at the nanoscale.

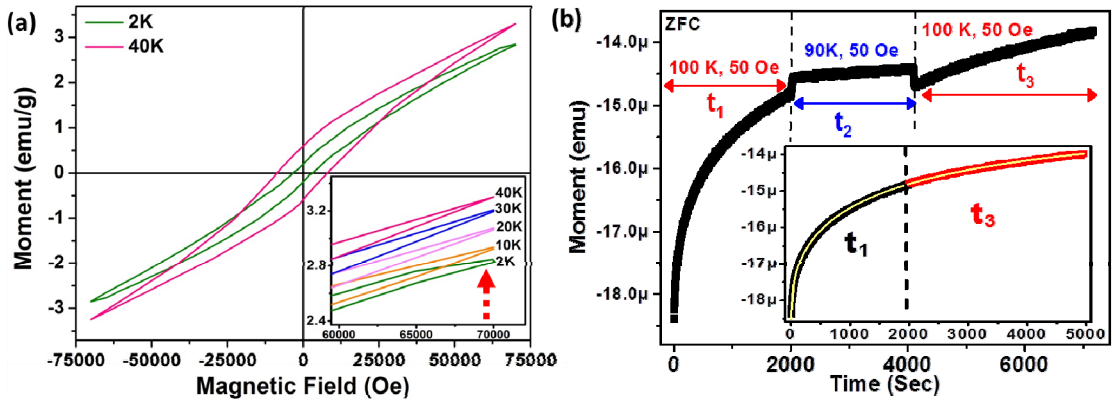

Fig. 1. (a) MH Hysteresis loop of the G-NiOOH at Low temperatures. Inset shows both magnetization and coercivity increases with temperature anomalously. (b) Thermoremnant dc relaxation curve shows the memory effect retained in the system.

Thermal Coupling in Nickel Studied with Time-resolved Pump-probe Techniques

Kyuhwe Kang[1*], Gyung-Min Choi[1,2†]

[1]Department of Energy Science, Sungkyunkwan University, Suwon 16419, Korea

[2]Center for Integrated Nanostructure Physics, Institute for Basic Science (IBS), Suwon 16419, Korea

Thermal relaxation in Ni is investigated in the ps time scale using time-resolved pump-probe techniques: the time domain thermoreflectance (TDTR) and the time-resolved magneto-optical Kerr effect (TR-MOKE). Also, two optical experimental configurations for thermal excitation of Ni are used. One is the direct optical excitation of the nano scale Ni layer and the other is the heat transport from the adjacent Au layer to the Ni layer. As a result, thermal coupling parameters are determined between three species of heat carriers in Ni. Besides that the thermal interaction between electron and magnon plays a significant role as expected, phonon and magnon are thermally coupled large enough so that the fast recovery of magnetization occurs. The determined coupling parameters have discrepancies less than 30% depending on the optical configurations.

Demagnetizing field effects on magnetization reversal in a narrow magnetoresistive element

Artem Talantsev[1*], Jaehoon Lee[1], SungJoon Kim[1], M. V. Bakhmetiev[2], A. I. Bezverkhnij[2], Cheol Gi Kim[1]

[1]Department of Emerging Materials Science, DGIST, Daegu, 42988, Republic of Korea

[2]Institute of Problems of Chemical Physics, Chernogolovka, Moscow, Russia

Demagnetizing field in a sensor's active element, affects the sensor's sensitivity. The strength of this effect depends on the sensor's operating field range and on the width of the sensor's active element. The operating field range is regulated by the exchange bias of the sensor's active layer [1]. For the sensors with ±10 Oe operating field range the 5 µm pattern width, the demagnetizing field effect results in 20-30 percent reduction of the amplitude of the PHR signal (Figure 1). The effect originates from magnetization misalignment, caused by the dependence of the demagnetizing field direction on the angle between the sensor's boundaries and the easy magnetization axis of the sensor's active element.

A local mapping of $M(H)$ loops along the sensor's pattern and comparison of the mapped $M(H)$ loops with the ones measured on a continuous thin film (Figure 2), allows determination of the angular incoherence of magnetization rotation in the active layer under applied external magnetic field. The value of demagnetizing field, determined by this technique, is in a good agreement with the data in references, calculated from micro-magnetic simulations [2].

The work was performed in accordance with the program of IPCP AAAA-A19-119092390079-8 and supported by Grant of President of Russian Federation for Scientific School 2644.2020.2.

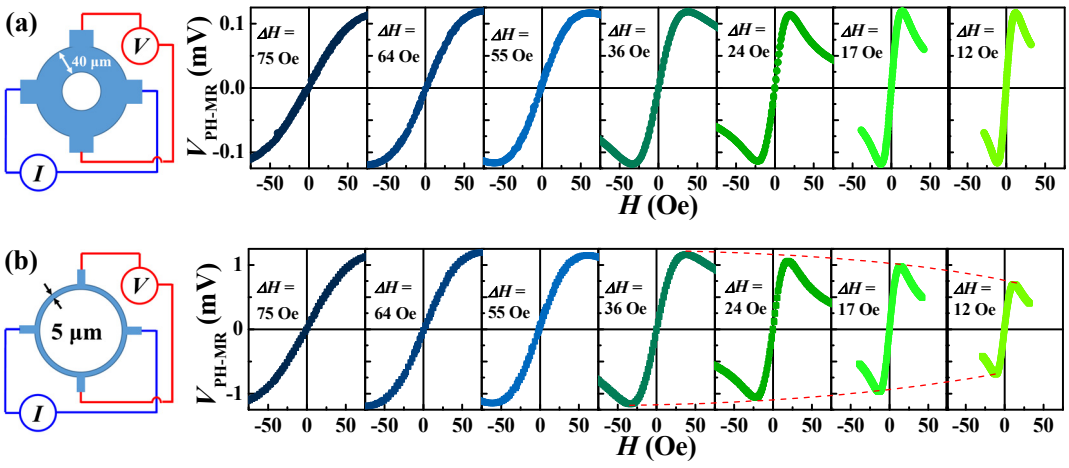

Fig. 1. PHR curves and output parameters for ring-shaped PHR sensors with 40 µm and 5 µm pattern widths. (a, b) PHR vs magnetic field profiles for two sets of ring-shaped PHR sensors with different pattern widths: (a) w = 40 µm and (b) w = 5 µm. In each set, the dynamic field range $\triangle H$ has been varied by the thickness of Cu spacer layer in NiFe/Cu/IrMn trilayer structure of sensor's active layer stack. The reduction of PHR signal amplitude at lower dynamic field ranges, observed in the sensors with w = 5 µm width, is indicated by dashed lines.

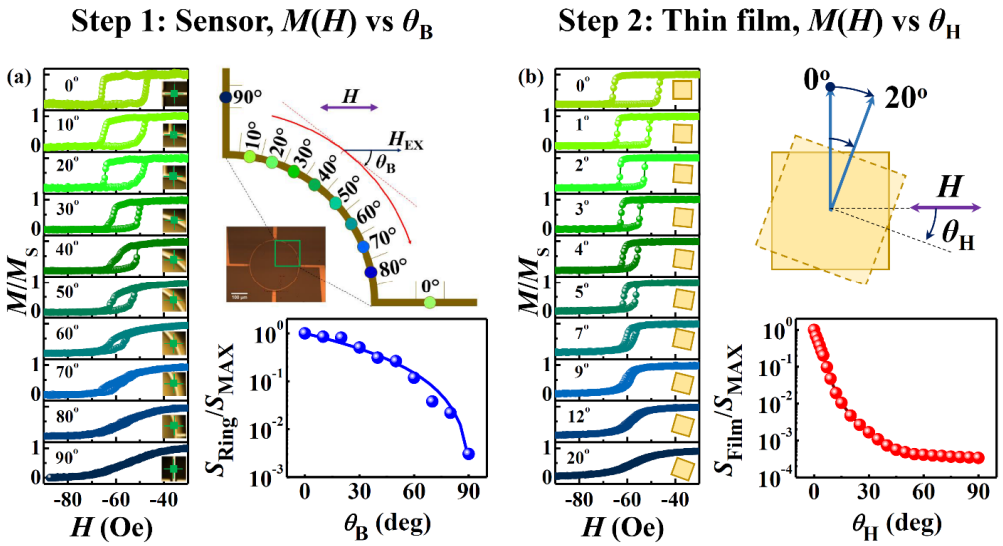

Fig. 2. Mapping of magnetization misalignment in PH-MR sensors of 5 μm pattern width. (a) mapping experiment: $M(H)$ loops vs the angle Θ_B between the easy axis and the sensor's boundary (measured on the sensor). Left panel: a set of $M(H)$ loops at the locations, indicated on micro-images in the insets. Right panel: top - schematics of measurements, bottom - the dependence of squareness $S_{Ring} = H_C \cdot M_R$ of the $M(H)$ loop on the angle Θ_B. (b) Reference experiment $M(H)$ loops vs the angle Θ_H between the easy axis and applied field (measured on a large area thin film). Left panel: a set of $M(H)$ loops at the selected angles Θ_H. Right panel: top - schematics of measurements, bottom - the dependence of squareness $S_{Film} = H_C \cdot M_R$ of the $M(H)$ loop on the angle Θ_H.

References

[1] S. J. Kim, et al. *Sensors* **20**, 434 (2020).

[2] M. Donolato et al. *J. Appl. Phys*. **109**, 064511 (2011).

Local magnetization reversal of CoFeB thin films under dipole field of ferromagnetic nanoparticles

R. B. Morgunov[1,2*], O. V. Koplak[1]

[1]Institute of Problems of Chemical Physics, 142432, Chernogolovka, Russia

[2]I.M. Sechenov First Moscow State Medical University, 119991 Moscow, Russia

Rapid development of giant magnetoresistance (GMR) sensors for registration, counting and selection of magnetically labeled living cells macromolecules became possible thanks to enhancement of sensors sensibility [1-2]. Magnetoresistive sensors are usually heterostructures, sensitive to the magnetic dipole fields of NP's [3-4]. The goal of our work is to study the magnetic responses of MgO/CoFeB/Ta/CoFeB/MgO/GaAs and MgO/ CoFeB/Ta/MgO thin film structures with perpendicular anisotropy after deposition of Fe/Fe_3O_4 nanoparticles on their surface. Atomic Force Microscope (AFM) and Magnetic Force Microscope (MFM) technique allow direct visualization of the film area, which magnetization is affected by the stray field of the single ferromagnetic Fe/Fe_3O_4 nanoparticles (Fig. 1a).

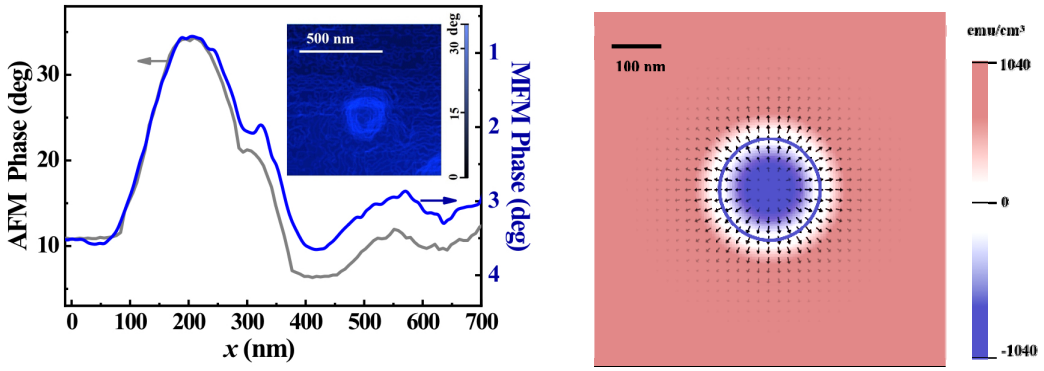

a b

Fig. 1. (a) Profiles of the MFM and MFM phase contrasts of Fe/Fe_3O_4 particle, deposited on CoFeB/Ta/CoFeB surface. Extraction of the AFM phase contrast from the MFM phase contrast is shown in the insertion. (b) Magnetic configuration in the bottom CoFeB layers of CoFeB/Ta/CoFeB platform under the magnetic field generated by 100 nm radius NP's cluster.

The size of Fe/Fe_3O_4 nanoparticles deposited on CoFeB ferromagnetic thin film given by the AFM and MFM phase contrasts was studied. Comparison between the two types of phase contrast allowed us to determine the magnetization area in the film reversed under the magnetic stray field of the ferromagnetic particle. Deposition of Fe/Fe_3O_4 particle on CoFeB film and CoFeB/Ta/CoFeB bilayer causes changed in the FMR measurements performed on the magnetic films due to the local effect of particles magnetic stray fields. Shift of the resonant fields of the Fe/Fe_3O_4 particles and magneto induced anisotropy of FMR spectrum of the nanoparticle clusters are observed. Theoretical estimation and OOMMF modeling of the diameter of the CoFeB film area, which magnetization is reversed under the dipolar magnetic field created by the Fe/Fe_3O_4 particle, are obtained (Fig.

1b). They are found to be in good agreements with the area observed experimentally. Proof of the interaction between the magnetization of the nanoparticles and the thin film can be observed at low temperatures ~ 2 K using SQUID magnetometer.

The work was performed in accordance with the program of IPCP AAAA-A19-119092390079-8 and supported by Grant of President of Russian Federation for Scientific School 2644.2020.2.

References

[1] O. Koplak, et al., Journal of Magnetism and Magnetic Materials, 433 (2017) 91-97.

[2] R. Morgunov, et al., Physical Review B 96 (2017), 05.

[3] O. Koplak, et al., Superlattices and Microstructures 121 (2018) 23-32.

[4] R.B.Morgunov, et al., Applied Surface Science 527 (2020) 146836.

Neuromorphic computing based on photon-magnon coupling

Loïc Millet*, Haechan Jeon, Bosung Kim, Biswanath Bhoi and Sang-Koog Kim†
National Creative Research Initiative Center for Spin Dynamics and Spin-Wave Devices,
Nanospinics Laboratory, Research Institute of Advanced Materials,
Department of Materials Science and Engineering, Seoul National University, Seoul 151-744, South Korea
†Correspondence and requests for materials should be addressed to S.-K. K. (sangkoog@snu.ac.kr)

Neuromorphic computing is a brain-inspired computing paradigm to outperform conventional computing on specific tasks. In particular, reservoir computing is a form of neuromorphic computing which uses a recurrent and randomly interconnected network of non-linear neurons, called a reservoir, to perform classification tasks. By using time-multiplexing on the input data, it becomes possible to emulate the full reservoir from a single neuron [1]. To improve further the power efficiency of neuromorphic computing, spintronics based neuromorphic computing devices are intensively studied [2]. A promising spintronics device, the spin-torque nano-oscillator, is able to perform waveform recognition by using reservoir computing [3]. Meanwhile, photon and magnon modes in a variety of hybrid systems can be strongly coupled in the anticrossing region [4]. In the anticrossing, the two magnon and photon modes can exchange energy at a rate given by the coupling strength and their frequencies are modified. Such hybrid systems open the path toward quantum technologies combining two different information-carriers with preserved coherence owing to the strong coupling. Photon-magnon coupling can be observed in a planar geometry consisting of a split-ring resonator (SRR) or its inverted pattern (ISRR) and a microstrip line to excite photons and an Yttrium Iron Garnet (YIG) film placed on the resonator to excite magnons [5]. As opposed to 3-dimensional cavities, this planar device geometry is compatible with 2-dimensional CMOS technologies.

In this work, we implement photon-magnon coupling towards the realization of several examples of neuromorphic computing tasks. As a first computational task, waveform recognition is investigated using 2D geometry hybrids. Performing waveform recognition with reservoir computing requires a device whose output is a non-linear function of an input, in which we encode the waveform. Because the photon mode frequency in photon-magnon coupling is a non-linear function of the magnon mode frequency, it is possible to use a single ISRR/YIG system as a neuron to perform waveform recognition. The input points are encoded in the magnon mode frequency whereas the output of the system is given by the ISRR resonant frequency. The feasibility of such a concept has been investigated by simulation. Using the equations describing the normal anticrossing in an ISRR/YIG coupled system [6], the success rate of a noiseless system reaches 100% over a wide range of encoding spin-waves frequencies. The system is robust against noise with more than 90% of success over a narrower encoding frequency region when considering noisy inputs. Further work will show experimental results of the waveform recognition as well as other neuromorphic computing tasks.

References

[1] Appeltant, L., Soriano, M., Van der Sande, G. et al. Nat Commun 2, 468 (2011).

[2] Grollier, J., Querlioz, D., Camsari, K.Y. et al. Nat Electron (2020).

[3] D. Markovic´, N. Leroux, M. Riou, F. Abreu Araujo, J. Torrejon, D. Querlioz, A. Fukushima, S. Yuasa, J. Trastoy, P. Bortolotti and J. Grollier, Appl. Phys. Lett. 114, 012409 (2019).

[4] H. Huebl, C. W. Zollitsch, J. Lotze, F. Hocke, M. Greifenstein, A. Marx, R. Gross, and S. T. B. Goennenwein, Phys. Rev. Lett. 111, 127003 (2013).

[5] Bhoi, B., Kim, B., Kim, J., Cho, Y.-J., Kim, S.-K., Sci Rep 7, 11930 (2017).

[6] B. Bhoi, B. Kim, S.-H. Jang, J. Kim, J. Yang, Y.-J. Cho, and S.-K. Kim, Phys. Rev. B 99, 134426 (2019).

Thermal intermixing effect on Gilbert damping of sputter-grown Pt/$Ni_{80}Fe_{20}$/Pt sandwich trilayers

Yongsub Kim[1*], Bosung Kim[1], Bhoi Biswanath[1], Young-Woon Kim[2] and Sang-Koog Kim[1†]

[1]National Creative Research Initiative Center for Spin Dynamics and Spin-Wave Devices, Nanospinics Laboratory, Research Institute of Advanced Materials, Department of Materials Science and Engineering, Seoul National University, Seoul 151-744, South Korea

[2]Department of Materials Science and Engineering, Seoul National University, Seoul, 08826, Republic of Korea

[†]Correspondence and requests for materials should be addressed to S.-K. K. (sangkoog@snu.ac.kr)

In this work, we investigated the annealing effect on Gilbert damping of Pt/Permalloy(Py: $Ni_{80}Fe_{20}$)/Pt sandwich trilayer films from ferromagnetic resonances (FMR) and vibrating sample magnetometer (VSM) measurements. We estimated the variation of the effective Gilbert damping constant α_{eff} according to post-annealing temperature T_a for 30 min in a range of T_a = 600 ~ 800 K. The damping constant for the as-grown sample was estimated to be α_{eff} = 0.021, but linearly increases with T_a until 700 K and then drastically increases up to α_{eff} = 0.093 at T_a = 800 K. The XRD and TEM measurements and delicate analysis revealed that the annealing temperature affects interface shifting, intermixing of Pt and Py at their interfaces and/or new phase formation.

The Gilbert damping constant is closely related to the structural characteristics of interfaces. It was found that α_{eff} in a temperature range of T_a = 600 – 700 K gradually increases with T_a due to alloying/intermixing between the Pt and the Py layers as well as the degradation of Pt(111) texture. In particular, for 800 K-post-annealed sample, the Gilbert damping constant increases up to 4 times larger than that of the as-grown sample, and the saturation magnetization decreases by 54%, suggesting that possible formation of new phases of stoichiometric compounds including non-magnetic $NiPt_3$ as well as NiPt, FePt, Fe_3Pt, Ni_3Pt, NiFePt at either interface of Py with Pt[1]. From energy dispersive X-ray spectroscopy (EDS) measurements, atomic diffusivity of Ni, Fe, and Pt were estimated, which is comparable to previously reported values[2.3]. These values indicate that intense intermixing and degradation of texture due to chemical disorder at interfaces occurred. This work allows for a better understanding of annealing effect on the Gilbert damping constant and offers a guideline to optimize complex multi-layered structures in potential spintronic devices.

References

[1] I.V. Vernyhora and S. M. Bokoch, ISRN Thermodynamics, 2012, 917836 (2012)

[2] V.D. Divya and A. Paul, J. Mater. Res., 26, 18, 2384-2393 (2011)

[3] T. Kaiser and W. Jäger, J. Appl. Phys., 103, 063913 (2008)

Negative Refraction in a Photon-Magnon Coupled Hybrid

Biswanath Bhoi*, Bosung Kim, Haechan Jeon and Sang-Koog Kim†
National Creative Research Initiative Center for Spin Dynamics and Spin-Wave Devices, Nanospinics Laboratory,
Research Institute of Advanced Materials, Department of Material Science and Engineering,
Seoul National University, Seoul 151-744, South Korea
†Correspondence and requests for materials should be addressed to S.-K. K. (sangkoog@snu.ac.kr)

Materials of positive refractive index are universal in nature, but its counterpart materials of negative refractive index (NRI) have been artificially synthesized owing to its fundamental interest as well as potential applications [1-3]. The NRI can be achieved by realizing both the negative permittivity (ε) and negative permeability (μ) [4]. Although the flexible controllability of NRI is challenging, a simplified planar structure of NRI with a broadband-frequency tunability as well as its on-off switching functionality remains challenging in terms of its practical accomplishment in high-frequency electromagnetic devices.

In this work, we report a novel phenomenon of negative refraction originated by photon-magnon coupling [5-7] in a specially designed hybrid system that consists of an Yttrium Iron Garnet (YIG) film and an inverted structure of split-ring resonator (ISRR). We fabricated an ISRR sample using common photolithography and chemical etching process. The dimensions of the ISRR and the YIG film are the same as those reported for previous experiments [4]. A commercially available epitaxial YIG film, grown on a Gadolinium Gallium Garnet (GGG) substrate was placed on the microstrip line of the ISRR sample. We measured scattering parameter S_{ij} (i, j = 1 or 2) of the ISRR/YIG hybrid sample using a calibrated two-port vector network analyzer. The input terminal was soldered to a subminiature version A connector, then, the S_{ij} parameters were measured by changing the external bias magnetic field from 40 to 100 mT. From the experimental results, the negative refraction signature was revealed from the negative values of both permittivity and permeability extracted from the experimental results of scattering parameters (S_{21} and S_{11}) for the hybrid system. In the anti-crossing region where two distinct modes of photon and magnon modes are resonantly coupled, negative refraction occurred, which is tunable by changing the frequency of ac currents and the strength of bias magnetic fields. This novel NRI characteristic of the ISRR/YIG hybrid system is the result of the strong interaction between the ISRR's photon and YIG's magnon modes. Our planar hybrid allows for a strong excitation of higher-order magnon modes, which can also couple to ISRR's photon and tune the frequency of negative refraction. This work provides an opportunity for the development of externally controllable negative refraction using various photon-magnon hybrid systems.

References

[1] D. R. Smith, J. B. Pendry, and M. C. K. Wiltshire, Science, 305, 788–792 (2004).
[2] A. Demetriadou and J. B. Pendry, J. Phys. Condens. Matter, 21, 376003 (2009).
[3] N. I. Landy, S. Sajuyigbe, J. J. Mock, D. R. Smith, and W. J. Padilla, Phys. Rev. Lett. 100, 207402 (2008).
[4] V. G. Veselago, Sov. Phys. Uspekhi, 10, 509 (1968).
[5] B. Bhoi, B. Kim, J. Kim, Y-J. Cho, and S-K. Kim, Sci. Rep., 7, 11930 (2017).
[6] B. Bhoi, B. Kim, S.-H. Jang, H. Kim, J. Yang, and S-K. Kim, Phys. Rev. B, 99, 134426 (2019).
[7] B. Bhoi and S-K. Kim, "Recent Advances in Topological Ferroics and their Dynamics", R.L. Stamps, H. Schultheib (Eds.), Solid State Physics, vol. 70, Academic Press, 2019, pp. 1-77 (Chapter One).

Measurement of temperature increment rates from magnetic nanoparticles

Jae-Hyeok Lee*, Bosung Kim, Youngsub Kim and Sang-Koog Kim†
National Creative Research Initiative Center for Spin Dynamics and Spin-Wave Devices, Nanospinics Laboratory,
Research Institute of Advanced Materials, Department of Materials Science and Engineering,
Seoul National University, Seoul 151-744, South Korea
†Correspondence and requests for materials should be addressed to S.-K. K. (sangkoog@snu.ac.kr)

Magnetic hyperthermia has been intensively studied to generate heat from magnetic particles for hyperthermia medical treatments. However, conventional magnetic hyperthermia is limited by very low specific loss power (below several hundred Watts per gram)in a kHz frequency range of AC magnetic fields at several hundreds of Oe. Also the conventional hyperthermia methods usually take more than tens of minutes to increase temperature up to 10 ^{o}C at the tumor site, making difficult a precise control of temperature in human bodies. In order to overcome such disadvantages of low power efficiency and delayed responding time, we for the first time set up a system for temperature measurements from magnetic nanoparticles combined with RF pumping for generating heat induced by resonant spin-excitation [1-4] in superparamagnetic Fe_3O_4 nanoparticles. The sample of Fe_3O_4 nanoparticles were deposited on the signal line in the microstrip, where the pumping RF power of GHz frequencies generated from a signal generator is transmitted. A thermal infrared (IR) camera was used to measure the temperature of particles via thermal radiation. DC magnetic fields are applied along the microstrip line where its field direction is perpendicular to the applied RF magnetic field direction. From this measurement setup, we achieved an extremely high initial temperature increment rates of 150 K/s, which is two orders of magnitude larger than other reported values by the conventional magnetic hyperthermia so far. This work offers a precisely controllable and highly efficient heat-generation technique for the realization of clinical treatment using magnetic hyperthermia.

References

[1] S.-K. Kim et al., Sci. Rep. 5, 11370 (2015)
[2] S.-K. Kim et al., Sci. Rep. 6, 31513 (2016)
[3] M.-K. Kim and S.-K. Kim et al., Phys. Rev. Applied 9, 054037 (2018)
[4] M.-K. Kim and S.-K. Kim et al., J. Appl. Phys. 125, 063901 (2019)

Toward Experimental Demonstration of Negative Refraction in Photon-Magnon Coupled Composite Antennas

Bosung Kim*, Biswanath Bhoi, Haechan Jeon and Sang-Koog Kim†
National Creative Research Initiative Center for Spin Dynamics and Spin-Wave Devices, Nanospinics Laboratory,
Research Institute of Advanced Materials, Department of Material Science and Engineering,
Seoul National University, Seoul 151-744, South Korea
†Correspondence and requests for materials should be addressed to S.-K. K. (sangkoog@snu.ac.kr)

Light-matter interaction in hybrid quantum systems has been studied for its potential applications to quantum information and communication devices [1]. A recent demonstration of photon-magnon (P-M) coupling [2-5] provides a powerful tool for reading and writing quantum states. However, most of the P-M relevant researches have focused on circuits of quantum computing processors. In this work, we report on the first experimental demonstration of P-M coupling based negative refraction in planar antennas that consist of Yttrium Iron Garnet (YIG) film and patch antenna, which is applicable to communication technologies with benefits of beamforming using a magnetic field.

We fabricated patch antennas using photolithography and chemical etching process along with conventional PCB technique. A substrate of a relative dielectric constant, $\varepsilon = 10$ was used. The frequency characteristic of the patch antenna was optimized using the CST-studio simulator. A commercially available epitaxial YIG (Yttrium Iron Garnet) film of 3.7 mm × 3.7 mm × 25 μm, grown on a Gadolinium Gallium Garnet (GGG) substrate by liquid phase epitaxy was placed on the feeding line of the patch antennas. We measured the reflection coefficient S_{11} of the composite antenna using a calibrated one-port vector network analyzer (VNA). The input of the antenna was soldered to a subminiature version A connector, then, the S_{11} parameter was measured by changing the external DC magnetic field from 50 to 100 mT. We observed normal anti-crossing from the patch antenna/YIG hybrid as similar to that in the inverted split-ring resonator (ISRR)/YIG hybrid [3,4]. Also, we modified the coupling strength by varying the position of the YIG film relative to the inset of the patch antenna. The coupling strength was observed to increase as the YIG position approaches to the inset of the patch antenna. Asymmetry of the intensity between the upper and lower branches was also observed. It might be originated from electric monopoles and magnetic dipoles induced by the curling flow of AC electric currents along with the inset of the antennas. Then, the radiation pattern of the composite antenna was measured in an anechoic chamber to characterize the optical behaviors of the antenna. The composite antenna was mounted in a rotation module for a three-dimensional (3D) scan of radiated electromagnetic-waves and connected to the port 1 of VNA. Static magnetic fields of strength in a range of 10 - 120 mT were applied by a pair of permanent magnets in the rotation module. A common type of pyramidal horn antenna connected to port 2 of VNA was placed 3 m away from the rotation module. From the antenna measurement, we observed radiation patterns similar to those from conventional antennas in the non-coupling region. However, unexpected radiation patterns are observed in the P-M coupling region. These radiation patterns have not been reported in patch antennas ever, rather quite similar to reverse Cherenkov radiation (or backward-wave radiation) in leaky-wave antennas with the negative refractive index [6]. The result implies that P-M coupling leads to reverse Cherenkov-radiation like patterns through negative

refraction. This work may pave a new way of controlling the bandwidth, beam pattern, as well as refractive index of the composite antennas by P-M coupling.

References

[1] H. J. Kimble, Nature, 453, 1023 (2008).

[2] L. Bai, M. Harder, Y. P. Chen, X. Fan, J. Q. Xiao, and C.-M. Hu, Phys. Rev. Lett., 114, 227201 (2015).

[3] B. Bhoi, B. Kim, J. Kim, Y-J. Cho, and S-K. Kim, Sci. Rep., 7, 11930 (2017).

[4] B. Bhoi, B. Kim, S.-H. Jang, H. Kim, J. Yang, and S-K. Kim, Phys. Rev. B, 99, 134426 (2019).

[5] B. Bhoi and S-K. Kim, "Recent Advances in Topological Ferroics and their Dynamics", R.L. Stamps, H. Schultheib (Eds.), Solid State Physics, vol. 70, Academic Press, 2019, pp. 1-77 (Chapter One).

[6] A. Grbic and G. V. Ekeftheriades, J. Appl. Phys., 92, 5930 (2002).

Abnormal dynamic modes of skyrmions in magnetic nanotubes

Jaehak Yang[1*], Junhoe Kim[1], Claas Abert[2], Dieter Suess[2] and Sang-Koog Kim[1†]
[1]National Creative Research Initiative Center for Spin Dynamics and Spin-Wave Devices, Nanospinics Laboratory, Research Institute of Advanced Materials, Department of Materials Science and Engineering, Seoul National University, Seoul 151-744, South Korea
[2]Christian Doppler Laboratory - Advanced Magnetic Sensing and Materials, University of Vienna, Austria
[†]Correspondence and requests for materials should be addressed to S.-K. K. (sangkoog@snu.ac.kr)

Magnetic skyrmions, one of topologically protected magnetization textures, are at the center of current magnetism research owing to its promising application to information processing devices [1] with benefits of its nano-scale dimensions and low-power-driven motions. Most of the earlier studies on dynamic motions of skyrmions have been focused in two-dimensional (2D) planar geometry such as nanostripes, nanodisks, and thin films. In those planar geometries, it was also found that a gyration mode and azimuthal spin-wave modes are excited by in-plane ac magnetic fields or currents, as well as one breathing mode excited by out-of-plane ac magnetic fields or currents.[2-3] To date, there have been no reports of static and dynamic modes of skyrmions formed in magnetic nanotubes. In soft magnetic nanotubes based on micromagnetic simulations, Yang et al.[4] reported on intrinsic spin-wave modes and corresponding vortex-type domain-wall motion. Since dynamic behaviors of skyrmions in such 3D elements are expected to differ from their known dynamic modes of 2D elements, here we performed micromagnetic numerical calculations to examine the stability of single skyrmions formed in magnetic nanotubes as well as their dynamic modes.

We report a robust stability of skyrmions in a curved geometry and their abnormal dynamic motions in nanotubes of perpendicular magnetic anisotropy with respect to the tube surface. Unlike planar geometry, skyrmions show elliptical shapes. Depending on the sign of the Dzyaloshinskii-Moriya Interaction (DMI) constant, the formed skyrmions are less or more stabilized by the curved geometry. The positive and negative signs of the DMI constant play a crucial role in the formation of skyrmions on the curved surface. These effects become stronger as the diameter of the tube decreases, quantitatively evidencing that the curvature-induced DM-like interaction also contributes to the stability of skyrmion formation. For the skyrmion core oriented along the outward direction, the dynamic modes of the skyrmion in the tubes are found to be not only a counterclockwise (CCW) gyration mode and a clockwise (CW) azimuthal spin-wave mode, but one breathing mode. On the other hand, in contrast to the planar geometry, initial CCW gyration motion turns out to be a linear translational motion in the circumferential direction of the tube when the strength of axial ac magnetic fields is greater than a certain threshold field strength. The direction of the translational motions is determined by the skyrmion helicity governed by the sign of the interfacial DMI constant. This work provides further physical insight into the static and dynamic properties of skyrmions formed in curved-geometry systems and also suggests its potential application to information processing devices.

References

[1] A. Fert, V. Cros, and J. Sampaio, Skyrmions on the track. Nature Nanotech. **8**, 152 (2013).

[2] K. Y. Guslienko, and Z. V. Gareeva, Gyrotropic Skyrmion Modes in Ultrathin Magnetic Circular Dots. IEEE Magnetics Letters, **8**, 1-5 (2017).

[3] M. Beg et al. Dynamics of skyrmionic states in confined helimagnetic nanostructures. Physical Review B, **95**(1), 014433 (2017).

[4] J. Yang, J. Kim, B. Kim, Y.-J. Cho, J.-H. Lee, and S.-K. Kim, Characteristic dynamic modes and domain-wall motion in magnetic nanotubes excited by resonant rotating magnetic fields, Phys. Rev. B **94**, 024425 (2016)

DMI-free skyrmion formation and robust dynamic behaviors in magnetic hemispherical shells

Jaehak Yang[1*], Claas Abert[2], Dieter Suess[2] and Sang-Koog Kim[1†]

[1]National Creative Research Initiative Center for Spin Dynamics and Spin-Wave Devices, Nanospinics Laboratory, Research Institute of Advanced Materials, Department of Materials Science and Engineering, Seoul National University, Seoul 151-744, South Korea

[2]Christian Doppler Laboratory - Advanced Magnetic Sensing and Materials, University of Vienna, Austria

[†]Correspondence and requests for materials should be addressed to S.-K. K. (sangkoog@snu.ac.kr)

Chiral spin textures such as domain walls, vortex, and skyrmions are considered as promising building blocks for prospective memory and logic devices in the field of spintronics and spin-orbitronics [1-2]. In particular, magnetic skyrmions have been intensively studied not only to understand their fundamental dynamic properties, but to reliably manipulate their static and dynamic properties [2-3]. However, most of those studies have been focused on 2D planar thin films with perpendicular magnetic anisotropy, while the statics and dynamic properties of magnetic textures can be modified in 3D curved geometries [4]. Recent theoretical and experimental works revealed that 3D curved and torsional magnets can introduce two effective magnetic interactions of curvature-induced effective anisotropy and DMI [5].

Here, thus we performed micromagnetic simulations to examine the formation of skyrmions in curved geometries, for example, magnetic hemispherical shells according to the strength of the uniaxial magnetic anisotropy and the diameter of hemispherical shells. Curvature-induced DMI-like term allows for the stabilization of skyrmions without the DMI term in hemispherical shells in a range of the uniaxial magnetic anisotropy above a certain threshold anisotropy constant K_u. As the curvature of shells, the threshold K_u increases, indicating that the curvature-induced DM-like interaction contributes to further stabilizations of skyrmions. The dynamic modes of skyrmions formed in the shells with no DMI are found to be two in-plane gyration modes in counterclockwise (CCW) and clockwise (CW) rotation senses, and one out-of-plane breathing mode, as similar to those found in planar geometries. Additional fine feature will be reported in this presentation. This work provides a further physical insight into the static and dynamic properties of skyrmions formed in curved-geometry systems even with no DMI.

References

[1] N. Nagaosa and Y. Tokura, Topological properties and dynamics of magnetic skyrmions, Nat. Nanotechnol. **8**, 899 (2013).

[2] A. Fert, N. Reyren, and V. Cros, Magnetic skyrmions: Advances in physics and potential applications, Nat. Rev. Mater. **2**, 17031 (2017).

[3] J. Seidel, ed., Topological Structures in Ferroic Materials (Springer International Publishing, Switzerland, 2016).

[4] R. Hertel, Curvature-induced magnetochirality, SPIN **03**, 1340009 (2013).

[5] O. V. Pylypovskyi, V. P. Kravchuk, D. D. Sheka, D. Makarov, O. G. Schmidt, and Y. Gaididei, Coupling of Chiralities in Spin and Physical Spaces: The Möbius Ring as a Case Study, Phys. Rev. Lett. **114**, 197204 (2015)

Carbon content effect of $Mn_{50}Al_{50-x}C_x$ on its magnetic properties and phase stability

Sumin Kim, Hyun-Sook Lee* and Wooyoung Lee†
Department of Materials Science and Engineering, Yonsei University,
50 Yonsei-ro, Seodaemun-gu, Seoul, 03722, Republic of Korea
Corresponding authors. E-mail addresses: wooyoung@yonsei.ac.kr (W. Lee), h-slee@yonsei.ac.kr (H.-S. Lee)

We have investigated the effect of carbon content in $Mn_{50}Al_{50-x}C_x$ (x = 0, 1.56, 2.35, and 3.12 at.%) on the magnetic properties and phase stability. We prepared a high content of the ferromagnetic τ-phase with different particle sizes in the powders. From the phase analysis using XRD, we found that the carbon content is critical for the stability of the τ-phase formation. The highest saturation (96.6 emu/g) and remanence (47.1 emu/g) magnetizations are observed at x = 2.35. These are the highest values reported so far. This is attributed to the high fraction of the τ-phase (~94 wt%) at this carbon content. The coercive field of $Mn_{50}Al_{50-x}C_x$ shows particle-size dependence. A high coercive field is observed at a smaller size of particles. From the analyses of the phase and magnetic properties, the solubility limit of carbon in $Mn_{50}Al_{50-x}C_x$ that yields the high-quality τ -phase was found to be x = ~2.35.

Keywords: Mn–Al–C alloy, carbon addition, phase stability, magnetic properties, permanent magnets

Si-doping effects on grain growth and magnetic properties in LaCaCo-substituted M-type hexaferrites

Pyeong-Yeol Yu[1*], Kyoung-Seok Moon[2], Young-Min Kang[1†]

[1]Department of Materials Science and Engineering, Korea National University of Transportation, Chungju, 27469, Republic of Korea

[2]School of Materials Science and Engineering, Gyeongsang National University, Jinju, 52828, Republic of Korea

La-Ca-Co substituted M-type Sr-hexaferrites ($Sr_{0.3}Ca_{0.4}La_{0.3}Fe_{9.8}Co_{0.2}O_{19-\delta}$) were prepared by a conventional solid-state reaction using two different procedures, where the SiO_2 additive was mixed either before calcination (pre-Si) or after calcination (post-Si). Phase analysis and lattice parameters were calculated based on the X-ray diffraction patterns. At the same sintering temperature, smaller cell volumes and reduced saturation magnetization (M_s) values were obtained for samples processed with the pre-Si method than those with the post-Si method. This implied that the pre-Si method resulted in a greater degree of Si substitution into the M-type lattice and increased Fe extrusion out of the M-type lattice. The difference in M_s between the two groups of samples decreased as the sintering temperature increased from 1200 °C to 1250 °C. The grain growth behavior was controlled by the SiO_2 amount and sintering temperature. It was found that abnormal grain growth occurs with a bimodal distribution in the 0.5 wt% SiO_2 samples sintered at 1240 °C, due to the increased critical driving force for growth caused by an increased amount of SiO_2 addition. When a larger amount of SiO_2 was added (≥ 1 wt%), the critical driving force was larger than the driving force for growth of all grains, which resulted in no grain growth in the initial stage of sintering. The M_s and coercivity values were altered with the control of Si diffusion and abnormal grain growth.

*This work was supported by Korea National University of Transportation in 2020.

Characterization of Mn-substituted M-type Sr-hexaferrites synthesized by sol-gel method

Jun-Ki Kim, Young-Min Kang*
Department of Materials Science and Engineering, Korea National University of Transportation, Chungju, 27469, Republic of Korea

Mn-substituted M-type Sr-hexaferrites, $SrFe_{12-x}Mn_xO_{19}$ (x = 0, 2, 4, 6, 8, 10, 12) were prepared by the sol-gel method. Precursors of $Sr(NO_3)_2$, $Fe(NO_3)_2 \cdot (9H_2O)$, and $Mn(NO_3)_2 \cdot 6H_2O$ in desired stoichiometric amounts were weighed and mixed with citric acid in a 1:1 weight ratio by using the minimum amount of distilled water needed to form an aqueous solution. Ammonia (NH_4OH) is added to the solution drop by drop to adjust the PH value to 7. The resulting solution was stirred at 100 °C and dried at 180 °C. The dried powders were annealed in air at various temperatures in range of 600 – 1000 °C for 4 h. XRD analysis on x=0 sample revealed that the crystalline M-type hexaferrite phase can be formed at the annealing temperature, $T_{ann} \geq 700$ °C. The powder samples of $SrFe_{12-x}Mn_xO_{19}$ (x = 0, 2, 4, 6, 8, 10, 12) annealed at 900 ℃ were ground, pressed into disk and toroidal types of pellets, and finally sintered in air at 1100 °C for 4 h, respectively. Single M-type hexaferrite phase was confirmed for the samples of $x \leq 6$. In the M-H measurement, the saturation magnetization value decreased and the coercivity increased with increasing x from 0 to 6. The resistivity of the sintered sample continuously and significantly decreased from 1.8×10^8 Ωcm to 5.5×10^3 Ωcm with increase of x from 0 to 6. Scanning electron microscope (SEM) was used for the study of microstructure. Complex permittivity and permeability were measured on the toroidal shaped samples of $SrFe_{12-x}Mn_xO_{19}$ (x = 0, 2, 4, 6, 8)-epoxy (10wt%) composites. The magnetic and electrical properties of these samples with (x = 0, 2, 4, 6, 8, 10, 12) and the correlation among the composition, structure, and the properties will be discussed.

NdFeB magnets studied by machine learning combined with micromagnetic simulations

Hyeon-Kyu Park[1*], Jehyun Lee[2], Jae-Hyuk Lee[1] and Sang-Koog Kim[1†]

[1]National Creative Research Initiative Center for Spin Dynamics and Spin-Wave Devices, Nanospinics Laboratory, Research Institute of Advanced Materials, Department of Materials Science and Engineering, Seoul National University, Seoul 151-744, South Korea

[2]Platform Technology laboratory, Korea Institute of Energy Research, 152 Gajeong-ro, Yuseong-gu, Daejeon, South Korea

[†]Correspondence and requests for materials should be addressed to S.-K. K. (sangkoog@snu.ac.kr)

NdFeB magnets are expected to have a theoretically calculated intrinsic value of BH_{max}, 64 MGOe, or 512 kJ/m^3 [1], but experimentally observed highest value is slightly less, BH_{max} ~ 56 MGOe [2]. In efforts to enhance the BH_{max} of NdFeB magnets, microstructural factors such as the thickness of grain boundaries [3], average grain size [4,5], and degree of misalignment of easy axes of individual grains [6] are required to be optimized. Here, we conduct a study of the effect of microstructural parameters on the performance of NdFeB magnets by machine learning combined with micromagnetic simulations, using a model of NdFeB magnets composed of 256 grains with an average grain size varying from 8 to 64 nm (see Fig. 1). In the modeling, intergranular exchange stiffness, the average size of grains, and the degree of misalignment of easy axes of the grains are varied to examine both coercivity and BH_{max} from demagnetization curves calculated by micromagnetic simulations using Mumax[3] (see Fig. 2). We employed the support vector regression (SVR) technique which adopts ε-insensitive linear loss function and a radial basis function as the kernel of the response function. Our preliminary result obtained from 300 datasets of the coercivity values demonstrates R^2 score 0.867 and root mean square error (RMSE) as low as 0.322 T (Figure 3), with optimized hyper-parameters of the regularization parameter C = 1000, ε = 0.01 and the coefficient of the radial basis function kernel γ = 1.0. Our results demonstrate the potential of machine learning methods for the design of microstructure of NdFeB magnets in the future when the underlying microstructure-property relationships are not yet clarified.

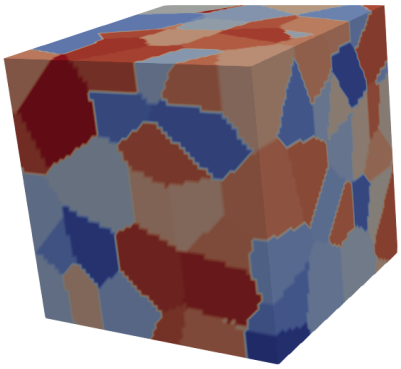

Fig. 1. An example of meshes of polycrystalline NdFeBs with an average grain size of 25.9 nm for micromagnetic simulations

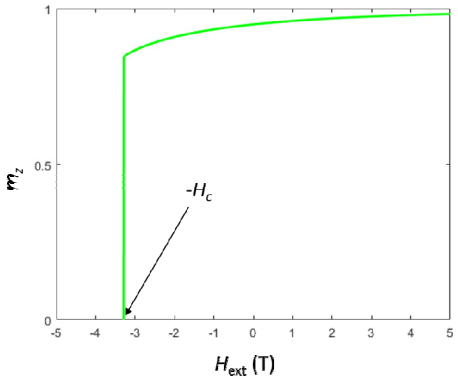

Fig. 2. Demagnetization curve obtained by micromagnetic simulation.

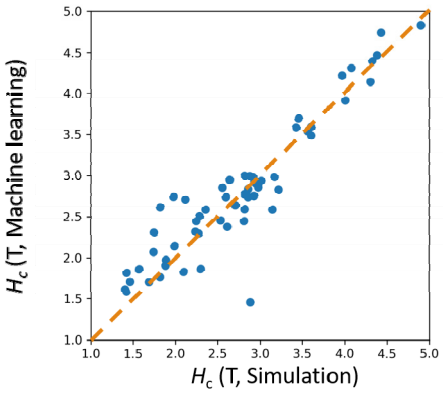

Fig. 3. Parity plot comparing coercivity data obtained from the micromagnetic simulation against that predicted from machine learning for 300 datasets.

References

[1] J. F. Herbst, *Rev. Mod. Phys.* **63**, 819 (1991).

[2] O. Gutfleisch, M. A. Willard, E. Brück, C. H. Chen, S. G. Sankar, and J. P. Liu, *Adv. Mater.* **23**, 821-842 (2011).

[3] T. T. Sasaki, T. Ohkubo, Y.Takada, T.Sato, A.Kato, Y.Kaneko, and K.Hono, *Scr. Mater.* **113**, 1 (2016).

[4] S. Bance, B. Seebacher, T. Schrefl, L. Exl, M. Winklhofer, G. Hrkac, G. Zimanyi, T. Shoji, M. Yano, N. Sakuma, M. Ito, A. Kato, and A. Manabe, *J. Appl. Phys.* **116**, 233903 (2014)

[5] H. Kronmüller and M. Fähnle, Micromagnetism and the Microstructure of Ferromagnetic Solids (Cambridge University Press, 2003).

[6] S.-K. Kim, S. Hwang, J.-H. Lee, *J. Magn. Magn. Mater.* **486**, 165257 (2019).

Magnetic properties of La-Co substituted Sr M-type hexaferrites in iron deficiency

Kanghyuk Lee*, Junho Park, Sung Joon Choi and Sang-Im Yoo†
Department of Material Science and Engineering, Research Institute of Advanced Materials (RIAM), Seoul National University, Seoul, Korea

The Sr M-type hexaferrites ($SrFe_{12}O_{19}$) are one of the most widely used magnetic material due to their cost efficiency, strong uniaxial magnetic anisotropy along the *c*-axis, and excellent chemical stability. Recently, many studies have improved the intrinsic magnetic properties of M-type hexaferrites by substitution, such as saturation magnetization and crystalline anisotropy. Previous reports have been mainly focused on La^{3+}substitution for the Sr^{2+} site and Co^{2+} substitution for the Fe^{3+} sites of M-type hexaferrites. In addition, there is generally requires a non-stoichiometric of iron ratio between 10 and 12 on Ba M-type hexaferrites. While iron deficiency is known to be helpful for the grain growth and the structure formation of NiZn spinel ferrites. However, the effect of La-Co substitution and iron deficiency on magnetic properties of the Sr-La-Co M-type hexaferrites remains unexplored. In this study, therefore, we tried to investigate La-Co substituted Sr M-type hexaferrites $Sr_{1-x}La_xFe_{12-x}Co_xO_{19,}$ ($0 \leq x \leq 0.5$) and the effect of iron deficiency on the magnetic properties of $Sr_{1-x}La_xFe_yCo_xO_{19-\delta}$ ($x = 0.15$, $10 \leq y \leq 12$-x) hexaferrites prepared by solid state reaction. The raw materials were ball-milled for 24 h with SiO_2 additive and calcined at 1280 ℃ for 2 h in air. as-calcined powder was pressed into pellets and sintered at 1230 ℃ for 1 h in air with SiO_2 and $CaCO_3$ additives. Samples were characterized by powder X-ray diffraction (XRD), vibrating sample magnetometer (VSM), and scanning electron microscope (SEM). In case of Iron deficient Sr-La-Co M-type hexaferrties, Powder XRD analyses revealed that M-type single phases were obtained with all Fe contents at sintering temperature. The saturation magnetization (M_s) of the Sr-La-Co M-type hexaferrite samples was around 72 emu/g. However, the coercivity (H_c) decreased with higher Fe content because the grain size was larger than the single domain size. The V_{cell} change due to substitution and iron deficiency seems to be inversely related to H_a obtained by magnetic hysteresis loops calculation. Detailed microstructures and magnetic properties will be presented for a discussion.

Keywords: Hexaferrite, magnetic property, iron deficiency, M-type hexaferrite

This research was supported by Future Materials Discovery Program through the National Research Foundation of Korea (NRF) funded by the Ministry of Science and ICT (2016M3D1A1027835)

Magnetic and electromagnetic wave absorbing properties of multi-hexaferrite-epoxy composites

Young-Min Kang*

Department of Materials Science and Engineering, Korea National University of Transportation, Chungju, 27469, Republic of Korea

Multi-hexaferrites ($Sr_{3-x}M_xCo_2Fe_{24}O_a$; M = none, La, Ca, Ce, Y; x = 0.3) with more than two types of hexaferrite phases were synthesized by solid-state reactions and doping of various cations in the Z-type Sr_3Co_2 hexaferrite. Multi-hexaferrites consisting of Z + U + W, W + M, X + W, W + M, and X + W + Z phases were formed in the samples with M = none, La, Ca, Ce, and Y, respectively, upon first and second calcinations at 1160 and 1210 °C. The microstructures were observed by scanning electron microscopy. *M–H* curves of the sintered bodies were measured using a *B–H* loop tracer. Complex permittivity and permeability measurements (100 MHz ≤ f ≤ 18 GHz) were performed on hexaferrite–epoxy composite samples. The microwave absorption properties were evaluated by reflection loss (RL) calculations based on the complex permittivity and permeability spectra. For the undoped sample, the minimum RL (-47.6 dB) corresponding to the maximum microwave absorption was obtained at f = 4.5 GHz and thickness d = 4.6 mm. The frequency corresponding to the RL peak was increased up to 17.3 GHz, while the optimal thickness gradually decreased upon the doping with Ca, Y, Ce, and La cations. The peak shift to high frequency is attributed to the increase of magnetic hardness of the mult-hexaferrites. Broad-band EM absorption properties are also achieved owing to the overlaps of the hard–soft magnetic properties of the multi-hexaferrites.

Phase- and Composition-tunable Exchange-coupled Nanomagnet: SmCo/Co and SmCo/Fe Nanofibers

Jimin Lee*, Eun Jae Lee, Jongryoul Kim, Yong-Ho Choa
Department of Materials Science and Chemical Engineering, Hanyang University, Korea

An exchange-spring magnet is a next-generation permanent magnetic model that possesses a synergistic effect of single-phased hard and soft magnets, thereby giving rise to enhanced magnetic performance. However, in spring magnet preparation thus far, it has remained a challenge to manipulate the magnetic properties via the exchange-coupling effect due to the lack of a synthetic method that enables the hard/soft interfacial magnetic interaction in a homogeneous manner. Here, we report an in-situ approach for the synthesis of a phase- and composition-tunable SmCo-based spring magnet based on a binary phase system. This is the first reported systematic and prospective approach to spring magnet preparation. An electrospinning technique with the use of a composition-tunable precursor enables the fabrication of bimagnetic nanofibers with a precisely controlled hard/soft magnet volume ratio (0 to 100%) and a good number of interfacial sites, leading to an effective magnetic coupling interaction. On the basis of a microstructural study and qualitative magnetic measurements, we demonstrate an enhancement in magnetic performance for binary-phased fibers and clearly manifest the elucidation of the exchange-coupling effect between nanograins across the interface in the one-dimensional nanomagnet. We envision that this work can provide a potential approach to develop exchange-coupled spring magnet and moreover, offering an ideal model to understand the nanomagnetism of a well-constructed one-dimensional spring nanostructure.

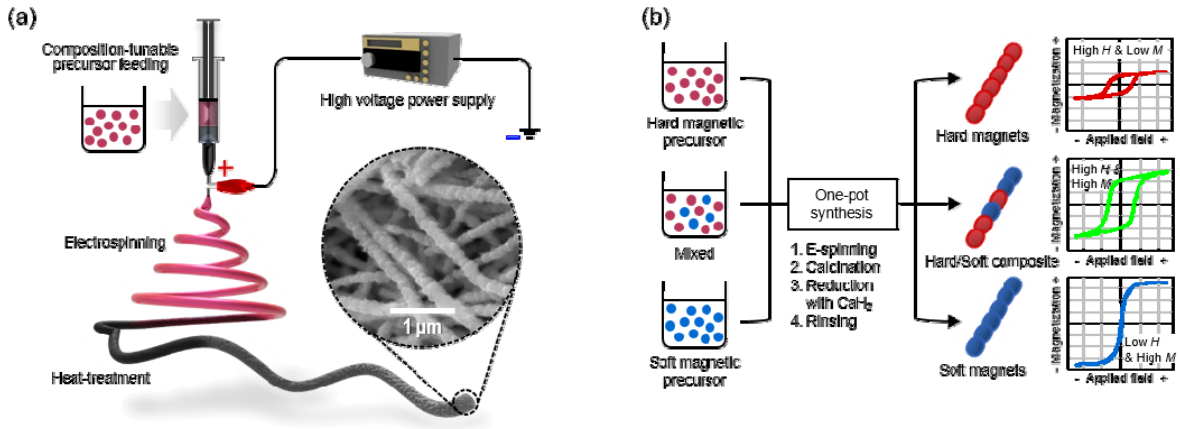

Fig. 1. Schematic illustrations of (a) basic electrospinning process for magnetic nanofiber preparation and (b) possible formation mechanism of phase-tunable magnetic composites by the one-pot synthesis using a composition-tunable precursor solution.

Effect of post-annealing on the coercivity and microstructure of (Nd, Ce) -Fe-B hot-deformed magnet

Ga-Yeong Kim[1,2*], Hee-Ryoung Cha[1], Dong-Hwan Kim[3], Yang-Do Kim[2] and Jung-Goo Lee[1†]

[1]Powder&Ceramics Division, Korea Institute of Materials Science, Changwon, Korea

[2]Department of Materials Science and Engineering, Pusan National University, Busan, Korea

[3]Research Center of SG Tech., Star Group Ind. Co., Daegu, Korea

Nd-Fe-B based magnets are widely used in industrial applications such as the traction motor of hybrid electric vehicles and electric vehicles due to its excellent magnetic properties. In general, Nd-Fe-B magnets are composed of ~30 wt.% rare-earth (RE) elements such as Nd, Pr and Dy which are less abundant in the natural rare earth resources, although Ce and La are the most abundant elements in the natural rare earth resources and its price is much cheaper than Nd, Pr and Dy. It is because that the intrinsic hard magnetic properties of $Ce_2Fe_{14}B$ ($4_{\pi M}$ = 11.7 kG, H_a = 26 kOe) and $La_2Fe_{14}B$ ($4_{\pi M}$ = 13.8 kG, H_a = 20 kOe) are much inferior to those of $Nd_2Fe_{14}B$ ($4_{\pi M}$ = 16 kG, H_a = 73 kOe). Furthermore, there exists secondary phase of $CeFe_2$ with high melting point in Ce-Fe-B magnet, which is reported to be suppressed by addition of La. On the other hand, It is well known that the modification of the microstructure by post-annealing (PA) is the most effective way to improve the coercivity of Nd-Fe-B magnets without degradation of their remanence. For the Nd-Fe-B sintered magnet, post-sinter annealing process is performed at a temperature ranging from 773 K and 873 K in order to improve Nd-rich grain boundary phase for high coercivity. However, most studies have been focused on sintered magnets and studies on annealing effect of hot-deformed magnets are quite limited.

In this study, post-annealing effect on the magnetic properties and microstructure of (Nd, M)-Fe-B hot-deformed magnets, was investigated. Initial ribbons with the nominal compositions of $(Nd_{1-x}M_x)_{13.6}Fe_{bal}B_{5.6}Ga_{0.6}Co_{6.6}$ (x=0, x=0.2/M=Ce, x=0.3/M=Ce and x=0.3/M=Ce+La, wt.%, named as ND, CE0.2, CE0.3 and CELA0.3, respectively) were prepared by melt-spinning and then pulverized into powders. The powders were hot-pressed at 973 K under 100 MPa and then subjected to die-upsetting at 973 K with a deformation rate of $\dot{\varepsilon}$ = 0.1 s^{-1}. From TEM observation, it was confirmed that the RE-rich phase distribution along grain-boundaries is quite different between CE0.3 and CELA0.3 magnets compared to ND. Especially, the grain boundary phase of CELA0.3 magnets was quite indistinct in almost area, whereas the grain boundary phase of ND was continuous and homogeneous. The post-annealing effect was different depending on the substitution elements. The post-annealing effect was highest in CELA0.3 magnet at 973K. Based upon these results, the post-annealing effect on coercivity and microstructure of M(Ce,La)-substituted (Nd, M)-Fe-B hot-deformed magnets will be discussed.

Effects of initial Nd-Fe-B HDDR powders' microstructure on the microstructure and magnetic properties of hot-deformed magnet

Jae-Gyeong Yoo[1,2*], Hee-Ryoung Cha[1], Yang-Do Kim[2], Jung-Goo Lee[1†]
[1]Powder & Ceramics Division, Korea Institute of Materials Science, Changwon, Korea
[2]Department of Materials Science and Engineering, Pusan National University, Busan, Korea

Nd–Fe–B hot-deformed magnets produced from ultra-fine grains of melt-spun (~50nm) or HDDR (~300nm) powder have much smaller average grain size than that of sintered magnets. Therefore, hot-deformed magnets have a great potential to obtain high coercivity and improve its temperature dependence even without using heavy rare earth elements which is usually used to obtain high coercivity in the sintered magnets. However, the coercivity of hot-deformed magnets is quite lower than that predicted from the empirical relationship between the grain size and coercivity. The low coercivity of the hot-deformed magnets with ultrafine grain size was reported to be due to the high content of Fe and Co in the intergranular phase, which exhibits ferromagnetism. The highly ferromagnetic grain boundary phase leads to a strong ferromagnetic exchange coupling between neighboring $Nd_2Fe_{14}B$ grains. Hence, the coercivity of hot-deformed magnet could be enhanced further by modifying the grain boundary phase into non-ferromagnetic state.

To modify the composition of the intergranular phase toward a lower Fe content, post-treatment such as grain boundary diffusion process(GBDP) with non-ferromagnetic material is necessary. The distribution and composition of grain boundaries optimized through GBDP, causing magnetic decoupling among neighboring $Nd_2Fe_{14}B$ grains, can contribute to the enhancement of coercivity of hot-deformed magnets.

In this study, the Nd-Fe-B bulk magnets were produced by hot-deformation process using HDDR powders. As-produced and annealing-treated HDDR powders, which have different microstructure but the same composition, are employed. Then, the hot-deformed magnets made from different initial HDDR powder were subjected to GBDP using NdHx-Cu mixed powders. The magnetic properties and microstructure of hot-deformed and subsequently GBDPed magnets were analyzed by VSM and FE-SEM. As an interesting result, the coercivity enhancement of hot-deformed magnet made from annealing-treated HDDR powders was higher than that of made from as-produced HDDR powder after GBDP. Based upon these results, effects of the initial Nd-Fe-B HDDR powders' microstructure on the microstructure and magnetic properties of hot-deformed magnet during GDBP will be discussed.

Ca-assisted Synthesis of well-size-controlled $Sm_2Fe_{17}N_3$ nanoparticles

Eun Jae Lee*, Jimin Lee, Min Kyu Kang, Jongryoul Kim, Yong-Ho Choa†
Department of Materials Science and Chemical Engineering, Hanyang University,
Ansan, Gyeonggi-do, 15588, Korea

Sm-Fe-N magnet with superior magnetic intrinsic properties is a promising alternative to conventional hard magnet such as Nd-Fe-B and Sm-Co. $Sm_2Fe_{17}N_3$ which is the basic nitrided phase in Sm-Fe system with hard magnetic behavior has comparatively high Curie temperature (749 K), uniaxial anisotropy field (260 kOe), and also relative high saturation magnetization (1.54 T).

In principal, hard magnetic particles achieve the highest coercivity at their single-domain size (i.e. 0.35 μm for $Sm_2Fe_{17}N_3$). Generally, most hard magnetic phases require submicron-scaled particle size. Several methods for the preparation of rare-earth based intermetallic compounds have been widely researched. Among them, top-down methods which contain pulverization cause inhomogeneity, surface defects. On the other hand, bottom-up approaches with controlling size of the metal oxide as a starting material have an advantages in the synthesis of the fine particles having uniform size, surface with low defect and homogeneous element mixing. Earlier research has been executed with co-precipitation, polymerized-complex. However, these methods have complex process or low production yield for the preparation of metal oxide. Besides, during subsequent reduction process, formation of coarse particle is unavoidable due to easy-aggregation of Fe particles.

In this work, we focused on the preparation of submicron $Sm_2Fe_{17}N_3$ particles possessing both less-aggregated and high coercivity. Self-sustained combustion method is a suitable for synthesizing metal oxide precursor particle in nano-scale. To prevent sintering between Fe particles, calcium oxide, served as a blocking agent between Fe particles, was employed. Moreover, in-situ nitridation(rinsing CaO after consecutive nitriding) led to synthesis of single-phased product without phase decomposition. In order to investigated the effects of Ca content on the size of $Sm_2Fe_{17}N_3$ particle and their magnetic properties, a precursor of CaO was employed in different concentrations. We fabricated $Sm_2Fe_{17}N_3$ particles with the average diameter of 0.68 ± 0.26 μm, which exhibited the coercivity of 17 kOe under Ca introduction.

Low melting-point diffusion salts of heavy rare-earth for enhancing coercivity of grain-boundary-diffusion-processed Nd-Fe-B-type magnet

J. Y. Choi[1*], H. W. Kwon[1*], B. A. Kim[1], Y. K. Kim[2] and J. G. Lee[2†]
[1]Pukyong National University, Busan, Republic of Korea 48513
[2]Korea Institute of Materials Science, Changwon, Republic of Korea 51508

Nd-Fe-B-type magnet has been exclusively used for rotor magnet in traction motor of HEV and EV, but it still has one big drawback: poor thermal stability (high temperature coefficient of coercivity (β)) due to low Curie temperature (T_c). Standard approach for solving this problem is sufficiently enhancing room temperature coercivity by means of grain boundary diffusion (GBD) of heavy rare-earth (HRE), such as Tb or Dy. Commonly used diffusion sources of the HRE for GBD are HRE fluoride or oxide salts. As these salts exist as solid during GBD process, diffusion of HRE towards interior is inherently sluggish. It is expected that using HRE diffusion sources in liquid form would lead to speedier diffusion of HRE, thus leading to more rapid and efficient coercivity enhancement. By a lucky chance, we could find a good candidate of diffusion source of Dy in DyF_3 – LiF binary system, which becomes liquid during GBD annealing. Promising liquid Dy diffusion source is available in two-phase region (solid DyF_3 + liquid (DyF_3 – LiF)) above the peritectic line (~ 815 °C) in DyF_3 – LiF binary system, and relative amount of the liquid phase can be controlled by choosing composition the low melting-point (DyF_3–LiF) diffusion source. On the plus side, the peritectic temperature (~ 815 °C) is desirably lower than typical GBD annealing temperature for Nd-Fe-B-type magnet. In this study, efficacy of using liquid phase Dy diffusion source for enhancing coercivity in GBD-processed Nd-Fe-B-type magnet was investigated. Commercial (Nd,Pr)-Fe-Co-Cu-B-type sintered magnet was coated with (DyF_3 – LiF) mixture having desired composition. Coated Nd-Fe-B magnet was annealed at 820 °C and then quenched, and followed by aging at 550 °C. It was found that the (DyF_3 – LiF) mixture having 10 vol% liquid (DyF_3 – LiF) + 90 vol% solid DyF_3 at annealing temperature was the best for enhancing coercivity of the Nd-Fe-B-type magnet (Fig. 1(a)). More importantly, it was also revealed that more rapid and consistently higher coercivity enhancement was achieved by using low melting-point (DyF_3–LiF) diffusion source with respect to solid DyF_3 diffusion source (Fig. 1(b)). Overall, the magnet GBD-processed with low melting-point (DyF_3–LiF) diffusion source outperformed the one processed with solid DyF_3.

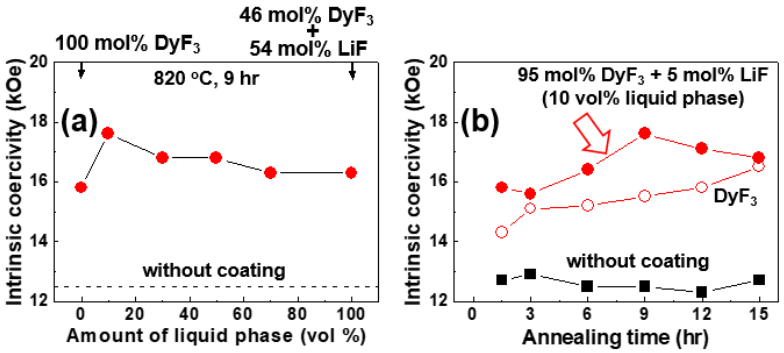

Fig. 1. Coercivity variation in Nd-Fe-B-type magnet GBD-processed using Dy diffusion source.

Nd-Fe-B계 폐자석을 이용한 이방성 HDDR 분말 제조

노태성[1,2*], 차희령[1], 김양도[2], 이정구[1*]
[1]한국기계연구원 부설 재료연구소, 기능분말연구실
[2]부산대학교, 재료공학과

Nd-Fe-B계 자석은 우수한 자기특성 때문에 다양한 분야에 광범위하게 사용되고 있다. 특히, 최근 친환경 자동차 시장이 성장함에 따라 하이브리드/전기자동차 구동모터용 Nd-Fe-B계 자석의 수요가 급격하게 증가하고 있다. 한편, Nd-Fe-B계 자석의 약 30 wt.%를 차지하는 희토류 자원은 대부분 중국에서 생산되고 있고, 수급 불안정 및 가격 문제가 지속적으로 대두되고 있는 실정이다. 또한 현재 소비되는 Nd-Fe-B계 자석은 향후 관련 부품의 노후화와 더불어 대량의 산업폐기물로 배출될 것으로 예상된다. 따라서, Nd-Fe-B계 폐자석을 효율적으로 활용하는 것이 급증하는 Nd-Fe-B계 자석의 수요와 이와 관련된 희토류 수급 불안정을 해소하기 위하여 방안으로 대두되고 있다.

Nd-Fe-B계 폐자석을 활용하는 방안으로 폐자석의 희토류를 추출하여 재활용하는 방법과 폐자석을 모합금으로 재이용하는 방법이 있다. 후자와 관련하여, 폐자석을 분쇄한 후 첨가물을 혼합하여 재소결하는 방법과 melt-spinning 또는 HDDR (hydrogenation-disproportion-desorption-recombination) 공정을 이용하여 나노 결정립 분말을 제조한 후 본드자석으로 제조하는 방법이 보고되고 있다. 이들 중 HDDR 공정법은 Nd-Fe-B계 자석의 결정립을 300nm 수준으로 미세화 할 수 있는 기술로 공정조건을 적절히 제어한다면 고보자력 이방성 분말로 제조가 가능하다. 하지만 폐자석의 경우 기존 자석에 비해 산소농도가 높고, 다량의 Dy를 포함하는 등 기존 HDDR 공정에 이용되는 합금과 상이하여, 고특성 분말을 개발하기 위해서는 폐자석에서의 HDDR 거동에 대한 정확한 이해와 공정조건의 최적화가 필요하다.

본 연구에서는 $Dy_{1.4}Nd_{21.8}Pr_{6.7}Fe_{bar}B_{0.9}M(Co, Al, Cu, Ga, Nb)_{2.0}$ (wt.%) 조성의 소결자석을 폐자석 대용으로 이용하여 나노결정립의 이방성 HDDR 분말을 제조하기 위한 연구를 수행하였다. 먼저 소결자석은 균일한 HDDR 반응를 위해 HD (Hydrogen Decrepitation) 처리하여 조분쇄 하였으며, 810~940℃의 온도범위에서 HDDR처리하여 이방성 분말로 제조하였다. 실험결과, HDDR 공정온도에 따라서 분말의 보자력 및 미세구조가 크게 변화됨을 확인하였으며, 920℃에서 처리한 분말이 11.4 kOe로 가장 높은 보자력을 나타내었다. 또한 공정온도가 810℃에서 940℃까지 증가함에 따라 결정립 크기가 300nm에서 500nm으로 증가되었다. 하지만 입계상은 온도가 증가함에 따라 점차 연속적이고 균일하게 분포하는 것을 확인하였다. 이러한 결과를 바탕으로 Nd-Fe-B계 폐자석의 HDDR 거동에 대해 논의하고자 한다.

초고보자력 산화철 나노 분말을 이용한 벌크 자석 제조

조기련[1,2*], 표민지[1,3], 손영국[2], 백연경[1†]
[1]한국기계연구원 부설 재료연구소, 한국
[2]부산대학교, 재료공학부, 한국
[3]부경대학교, 재료공학과, 한국

4차 산업혁명 시대가 도래하여 전동 모터의 사용이 급증함에 따라 영구자석의 수요가 증가하였다. 그러나 현재 사용되고 있는 고특성 영구자석은 희토류 기반이며, 이는 제한된 자원량으로 인한 공급의 문제점이 있다. 반면, 3d 천이 금속은 양적으로 풍부하여 수급에 용이하므로 이를 기반으로 우수한 자기특성을 가지는 영구자석 소재를 개발한다면 4차 산업 핵심분야를 견인할 수 있는 부품소재로 활용할 수 있을 것이라 기대된다. 입실론 산화철 (ε-Fe_2O_3)은 25 kOe 이상의 산화물 계열임에도 불구하고 높은 보자력을 가지므로 비희토류 영구자석 소재로서 잠재력이 있으나 준 안정상이므로 합성된 분말을 실제 산업에 적용하기 위해 벌크화 공정 개발이 필요하다. 이에 따라 우리는 역마이셀-졸젤 공정을 통해 분말을 합성하고 이를 저온 저압 공정을 통해 벌크화 하였다. 이때, 벌크화 공정 단계에서 압력 및 온도에 따라 제조된 자석의 입실론 상 함량이 변하는 것을 확인하였고, 이의 자기적 특성을 비교 및 분석하였다.

Keywords: rare-earth free, ε-Fe_2O_3, bulk, hard magnet, iron oxide

Synthesis and electromagnetic wave absorbing properties of Ni-substituted Z-type Sr_3Co_2 hexaferrite-epoxy composites

Jin-Young Yu*, Young-Min Kang†
Department of Materials Science and Engineering, Korea National University of Transportation, Chungju, 27469, Republic of Korea

Z-type hexaferrites are one of the promising materials for electromagnetic wave absorber or antenna miniaturization applications owing to their suitable magnetic and dielectric properties. Thus, modulating of the permeability and permittivity properties in the corresponding frequency range is very important. In this research, Ni-substituted Z-type Sr_3Co_2 ($Sr_3Co_{2-x}Ni_xFe_{24-d}O_{41}$, x=0, 0.1, 0.2, 0.3, 0.4, 0.5) were prepared by solid-state reaction processes. Based on our previous research, the Fe-deficient composition (d=1) were employed to obtain almost single Z-type phase.

XRD analysis revealed that almost single Z-type hexaferrite phase could be obtained for the samples with Ni substitution composition of $0 \leq x \leq 0.5$ when the samples were sintered at 1235 ºC for 2 h in air. The Ni substitution into the Co site of the Z-type hexaferrite did not cause noticeable changes both on lattice parameter and microstructure of the samples. For the grounded powder samples of $Sr_3Co_{2-x}Ni_xFe_{24-d}O_{41}$ (x=0, 0.1, 0.2, 0.3, 0.4, 0.5), 10 wt% of epoxy binder was added and mixed together. Then, the mixed powder was pressed into toroidal-shaped green compacts, and finally cured at 180 ºC for 1 h in air. After the complex permittivity (ε', ε") and permeability (μ', μ") measurements (100 MHz $\leq f \leq$ 18 GHz) on the toroidal hexaferrite powder–epoxy composites, the reflection losses (RLs) was calculated as functions of the sample thickness (d) and frequency (f) and plotted as 2D maps for these composite samples, respectively. With increasing Ni substitution x, the permeability spectra continuously shifted to low frequency. The peak frequency of μ" gradually decreased from 3.2 GHz to 2.0 GHz. The frequency corresponding to the minimum RL peak was also decreased from 3.3 GHz to 2.3 GH with the increase of x from 0 to 0.5. The Ni substitution is very effective for the tuning of EM absorption frequency.

Effect of Co Addition on Magnetic Properties in FINEMET-based Alloy System

Hyunsol Son*, Haein Choi-Yim†
Department of Physics, Sookmyung Women's University, Seoul 04310, Korea

Fe-based amorphous alloy systems have attracted the interest in the remarkable soft magnetic properties, high saturation magnetization, and the low cost of manufacture. We substitute Copper in FINEMET with Cobalt to improve glass forming ability(GFA) and soft magnetic properties with good thermal stability. We investigated the Fe-based amorphous soft magnetic alloys of $(Co_{1-x}Fe_x)_{72}B_{19.2}Si_{4.8}Nb_4$ prepared by arc-melting system with high purity metals under Ti-gettered Argon atmosphere. Then, with these samples, we produced ribbons with 2-3mm widths and 20-30 μm thicknesses by using melt spinning technique. After processing these ribbons, we analyzed the alloys' thermal and magnetic properties. $(Co_{1-x}Fe_x)_{72}B_{19.2}Si_{4.8}Nb_4$ alloy system was verified as fully amorphous by using X-ray diffraction (XRD). The thermal properties including crystallization temperature (T_x) were measured by differential scanning calorimetry (DSC) and turned out to have T_x between 570℃ and 620℃. Magnetic properties of the amorphous ribbons were measured by a vibrating sample magnetometer (VSM). The amorphous ribbons of $(Co_{1-x}Fe_x)_{72}B_{19.2}Si_{4.8}Nb_4$ identified soft magnetic properties with high saturation magnetization (Ms) at most 126.26emu/g.

Hysteresis Loop Characteristics Change of Co-based Amorphous $Co_{67}Fe_3Cr_3Si_{15}B_{12}$ Ribbon

Deok Young Lee[1*], Sin Hyuk Yim[1], Derac Son[2]
[1]Agency for Defense Development, Daejeon, Korea
[2]Dept. of Information and Communication Engineering, Hannam university, Daejeon, Korea

Study of soft magnets has been important research topic because of their various applications such as transformers, magnetic shielding, magnetometer, and large variety of apparatus. Amorphous alloys are versatile materials in application of those apparatus, because amorphous alloys have excellent soft magnetic properties.

In particular, large permeability and small coercive force of Co-based amorphous alloy is recommended in sensors application. We synthesize Co-based amorphous alloy, $Co_{67}Fe_3Cr_3Si_{15}B_{12}$, using melt-spinning process. We have measured hysteresis loops of amorphous alloys. Loops are recorded at room temperature for annealing with different temperature. By controlling annealing temperature, coercive field of sample decreased that means sample has more excellent soft magnetic properties. Here, we propose an optimal condition for annealing Co-based amorphous alloy, $Co_{67}Fe_3Cr_3Si_{15}B_{12}$.

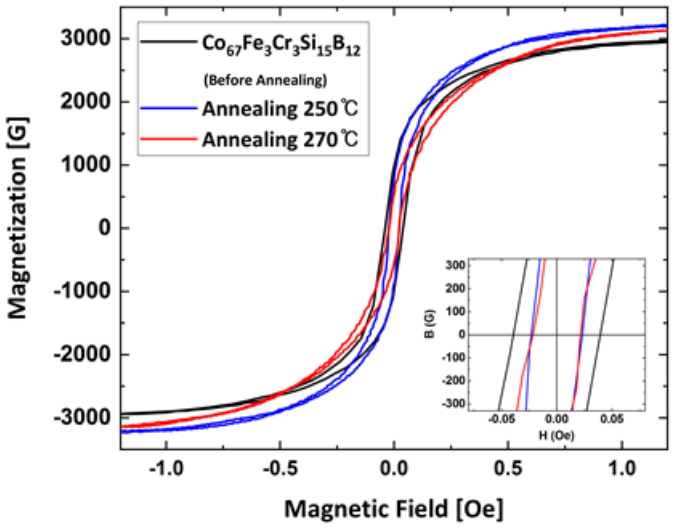

Fig. 1. Hysteresis loops of $Co_{67}Fe_3Cr_3Si_{15}B_{12}$ with different annealing conditions

Magnetic Field-induced Switching of Asymmetric Bloch wall in a Ferromagnetic Rectangular disk

Sooseok Lee[1*], Hee-Sung Han[1], Myeonghwan Kang[1], Hye-Jin Ok[1],
Namkyu Kim[1], Mi-Young Im[2], Ki-Suk Lee[1]
[1]Ulsan National Institute of Science and Technology, Korea
[2]Lawrence Berkeley National Laboratory, USA

In a rectangular shaped ferromagnetic thin film, usually flux closure domain structure is formed from the competition between demagnetization and exchange energies [1]. At the center of this closure domain, the typical 180 degree domain wall, Bloch wall appears in the middle of part. Near the top and bottom surfaces the magnetization direction changes by rotating parallel to the surface in the x-direction, the so called Néel caps [2] (Shown in Fig.). This over all arrangement was named Asymmetric Bloch wall [3]. The ABW can be classified by direction of Neel cap, the bottom and top NCs, i.e., (+,−) and (−, +) [4]. It has high potential for multi bit applications in a well ordered array of lithographically patterned magnetic dot because of its multiple ground states (8 ground states). To utilize them, it is important to understand their complex three-dimensional magnetic structure and physical behavior. Since both (+,−) and (−,+) states have exactly same energy, they appear almost same probability. Therefore, breaking their symmetry is necessary by external factor. For example, an asymmetric geometry was utilized for control the ABW states [4]. In this presentation, we are suggesting another way to control the ABW states efficiently by using micromagnetic simulations in a rectangular ferromagnetic disk. We also observed the controlled ABW structures experimentally by means of the magnetic transmission soft x-ray microscopy (MTXM) at the Advanced Light Source [5].

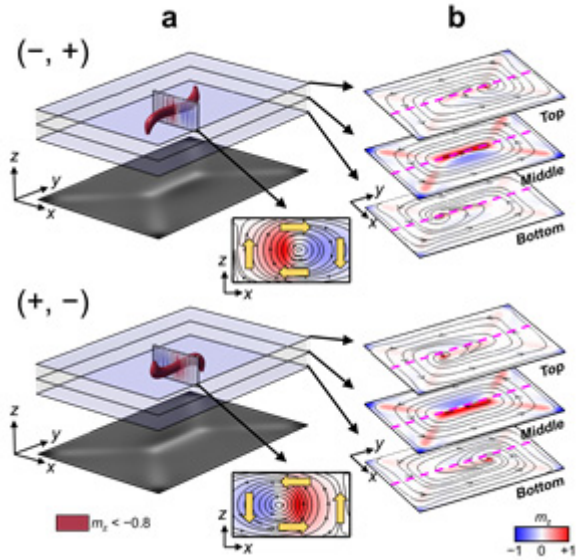

Fig. 1. The simulation results to show the two degenerated state of asymmetric Bloch wall in permalloy ($Ni_{80}Fe20$) rectangular disk. The blue (red) surface is the area where $m_z < -0.8$ ($m_z > +0.8$).

References

[1] A. Hubert and R, Schäfer. Magnetic Domains. (Springer, Berlin, 1999)

[2] A. Hubert, Phys. Status Solidi 32, 519 (1969).

[3] A. E. Labonte, J Appl. Phys. 40, 2450 (1969)

[4] F. Cheynis et al., Phys. Rev. Lett. 102, 107201 (2009)

[5] Fischer, P. et al. Mater. Today 9, 26-33 (2006).

SnO_2 도핑에 따른 $BaCoFe_{12}O_{19}$의 자기적 특성 및 마이크로파 흡수 특성 연구

W. H. Jeong*, S. W. Kim, B. W. Lee†
Department of Physics and Oxide Research Center, Hankuk University of Foreign Studies, Yongin 17035, South Korea

일상생활에서 전자기기의 사용빈도가 많아지면서 전자기기에서 발생하는 전자파 간섭(EMI)으로 인한 오작동 및 인체유해의 문제가 대두되고 있다. 본 연구는 전자파 차폐 효과가 뛰어나다고 알려진 M-type hexaferrite를 기반으로 금속 산화물인 SnO_2를 도핑하여 이에 따른 상호작용을 통한 특성 변화를 분석 하였다.[1,2] 공침법에 의해 제조된 $BaCo_xFe_{12-x}O_{19}$ (x = 1) M-type hexaferrite 에 첨가하는 SnO_2의 함량에 따라 물리적 특성들을 확인하였다. 졸-겔 방법을 통해 전구물질인 tin chloride ($SnCl_2$)를 tin dioxide (SnO_2)로 치환한 후 졸 형태로 첨가하였다.[3] X-ray diffraction patterns 을 통해 샘플이 결정화 되었다는 걸 확인하였다. 또한 표면의 형태를 SEM 을 통해 확인하였고 EDS 분석으로 해당 시료의 구성원소를 확인할 수 있었다. VSM 분석을 통해 Ms, Hc 등의 자기적 특성을 분석하였다. 해당 파우더를 조건 별 토로이달 형태로 성형 후 network analyzer 분석을 통해 마이크로 웨이브 영역대의 반사손실을 확인하였다. SnO_2의 함량의 변화에 따라 전자파의 차폐효과를 보이는 공명 주파수가 이동하는 것을 확인하였다. 본 연구를 통해 sol 형태의 SnO_2 함량 변화로 원하는 차폐가능 주파수를 구현 할 수 있음을 확인하였다.

References

[1] N. Tran, et al, Current applied Physics, 19 (2019)
[2] Biao Zhao, et al, Mater Electron, 26 (2015)
[3] H. Kose, et al, Acta Physica Polonica A, 1, 121 (2012)

Al 도핑된 ZnO 와 연자성 NiZn Ferrite 합성물의 EMI 차폐

Y. R. Kim*, J. H. Ahn, B. W. Lee†
Department of Physics and Oxide Research Center, Hankuk University of Foreign Studies,
Yongin 17035, South Korea

Al이 도핑된 ZnO(AZO)와 NiZn ferrite를 혼합하여 만든 EMI 차폐제의 특성을 연구하였다. Al의 도핑으로 우수한 전기전도도를 가지는 AZO를 합성 후, NiZn ferrite와 혼합하면, NiZn ferrite의 전기 전도도 뿐만 아니라 차폐 기능을 향상 시킬 수 있을 것이라 예상하였다.

AZO는 sol-gel 방법으로 합성 한 뒤, 600℃로 calcination 시켜 결정화 상태의 AZO를 만들었으며, NiZn ferrite는 solid state 방법으로 합성하였다. XRD, SEM, EDS 측정 결과, 시료가 성공적으로 합성되었음을 확인하였다. 이후, NiZn ferrite, AZO, NiZn ferrite와 AZO의 혼합물, 세가지 시료에 적정량의 epoxy를 각각 혼합하여 EMI 차폐를 특성을 확인하였다.

AZO는 S-band에서 가장 우수한 EMI 차폐능력을 나타냈다. 이는 스마트폰이 주로 사용되는 주파수 영역대인 2.4 GHz 대역에서 차폐물질로서 사용 가능할 것으로 보인다. 한편, NiZn ferrite와 AZO를 epoxy에 적정량 혼합 한 시료의 EMI 차폐 측정 결과, NiZn ferrite와 AZO의 혼합물은 S-band뿐만 아니라 KU-band까지 EMI 차폐를 할 수 있는 멀티밴드용 차폐제로의 응용이 가능할 것으로 보인다.

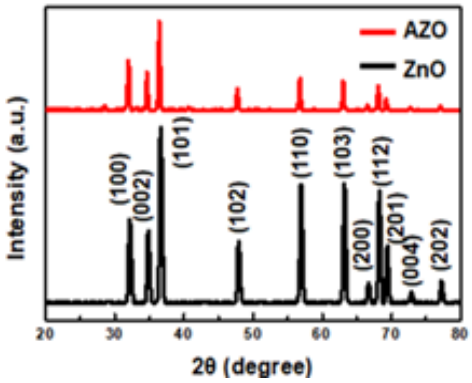

Fig. 1. XRD result

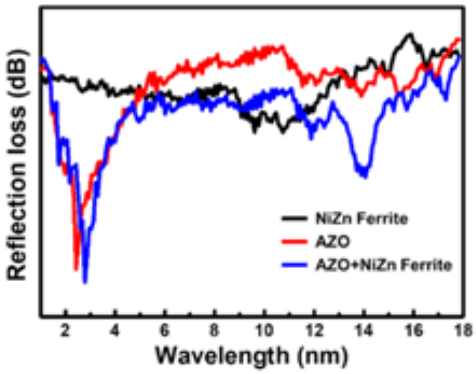

Fig. 2. EMI shielding result

멕센($Ti_3C_2T_x$) 첨가량에 따른 스피넬 페라이트의 차폐 성능의 향상

우혁준*, 이민영, 이보화†
한국외국어대학교 물리학과, 산화물 연구센터
*bwlee@hufs.ac.kr

전자기기의 작동주파수가 높아짐에 따라 전자파는 인체의 건강과 전자기기의 작동에 영향을 미친다. 전자기파 차폐는 해결해야할 사회적 문제로, 고주파 대역에서의 우수한 전자파 차폐 성능을 구현할 수 있는 다양한 차폐제에 관한 연구가 활발하게 진행되고 있다. 특히 2D 물질은 이러한 전자파 차폐재로서 우수한 성능을 나타내기 때문에 최근 MXene이 차폐재료로써 많은 연구가 진행되고 있다. 하지만 MXene의 경우 원재료가 수입에 의존하고 있으며, 제조단가가 높으며, 대량생산이 어렵다는 단점을 가지고 있다. 이를 해결하기 위해 우리는 기존에 많이 사용되는 전자파 차폐소재인 스피넬 페라이트에 MXene을 첨가하였다. 스피넬 페라이트는 생산단가가 저렴하고 대량생산이 가능하며, 8 GHz에서 5 dB의 반사손실을 갖는다. 여기에 MXene을 1-5wt%까지 첨가하였을 때 반사손실값이 점차 증가하였으며 차폐 주파수 대역이 이동하였다. 3wt% 샘플에서 9 GHz(10dB), 4 wt% 샘플에서 12 GHz(14dB)로 반사손실값이 향상되었으며, 전자파 차폐 주파수 영역이 고주파 대역으로 이동하는 경향을 보였다. 이를 통해 MXene이 첨가된 스피넬 페라이트는 MXene의 대체재로의 가능성을 확인하였다.

Influence of Zr/Hf content on soft magnetic properties of the Fe-Co-M-Nb-B alloy system (M = Zr, Hf)

JongHee Han*, Haein Choi-Yim
Department of Physics, Sookmyung Women's University

The Fe-rich Fe-Zr alloy system attracted considerable interests in the past few years because of their spin-glass behavior. However, Fe-Zr alloy systems have trouble in forming the amorphous phase. It is well known that the small addition of B in Fe-Zr and Fe-Hf alloys improves glass forming ability (GFA). It has been reported that Fe-(Zr, Hf)-B alloy system has high B_s of 1.5 T and long glass formation range. Furthermore, substitution Zr with Hf decreases H_c in Fe-(Zr/Hf)-B alloy system. The soft magnetic amorphous ribbons of $(Fe_xCo_{1-x})_{85}M_9Nb_1B_5$ (M = Zr and Hf) were investigated in this study. Fe-Co-based amorphous materials have excellent soft magnetic properties such as high saturation magnetic flux density (B_s) and low coercivity (H_c). To analyze soft magnetic properties of Fe-Co-(Zr/Hf)-Nb-B alloy system, vibrating sample magnetometer (VSM) and DC B-H loop tracer were used in this study. Also, we used X-ray Diffraction to observe the amorphous phase and differential scanning calorimeter (DSC) to measure the crystallization temperature (T_x) of Fe-Co-(Zr/Hf)-Nb-B alloy system. Most of the compositions exhibit excellent soft magnetic properties such as high B_s and low H_c. Especially, the highest B_s value is 1.62 T which is an excellent value in soft magnetic materials, and the lowest H_c value is 11 A/m. We observed that substituting Zr with Hf enhanced soft magnetic properties and the increasing Fe/Co ratio enhanced values of T_x and H_c.

Fabrication of a-Fe@SiO_2 Core-Shell Nanorod Particles for the Electromagnetic Waves Control

Min-Ji Pyo[1,2*], Gi-Ryeon Jo[1,3], Hee-Lack Choi[2], Youn-Kyoung Baek[1†]

[1]Powder and Ceramics Division, Korea Institute of Materials and Science, Chang-won, Korea

[2]Department of Materials Science and Engineering, Pukyong National University, Busan, korea

[3]School of Materials Science and Engineering, Pusan National University, Busan, Korea

With the development of electronic devices, research focusing on high frequency and superior characteristics for power conversion materials have been conducted to achieve high efficiency of electromagnetic (EM) equipment. Especially, as soft magnetic composites (SMCs), Fe-based magnetic powder coated by insulated layers is suitable for frequency control device materials applied for motors and inductors due to their giant saturation magnetization. However, iron has a problem in that EM wave control performance is decreased due to a drop in permeability above a specific frequency. Thus, researchers have investigated the method to increase anisotropy of the magnetic powders via fabricating 1d structure for maintaining permeability. In this study, we have synthesized 1d structured Fe nanoparticles via SiO_2 coating of Fe_2O_3 cores combined with hydrogen (H_2) reduction. It was confirmed that the iron nanocores in the shell can be adjusted from sphere to rod shapes according to reduction conditions. Thus, our strategy shows the possibility to utilize anisotropic shaped Fe as SMCs materials for EM wave control.

Transit gate for programmable manipulation of micro magnetic particles

Byeonghwa Lim*, Keonmok Kim, Jonghwan Yoon, Hyeonseol Kim, Cheol Gi Kim†
Department of Emerging Materials Science DGIST, Daegu 42988, Republic of Korea
cgkim@dgist.ac.kr

Micro-particle manipulation techniques have been studied in a variety of fields due to their potential applications. Since it operates in a small environment, sample/reagent consumption and energy consumption can be reduced, and measurement time can be reduced by processing many samples in parallel. Programmable particle manipulation is essential for large-capacity arrays and individual bead manipulation. The digital manipulation of single particles was implemented by a magnetophoretic circuit using a current wire, but the complicated manufacturing process and multiple current operation steps limit the practical application of large-capacity arrays. In this study, we propose a method of digital manipulating magnetic particles using a transit gate operated by a time-dependent pulsed magnetic field instead of a current wire. The transit gate consists of return, delay, and resistance linear gates and dividing, reversed, and rectifying T-junction gates, and has been studied through simulations and experiments for programmable digital manipulation of magnetic particles. The results show that it is important to operate the transit gate at the desired point in time through a magnetic field applied in the correct direction at the correct time, and it can be seen how to manipulate the magnetic particles to the desired path.

Magnetic and microwave absorbing properties of Zn-substituted BaW-type hexaferrites in Ka-band for 5G application

Sungjoon Choi[1*], Seung-Young Park[2], Seong Jin Choi[3] and Sang-Im Yoo[1]

[1]Department of Materials Science and Engineering, and Research Institute of Advanced Materials, Seoul National University, Seoul 151-744, Korea

[2]Spin Engineering Physics Team, Division of Scientific Instrumentation, Korea Basic Science Institute, Daejeon 34133, Korea

[3]Chang Sung Co Ltd, R&D Ctr, 11-9 Namdong Ind Area, Inchon 405100, Republic of Korea

The microwave absorption properties of Zn-substituted Barium W-type hexaferrites ($BaFe_{2-x}Zn_xFe_{16}O_{27}$; $BaFe_{2-x}Zn_xW$, where x = 0.0, 0.5, 1.0, and 2.0) in Ka-band were investigated. The partial substitution of Zn^{2+} for the Fe^{2+} site is known to increase both real and imaginary permittivity. The $BaFe_{2-x}Zn_xW$ samples were annealed at the temperature region of 1000–1350 ˚C for 2 h in the PO_2 of 10^{-3} atm. Magnetic hysteresis loops were measured at room temperature with a vibrating sample magnetometer (VSM, Lake Shore VSM-7410) in the applied filed up to 2.7 T. The composites, having epoxy resin and $BaFe_{2-x}Zn_xW$ (x=0.0, 0.5, 1.0, and 2.0) as a matrix and fillers, respectively, were fabricated with the ferrite volume factions of 30, 60, and 90 vol%. The complex permittivity ($\varepsilon_r = \varepsilon' - j\varepsilon''$) and permeability ($\mu_r = \mu' - j\mu''$) of $BaFe_{2-x}Zn_xW$ in Ka-band were measured by vector network analyzer (VNA, Agilent PNA N5525A) with a waveguide and the reflection losses were calculated based on the transmission line theory. Excellent microwave absorbance having the reflection loss (RL) blow -20 dB could be achievable in Ka band from our samples with the absorber thickness less than 1 mm. Detailed results will be presented for discussion.

This work was supported by a Grant from Chang Sung Co.

Unconventional Hall effect in ferrimagnet/oxide/silicon tri-layers

Jun-Ho Kang[1*], Soogil Lee[1,2], Dohyoung Kim[2], Seyeop Jung[3], Sanghoon Kim[3], Byong-Guk Park[2] and Kab-Jin Kim[1]

[1]Department of Physics, KAIST, Daejeon 34141, Korea
[2]Department of Materials Science and Engineering, KAIST, Daejeon 34141, Korea
[3]Department of Physics, University of Ulsan, Ulsan 44610, Korea

Conventional spintronic devices are composed of magnet/non-magnet bi-layer structures, because the bi-layers can serve as convenient platform to study spin orbit torque-related phenomena. In those bi-layers, the spin current generated in the non-magnetic layer exerts torque to the magnetic layer, resulting in a switching or domain wall motion in magnetic layer. Contrary to this conventional approach, here we investigate the transport properties in tri-layer structure. Our tri-layer consist of ferrimagnet/oxide/silicon, in which the electron tunneling occurs between ferrimagnet and silicon through the thin oxide layer. We found an unconventional Hall effect in the tri-layers: Hall resistance increases at higher temperature and depends on the current as well as external magnetic field in a unique way. We ascribe the observed unconventional Hall resistance to the combined effect of spin tunneling and inverse Rashba effect. In the presentation, we will also discuss how the ferrimagnetic properties affect the unconventional Hall resistance.

Performance Validation of a Planar Hall Resistance Biosensor through Beta-Amyloid Biomarker

Jinwoo Kim[1*], Sung Joon Kim[1], Sri Ramulu Torati[1], Artem Talantsev[1], Chang Yeop Jeon[1], Sung Bae Lee[2] and Cheol Gi Kim[1†]

[1]Department of Emerging Material Science, DGIST, Daegu 42988, Korea

[2]Departmant of Brain & Cognitive Science, DGIST, Daegu 42988, Korea

Biosensors detect and analyze target biomaterial selectively for biomedical research and diagnostic. Biosensor based magnetoresistance have raised interest and become dominant player in the vast world of biosensor with high detectivity. Especially magnetoresistance sensor using Planar Hall effect has high sensitivity and thermal stability. In this work, Portable biosensor platform was designed to detect magnetic labels without external magnetic field. The PHR sensor with tri-layer structure with a composition of Ta (5 nm) / NiFe (10 nm) / Cu (x = 0 nm ~ 1.2 nm) / IrMn (10 nm) / Ta (5 nm) using DC magneton sputter and Photolithography. The optimized sensitivity of sensor was 6 μV/Oe. We compared the signals from magnetic particles in first harmonic AC mode (1f mode) using an external magnetic field and in the second harmonic AC mode (2f mode) using a self-field generated by current passing through sensor. To detect a series of concentrations of magnetic labels using 2f mode method where the high signal-to-noise ratio (SNR), we demonstrated a β-amyloid biomarker based antibody-antigen sandwich model. The generated self-field from sensor was sufficient to detect an immobilized magnetic tag without external magnetic field. Therefore, this allows to reduce device sizes to use the point-of-care testing using a portable circuit system.

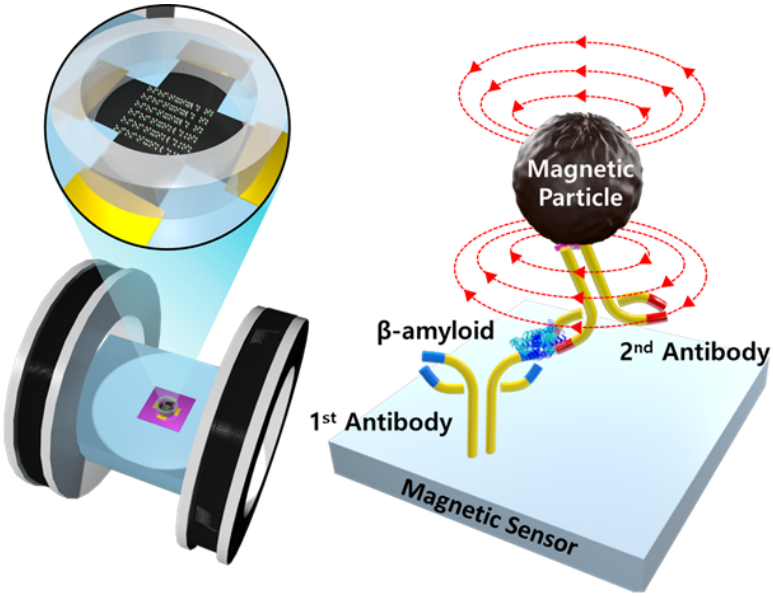

Fig. 1. Schematics of the planar Hall resistance (PHR) biosensor working principle in 1f and 2f detection mode.

Electric-field control of spin orbit torque behaviors by bias-dependent TaO_x oxide dynamics

Jeonghun Shin[1*], Jeongwoo Seo[2], Jungyup Yang[3] and Jinpyo Hong[1,2]

[1]Division of Nano-scale Semiconductor Engineering and Physics Hanyang University, Seoul 133-791, South Korea

[2]Department of physics, Hanyang University, Seoul 133-791, South Korea

[3]Department of physics, Kunsan national University, South Korea 54150

Intentional manipulation of Spin-Orbit Torque (SOT) efficiency and its devices inevitably requires precise adjustment of heavy metal layer in a Heavy Metal (HM)/Ferromagnet Metal (FM)/oxide frame. One approach developed up to now is the possible displacement of the domain walls which are highly dependent on the angle between the direction of the current and domain wall motion, and asymmetric and nonlinear with respect to the current polarity. The other approach is the choice of other HM layer, topological insulator, or antiferromagnet/ ferromagnet to provide the advancing SOT features. Here, we address the influence of bias-dependent oxygen ion drifts in ferromagnet/oxide layers generated by an external voltage. We note that samples have Perpendicular Magnetic Anisotropy (PMA), as shown in Fig. 1, in which the normalized RH versus perpendicular magnetic field curves are presented. The RH values are monitored under a gate voltage of +5V, 0V and -5V, demonstrating that the PMA is markedly influenced by electric field. The bias voltage is expected to strongly affect the ferromagnetic material's interface and perpendicular magnetic anisotropy features, thus enabling the HM layers' spin polarity and SOT spin current to be modified.

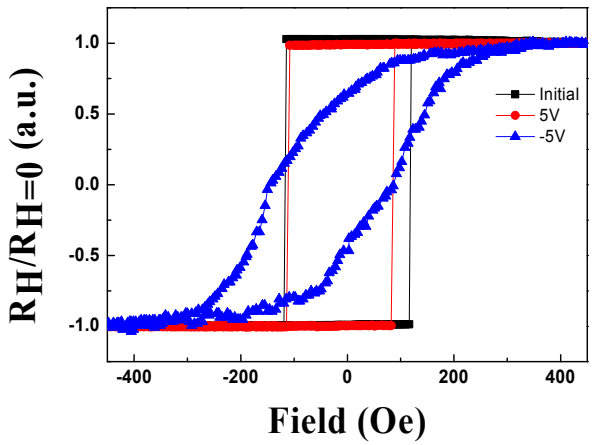

Fig. 1. Anomalous Hall resistance versus out of plane magnetic field in various gate voltages.

Unconventional Magnetoresistance Induced by Sperimagnetism of GdFeCo

Jaehyeon Park[1*], Hirata Yuushou[2], Jun-Ho Kang[1], Soogil Lee[1], Sanghoon Kim[3], Jong-Ryul Jeong[4], Seung-Young Park[5], Younghun Jo[5], Arata Tsukamoto[6], Teruo Ono[2,7], Se Kwon Kim[1,8], Kab-Jin Kim[1]

[1]Department of Physics, Korea Advanced Institute of Science and Technology, Daejeon, Korea
[2]Institute for Chemical Research, Kyoto University, Gokasho, Uji, Kyoto 611-0011, Japan
[3]Department of Physics, University of Ulsan, Ulsan, 44610, Korea
[4]Department of Materials Science and Engineering, Graduate School of Energy Science and Technology, Chungnam National University, Daejeon 34134, South Korea
[5]Center for Scientific Instrumentation, KBSI, Daejeon 34133, South Korea
[6]College of Science and Technology, Nihon University, Funabashi, Chiba 274-8501, Japan
[7]Center for Spintronics Research Network (CSRN), Graduate School of Engineering Science, Osaka University, Osaka 560-8531, Japan
[8]Department of Physics and Astronomy, University of Missouri, Columbia, MO, USA

Recently, ferrimagnets have drawn much attention because of their intriguing properties near the compensation temperatures. For example, high domain wall velocity[1] and negligible skyrmion Hall effect[2] have been observed near the angular momentum compensation temperature (T_A), while the enhanced spin orbit torque efficiency has been reported near the magnetization compensation temperature (T_M) [3]. However, the phenomena mentioned above are all related to the spin dynamics property. There are only few results reported on the spin transport properties which is another important aspect of spintronic research.

In this study, we investigate magnetoresistance (MR) of $Gd_{23.5}Fe_{66.9}Co_{9.6}$, a representative rare earth-transition metal ferrimagnetic material. The MR changes linearly to the external magnetic field at high field regime, which seems to be similar to the magnon-based MR[4]. However, the observed MR is in stark contrast to the previously reported magnon-based MR: the magnitude of the MR becomes larger as the temperature decreases, which is opposite to the conventional magnon-based MR. Furthermore, the slope of the MR changes its sign at T_M. These results imply that the observed MR may not caused by magnon, but originates from the ferrimagnetic characteristics.

To interpret the interesting MR trend, we may suggest the GdFeCo is a sperimagnet whose Gd and Fe net moments are directing antiparallel to each other with forming their own cone angles. Because of the negative anisotropic magnetoresistance (AMR) of Gd[5], the MR change of Fe and Gd are constructively additive even though the two cone angles are reacting oppositely to the external magnetic field. Despite of the considerable MR change, the anomalous Hall resistivity does not alter as much as it expected to be. From this, we can guess the contribution of the Gd to the spin transport property is comparable to that of the FeCo . Therefore, we might be able to understand the antiferromagnetic spin transport by studying on the ferrimagnets.

References

[1] Kim, Kab-Jin, et al. “Fast domain wall motion in the vicinity of the angular momentum compensation temperature of ferrimagnets.” *Nature materials* 16.12 (2017): 1187.

[2] Hirata, Yuushou, et al. “Vanishing skyrmion Hall effect at the angular momentum compensation temperature of a ferrimagnet.” *Nature nanotechnology* 14.3 (2019): 232.

[3] Ham, Wooseung, et al. “Temperature dependence of spin-orbit effective fields in Pt/GdFeCo bilayers.” *Applied Physics Letters* 110.24 (2017): 242405.

[4] Nguyen, V. D., et al. “Detection of domain-wall position and magnetization reversal in nanostructures using the magnon contribution to the resistivity.” Physical review letters 107.13 (2011): 136605.

[5] McEwen, K. A., G. D. Webber, and L. W. Roeland. “Magnetoresistance of gadolinium.” Physica B+ C 86 (1977): 533-534.

Effect of MgO spacer layer between Pt and CoFeSiB on interfacial Dzyaloshinskii-Moriya interaction

Taehyun Kim[1*], In Ho Cha[1], Yong Jin Kim[1], Gyu Won Kim[1], A. A. Stashkevich[2], Y. Roussigné[2], M. Belmeguenai[2], S. M. Chérif[2], A. S. Samardak[3] and Young Keun Kim[1]

[1]Department of Materials Science and Engineering, Korea University, Seoul 02841, Korea

[2]Université Paris 13, Sorbonne Paris Cite, 93430 Villetaneuse, France

[3]School of Natural Sciences, Far Eastern Federal University, Vladivostok 690950, Russia

The interfacial phenomena have been recently revisited and experimentally illustrated because of its huge potential to explore novel magnetic behaviors such as Skyrmions, chiral domain wall dynamics, and spin-Hall effects [1,2]. Among various interfacial effects, interfacial Dzyaloshinskii-Moriya interaction (iDMI) is drawing attention [3]. Number of different studies have previously been conducted to control the magnitude of iDMI in nonmagnet/ferromagnet/oxide trilayer; they showed how modification of top and bottom interface of ferromagnets can affect iDMI [4]. From the previous study, the interface between nonmagnet (NM) and ferromagnet (FM) layer is known to be the origin of iDMI due to the large spin-orbit coupling with the broken inversion symmetry at NM/FM interface, and experimental study reported a reduction of iDMI energy density as Cu, a well-known material for negligible spin-orbit coupling, is inserted at the interface [5]. Here, we have experimentally shown that iDMI can also be derived from FM/oxide interface by inserting MgO spacer layer between NM and FM.

A DC and RF magnetron sputtering system was used to deposit Ta/Pt/MgO(t_{MgO})/CoFeSiB/MgO/Ta structure under base pressure of $5x10^{-9}$ Torr. Ta is used to enhance crystallinity of Pt layer, a major source of spin-orbit coupling in our structure. The CoFeSiB is used as a magnetic layer and MgO with a thickness varying from 0 to 2.1 nm is inserted between Pt and CoFeSiB to see the effect of insertion layer on iDMI energy density. Vibrating sample magnetometer (VSM) is used to observe magnetic properties of the samples. Brillouin light scattering (BLS) spectroscopy is utilized to measure iDMI energy density by detecting non-reciprocal spin wave dispersions in Damon-Eshbach geometry. Transmission electron microscope (TEM) and X-ray diffraction (XRD) is done to confirm the crystal structure of Pt and Secondary ion mass spectroscope (SIMS) is used to show the structure of the stack.

All samples are studied in as-deposited state and showed in-plane anisotropy. Samples with 0 and 1.2 nm of MgO spacer layer are used to calculate magnetic dead layer using t_{FM} vs. $M_s t_{FM}$ plot and both samples show negligible amount of magnetically dead layer. An oscillating behavior of iDMI energy density, which is far from the common belief of instant decrease of iDMI energy density as insertion of MgO occurs. The maximum iDMI energy density of -0.78 mJ/m^2 was observed at 0 nm of t_{MgO}. TEM and XRD results show concrete Pt layer and SIMS result support the existence of MgO spacer layer between Pt and CoFeSiB. The potential physical mechanism is suggested based on the tunneling of conduction electrons through dielectric spacer. The indirect exchange coupling of Ruderman-Kittel-Kasuya-Yosida type interaction gives rise to the oscillating behavior of iDMI energy density.

References

[1] A. Soumyanarayanan et al., Nat. 539, 509 (2016).

[2] S. Woo et al., Nat. Mater. 15, 501 (2016).

[3] J. Cho et al., Nat. Commun. 6, 7635 (2015).

[4] A. Belabbes et al., Phys. Rev. Lett. 117, 247202 (2016).

[5] N.-H. Kim et al., AIP Adv. 7, 035213 (2017)

Interfacial Engineering Induced Spin-Orbit Torque Switching Current Reduction in W/W-N/CoFeB structures

Minhyeok Lee*, Yong Jin Kim, Gyu Won Kim, Taehyun Kim, In Ho Cha, Young Keun Kim*
Department of Materials Science and Engineering, Korea University, Seoul 02481, Republic of Korea

For the development of energy-efficient nonvolatile memory devices, a brand-new writing method, which defined as spin-orbit torque (SOT), has drawn huge attention. SOT is a torque triggered by angular momentum transfer from the spin current generated at the normal metal (NM) layer to the magnetization of an adjacent ferromagnetic (FM) layer. SOT can manipulate the direction of the magnetization of FM more fastly and provide lower energy consumption compared with conventional spin-transfer-torque devices [1]. However, the critical switching current required for magnetization reversal is still too large for the memory and logic device applications. The magnitude of the critical switching current is inversely proportional to the spin Hall angle (SHA) which defined as the ratio of the generated spin current over the injected in-plane electric current [2]. Recent studies have reported SHA of the various NMs: ~0.33 for β-W [3], ~0.15 for Ta [4], and ~0.10 for Pt [5] which are insufficient for applications. To further enlarge SHA, interface engineering approaches that manipulate NM/FM interfaces have been studied [6]. In this study, we report the large reduction of the critical switching current via interface engineering which employing the W-N interfacial layer between W/CoFeB heterostructure. The ultrathin W-N layer was deposited using reactive DC magnetron sputtering under an N_2 atmosphere. We measured SOT efficiency and microstructure as varying the concentration of N in the W-N interlayer. When a device comprising with 0.2 nm of W-N interlayer containing 42 at% N, SOT efficiency is obtained as 0.54 and the measured critical switching current is also reduced to one-fifth compared to that of W/CoFeB heterostructure. Our results suggest that we can obtain dramatic changes in the SOT efficiency as varying the composition of the layer even in an 0.2 nm-ultrathin layer showing that interfacial engineering is the right direction to approach the commercialization of SOT technology.

References

[1] I. M. Miron *et al*., Perpendicular switching of a single ferromagnetic layer induced by in-plane current injection, *Nature* 476 (2011) 189–193.

[2] K.-S. Lee *et al*., Threshold current for switching of a perpendicular magnetic layer induced by spin Hall effect, *Appl. Phys. Lett*. 102 (2013) 112410.

[3] C.-F. Pai *et al*., Spin transfer torque devices utilizing the giant spin Hall effect of tungsten, *Appl. Phys. Lett*. 101 (2012) 122404.

[4] Q. Hao, G. Xiao, Giant spin Hall effect and magnetotransport in a Ta/CoFeB/MgO layered structure: A temperature dependence study, *Phys. Rev. B* 91 (2015) 224413.

[5] H. L. Wang *et al*., Scaling of spin Hall angle in 3d, 4d, and 5d metals from Y3Fe5O12/metal spin pumping, *Phys. Rev. Lett.* 112 (2014) 197201.

[6] H.-Y. Lee *et al*., Enhanced spin-orbit torque via interface engineering in Pt/CoFeB/MgO heterostructures, *APL Mater*. 7 (2019) 031110.

Cation distribution and element resolved magnetic property for the Pb-based perovskite showing multiferroicity

Nyun Jong Lee[1*], Jae-Hyeon Cho[2], Ju-Hyeon Lee[2], Wook Jo[2] and Sanghoon Kim[1*]
[1]Department of Physics and EHSRC, University of Ulsan, Ulsan 44610, Korea
[2]School of Materials Science and Engineering, Ulsan National Institute of Science and Technology, Ulsan 44919, Republic of Korea
[*]Corresponding author: sanghoon.kim@ulsan.ac.kr

Multiferroicity has great potential for the next generation electronic applications such as ferroelectric photovoltaics and next-generation memory devices. For practical application, multiferroicity between ferromagnetism and ferroelectricity is desired to operate at room temperature [1-3]. An epitaxially-grown antiferromagnetic $BiFeO_3$ is representative material [4, 5] which shows the multiferroicity with single phase, while a ferromagnetic-ferroelectrically coupled material at room temperature has not been reported yet.

In this presentation, we show a Pb-based perovskite which is magnetoelectrically coupled above even room temperature. To understand the multiferroic property based on the correlation between crystal and electronic structures, X-ray absorption spectroscopy was conducted at both near (XAS and XMCD) and extended edges (EXAFS). Our results have confirmed that the ferrimagnetic property of perovskite has been induced by the A-site substitution of Ni.

References

[1] S. Dong, J.-M. Liu, S.-W. Cheong, Z. Ren, Multiferroic materials and magnetoelectric physics: symmetry, entanglement, excitation, and topology. *Adv. Phys*. **64**, 519-626 (2015).
[2] Y. Tokura, S. Seki, Multiferroics with spiral spin orders. *Adv. Mater*. **22**, 1554-1565 (2010).
[3] U. Lüders et al., $NiFe_2O_4$: A Versatile Spinel Material Brings New Opportunities for Spintronics. Adv. Mater. **18**, 1733-1736 (2006).
[4] J. Wang *et al.*, Epitaxial $BiFeO_3$ multiferroic thin film heterostructures. *science* **299**, 1719-1722 (2003).
[5] J. B. Neaton, C. Ederer, U. V. Waghmare, N. A. Spaldin, K. M. Rabe, First-principles study of spontaneous polarization in multiferroic$BiFeO_3$. *Phys. Rev. B* **71**, (2005).

Room-temperature Spin Hall Magnetoresistance in Pt/Co/Graphene Heterostructures

Thi Nga Do[1,2*], Sehee Lee[3], Chanyong Hwang[3], Tae Hee Kim[1,2†]
[1]IBS Center for Quantum Nanoscience, Ewha Womans University, Seoul, Korea
[2]Department of Physics, Ewha Womans University, Seoul, Korea
[3]Korea Research Institute of Standards and Science, Daejeon, Korea

Making graphene magnetic has attracted considerable interest from both the basic scientific and technological standpoints, which could meet the ever-increasing demand for more storage capacity by engineering ultimately thin, two-dimensional (2D) magnetic materials. There have been many theoretical and experimental studies of magnetic moments in graphene as a result of vacancy defects, deposition of adatoms, and coupling to ferromagnetic (FM) substrates [1,2]. Evidences of spin transport modulation by proximity effects have been also reported in heterostructures of graphene and FM materials [3]. However, making graphene magnetic still remains a non-trivial task, and little is known about how the spin-orbit proximity effects influence spin dynamics and the emergence of the spin Hall effect (SHE).

Here we demonstrate high spintronic performance in Chemical Vapor Deposition (CVD)-grown multilayer graphene on industrial standard SiO_2/Si substrates. 3-nm Pt/2.5-nm Co bilayers were fabricated using Ultra-High Vacuum (UHV)-Molecular Beam Epitaxy (MBE) deposition technique on top of large-area graphene films. Simultaneously, the Hall bar devices of Pt/Co were provided using the *in-situ* shadow mask patterning technique. Then, the Al_2O_3 capping layer was deposited by the UHE-MBE technique at room temperature to prevent surface oxidation.

For microstructural characterization of the heterostructures, the careful analysis of interface properties was performed using High Resolution (HR)-Transmission Electron Microscopy (TEM) and atomic force microscope (AFM), and the chemical properties of ultra-thin trilayered heterostructures were characterized by Raman Spectroscopy. The confirmation of the layered nature (RMS roughness less than 0.3 nm) within the heterostructures was confirmed by these surface analysis techniques. The Raman images of the thin film heterostructures suggested high purity of the grown films on the graphene. The fundamental properties have been employed to analyze the states and effects of graphene materials present in the heterostructures and devices.

The field-dependent magnetoresistance (FDMR) and angular-dependent magnetoresistance (ADMR) results provide evidence for the spin Hall magnetoresistance (SMR) effect. Considerably large spin Hall magnetoresistance (SMR) values of ~2.5% were observed at room temperature. In order to investigate the interface effects between the graphene and Co layer, a comparative study of spin transport was carried out for the Pt/Co devices with and without an ultra-thin MgO interlayer at the Co/graphene interface. For the Pt/Co Hall bar devices with the MgO interlayer, a decrease in the SMR effect was seen, as compared with the SMR effect measured in the Hall bar device without the MgO interlayer.

Our findings provide insights into the spin-orbit proximity effects in graphene-based heterostructures and guidelines for potential applications of two-dimensional materials for their integration towards next-generation spintronics.

Keywords: Spin Hall magnetoresistance, Graphene films , proximity effects, Two-dimensional materials

References

[1] W. Han, R. K. Kawakami and M. Gmitra, Nat. Nanotechnol., Vol. 9, p. 796 (2014)

[2] S.-Y. Huang, H.-L. Li and C.-W. Chong1, Sci. Rep., Vol.8, p. 108 (2018)

[3] J. Sawinska and J. I. Cerdá, New J. Phys., Vol.21, p. 073018 (2019)

Perpendicular Magnetoresistance sensor with Improved Thermal Stability

Taehyeong Jeon*, Jae Hoon Lee, Artem Talantsev and Cheol Gi Kim*
Department of Emerging Materials, DGIST, Daegu, 42988, Republic of Korea

Cross-junction과 Wheatstone bridge 모양으로 제작한 perpendicular magnetoresistance (PMR) sensor에서 뛰어난 온도안정성을 확인하였다. PMR 신호의 thermal drift는 zero-field PMR offset에 비례하며, 같은 제작방식을 가지는 anisotropic magnetoresistance (AMR) sensor와 비교하여 약 천 배 작은 thermal drift를 보였다. PMR의 thermal drift는 baseline drift와 signal amplitude drift로 나누어 생각할 수 있다. PMR offset으로 normalize한 baseline drift의 온도의존도는 전기저항의 온도의존도와 비슷하다. 따라서 PMR baseline drift의 온도의존도를 이용하면 한 번의 PMR 측정으로부터 thermal baseline drift를 계산할 수 있다. Signal amplitude drift는 PMR sensor의 패턴의 형태에 따라 다르게 관찰되었으며 선폭이 좁은 패턴에서 더 큰 demagnetizing field로 인한 magnetization misalignment 때문에 더 큰 signal amplitude drift가 나타난다. Baseline drift의 온도의존도와 signal amplitude drift의 온도의존도가 반대의 부호를 가지고 비슷한 크기의 진폭을 가지기 때문에 bridge-type PMR sensor에 조금의 비대칭성을 주어 baseline drift와 signal amplitude drift를 서로 상쇄시킬 수 있는 가능성을 확인하였다.

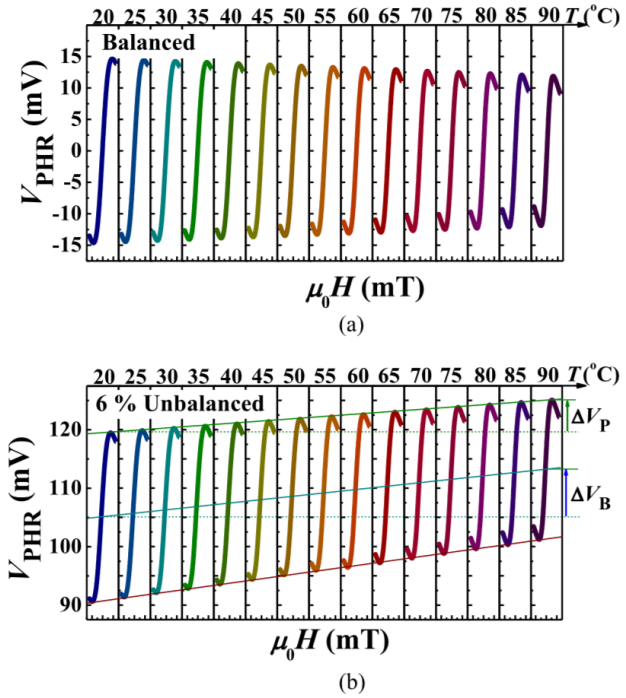

Fig. 1. PMR curves for (a) balanced and (b) unbalanced multiring PMR bridge sensor at 20-90℃

NS01

헬륨 이온조사를 이용한 CoO_X 박막의 국소적인 환원 현상

김지수[1*], 박은강[1], 이년종[1,2], 이택현[3], 양지석[3], 이기승[2], 유천열[2], 김갑진[3], 김상훈[1]
[1]울산대학교 물리학과
[2]대구경북과학기술원 신물질과학 전공
[3]한국과학기술원 물리학과

정보 저장 기술에서 자성체의 나노 패터닝은 아주 중요한 기술이라고 할 수 있다. 자성체의 경우 화학적 식각에 의한 패터닝을 사용하면, 자성체가 화학물질에 손상을 받기 쉽기 때문에 Ar 이온 등을 이용한 물리적 식각 방식을 주로 사용해 왔다. 그럼에도 불구하고, 자성체의 식각면에 발생하는 물리적 손상은 피할 수 없는 문제가 되어 왔다. 2012년, 수소이온에 의해 산화물인 Co_3O_4가 자성체이자 도체인 Co로의 환원이 가능하고, 그 현상을 이용하면 물리적인 식각 없이 자성 나노 패터닝이 가능하다고 보고가 되었다.[1] 물리적인 식각이 없을 뿐만 아니라 부도체 특성을 갖는 물질이 도체 특성을 갖게 되면서 자성 패터닝뿐만 아니라 전극 패턴이 가능하다는 것을 의미하기도 한다. 그러나, 수소이온의 경우 산화물이 가지고 있는 산소와 쉽게 반응을 하기 때문에 수소이온을 이용한 패터닝 방법은 게이트 산화물이 사용되는 반도체 회로 공정 단계에 쉽사리 포함되기 어렵다고 할 수 있다.

본 발표에서는 헬륨 이온 조사법을 이용하여 산화된 Co 박막의 국소적인 패턴이 가능함을 보여준다. 다양한 이온 조사법이 있으나 (Ar, PH_3, AsH_3 등) 조사되는 이온의 상대적으로 큰 질량으로 인해 발생하는 강한 kinetic energy 때문에 얇은 박막의 경우 손상을 피하기 어렵다. 이러한 시료의 손상을 최소화시키기 위해 상대적으로 질량이 가벼운 헬륨 이온을 사용하였다. 본 연구에서는 나노미터 이하 크기의 ion probe 덕분에 나노 구조의 이미징 및 제작이 가능한 헬륨 이온 현미경 시스템(HIM: He-Ion Microscope)이 활용되었다. 본 연구는 헬륨 이온을 통해 국소적인 나노 자성 및 전극 패터닝이 가능하다는 것을 보여주며, 이를 이용한 다양한 스핀트로닉스 소자의 개발을 기대할 수 있다.

Reference

[1] S Kim, et al. “Nanoscale patterning of complex magnetic nanostructures by reduction with low-energy protons” Nature Nanotechnology 7.9 (2012): 567-571.

입상 박막에서의 온도에 의한 보자력 특성

이동현[1*], Suzuki Ippei[2], Takahashi Yukiko[2], 김상훈[1*]
[1]울산대학교 물리학과
[2]National Institute for Materials Science (NIMS), Tsukuba 305-0047, Japan

자성박막은 초격자 물질, 다층 구조 물질과 같은 구조적 변화를 통해 수직 자화 이방성, 자기 저항 효과 등과 같은 다양한 현상을 유도하는 방식으로 연구가 진행되어왔다. 그중 입상 박막 (granular thin film)이란 한 자성층에서 지름이 수 나노 미터 크기의 자성 알갱이들이 형성되어진 것을 말한다. 이러한 입상 자성 박막은 열적 안정성이 아주 우수하면서도 작은 단위의 자구 (magnetic domain)을 형성할 수 있어 하드디스크 드라이브의 미디어 재료로 많은 연구가 되고 있다.

본 연구에서는 FePt-C 의 입상 박막의 온도에 따른 보자력 변화를 관찰하고, Sharrock 모델을 이용하여 열적 안정성을 평가한다.[1]

Reference

[1] M.P.Sharrock. “Time dependence of switching fields in magnetic recording media” *Applied Physics Letters* 76.10 (1994): 6413.

Structural and Magnetic Properties of Pure-Phase $BiFeO_3$ and $MnFe_2O_4$ Nanoparticles and their Nanocomposites

Inna Yusnila Khairani[1], Anindityo Nugra Arifiadi[1*], Jae-Hyeok Lee[1], Biswanath Bhoi[1], Sandeep Kumar Singh Patel[2], Sang-koog Kim[1]

[1]National Creative Research Center for Spin Dynamics and Spin-Wave Devices, Nanospinics Laboratory, Research Institute of Advanced Materials, Department of Materials Science and Engineering, Seoul National University, Seoul 151-744, South Korea

[2]Department of Chemistry, MMV, Banaras Hindu University, Varanasi-211005, India

This work reports the synthesis and the investigation of structural and magnetic properties of pure phase $BiFeO_3$ (BFO) and $MnFe_2O_4$ (MFO) nanoparticles and their nanocomposites (BMFO). BFO nanoparticles with an average size of 93.3 nm were synthesized using the sol-gel method while MFO nanoparticles with an average size of 70.5 nm were synthesized using the co-precipitation method. An equal molar of BFO and MFO were then mixed up, pressed and sintered to produce their nanocomposites. X-ray diffraction patterns show that the phase purities of BFO and MFO were maintained even after sintering of the composite. The saturation magnetization values (M_s) of BFO, MFO, and BMFO were 4.9, 52, and 33 emu/g, respectively. The BMFO nanocomposite shows an enhanced value of M_s compared to those of BFO-MFO bulk composite previously reported [1]. This enhanced M_s value can be attributed to the presence of Fe^{2+} in BFO.

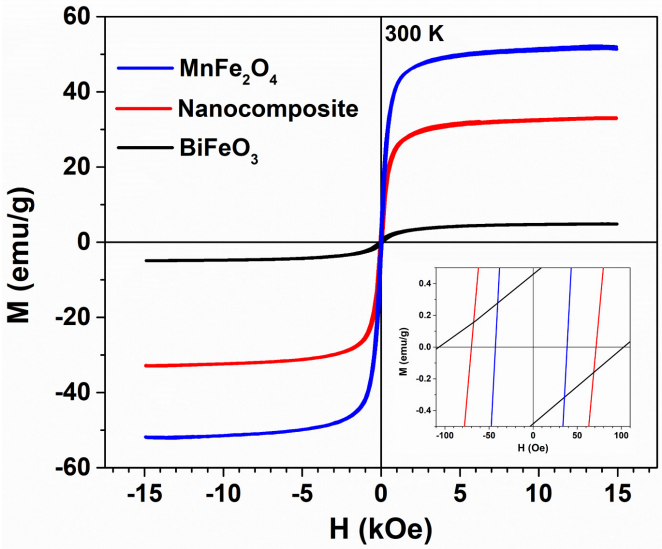

Fig. 1. M-H loops of BFO, MFO and their nanocomposite measured ad 300K. The inset shows the magnification at low field strength

Reference

[1] A. Kumar, K.L. Yadav, Synthesis and characterization of $MnFe_2O_4$–$BiFeO_3$ multiferroic composites, Physica B, 406 (2011) 1763-1766. https://doi.org/10.1016/j.physb.2011.02.023

Wireless Controllable, 2D and 3D Actuations of Magnetic Kirigami Patterns

Trivoramai Jiralerspong[2], Geonhee Bae[3], Minho Yun[1*], Jae-Hyeok Lee[1], Sang-Koog Kim[1†]
[1]National Creative Research Initiative Center for Spin Dynamics and Spin-Wave Devices, Nanospinics Laboratory, Research Institute of Advanced Materials, Department of Materials Science and Engineering, Seoul National University, Seoul 151-744, Republic of Korea
[2]Current address: 15/2 Montri Road, Tambol TaladYai, Amphur Muang, Phuket, Thailand
[3]Current address: 1, Samsungjeonja-ro, Hwaseong-si, Gyeonggi-do, Republic of Korea
Corresponding author: sangkoog@snu.ac.kr

1. Introduction

The art of paper cutting, kirigami, and its shape transformation capabilities have shown remarkable advancements in the field of science and engineering. A kirigami pattern consists of cuts that are made on a single sheet of material, where planar mechanical deformations could induce shape transformations in both two-dimensional (2D) and three-dimensional (3D) [1]. Due to this remarkable property, kirigami patterns could give rise to complex material properties such as auxetics and mechanical metamaterials where they expand when subjected planar deformations [2]. However, the mechanical deformations of kirigami structures are usually performed physically by hand or machine, and therefore limiting its application in small and tight spaces where access is difficult [3]. To counter this problem, this study proposes a remote-control technique of kirigami patterns using magnetic fields as an external stimulus [4].

2. Method and Results

In this study, the remote control of kirigami patterns in 2D and 3D are achieved by programming the magnetic anisotropy of magnetic nanoparticle (MNP) chains within the magnetic-elastomer composite [5]. The magnetic-elastomer composite is a type of magnetorheological elastomer that is composed of iron oxide (Fe_3O_4) nanoparticles and silicone elastomer. To bring about the 2D and 3D shape transformation, the MNP chains are aligned in-plane and out-of-plane, respectively. The in-plane orientation is performed by aligning the mold and hence the MNP chains along the xy-plane. Likewise, the out-of-plane chain orientation is obtained by placing the mold along the xz-plane by means of a 3D printed jig. The chains are permanently embedded within the composite once the elastomer is cured, even after the removal of the field. The kirigami patterns considered consists of multiple unit shapes that are connected by hinges [6]. Various 2D and 3D shape transformations are produced by changing the magnetic anisotropy within each unit shape and the placement of the hinges. The fabrication and the experimental procedures are performed under a uniform magnetic field that is generated by an electromagnet. The experiment is conducted under a uniform magnetic field of approximately 180 mT that is produced by an electromagnet. Experimental results show that the embedded chains within the kirigami patterns respond quickly to align its magnetic moment along the direction of the applied magnetic field.

3. Discussion

This study has demonstrated the remote 2D and 3D actuation of magnetic kirigami patterns by programming the magnetic anisotropy of each unit shape within the kirigami pattern, which allow the kirigami patterns to be controllable under an applied uniform magnetic field. In other words, by aligning the MNP chains within each unit shape in-plane and out-of-plane, 2D and 3D shape transformation can be achieved, respectively. Due to magnetic anisotropy, the functionalized unit shapes turn to align the embedded chains with the direction of the applied external magnetic field. Depending on the direction and the angle that the chains make with respect to the applied field, as well as the location of the hinges of the kirigami patterns, a variety of kirigami structures can be fabricated.

4. Conclusion

Remote actuation of kirigami patterns in 2D and 3D can be realized through in-plane and out-of-plane alignment of the MNPs, respectively. It is shown that by aligning the MNP chains in different directions and changing the hinge location within the kirigami pattern, several shape transformation can be obtained. This untethered actuation of kirigami patterns therefore have potential applications in areas such as drug delivery, medical patches, and artificial valves.

References

[1] X. Ren, R. Das, P. Tran, T. D. Ngo, and Y. M. Xie, Smart Mater. Struct. 27, 2018.

[2] A. Rafsanjani and K. Bertoldi, Phys. Rev. Lett. 118, 1, 2017.

[3] K. Bertoldi, V. Vitelli, J. Christensen, and M. Van Hecke, Nat. Rev. Mater. 2, 2017.

[4] R. M. Erb, J. J. Martin, R. Soheilian, C. Pan, and J. R. Barber, Adv. Funct. Mater. 26, 3859, 2016.

[5] Geonhee Bae, “Motion Control of Fractal Structure Magnetic Actuator Embedded with Chained Iron Oxide Nanoparticles”, Master’s thesis, Seoul National University, 2018; Trivoramai Jiralerspong, “Controllable Actuation of Magnetic Kirigami Patterns”, Master’s thesis, Seoul National University, 2019.

[6] V. Kunin, S. Yang, Y. Cho, P. Deymier, and D. J. Srolovitz, Extrem. Mech. Lett. 6, 103, 2016.

This research was supported by the Basic Science Research Program through the National Research Foundation of Korea (NRF) funded by the Ministry of Science, ICT & Future Planning (NRF-2018R1A2A1A05078913).

Electromagnetic Wave Absorption Properties of Core-Shell Ni/CuSiO3 Nanocomposite

Taha Latif*, Rambabu Kuchi, Jong-Ryul Jeong†
Department of Materials Science and Engineering, Graduate School of Energy Science and Technology, Chungnam Nationa University, Daejeon 34134, South Korea

In this study, we have investigated core-shell Ni/CuSiO3 nanospheres with a controllable shell (CuSiO3) thickness to enhance microwave wave absorption properties. The effects of shell thickness on electromagnetic wave properties were investigated. The electromagnetic wave absorption measurement demonstrates that the Ni/CuSiO3 core-shell nanocomposites with shell thickness of 30 nm, show a strong reflection loss peak of –39.5 dB, and have a wide effective absorbing bandwidth from 7.8 GHz to 12.6 GHz. It was also found that the rambutan-like core-shell Ni/CuSiO3 composite nanospheres with a proper shell thickness resulting in the high microwave absorption performance. It can be attributed to the novel structure which could enhances the interfacial polarization, controlled shell thickness results the good match between electromagnetic properties (ε, μ) and magnetic loss from the ferromagnetic Ni. Thus, we believe that a controlled shell thickness in core-shell Ni/CuSiO3 composite nanospheres establishes a novel approach to attain high-performance electromagnetic wave absorbers in the field of electromagnetic wave absorption.

Synthesis of Bi-YIG Thin Films and Role of poly[vinylpyrrolidone](PVP) in Metallo-Organic Decomposition (MOD) Method

Trinh Nguyen Thi*, Viet Dongquoc, Jong-Ryul Jeong†
Department of Materials Science and Engineering, Graduate School of Energy Science and Technology, Chungnam Nationa University, Daejeon 34134, South Korea

In this study, we have synthesized Bi-YIG (Bi substituted yttrium iron garnet) thin film using modified metallo-organic decomposition method. To control the structural and magnetic properties of Bi-YIG thin film, we have introduced polyvinylpyrrolidone (PVP) as a reducing agent and growth modifier. The magneto-optical properties of the Bi-YIG film including Faraday rotation were measured. We obtained the highest value of Faraday rotation up −8.0°/μm by using a SiO_2 substrate. $Bi_xY_{3-x}Fe_5O_{12}$ films with different Bi concentration were also investigated to enhance the magneto-optical properties of Bi-YIG films. This study demonstrates that high-quality Bi-YIG thin films can be grown on a SiO_2 substrate by using an all metal nitrate precursor with PVP additive.

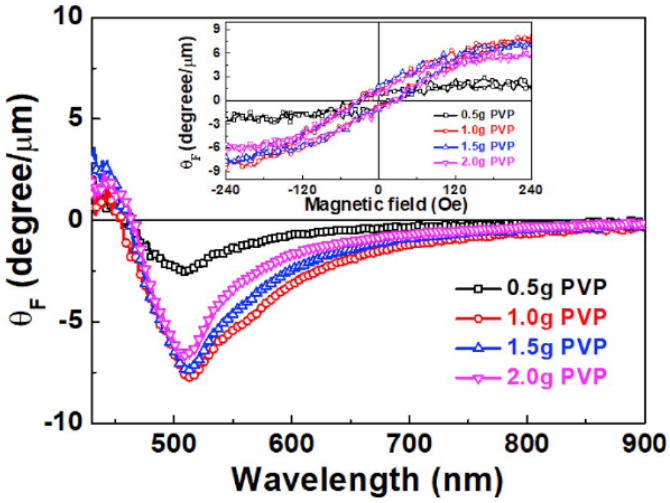

Fig. 1. Dependence of Faraday rotation spectrum of Bi-YIG/SiO_2 thin films on PVP concentration.

Effect of target composition on surface morphology and magnetic properties of thulium iron garnet thin films deposited by facing target sputtering

Duc Duong Viet*, Phuoc Cao Van, Hayeong Ahn, Trinh Nguyen Thi, Jong-Ryul Jeong†
Department of Materials Science and Engineering, Graduate School of Energy Science and Technology, Chungnam Nationa University, Daejeon 34134, South Korea

In this study, we have investigated the effect of target composition on the magnetic properties and surface morphology of thulium iron garnet (TmIG – Tm3Fe5O12) thin films which are grown on {111} gadolinium gallium garnet (GGG – Gd3Ga5O12) substrates via facing target sputtering method. The composition of films was controlled by changing the ratio of precursor powders which were used as the source of the target material. Then the quality of the prepared films was analyzed by atomic force microscopy (AFM), vibration sample magnetometer (VSM) to investigate surface morphology, magnetic properties, respectively. Other techniques such as X-ray photoelectron spectroscopy (XPS), transmission electron microscopy (TEM) have also been introduced to study the crystalline structure of TmIG films. The results show the strong dependence of magnetic anisotropy as well as surface morphology to the composition of the TmIG films. It proved the importance of stoichiometry to the overall quality of the films. Moreover, we also observed that the magnetic anisotropy of sputtered films is significantly changed corresponding to the film of 20 - 60nm thick. The high-quality 20nm film exhibited the strongest perpendicular magnetic anisotropy (PMA), and the saturation magnetization at room temperature was estimated at approximately 90 emu/cm^3 with a low coercivity value (13 Oe).

Plasmon resonance induced thermal gradient in Au nanoparticle embedded Pt/YIG bilayers

Phuoc Cao Van*, Srivathsava Surabhi, Jong-Ryul Jeong†
Department of Materials Science and Engineering, Graduate School of Energy Science and Technology,
Chungnam Nationa University, Daejeon 34134, South Korea

In this study, we have investigated the variation of longitudinal Spin Seebeck effect (LSSE) in Au nanoparticle embedded Pt/Y3Fe5O12 (YIG) bilayers grown on Gd3Ga5O12 (GGG) substrate via rf-sputtering method. Specifically, detailed mechanism of the plasmonic spin current in company with plasmonic heating phenomena induced by continuous laser illumination was studied. The effects of each type of spin generation was observed by using particular samples under different laser power and wavelength. In the Pt/YIG/Au NPs/GGG sample, the relative position of Au NPs to YIG makes it generating the inverse thermal gradient (∇T) to the external ∇T caused by the laser source. When laser's wavelength fulfils the SPR condition, there is breakdown point of the SSE voltage dependence on laser power around 25 mW. The experimental results show the dominance of plasmonic spin current generation effect over the SSE signal caused by the plasmonic heating effect at the low laser power region.

펄스자기장이 적혈구의 응집성과 변형성에 미치는 영향

방승환[*], **이현숙**[†]
상지대학교 보건과학대학 한방의료공학과, 강원 원주시 상지대길 84, 26339

적혈구의 유변학적 특징인 응집성과 변형성은 인체내 혈액순환에 중요한 역할을 하고 있기에, 본 연구에서는 펄스 자기장 자극 시 적혈구의 응집성과 변형성이 어떤 영향을 받는지 관측하여 혈액순환 장애와 관련된 질병 예측 및 치료에 대한 자기장의 역할을 규명하고자 하였다. ESR(erythrocyte sedimentation rate) 실험을 이용하여 자기장의 유무에 따른 적혈구의 응집성을 측정하였으며, 펄스자기장의 자극 세기를 조절함으로써 자기장세기에 따른 적혈구 응집성 변화를 확인하였고 산화제인 tBhp(tert-Butyl hydroperoxide)를 이용하여 인위적인 병증을 적혈구에 유발시킨 후 산화 처리에 따른 자기장의 효과를 측정하였다. 자기장을 인가한 적혈구는 자기장을 인가하지 않은 적혈구보다 19% 적게 침강하는 것으로 관측되어 적혈구 응집성이 개선됨을 확인하였다. 또한 산화 처리한 적혈구 또한 자기장인가 후 응집성이 감소되어 펄스자기장 자극이 적혈구 응집성에 치료효과를 주는 것으로 예상된다. 적혈구 변형성은 5㎛의 크기를 갖는 필터를 이용하여 필터 크기보다 큰 7-8㎛ 크기를 갖는 여과된 적혈구의 개수를 측정함으로서 관측하였는데, 자기장자극 세기와 산화처리된 적혈구, verapamil로 환원한 적혈구에 대해 자기장의 효과에 대한 분석을 하였다. Fig. 1은 필터에 여과된 상대적 적혈구의 개수를 대조군과 비교하여 나타낸 것이다. 400G, 1000G, 2700G를 인가하였을 때 인가하지 않은 적혈구보다 여과된 적혈구의 개수가 증가하여 verapamil과 같이 적혈구의 변형성을 개선시켜주는 것을 확인할 수 있었으며 최적의 자기장 세기는 2700G로 알 수 있었다. 또한 병증이 유발된 tBhp 처리군에 자기장을 인가 하였을 때 적혈구의 변형성이 개선되는 것을 확인하였다. 이는 강한 펄스자기장 자극이 적혈구 막 전하에 영향을 줌으로서 zeta potential의 변화로 적혈구의 응집성과 변형성에 영향을 미치는 것으로 생각된다. 그러므로 펄스자기장의 자극은 인체의 혈액순환, 장애인 협심증, 심혈관 질환, 심근경색증과 같은 질병 예방과 치료에 비침습적인 치료법으로 제안될 수 있다.

주제어: 펄스 자기장, 적혈구 변형성, 적혈구 응집성

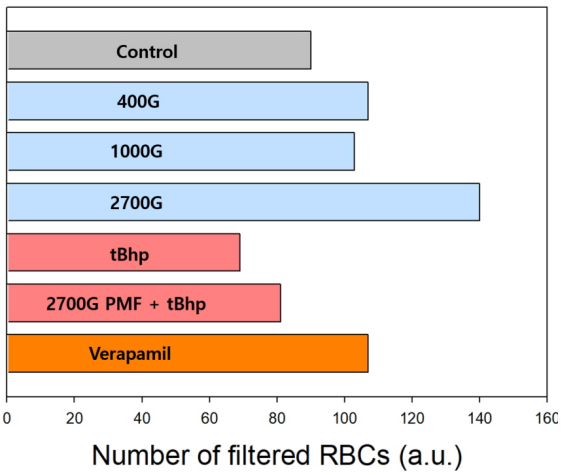

Fig. 1. Numbers of filtered RBCs under pulsed magnetic field of 400G, 1000G and 2700G

Optical spin-polarization and NMR detection of Xe isotopes in Rb-^{129}Xe/^{131}Xe-N_2 gas cells for Atom Spin Gyroscopes

Deok Young Lee*, Sangkyung Lee, Sin Hyuk Yim, Kyumin Shim
Agency for Defense Development, Daejeon, Korea

Atom spin gyroscopes(ASG) sense rotation rates based on Larmor frequency measurement of spin-polarized noble gas atoms. In ASGs, the pump beam for optically spin-polarizing alkali atoms and the probe beam for detecting optical Faraday rotation propagate perpendicularly to each other in the alkali-noble gas-buffer gas cell. Collisions between optically spin-polarized alkali atoms and noble gas atoms transfer spin polarization from alkali atoms to noble gas atoms and vice-versa. They cause a nuclear spin polarization of noble gas atoms and impart precession of the nuclear spin polarization to the alkali spin polarization.

In our experiment, the atomic vapor cell filled with gas mixture containing vapor Rb, ^{129}Xe, ^{131}Xe, and N_2(4% H_2) is applied. The transverse spin relaxation time (T_2) of each ^{129}Xe and ^{131}Xe in the gas cell is measured by the free induction decay(FID) method. The FID signal is measured by applying a $\pi/2$ pulse along y-axis and recording the Faraday rotation angle depending on the nuclear spin precession projected on the xy-plane. We extract the T_2 time by fitting the damping FID signal to an exponential function. Specifically, we measure the transverse relaxation time as a function of magnetic field gradients in order to maximize the transverse relaxation time. This magnetic field gradient optimization is able to reduce the angular random walk of our ASG.

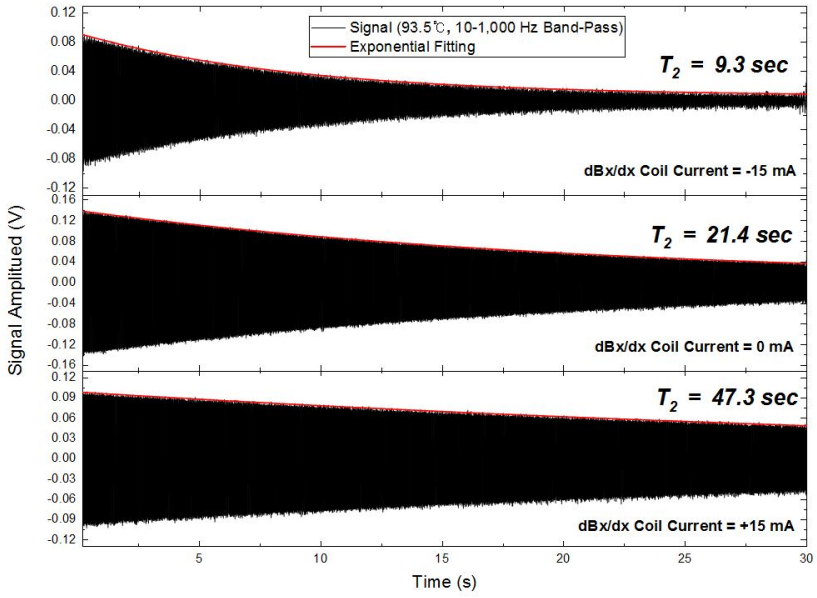

Fig. 1. FID signal and Transverse relaxation time of ^{129}Xe with various magnetic field gradient($\partial B_x/\partial x$).

Development of DOI Detector for PET using Different Kinds of Reflectors

Seung-Jae Lee[1*], Cheol-Ha Baek[2†]
[1]Department of Radiological Science, Dongseo University, Korea
[2]Department of Radiological Science, Kangwon National University, Korea

We developed a depth of interaction (DOI) detector for positron emission tomography (PET) using different kinds of reflectors. The detector module consists of two layers of scintillator arrays, which was composed of 4 x 4 Gadolinium Aluminum Gallium Garnet (GAGG) crystals of size 3 mm x 3 mm x 10 mm, and 4 x 4 silicon photomultiplier (SiPM) arrays. The bottom layer optically coupled to the SiPM used a diffuse reflector and the top layer used a specular reflector. The layer interacted with gamma ray and crystal could be determined by analyzing the signal size because it obtained for each layer is different by using different reflectors for the crystals for each layer. The detector performance was analyzed by the flood image, energy spectrum with two photoelectric peaks, and energy resolution. In the experiment for the detector module performance, all pixels in the flood map were well decoded, and the energy spectrum of each pixel is measured with two photo peaks.

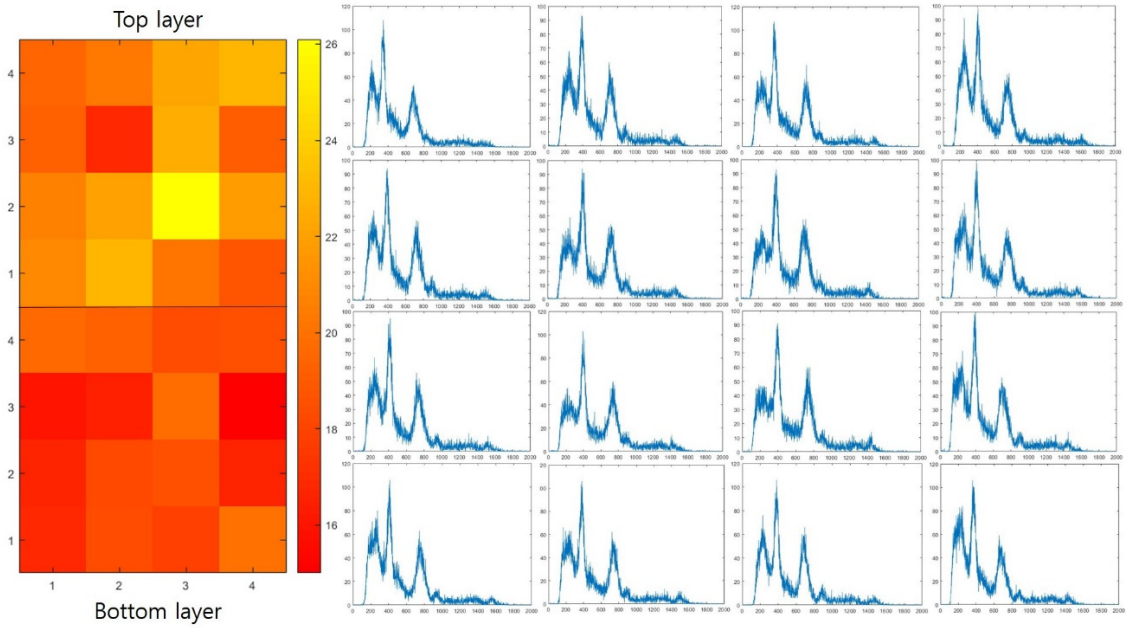

Fig. 1. Energy resolution distribution (left) and energy spectra (right) corresponding to each pixel position in the flood image

입력 임피던스 측정을 통한 자기 클러치 변위 계측

김경원*, 신광호†
경성대학교 정보통신공학과

자기 클러치는 자동차 파워트레인에 사용되는 부품 중 하나로서, 특히 사륜구동차량의 동력전달을 조절하기 위해서 필수적으로 사용된다. 자기 클러치는 솔레노이드형태의 코일과 자성체(저탄소강) 자기회로를 이용하여서 제작되며, 솔레노이드 코일에 일정 크기 이상의 전류를 인가하면 자기회로의 일부분인 Plunger가 변위와 힘을 발생시키는 구조를 가지고 있다. 자기클러치의 Plunger는 부품의 노화, 철가루 등 이물질의 삽입, 편심 발생 등의 요인에 의해서 오동작을 일으킬 수 있으며, 이러한 경우에는 정해진 크기 이상의 전류를 인가함으로써 오동작을 방지하여야 한다. 또한, 자기클러치의 작동이 정상적인 경우에는 Plunger가 변위를 일으키는 최소한의 전류를 인가하여 동작시킬 수 있다면 에너지 절감에 도움이 된다. 이러한 상황을 위해서는, 자기클러치의 Plunger의 변위를 계측할 수 있는 방안이 마련되어야 하며, 변위센서를 이용할 수 있다. 본 연구에서는 자기클러치의 Plunger변위 계측을 위해서 입력 전력 임피던스의 이용 가능성에 대해서 조사하고 있다. 자기클러치에 인가되는 전류는 물론 Plunger의 변위에 의해서 자기회로에 변화가 야기되기 때문에 전류인가 및 변위에 따르는 임피던스의 변화가 발생하게 된다. 본 발표에서는 임피던스 계측을 통한 자기클러치의 변위 계측에 대한 실험결과에 대해서 보고 한다.

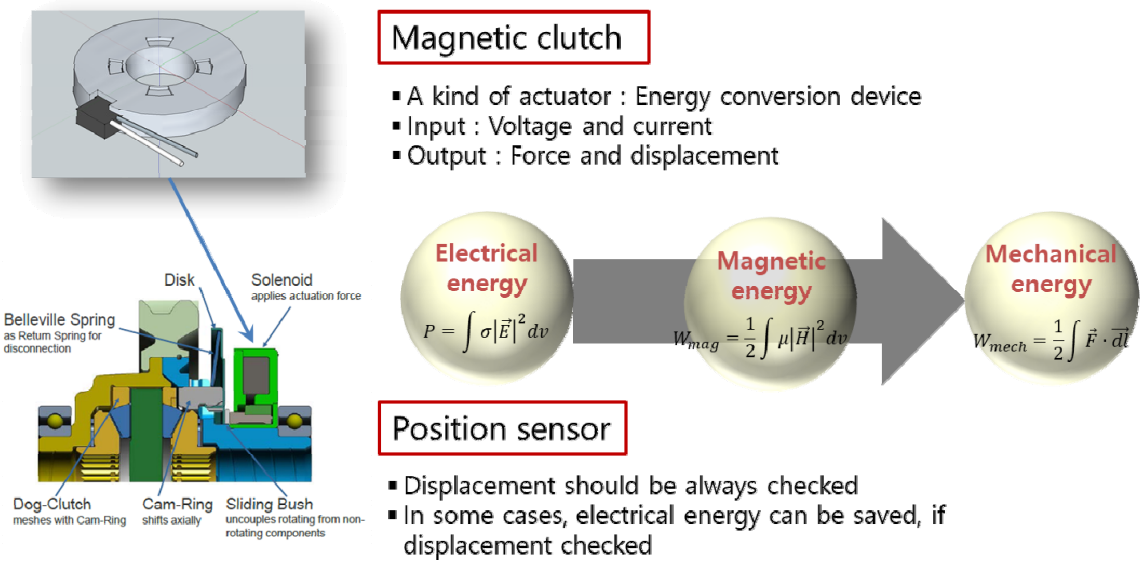

Fig. 1. Magnetic clutch and its position sensor.

KMS 2020 Summer Conference

Special Session I

‘Magnetic For IOT’

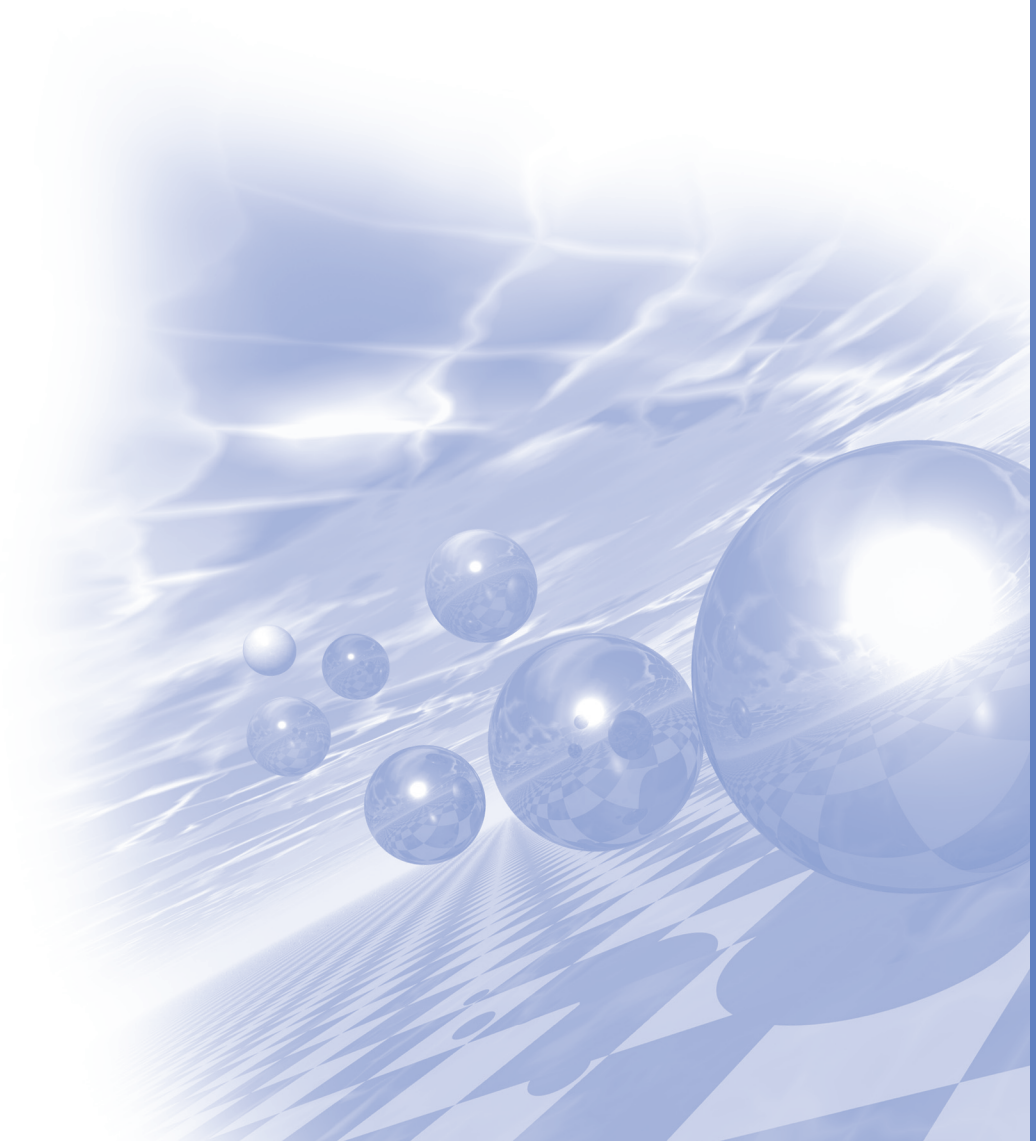

해저 매설 자기 센서의 해수 유동 영향 분석

배기웅[1*], 정현주[1], 조진석[2]
[1]해양기술연구원, 국방과학연구소
[2]해양2연구소, LIGNex1

강자성체에 의해 발생되는 자기 신호는 전자기파에 비해 수중에서 상대적으로 신호 감쇄가 적으므로, 음향 신호와 더불어 대표적인 수중 탐지 수단으로 활용되고 있다. 플럭스게이트(fluxgate) 센서는 부피, 소모 전력, 비용, 안정도, 잡음 수준 등의 측면에서 해저 매설에 적합한 자기센서 중의 하나이다. 최근 센서 제작 공정과 신호처리기술의 발전으로 플럭스게이트 센서의 자체 잡음 수준이 수백 pT 이하로 개선됨에 따라, 과거에 비해 탐지 범위가 더 넓어지고 있다. 국내에서도 수중 침투 위협 세력을 탐지하기 위해 플럭스게이트 자기센서로 구성된 해저 매설형 센서 시스템이 개발되어 운용 중이다. [1]

해저에 매설된 자기센서는 지구 자기장 변화, 해수 유동에 의한 자기장 변화, 인간 활동으로 인한 환경 자기장 변화 등 다양한 환경 잡음에 노출되어 있다. 이러한 잡음은 자기센서의 표적 탐지 정확도에 민감한 영향을 주므로, 정밀 분석이 필요하다. 본 논문에서는 해저에 매설된 자기센서의 파고에 따른 신호 관측 결과를 분석하였다. 또 기상청 청양 육상 관측소에 설치된 자기센서 측정값과의 비교를 통해 매설한 자기센서의 정확도를 검증하였다.

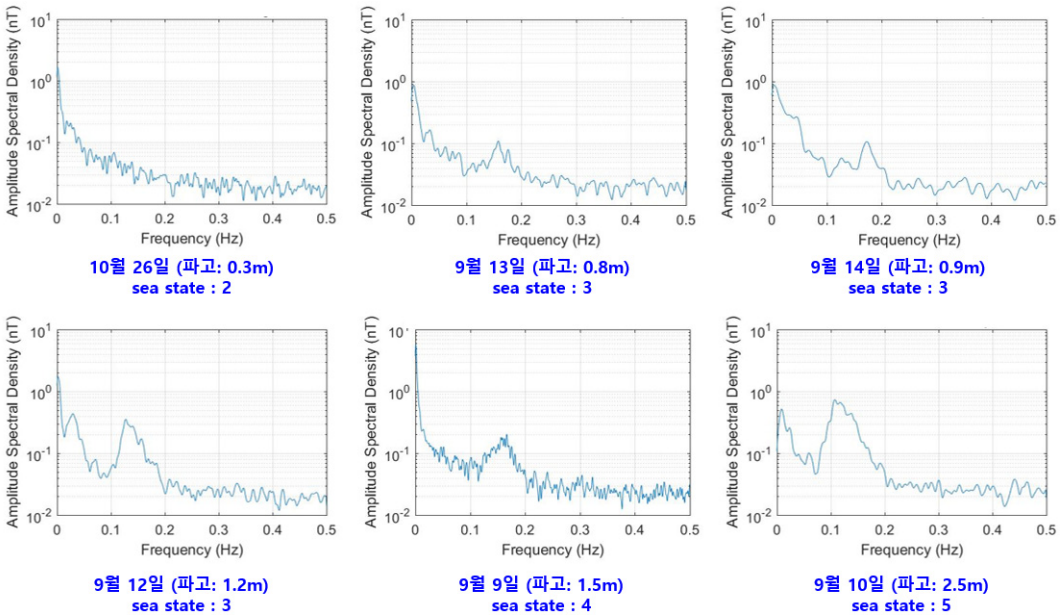

그림 1. 매설 지역의 파고에 따른 자기장 크기(주파수 영역)

그림 1은 매설 장소에서 2018년 9월~10월 간에 발생한 다양한 파고 상황 하에서 관측한 자기장 값이다. 관측 시간은 20분 이상이었고, Welch 기법을 적용하여 스펙트럼 밀도를 계산하였다. 파고는 매설 해역에서 약 20km 거리에 위치한 기상청 파고 부이 관측 기록을 참고하였다. 기상청 기록에 따르면, 측정 시 파의 주기는 4~8초였으며, 이는 0.125~0.25Hz 주파수 대역에 해당한다. 그림 1에서 0.1~0.2Hz 대역에서 피크가 관측된 것을 확인할 수 있다. 파고가 0.3m 일 때는 자기센서 잡음 수준 이하이므로 관측되지 않았으며, 파고 0.8m 이상

일 때는 관측되었다. 대체로 파고에 비례하여 피크의 크기가 커지는 것을 확인할 수 있었다. 다만 9월 9일에는 9월 12일보다 파고가 높았음에도 자기 신호 피크값은 더 감소하였다. 이는, 0.1～0.2Hz 대역에서 자기센서 측정값에 영향을 미치는 요인이 파고 이외에 장 주기의 너울(long-term swell) 등이 포함되어 있기 때문이다. 피크 주파수 대역 및 크기가 대체로 파고에 비례하는 점을 고려할 때, 해당 신호는 해수 유동으로 인한 신호로 추정할 수 있다. [2]

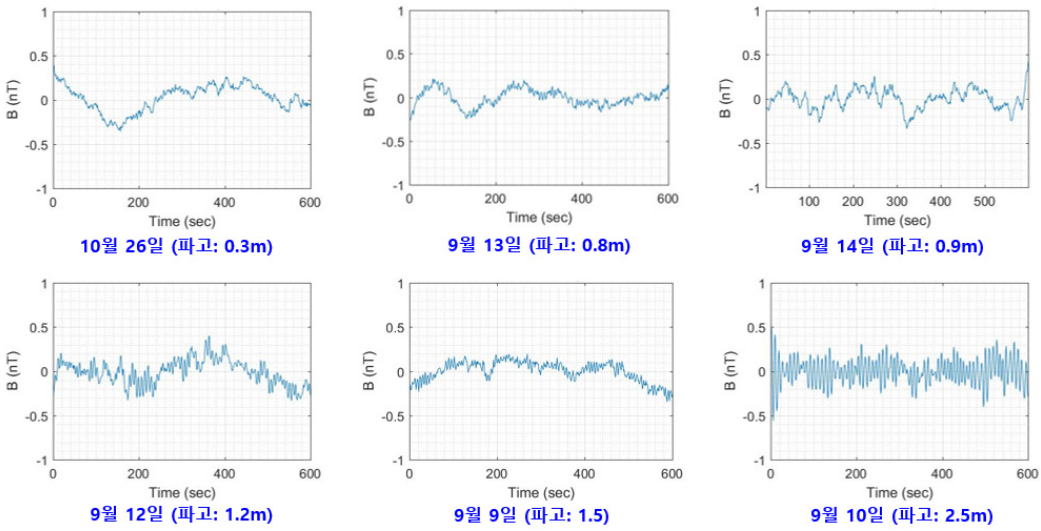

그림 2. 매설 지역의 파고에 따른 자기장 크기(시간 영역)

그림 2는 그림 1의 시간 영역 데이터이며, 10분간 계측된 합성 자기장 신호이다. 5차 함수로 곡선 보정하여 지구자기장에 의한 일변화를 제거하였고, 신호 리플의 크기와 파고가 대체로 비례함을 볼 수 있다.

그림 3은 해저 매설 지역에 부설된 자기센서와 매설 지역으로부터 약 250km 거리에 있는 기상청 청양 육상 관측소에서 표준 자기센서로부터 계측된 자기장 변화를 보여주고 있다. 관측 기간은 2018년 12월 14일 금요일 15시～16일 일요일 17시이며, 50시간이다. 두 장소 간 자기장의 평균 차이는 약 687nT였고, 이는 두 장소 간 지구 자기장 크기 차이로 추정된다. 두 관측 장소에서의 그래프 변화 양상이 유사한 점으로 볼 때, 해저 매설된 자기센서의 성능은 우수한 것으로 확인되며, 또한 이 양상은 자성체의 이동, 해수 유동 등의 국부적인 영향이 아니라, 지구 자기장의 일변화 등의 거시적 영향임을 알 수 있다. 향후 매설 자기센서의 표적 탐지 정확도 향상을 위해 추가 연구를 진행할 예정이다.

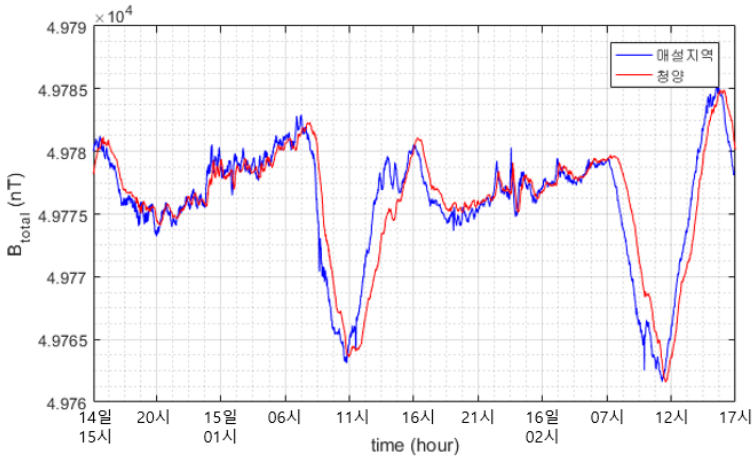

그림 3. 매설 지역 및 청양 지역 자기센서 측정값 비교

References

[1] 신증호, “해저매설형 음향센서 시스템의 내구성 검증 방안에 대한 연구,” 한국해안・해양공학회논문집, 29(3), pp.147-153, 2017년 6월.

[2] T. H. C. Herbers, P. F. Jessen, “Observing Ocean Surface Waves with GPS-Tracked Buoys,” Journal of Atmospheric and Oceanic Technology, vol. 29, pp.944-959, July 2012.

The RPM measurement techniques of the shell using by the magnetic sensor

Dong-Phil Han*, Se-Keun Oh, Young-Won Kim
㈜한화 종합연구소
*Corresponding author: 042-336-0493, dphan@hanwha.com

포탄과 같은 고충격 조건에서 5,000RPM이상으로 고속 회전하는 포탄의 회전수를 정밀하게 측정하는 방법을 개발하였다. 회전수 측정을 위해 계측용 신관에 자기센서를 장착하고 원격측정장치(Telemetry)를 통하여 데이터를 수집하였다. 데이터를 분석하여 포탄의 비행 초기구간부터 종말 단계까지 포탄의 회전수를 도출하였다.

1. 서론

포탄 개발시 탄도계산을 위해 포탄의 정확한 회전수 측정이 필요하다. 과거 포탄의 회전수는 포탄이 발사될 때 초고속카메라로 측정하였다. 초고속카메라는 정확하게 측정이 가능하지만, 발사 초기에만 측정 가능한 단점이 있다. 포탄 비행 전구간에서 회전수를 측정하기 위해서는 포발사시 발생하는 고충격 상황에서 생존하는 센서가 필요하고, 센서에서 측정된 값을 지상으로 송신하는 원격측정기술도 필요하다. 선진국에서는 각종센서(광센서와 자기센서)를 신관에 장착하여 회전수를 측정하는 계측용 신관을 개발하였다.[1][2]

2. 본론

회전수 계측용신관은 내부에 자기장에 반응하는 자기센서를 탑재하고, 계측된 값을 지상으로 전송하는 원격측정장치가 장착된다. 계측용 신관은 155mm탄에 장착 가능한 외형을 가진다. 주요 구성품인 배터리 모듈, 원격측정장치 모듈, 계측센서모듈로 구성되며 00,000G's의 내고충격성을 가져야 한다. 2축 자기센서(0 °, 90°)와 안테나는 신관의 앞쪽의 비금속 부분에 배치하여 지구자기장에 반응하도록 하였다.

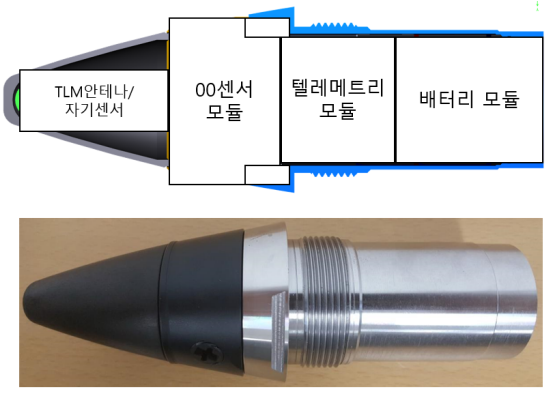

Fig. 1. 계측신관

2.1 전송데이터

지구자기장에 반응한 자기센서 값은 계측신관 최대 회전수의 20배인 6kHz 샘플링 하였다. 지상으로 전송되는 프레임의 주기는 100Hz이므로 빠짐없이 계측데이터를 전송하기 위해서 프레임당 60개의 측정데이터를 배치하였다.

시간(sec)	Magnetic-01	Magnetic-02	Magnetic-03	Magnetic-04	...	Magnetic-60
0	1.63365625	1.68721875	1.74078125	1.821125		1.821125
0.01	1.68721875	1.620265625	1.593484375	1.620265625		1.593484375
0.02	1.821125	1.861296875	1.861296875	1.861296875		1.8746875
0.03	1.539921875	1.593484375	1.606875	1.647046875		1.63365625
0.04	1.861296875	1.821125	1.79434375	1.754171875		1.700609375
0.05	1.6604375	1.68721875	1.754171875	1.7675625		1.79434375
0.06	1.620265625	1.620265625	1.593484375	1.593484375		1.566703125
0.07	1.834515625	1.888078125	1.888078125	1.888078125		1.821125
0.08	1.52653125	1.593484375	1.606875	1.620265625		1.63365625
0.09	1.834515625	1.780953125	1.7675625	1.700609375		1.63365625
0.1	1.74078125	1.7675625	1.780953125	1.807734375		1.807734375

Fig. 2. 전송데이터

2.2 시험결과

포발사 조건은 K-9화포, 추진장약 00, 포발사 고각은 00°이다. 총 4발을 발사하여 회전수를 측정하였으며, 측정결과 발사초기 회전수는 예측치와 유사함을 확인하였다. 종말단계에서는 500RPM 감소됨을 알 수 있었다.

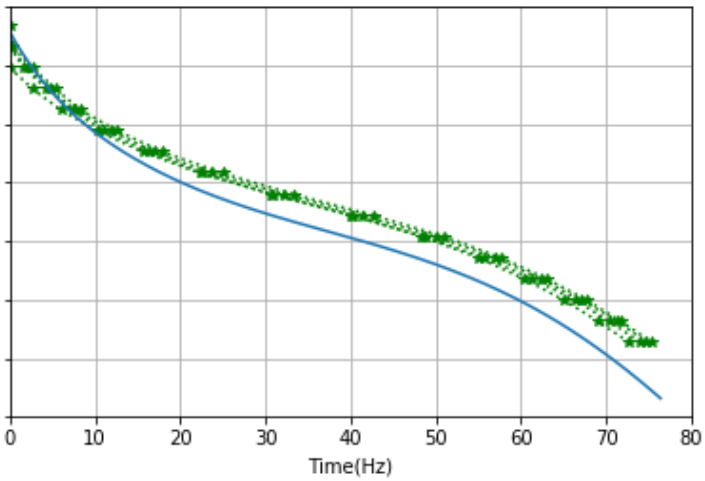

Fig. 3. 회전수 측정결과

3. 결론

자기센서와 원격측정장치가 내장된 회전수 계측용 신관을 개발하였고, 포발사시험을 통해 비행 전구간에 대한 회전수를 측정하였다. 회전수 측정결과 포탄의 종말 회전수는 그림 3과 같이 예측치에 비해 평균 500RPM 감소됨을 알 수 있었다.

후기

본 연구는 국방과학연구소 지상기술연구원 1부의 지원을 받아 이루어졌음에 감사드립니다.

References

[1] Martin Becker, “Yaw sonde and radar data reduction to obtain aerodynamic coefficients”, AD-787074, Naval Weapons Laboratory, 1974

[2] Eugene M. Ferguson, David J. Hepner, Wallace H. Clay, “Multisensor Pinhole Yawsonde, AD-A271715, U.S. Army Research Laboratory, 1993

알칼리 원자 - 버퍼가스 셀을 이용한 센서

김태현*, 임신혁, 이상경, 심규민
국방과학연구소 국방첨단기술연구원

美 DARPA(Defense Advanced Research Projects Agency)에서는 CSACs(chip scale atomic clocks), Micro-PNT (Micro-Technology for positioning, Navigation and time) 프로그램 등과 같이 원자를 이용하여 기존 센서보다 더 우수한 센서에 대해서 투자하고 있다. 특히, 원자를 이용한 센서들 중 초소형 원자시계 및 원자 자력계는 상용화가 되어 위성항법시스템, 군용 및 상용 장치로 개발되었다. 이에 국방과학연구소에서도 알칼리 원자 – 버퍼가스 셀에서 특정 원자의 스핀정보를 활용한 센서에 대해 연구를 하고 있다.

본 발표에서는 잠수함 탐지에 쓰이는 해외의 원자 자력계 및 원자 스핀 자이로스코프에 대해서 소개하고 이 원자 센서에 핵심인 국방과학연구소에서 제작한 알칼리 원자 – 버퍼가스 셀제작 시스템 및 제작된 셀을 소개하려 한다.

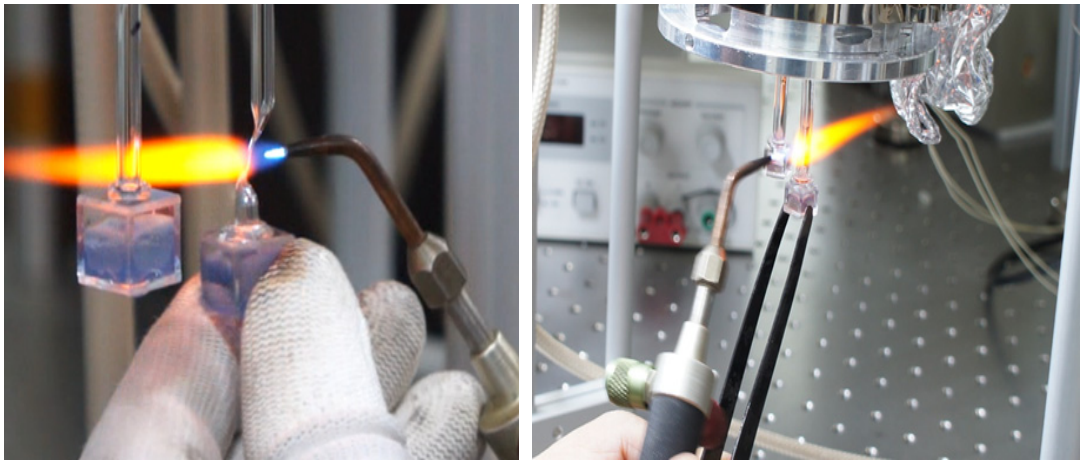

그림 1. 알칼리원자-버퍼가스셀 제작 공정 (좌) 내부 12.5mm 셀, (우) 내부 5 mm 셀

UXO 탐지용 자력계의 무인기적용에 관한 연구

손대락[1*], 김은애[2], 정순목[2]
[1]한남대학교
[2]주)센서피아

컴퓨터와 통신기술의 발달로 많은 분야에서 무인기술이 적용되고 있다. 군사분야에서도 병역자원의 한계에 의한 무인감시, 안전성이 고려된 위험지역의 지뢰탐지 및 제거가 그 대표적인 예이다. 군방분야에 사용되는 대부분의 무기체계가 철강재로 되어있고, 지구가 거대한 자석이기 때문에 군사분야에서 자기장을 측정하는 기술은 2차 세계대전이후 많은 연구가 계속되어 왔다.

본 연구에서는 불발병기(UXO:UneXploded Ordnance)를 자기적 방법으로 무인기에 적용하여 탐지하는 방법에 대하여 연구를 하고 있다. UXO를 자기적 방법으로 탐지하는 원리는 EMI (EletroMagnetic Impedance)방식, EMI(ElectroMagnetic Induction)방식, 및 자력계(Magnetometer)방식으로 나누어진다. EMI방식의 경우 측정감도는 피탐지물체로부터 가까운 거리에서는 유리하나 거리가 멀어지면 자력계방식이 유리하여진다. 또한 무인기인 UGV, UAV, USV, 및 UUV에 적용하기 위해서는 다음의 문제가 극복되어야 한다.

- 무인기로부터 발생되는 자기잡음문제,
- 자세의 불안정에 의한 측정불확도,
- 센서의 질량
- 센서의 전력소비 및
- 센서의 측정속도.

자력계(Magnetometer)방식으로 UXO를 탐지하기 위하여 자세의 불안정과 관계가 없는 total field를 측정하는 scalar magnetometer(atomic magnetometer)를 사용하고 있다. Cs^{133} magnetometer의 경우 Lamour precission 주파수가 3.49872 Hz/nT로 1 nT의 분해능으로 초당 3번 정도 가능하다[1]. 그리고 질량이 수 kg이고 전력소모가 수십 Watt 이상 되어 소형 드론의 경우 어려워진다. 본 연구에서는 3-축의 flux-gate magnetometer를 사용하여 total field를 측정하는 자력계를 만들기 위하여 3-축의 직각도를 보정하고, 동특성을 향상시키기 위하여 그림 1과같이 3-축의 자기장 성분을 동시에 측정하여 atomic magnetometer보다 동특성이 우수한 자력계를 제작하였다.

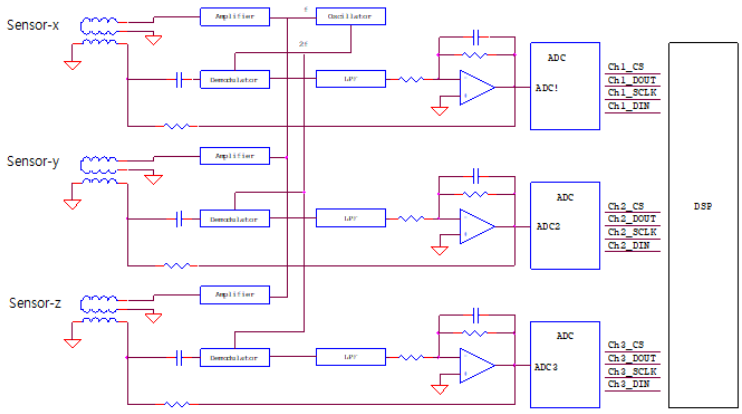

Fig. 1. Schematic diagram of 3-axis simultaneous measuring flux-gate magnetometer for scalar magnetometer.

자기센서용 연자성 코어의 자화곡선 모델링

신광호*, 김경원
경성대학교 정보통신공학과

플럭스게이트센서, 자기임피던스센서, 자기저항센서 등과 같이 연자성 코어를 이용하여서 제작되는 자기센서의 성능은 연자성코어의 자기적 특성에 크게 의존된다. 자기센서의 감도를 높이기 위해서 연자성코어의 투자율이 높아야 하고, 높은 분해능을 얻기 위해서는 연자성코어의 보자력과 자기이방성분산이 작아야 한다. 자기센서의 성능을 예측하기 위해서는 자기센서를 구성하는 전자회로는 물론 자성체코어와 검출코일의 전기적 연결을 해석하여야 하며, 정밀한 성능예측을 위해서는 연자성코어의 자화특성을 정확히 모델링할 수 있어야 한다. 자성체의 자화특성을 해석하거나 모델링하기 위해서 다양한 방법들이 제안되어 있다. 그러나, 연자성이 극히 우수한 자성체의 경우, 자성체에 축적되는 자기에너지의 양이 작아서 정밀한 해석 및 모델링이 용이하지 않다. 본 연구에서는 Jiles-Atherton hysteresis 모델링기법을 이용하여서 유도자기이방성을 가진 연자성체의 자화곡선을 모델링하고 연자성체를 이용하여서 구성한 Orthogonal fluxgate 자기센서의 특성을 해석하는 방법에 대해서 조사하고 있다. 본 발표에서는 Jiles-Atherton hysteresis 모델링기법을 유도자기이방성을 가진 연자성체에 적용하는 방법, 측정된 데이터에 맞추어서 Hysteresis 모델에 필요한 파라메터들을 도출하는 방법 등에 대해서 소개하고자 한다.

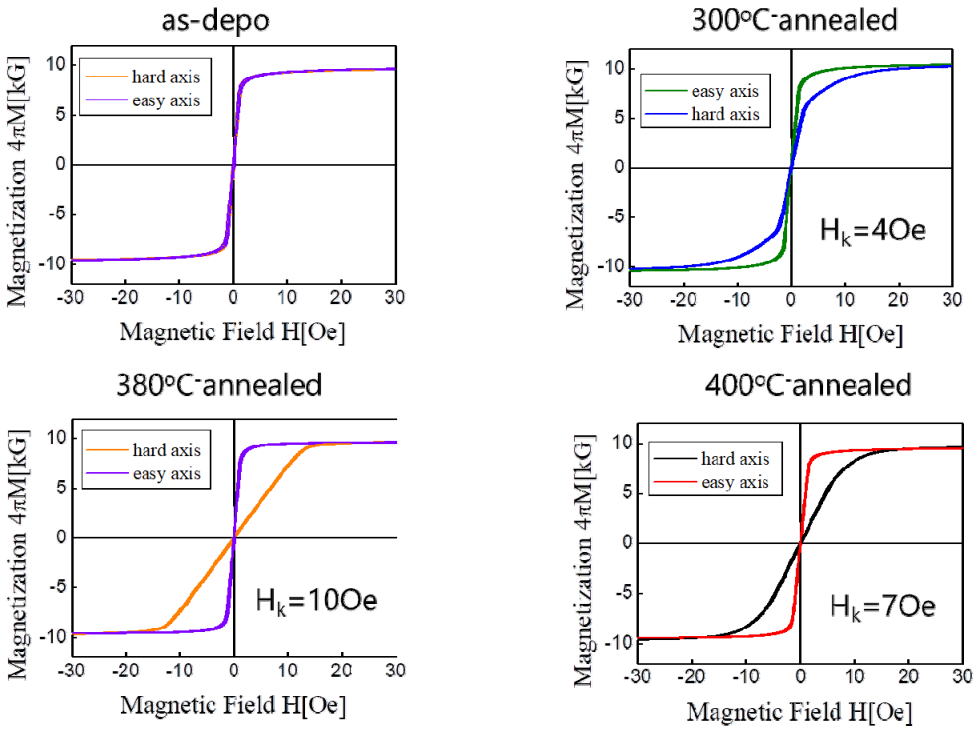

Fig. 1. Magnetization curves of CoZrNb films annealed in various temperatures.

자기장을 활용한 콘크리트 보강재 비파괴평가

조창빈[1*], 손대락[2], 곽임종[1], 이정우[1], 박광연[1]
[1]한국건설기술연구원 경기도 고양시 일산서구 고양대로 283
[2]한남대학교 광센서공학과 대전광역시 대덕구 한남로 70

1. 보강재의 자기이력곡선 측정

콘크리트의 취성적인 거동을 보완하는 철근・텐던(Tendon) 같은 보강재의 상태평가는 콘크리트 구조물의 유지관리에 필수적인 요소 중 하나로, 보강재의 응력・단면손상과 같은 상태평가를 위해 보강재가 자성체인 점을 활용한 연구가 진행되어왔다. 한국건설기술연구원에서도 2013년 타당성 연구[1]로 시작하여, Prestress를 받고 있는 보강재인 텐던의 응력・단면손상을 측정하기 위한 비파괴평가기술에 자기장을 활용하는 연구를 수행하고 있다. 본격적으로 자기장을 활용하기 위한 첫걸음으로 한남대학교 연구진과 공동으로 응력상태에 따른 텐던의 자화곡선을 측정하고 응력과 자화곡선의 관계인 Villrai 효과를 확인하였다(그림 1).

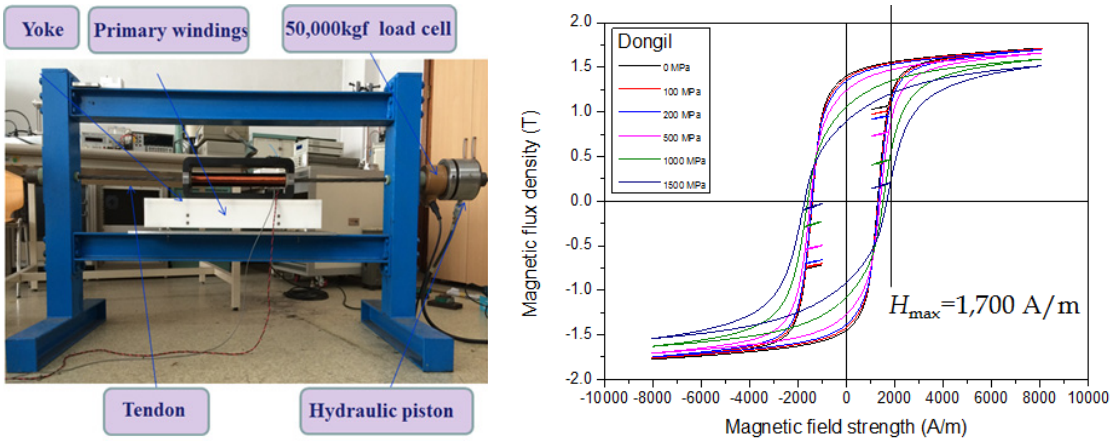

그림 1. 텐던 자기이력곡선 측정 장치 및 텐던(동일제강)의 자기이력곡선

2. 보강재의 응력과 단면손상 측정

이를 바탕으로 기존 외부텐던 구조에 설치하여 텐던의 응력・단면손상을 측정할 수 있는 착탈식 요크를 개발하여, 15가닥의 강선으로 이루어진 외부텐던의 응력과 투자율의 선형관계를 이용, 응력을 측정하는 기술을 개발

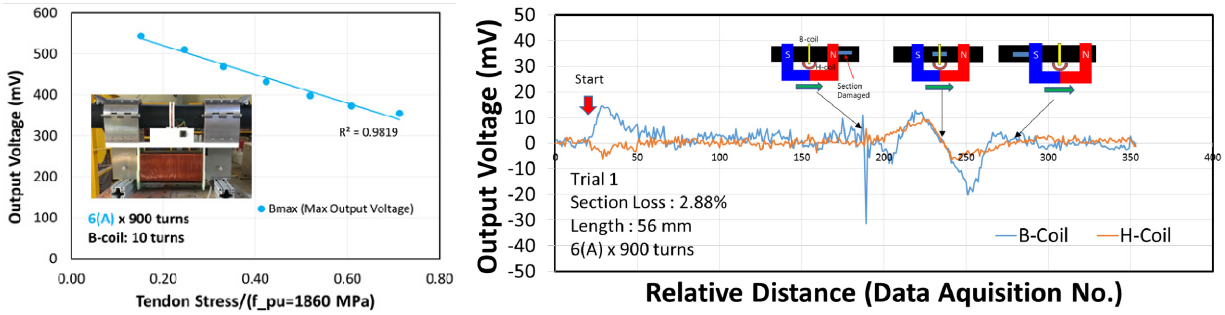

그림 2. 탈부착식 요크와 이를 활용한 텐던의 응력측정 및 단면손상 측정[3]

하였다(그림 2 좌). 또한 요크가 텐던을 따라 이동할 때 손상단면의 자속이 감속하는 것을 2차 코일(유도전압 측정)과 H 코일(자기포텐셜 측정)로 측정하여 텐던의 단면손상을 찾을 수 있는 기술도 개발하였다(그림 2 우). 접근이 어려운 콘크리트 내부의 텐던의 응력 평가를 위한 비더만효과 활용 등 다양한 기술도 제안하였다[4][5].

기본적인 개념은 같지만 개발된 기술의 실용적인 측면을 강화하기 위해, 요크의 무게를 줄이고 탈부착을 좀 더 쉽게 할 수 있는 장비를 개발하였다. 기존 100kg 정도였던 요크의 무게를 10kg 이하로 줄이고 가능한 폐자기회로를 구성할 수 있는 분절형 요크를 개발하고 실험을 통해서 성능을 확인하였다(그림 3 좌).

이후 보다 가볍고 손쉽게 자기장을 인가하기 위해, 텐던에 반구형 실린더 두 개를 결합하여 원통을 만들고 평면케이블(Flat Cable)로 감싼 후 엇갈리게 단자를 연결하는 개념의 Wrapping 솔레노이드를 개발하였다. 이 장치의 무게는 2kg 이하이고 3분이하로도 설치가 가능하였다. Wrapping 솔레노이드로는 기존의 요크를 이용하는 기술과는 달리 폐자기회로를 구성하기는 어렵지만, 실험결과 실용적인 정확도 내에서는 텐던의 응력과 손상을 측정할 수 있는 가능성을 확인하였다(그림 3 우).

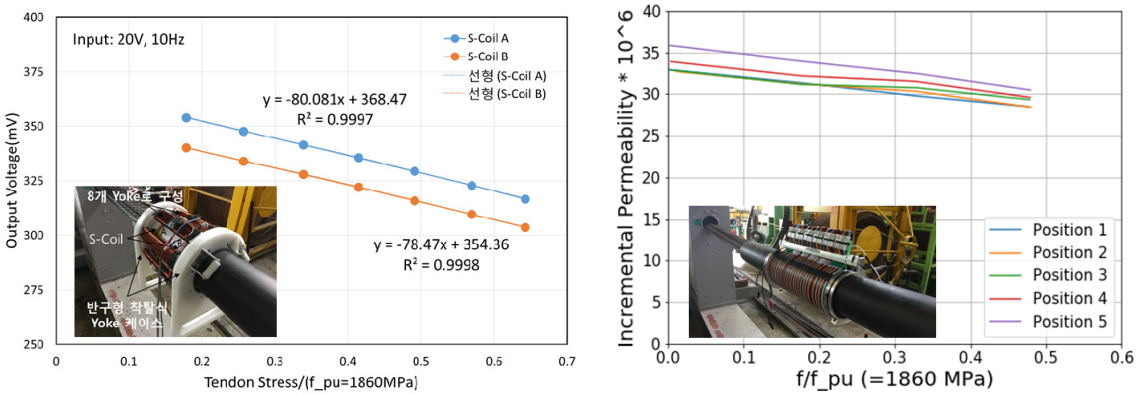

그림 3. 가벼운 분절형 요크와 탈부착이 쉬운 Wrapping 솔레노이드를 활용한 텐던의 응력측정

3. 분절형 요크・Wrapping 솔레노이드를 활용한 실용기술 개발

현재, 분절형 요크나 Wrapping 솔레노이드를 활용하는 기술을 실무에 적용하게 하기 위해 실용적인 완성도를 높이는 연구가 진행 중이다. 우선 다양한 종류의 텐던의 자기적인 특성에 대한 데이터베이스를 구축하고 있다. 또한 측정의 정확도・정밀도를 향상시키는 한편, 텐던에서 측정된 자기적인 신호를 분석하기 위한 신호처리・역해석 기술과 텐던 상태판정을 쉽게 하기 위한 보조적인 분석 방법으로 머신러닝 기법을 활용하는 연구가 진행 중이다.

감사의 글

이 논문은 2019년 한국건설기술연구원 주요사업((20주요-대1-임무)PSC 구조물 비파괴평가기술(PSC 청진기) 개발 (2/3))의 연구비 지원에 의해 수행 되었습니다.

References

[1] Joh, C., Lee, J., & Kwahk, I. (2013). Feasibility study of stress measurement in prestressing tendons using Villari effect and induced magnetic field. *International Journal of Distributed Sensor Networks*, *9*(11), 249829.

[2] Kang, S. J., Joh, C, Lee, J., & Son, D. R. (2014). Tendon 의 Villari 효과 특성 측정에 관한 연구. In *Proceedings of the Korean Magnestics Society Conference* (pp. 110-111). The Korean Magnetics Society.

[3] Joh, C., Lee, J., Park, Y., & Son, D. (2017). Measurements of Tensile Stress and Cross Sectional Area

Loss of Tendon by Means of Non-contact Movable Yoke. *JOURNAL OF THE KOREAN MAGNETICS SOCIETY*, *27*(5), 168-174.

[4] Kang, S., Son, D., Joh, C., & Lee, J. (2016). Tensile Stress Measurement of Tendon with Wiedemann Effect. *Journal of the Korean Magnetics Society*, *26*(4), 133-136.

[5] Kang, S., Son, D., Joh, C., & Lee, J. (2016). Tensile Stress Measurement of Tendon by Means of Non-contact Yoke Method. *Journal of the Korean Magnetics Society*, *26*(1), 19-23.

Evaluation of Railway Track Safety using Magnetic Barkhausen Noise method

Nam-Hyoung Lim[1*], Ki Hwan Jee[2], Gen Han Yoo[3], Soo Yeol Lee[4], Derac Son[5]
[1]Department of Civil Engineering, Chungnam National University, Daejeon, Korea
[2]Korea Measuring Technology Laboratory Co. LTD., Seoul, Korea
[3]Cnu Rail Research Institute, Chungnam National University, Daejeon, Korea
[4]Department of Materials Science and Engineering, Chungnam National University, Daejeon, Korea
[5]Department of Computer, Communication and Unmanned Technology, Hannam University, Daejeon, Korea

Unlike long or standard-length rail, the use of the continuous welded rail track results in thermally induced stresses in the rail. The stress caused by the temperature change is a major factor of rail fracture in cold weather condition and rail buckling in hot weather conditions. Therefore, the monitoring system of the rail stress is considered as one of the main concerns in the operating performance of railway. Strain gauges commonly used to measure stress do not apply to this monitoring systems. This is because when a temperature change occurs on continuous welded rail of several km, the strain due to temperature is zero. Other non-destructive measurement methods include ultrasonic and vibration measurement, but they are not widely applied due to problems in accuracy and precision. The method for measuring rail stress adopted in Korea is a semi-destructive method using VERSE equipment. This equipment calculates rail stress from the bending displacement measured in the field test using the relation between the axial stress and the bending displacement of the rail developed based on the beam-column theory. VERSE equipment is used in many countries due to its high precision and accuracy compared to other methods, but it has the disadvantage that it takes a lot of time and manpower, such as dismantling the rails on tracks, and operates only in a certain rail temperature range. Recently, to overcome the shortcomings of VERSE equipment, research to develop evaluation methods and equipment using the Magnetic Barkhausen Noise (MBN) method has been actively conducted. In this paper, we propose the MBN characteristics of rail steel, the location of MBN measurement, and the safety evaluation method of railway track.

펄스와전류 기술의 소개와 적용 분야

박덕근[1,2*], 신정우[2]
[1]한국원자력연구원
[2](주) 아이피트

정유, 가스, 전력 철도 등 우리나라의 중화학 산업의 역사는 60년을 넘었으나, 산업의 핵심인 시설・장비의 안전성에 대하여는 그리 큰 주의를 하고 있지 않은 편이다. 시설을 이루고 있는 재료도 시간이 지남에 따라 노화되며, 노화 상태를 측정하는 것은 산업 설비의 안전성을 측정하는 것은 매우 어렵다. 특히 항공기, 배관, 교량 등에서 자주 발생하는 부식이나 피로 등과 같은 재료의 열화를 측정하는 것은 공학적인 면에서도 새로운 도전이 되고 있다. 현재 사용되고 있는 설비 구조물은 대부분 탄소강 계열의 재료로 이루어져 있다. 탄소강 계열의 재료는 값이 싸고 내구성이 좋아 대부분의 산업 현장에서 널리 사용되고 있다. 그러나 부식과 마모 등에 취약해 유지보수에 많은 주의가 필요하다. 특히 유지보수에 필수적인 비파괴 검사를 위한 특화된 기술이 거의 없는 실정이다. 현재 실용화된 비파괴 기술은 대부분 와전류와 초음파 기술로서, 이들 기술은 배관, 교량 등 탄소강 계열의 재질에 적용하기에는 많은 한계성을 가지고 있다. 특히 여러 겹으로 구성된 재질에서는 기존의 비파괴방법인 초음파나 와전류 기술이 적용되지 않는다. 산업 현장에서 대부분의 배관은 배관의 열 손실을 방지하기 위하여 열전도도가 낮은 물질로 이루어진 보온재로 덮여있는데, 이들 배관 등에서 일어나는 국소적인 감육현상을 비파괴적으로 측정하는 것은 매우 중요하다. 펄스와전류 기술은 기존의 와전류 기술의 단점을 극복하고 적용성을 넓히기 위하여 고안된 기술로서, 기존의 와전류 기술이 주로 스텐레스나 인코넬과 같은 비자성체 이면서 표면 결함 탐지에만 적용되는 것을 재료가 자성체이면서 결함이 깊숙이 들어가 있는 이면결함의 탐지에도 적용될 수 있도록 고안된 기술이다. 본고에서는 펄스와전류(PEC) 기술의 원리와 특징을 설명하고 이 기술을 사용하여 보온재로 덮여있는 배관의 손상을 보온재를 제거하지 않고 보온재 외부에서 측정하는 기술에 대해 소개했다. 펄스와전류 기술은 보온재로 덮혀 있거나 자성체인 배관이나 철골 구조물 등에 적용하기

그림 1. 배관의 감육을 측정하는 펄스와전류 시스템

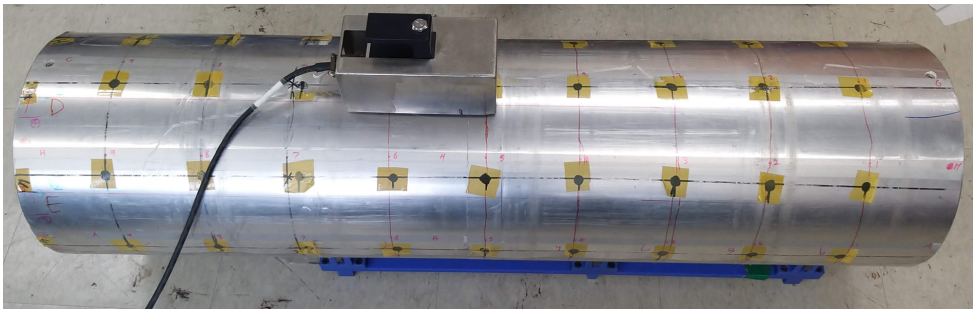

그림 2. 목업 용 배관

좋은 기술이다. 그러나 펄스와전류 기술은 범용장비가 존재하지 않으며, 특성상 범용장비가 존재하기도 힘든 기술이다. 이는 자기적 방법을 이용하는 기술의 특성상 대상물질의 모양, 재질 등에 따라 자기 특성이 달라지는 자기이력 특성으로 인하여 일률적인 적용하기 힘들며, 범용장비를 제작하기도 어렵다. 본 기술의 적용으로서 보온재와 보온재를 보호하는 스텐레스 크래딩으로 덮혀 있는 강자성체 배관에서 배관의 감육을 측정하는 펄스와전류 시스템을 개발하였다 (그림 1). 목업 용 배관은 두께가 15mm인 1,500mm 길이의 10인치 배관 외부에 65mm 두께의 보온재를 설치하였으며, 보온재 외부에는 0.6mm 두께의 스텐레스 피복재가 둘러싸여 있다(그림 2). 배관의 내부는 각각의 단차가 0.8mm에서 1.2mm인 계단식 모양으로 가공했다. 개발된 PEC 시스템은 8cm 두께의 보온재가 설치된 배관에서도 두께 변화를 탐지할 수 있었다. 이 장치는 여러 중화학 시설에 상업적으로 적용하기 위하여 개발했으며, 보온재로 둘러 쌓인 배관의 손상을 보온재를 해체하지 않고 보온재 외부에서 내부 배관의 손상 정도를 측정하는데 사용될 수 있다.

References

[1] J. Blitz, Electrical and magnetic Methods of nondestructive testing, Chapman & Hall, London(1997) pp100

[2] M. J. Cohn, J. W. Norton, In: Proceeding of PVP2008 ASME Pressure Vessels and Piping Division Conference (2008).

Special Session II

'Theory'

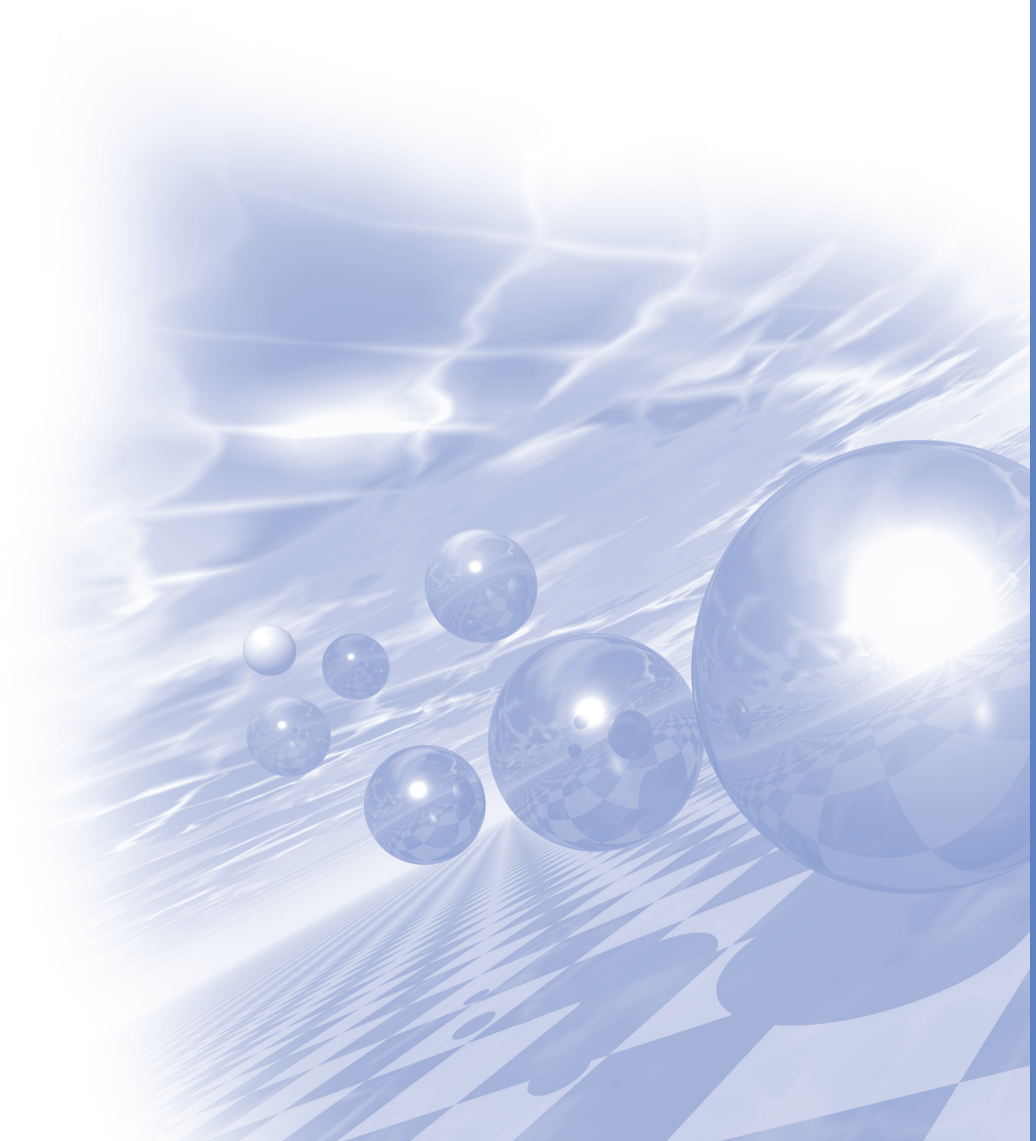

Lattice dynamics study on charge density wave and superconductivity in low-dimensional systems; CuTe and MgC_2

Sooran Kim*
Department of Physics Education, Kyungpook National University, Daegu, Korea

Low-dimensional systems often suffer from intrinsic instabilities, revealing diverse interesting phase transitions upon cooling, such as charge density wave (CDW), spin density wave, and superconductivity (SC). Lattice dynamics/phonon study is a useful approach to investigate those instabilities. In this talk, I will introduce two systems; CuTe with a CDW transition and MgC_2 with superconductivity. A quasi-one-dimensional layered material CuTe undergoes a CDW transition in Te chains with a modulation vector of qCDW = (0.4, 0.0, 0.5). Despite the clear experimental evidence for the CDW, the theoretical understanding, especially the role of the electron-electron correlation in the CDW, has not been fully explored. Here, using first-principles calculations, we demonstrate that the CDW transition in CuTe originates from the interplay of the Coulomb correlation and electron-phonon interaction. As a second part, our proposed MgC_2 consists of extended carbon bonds, one-dimensional graphene layers, and Mg atomic layers, which provides a good platform to study superconductivity of metal intercalated graphene nano-ribbons. The new phase of MgC_2 exhibit a strong electron-phonon coupling (EPC) strength of 0.6 whose corresponding superconductivity transition temperature reached 15 K. The EPC originated from the cooperation of the out-of-plane and the in-plane phonon modes. We found that the geometry confinement and the hybridization between the Mg and C bands significantly affect the coupling of phonon modes and electrons.

Mimicking superconductivity of Sr_2RuO_4 using $SrRuO_3$-$SrTiO_3$ superlattice

Bongjae Kim[1*], Sergii Khmelevskyi[2], Cesare Franchini[3], Igor I. Mazin[4] and Kyoo Kim[5]
[1]Kunsan National University, Korea
[2]TU Wien, Austria
[3]University of Vienna, Austria
[4]George Mason University, U.S.A.
[5]Korea Atomic Energy Research Institute (KAERI), Korea

The superconductivity in Sr_2RuO_4 has been one of the most challenging topics. Unlike cuprates whose mechanisms for superconductivity is understood with comparative studies within rich family, Sr_2RuO_4 is a lone superconductor. Using first-principles study, we show that $SrRuO_3$-$SrTiO_3$ (SRO-STO) heterostructure is endowed with all key characteristics of Sr_2RuO_4 such as two-dimensional electronic structures, spin-density-wave type magnetic instability, and strong nesting feature. Stronger and more frustrated magnetic instability in SRO-STO offers a unique opportunity of tunable magnetic and superconducting phases, which can be experimentally accessible for further intensitve studies and open a new platform to investigate the unconventional superconductivity in ruthenates.

브릴루앙 산란으로 연구된 Co_xGd_{1-x} 준강자성체의 스핀파 특성

김창수[1,2*], 이수길[2,3], 김현규[2], 박지호[2], 문경웅[1], 박재열[3], 육종민[3], 이경진[4,5,6], 박병국[3], 김세권[7], 김갑진[2], 황찬용[1]

[1]Quantum Spin Team, Korea Research Institute of Standards and Science, Daejeon 34113, Republic of Korea
[2]Department of Physics, KAIST, Daejeon 34141, Republic of Korea
[3]Department of Materials Science and Engineering and KI for Nanocentury, KAIST, Daejeon 34141, Republic of Korea
[4]Department of Nano-Semiconductor and Engineering, Korea University, Seoul 02841, Republic of Korea
[5]Department of Materials Science & Engineering, Korea University, Seoul 02841, Republic of Korea
[6]KU-KIST Graduate School of Converging Science and Technology, Korea University, Seoul 02841, Republic of Korea
[7]Department of Physics and Astronomy, University of Missouri, Columbia, MO 65211, United States of America

반강자성 정렬된 준강자성체는 총자화와 총각운동량이 0으로 수렴하는 자화보상온도 (T_M)와 각운동량보상온도 (T_A)에서 관찰되는 특이한 동역학으로 많은 주목을 받았다. Co_xGd_{1-x} 준강자성체는 전이금속인 코발트 (Co)와 희토류금속인 가돌리늄 (Gd)의 두 가지 서로 다른 자성원소로 이루어져 있어서 두 가지 모드 (mode)의 동역학이 나타난다고 알려져 있다. 우리는 300~440 K로 온도를 변화시키면서 자화보상온도와 각운동량보상온도 근처에서 브릴루앙 (Brillouin) 산란 분광법으로 스핀파 (spin wave) 동역학을 관찰하였다. 이론의 예측대로 두 모드를 관찰할 수 있었으며, 낮은 주파수 모드 (Low frequency mode, LF mode)는 자화보상온도에서 에너지가 0 근처로 수렴하고 각운동량보상온도 근처에서 최대가 되는 것을 확인하였다. 이와 반대로 높은 주파수 모드 (High frequency mode, HF mode)는 각운동량보상온도 근처에서 에너지가 최소가 되는 것을 확인하였다. 또한 자기장의 증가에 따라 두 모드의 교차 온도 (mode crossing temperature)가 증가하는 것을 관찰하였으며 두 보상 온도 근처에서 쟐로신스키-모리야 (Dzyaloshinskii-Moriya) 상호작용에 의한 스톡스-안티스톡스 (Stokes-Antistokes) 스핀파 모드의 에너지 차이를 측정하였다.

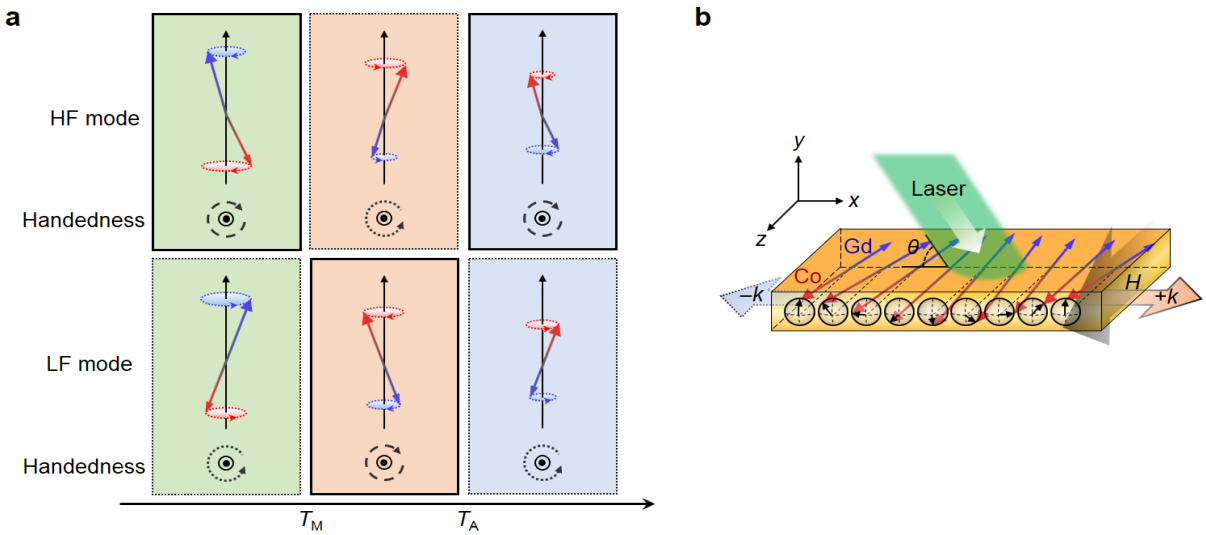

Fig. 1. a. 온도에 따른 Co_xGd_{1-x}의 자화동역학 b. 브릴루앙 산란과 스핀파 모식도

Self-Generated Spin-Orbit Torque and Spin Pumping by Spin-Orbit Coupled Ferromagnets

Kyoung-Whan Kim[1*] and Kyung-Jin Lee[2]
[1]Center for Spintronics, Korea Institute of Science and Technology
[2]Department of Materials Science and Engineering, Korea University

Electrical manipulation of magnetization is a central topic in spintronics. So far, spin torque induced by an external spin current has been mainly considered. For instance, spin-transfer torque utilizes a spin-polarized current from another magnetic layer and spin-orbit torque utilizes the spin Hall current generated by an adjacent layer or an interface. Since the conservation of angular momentum requires change of the total angular momentum in the ferromagnet to manipulate its magnetization, the injection of an external angular momentum has been considered to be essential for magnetization control.

In this talk, we present another route to manipulate the magnetization which does not require requiring an external source of spin current. A recent report of an intrinsic spin current generated in a ferromagnet itself opens the possibility. We generalize the drift-diffusion formalism for spin-orbit coupled ferromagnets and explicitly demonstrate that the intrinsic spin current can be extracted from the ferromagnetic layer and its backaction to the magnetic layer can generate a spin torque. In this case, the spin-orbit coupling in the ferromagnet converts the angular momentum stored in the lattice to the spin angular momentum, which eventually gives rise to a self-generated spin torque. The Onsager reciprocity of the self-generated spin torque describes a self-generated spin pumping. The self-generated spin-orbit torque and spin pumping depend on the thickness of the ferromagnet and thus experimentally distinguishable from the conventional spin-orbit torque. Our work not only generalizes the traditional theory used for a few decades but also changes the paradigm of spin torque.

Exotic electronic structures of the superconducting nickelate

Kwan-Woo Lee*
Division of Display and Semiconductor Physics, Korea University, Sejong
Department of Applied Physics, Graduate School, Korea University, Sejong

About one year ago, H. Hwang and coworkers [Nature 572, 624 (2019)] found the superconductivity up to T_c= 15 K in thin film $NdNiO_2$ when hole-doped. A dome-shape-like phase diagram was observed in the superconductor very recently. This is the three-decade-long sought cuprate-like nickelate superconductor. The $NdNiO_2$ and $LaNiO_2$ with Ni^{1+} ions are isostructural and isovalent with infinite layer $CaCuO_2$ (Cu^{2+}, d^9) that superconducts up to 110 K when doped. For a few decades, doped $LaNiO_2$ has been investigated as a most promising candidate for the superconductor, but not succeed yet.

In this presentation, we will address two fundamental aspects of the parent compounds. First, why is only hole-doped $NdNiO_2$ superconducting, although the crystal and underlying electronic structures of $LaNiO_2$ and $NdNiO_2$ are very close? Second, $NdNiO_2$ is metallic and not magnetically ordered, while undoped cuprates are insulating and antiferromagnetic. For the first issue, we will propose a crucial role of the open-shell Nd 4f orbital. Then, for the second issue, our results show a competition of potential instabilities due to a 1D van Hove singularity and quantum zero-point fluctuations. In any class of exotic superconductors such a competition has not been seen before.

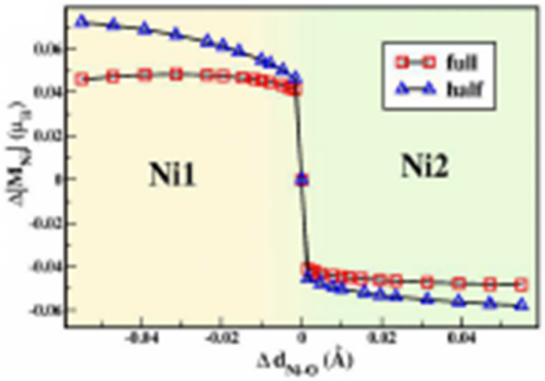

Fig. 1. Change of Ni magnetic moments by oxygen breathing modes

Acknowledgements

These researches were collaborated with Mi-Young Choi and W. E. Pickett. This research was supported by NRF of Korea Grants NRF-2019R1A2C1009588.

References

[1] M.-Y. Choi, K.-W. Lee, and W. E. Pickett, Phys. Rev. B 101, 020503(R) (2020).
[2] M.-Y. Choi, W. E. Pickett, and K.-W. Lee, arXiv:2005.03234.

Torque generation by orbital current: Orbital torque

Dongwook Go[1,2†] and Hyun-Woo Lee[3*]

[1]Peter Grunberg Institut and Institute for Advanced Simulation, Forschungszentrum Julich and JARA, 52425 Julich, Germany

[2]Institute of Physics, Johannes Gutenberg University Mainz, 55099 Mainz, Germany

[3]Department of Physics, Pohang University of Science and Technology, Pohang 37673, Korea

We propose a mechanism of torque generation by injection of an orbital current, which we call orbital torque. In a magnetic bilayer consisting of a nonmagnet (NM) and a ferromagnet (FM), we consider a situation where the spin-orbit coupling (SOC) is absent in the NM and thus there is no spin current injection from the NM to the FM. Despite the absence of the SOC in the NM, an orbital Hall current can be still generated in the NM and injected into the FM. Upon its injection, the orbital current may generate a nonequilibrium spin density in the FM and induces a torque. The magnitude of this orbital torque depends on the SOC of the FM. Remarkably, even for small SOC strength comparable to that of 3d FMs, the orbital torque can be comparable to the spin torque induced by the spin Hall effect of the NM with strong SOC. This provides a way to experimentally probe the OHE and opens a venue to achieving spin-torque devices based on light elements that exhibit gigantic orbital response. Experimental implications are discussed.

수직자성박막에 스커미온을 형성하는 방법

문경웅[1*], 양승모[1], 주태성[1,2], 김창수[1], 전병선[1], 박성균[2], 황찬용[1]
[1]한국표준과학연구원 양자스핀팀, 대전 34113, 대한민국
[2]부산대학교 물리학부, 부산 34113, 대한민국

자성벡터들로 이루어진 스커미온이 발견된 이래 스커미온에 대한 활발한 연구가 진행 중이다. 이러한 스커미온을 실험적으로 연구하는데 있어 극복해야 하는 난관은 스커미온이 형성되는 시료를 제작하는 것이다. 스커미온 시료를 만들기 위한 간단한 접근 방법은 업 다운이 반복되고 각 도메인이 일정한 폭을 가지고 있는 스트라잎 상태가 안정되어 있는 시료를 제작 하는 것이다. 왜냐하면 스트라잎 상태는 수직자성을 가지고 있는 시료에서 흔히 관찰되는 자화상태이고 스트라잎 상태와 스커미온 상태의 에너지 차이가 그리 크지 않다고 알려져 있기 때문이다. 실제 실험적으로도 스트라잎 상태가 쉽게 형성되는 시료에 수직 자기장을 인가하여 스커미온이 가득 차 있는 상태로 만들고 있다. 하지만 이러한 접근 방법은 스트라잎이 충분히 얇을 때만 성공적이었다. 이번 발표에서는 폭이 두꺼운 스트라잎에서 스커미온 상태를 만들지 못했던 원인에서부터 논의를 시작하여 모든 스트라잎 구조를 스커미온 상태로 변화 시키는 일반적인 방법에 대해 설명하고자 한다.

KMS 2020 Summer Conference

Special Session III

'Medical Magnetics'

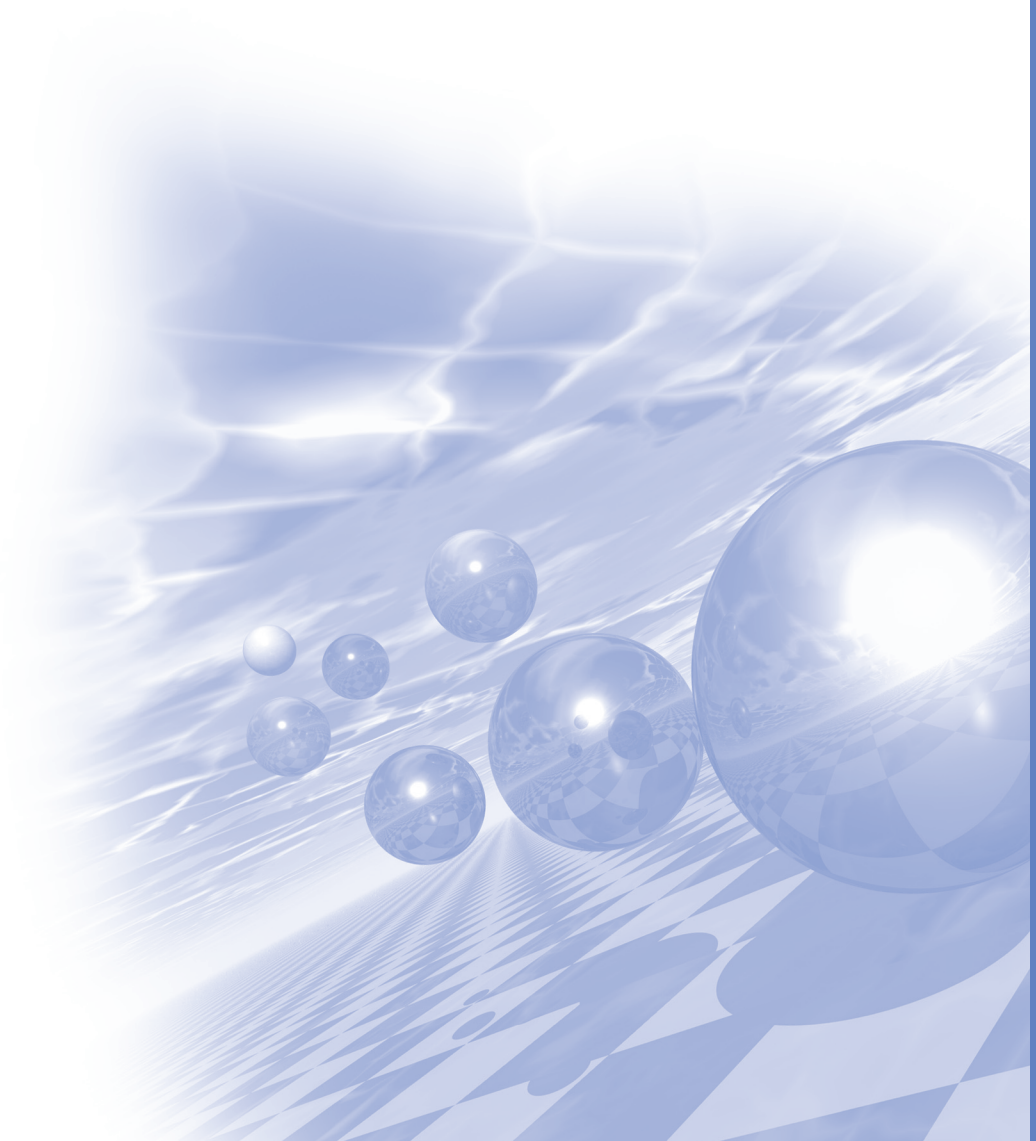

Brain segmentation analysis using brain magnetic resonance imaging (MRI) measurements for comparison between normal controls and Alzheimer's disease (AD) patients

Sang-Won Park[1*], Na-Young Yeo[2], Jae-Won Jang[1,3]

[1]Kangwon National University School of Medicine, Chuncheon, Republic of Korea

[2]Advanced R&D Team of Hanhwa High-tech Co. Ltd., Daejeon, Republic of Korea

[3]Department of Neurology, Kangwon National University Hospital, Chuncheon, Republic of Korea

Purpose: Alzheimer's disease (AD) is a chronic neurodegenerative disease known to be accompanied by a decreasing cognitive function. Changes in brain structures such as the hippocampal and cortical thicknesses measured on magnetic resonance images could be used as major indicators of cognitive decline in patients with AD. Thus, brain segmentation analysis is essential for obtaining more specific data. In this study, we performed a statistical analysis of cortical thickness and volume measurements and prepared a database for artificial intelligence (AI) analysis of brain structural changes using the FreeSurfer software, which is based on the Linux OS, in the future for comparison between normal controls and patients with AD.

Materials and Methods: All the magnetic resonance images used in this study were acquired from the Alzheimer's Disease Neuroimaging Initiative and obtained using a 3-T magnetic resonance imaging (MRI) scanner (GE, Siemens, or Philips). The MRI standard protocol was developed by comparing and evaluating three-dimensional (3-D) T1-weighted sequences for morphometric analysis. After brain segmentation, brain structural changes were analyzed to compare between patients with AD and healthy controls. Each group consisted of 7 patients. Briefly, brain images stored in the Digital Imaging and Communication in Medicine format (.dcm), a medical digital imaging standard protocol, were converted to Neuroimaging Informatics Technology Initiative format (.nii) to allow measurement of cortical volume using the FreeSurfer software. After that, brain segmentation and smoothing were performed to calculate cortical thickness. The individual images and demographics data were normalized for observation and analysis in this study. In addition, age and sex were used as covariates. A general linear model regression analysis was performed to identify differences between the normal controls and the patients with AD ($p < 0.05$). All the analyses were performed in our laboratory using FreeSurfer codes.

Results: The change in cortical thickness measured on magnetic resonance images using brain segmentation showed that the cortical volume in the patients with AD decreased as compared with that in the normal controls. In the healthy controls and patients with AD, the cortical thicknesses ranged from 1.36 to 3.87 mm^3 and from 1.41 to 3.60 mm^3, respectively, and the cortical volumes (mean ± SD) were 81.94 ± 1.59 mm^3 and 77.18 ± 1.76 mm^3, respectively, in the left hemisphere. In the right hemisphere, the cortical thicknesses ranged from 1.54 to 3.92 mm^3 and from 1.42 to 3.32 mm^3, respectively, and the cortical volumes (mean ± SD) were 82.64 ± 3.93 mm^3 and 76.64 ± 4.28 mm^3, respectively. The differences in cortical thickness and volume between the two groups were 6% and 8%, respectively. These results show that the normal controls maintained a significant normal

cortical thickness as compared with the patients with AD. In the patients with AD, we found a statistically significant change ($p < 0.05$) in the corresponding brain region on MRI.

Discussion and Conclusions: We assessed brain structural changes using MRI with the FreeSurfer software to compare between healthy controls and patients with AD. The results of the brain segmentation analysis and extracted values could be used in the first step of an AI analysis. The magnetic resonance images used in this study, which could be applied in the future, consisted of time-series sequences. In addition, on the basis of these images, the progression of brain structural changes to AD could be analyzed longitudinally using the recurrent neural network-long short-term memory AI model. However, more demographic data are needed as covariates, and a more sophisticated work is required for troubleshooting after image segmentation. These limitations could be improved in future studies.

MRI 시스템에 따른 GBCA의 신호 변화 Signal Change of GBCA according to MRI System

정현근*, 유재원, 배규성, 배서현, 김성호, 유세종, 전민철, 고현철
HK리서치센터 의생명공학연구실 (Biomedical Engineering Lab, HK Research Center Inc.)

1. 서 론

금속성 전이원소 가돌리늄은 원자량 157.25g/mol에 7.9g/cm^{3}의 밀도를 지니며, [Xe]4f^{7}5d^{1}6s^{2}의 전자배열로서 8개의 비쌍전자(unpaired electron)를 갖고 있어, $_1$H 양자와 결합하여 자기장 내에서 강한 상자성 효과를 지닌다. 이 때 in vivo에서의 가돌리늄은 통상적인 $_1$H spin과 상호작용하여 M_z, M_{xy} 변화에 따른 R_1, R_2 이완시간을 단축시키는데, 이는 동일한 자장 조건하에서 가돌리늄과 결합하지 않은 $_1$H spin에 비해 빠른 이완율(relaxivity)를 형성시켜 MR영상에서 높은 신호강도를 보여주게 된다[1～6]. 해당실험에서는 동일한 자장을 지니는 각 업체의 3.0T MRI장비에서 GBCA(Gadolinium Based Contrast Agent)반응을 확인해보고자 하였다. 그 이유는 동일한 3.0T의 자장강도라 하더라도 MR장비의 스펙, 자장의 균질도, 파라메타 등의 외부환경 인자에 따라 GBCA의 반응이 모두 다를 것으로 유추해 볼 수 있기 때문이다. 이에 본 연구에서는 GE, Philips, Siemens의 서로 다른 업체에서 제작된 각각의 3.0T MRI(750w, Archeiva, Skyra)에서 GBCA반응정도를 정량화하여 분석해보고자 하였다. 이를 위해 직접 제작한 MRI팬텀을 통하여 연구를 진행하였다.

2. 실험방법과 결과

본 연구를 위하여 29개의 용기로 구성된 하나의 MR팬텀을 사용하였다. 1실험은 서로 다른 모델의 3.0 T 초전도 MRI 장비를 사용 하였고, 팬텀 장착은 그림 2(a,b,c)와 같이 임상에서 실제 사용 중인 표준형 브레인 코일을 사용하였다.

각 장비별로 20회 추출한 그림 4(a,b,c)의 팬텀 단면영상에서 그림4(a)와 같은 녹색의 원형 ROI(Area=2.5m^2, 650px)를 설정 후 SI(Signal Intensity)를 측정하였고, 스캔횟수에 따른 평균값을 구하여 이를 분석하였다. 각 장비에서 스캔한 MR 팬텀 영상의 물질별 신호강도를 확인할 수 있으며, 각각의 물질 단면영상에서 ROI를 설정하고 SI(Signal Intensity) 및 대조도를 계산하였다. 팬텀실험결과 750w, Archeiva, Skyra 각 장비에서의 RSP는 20, 20, 50 mmol로 기록되었고, MPSI는 1377, 1495, 3459 [a.u.]를 보였다. MPP는 0.8, 0.6, 4 mmol로 기록되었고, CPFS는 276.3, 716.7, 287.3 [%]를 보였다. EPMF는 96.7, 47.6, 69.1[%]를 각각 기록하였고, EPMS는 640.3, 1105.6, 555.1 [%]를 보였다.

3. 고 찰

본 실험을 통하여 각 MRI장비 모델에서의 가돌리늄의 반응정도를 정량화 할 수 있었다. 임상에서는 통상적으로 1.5T, 3.0T MRI장비를 많이 사용하고 있다. 자장 세기만 고려했을 때는 단순해 보이지만, 다양한 업체에서 다양한 시스템이 있어 본 연구와 같은 GBCA반응 주제를 놓고 보면 단순한 문제는 아니다. 또한 장비를 세팅하는 외부 환경도 다르고, 이 후 임상환경에 맞춘 다양한 파라메타가 사용되고 있다. 즉, 본 연구결과에 따르면 동일한 자장세기의 3.0T 장비라 하더라도 다양한 시스템에 따라 GBCA의 신호가 모두 다르다는 것이다. 그러나 통상적으로 임상에서는 이와 같은 부분을 염두 하지 않고, GBCA를 사용하고 있다. 하지만 그 결과가 임상영상의 판독에 영향을 미칠 수 있다는 점을 감안하면, GBCA 반응 정량화 작업을 통하여 사용 중인 MRI장비를 적정하게 사용하고 있는지를 고려해 보아야 한다.

4. 결 론

본 팬텀 연구를 통하여 여러 종류 모델의 3.0T MRI장비에서 GBCA의 반응정도를 정량화 할 수 있었다. 그 결과는 각 업체에서의 서로 다른 MR시스템 따라 다른 반응을 보였다. GBCA 투약 후 적정한 T1검사가 이루어지는지 판단하기 위해서는 본 연구와 같은 정량화 분석 후 파라메타와 같은 외부환경 조정이 이루어진다면, 진단학적으로 더 유용한 검사가 가능하다고 사료된다.

References

[1] HK Jeong, KH Lee, MH Kim, SH Kim, MG Kim and HC Kim, “Signal Intensity of Contrast Enhancement according to TE in 3.0T MRI T1 Imaging” by Journal of Applied Science, 2018, 8.

[2] SH Kim, SY Kwon, CH Kang, HK Jeong, SW Kim, YJ Park, DK Han, JW Hong and YC Heo, “Analysis of Peak Velocity and Mean Velocity According to Shimming Technique in 2D Phase Contrast : Comparison of 1.5T Tesla and 3.0 Tesla” by Journal of Magnetics, 23(2), 201-206(2018).

[3] E. Hagberg, and K. Scheffler, “Effect of r(1) and r(2) relaxivity of gadolinium-based contrast agents on the T(1)-weighted MR signal at increasing magnetic field strengths”, Contrast Media MolImaging vol. 8, no. 6, pp. 456-65, Nov-Dec, 2013.

[4] Z. Seidl, J. Vymazal, M. Mechl, M. Goyal, M. Herman, C. Colosimo, M. Pasowicz, R. Yeung, B. Paraniak-Gieszczyk, B. Yemen, N. Anzalone, A. Citterio, G. Schneider, S. Bastianello, and J. Ruscalleda, “Does higher gadolinium concentration play a role in the morphologic assessment of brain tumors? Results of a multicenter intraindividual crossover comparison of gadobutrol versus gadobenate dimeglumine (the MERIT Study)”, AJNRAmJNeuroradiol, vol. 33, no. 6, pp. 1050-8, Jun, 2012.

[5] Bloembergen N, Purcell EM, Pound RV, “Relaxation effects in nuclear magnetic resonance absorption”, Phys Rev vol. 73, pp. 679, 1948.

[6] Bloembergen N, “Proton relaxation times in paramagnetic solution”, J Chem Phys vol. 27, pp. 572, 1957.

Rotatable LYSO-GAPD DEXA Detector Providing Normal-Resolution- and High-Resolution-mode

허희선[1*], 양진규[1], 강지훈[1,2†]
[1]전남대학교 의공학과
[2]전남대학교 헬스케어의공학연구소

본 연구에서는 하나의 검출기를 사용하여 일반해상도 및 고해상도 모드를 선택적으로 제공할 수 있는 회전형 LYSO-GAPD DEXA검출기를 개발하고 평가하였다.

3 × 3 × 2 mm^3 LYSO 섬광결정과 3 × 3 mm^2 GAPD는 광학그리스로 접합하여 DEXA 검출기를 구성하였다. 아날로그 출력신호는 전치증폭기와 DAQ장치를 이용하여 디지털로 변환되고, 후처리 과정을 통해 유효데이터를 추출한다. 검출기는 종축방향에서 횡축방향으로 90º 회전함으로써 일반해상도모드에서 고해상도 모드로 변환된다. 따라서, 일반 해상도 모드에서는 3 × 3 mm^2 입사면적에서 엑스선을 수집하고, 고해상도 모드에서는 2 × 3 mm^2 입사면적에서 엑스선을 수집함으로써 고유해상도는 33% 향상될 수 있다. K-edge Ce 필터에 의해 생성된 이중 에너지 엑스선 스펙트럼을 획득하고 광절정위치, 피크 대 골짜기 비율, 계수율 등을 평가하였다. 또한, 테스트 팬텀을 이용한 영상을 획득하고 두 모드의 비교평가를 수행하였다.

광절정 위치와 피크 대 골짜기 비율에서 유의한 차이점이 나타나지 않았다. 두 가지 모드에서 저에너지 및 고에너지의 광절정위치는 ~588 mV 및 ~1093 mV이고, PVR(Peak to Valley Ratio)는 ~3.4 및 ~1.6로 분석되었다. 일반해상도 모드에서 저에너지 및 고에너지 대역의 계수율은 각각 869 cps 및 663 cps이고, 고해상도 모드에서는 각각 613 cps 및 444 cps로 측정되었다. 이러한 실험결과는 고분해능 모드에서 에너지 성능에 변화가 없고, 획득한 계수율의 감소량(~31.3%)은 예상되는 감소량(~33.3%)과 일치함을 증명한다. 또한, DEXA 팬텀 영상을 성공적으로 획득하였다. 특히, 고해상도 모드에서 획득한 팬텀 영상은 미세한 디테일, 대조도 및 공간분해능이 우수한 것으로 평가되었다.

본 연구에서는 일반해상도 및 고해상도 모드를 제공하는 DEXA 검출기를 개발하고, 상호비교평가를 성공적으로 수행하였다. LYSO-GAPD 검출기는 간단한 회전장치를 추가함으로써 선택적으로 공간분해능을 제공할 수 있는 DEXA 검출기 및 시스템 개발에 적용가능하고, 다양한 엑스선 검출기 응용분야에 활용될 것으로 사료된다.

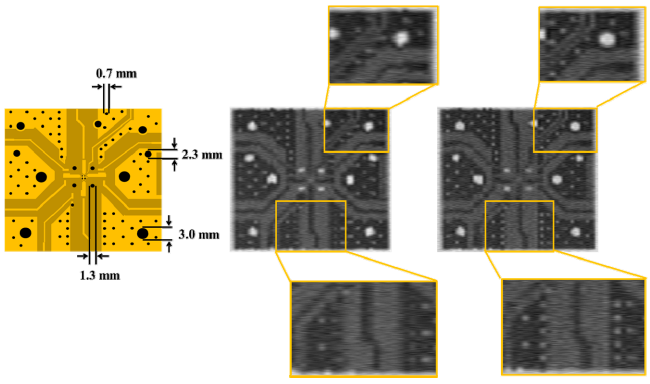

Fig. 1. 팬텀을 이용한 영상획득실험결과. 다양한 구멍크기와 라인패턴을 갖는 테스트 팬텀(왼쪽), 일반해상도 모드(가운데) 및 고해상도 모드(오른쪽)에서 획득한 DEXA영상

Optimization of variable collimator Thickness for disaster environmental monitoring

Jong-Hun Won[1*], Dong-Hee Han[1], Seung-Jae Lee[3], Hak-Jae Lee[4], Cheol-Ha Baek[2†]
[1]Department of Medical Health Science, Kangwon National University, SamCheok, Republic of Korea
[2]Department of Radiological Science, Kangwon National University, SamCheok, Republic of Korea
[3]Department of Radiological Science, Dongseo University, Busan, Republic of Korea
[4]ARALE Laboratory, Inc, Seoul, Republic of Korea

Gamma cameras are widely used in the radiation industry to respond to a wide range of changes to safety accidents and natural disasters.[1] Pinhole collimators are used for wide-area gamma-ray imaging, where gamma-rays can be acquired through a single small hole to obtain high-resolution images, but they have very low sensitivity.[2] Thus, this study derived optimized design variable values by setting parameters for the study of thickness optimization of variable pinhole collimators to be used in high resolution gamma-ray cameras for wide area monitoring. The Monte-Carlo simulation tool, GATE (geant4 application for tomographic emission), was used for optimization research. In gamma-camera, the scintillator set the gadolinium aluminum gallium garnet (GAGG) to 25.8 × 25.8 × 3 mm, and the radiation source positioned a point source of ^{137}Cs (662 keV) isotope 10 mCi at a distance of 60 mm from the center axis of the detector. For setting the variable collimator thickness, the total thickness of the collimator was set by testing the penetration of the tungsten material. Based on the total thickness variables, the leaf of the variable collimator was composed of five layers and the thickness optimization study was conducted for each leaf. In order to derive optimization design variables, the sensitivity and resolution of the dotted source were obtained and the trade-off result was obtained. As a result, the height of variable pinhole can be variously constructed, and based on the results of spatial resolution and sensitivity, the thickness of the five layers of leaf was derived as 6 mm on the first floor, 2 mm on the second floor, 4 mm on the third floor, 2 mm on the fourth floor, and 6 mm on the fifth floor. Based on the values of the optimization design variables, this study optimized the leaf thickness of the variable collimator for gamma-ray imaging for wide-area monitoring. It is expected that it will be applied to various industries where radiation is used in various fields by using gamma cameras that use collimators with variable systems.

Acknowledgement

This work was supported by National disaster management research Grant funded by the Korea government (2019-MOIS32-024).

References

[1] S. G. Jeong, Y. J. Jung, K. D. Kim, J. K. Bae, H. J. Lee, K. S. Lee, “Development of Wide Area Monitoring Radiation System Using Variable Collimator”, The Institute of Electronics and Information Engineers, Vol. 2016, No. 6, pp. 1254-1257, 2016.

[2] C. H. Baek, S. J. An, H. Kim, S. W. Kwak, and Y. H. Chung, “Development of a pinhole gamma camera for environmental monitoring”, Radiation Measurements, vol. 59, pp. 114-118, Dec. 2013.

A Feasibility Study on the Clinical Application of alanine/ESR Dosimetry

Ki-Tek Han[1*], Woo-sang Ahn[2], Eunhyuk Shin[3], Jeho Min[1], Do Hyeon Yoo[4], Hyojun Park[4], Chul Hee Min[4], Han-Ki Jang[1†]

[1]Radiation Technology and Research Center, Korean Association for Radiation Application, Jeongup, Korea
[2]Gangneung Asan Hospital, University of Ulsan College of Medicine, Gangneung, Korea
[3]Department of Radiation Oncology, Samsung Medical Center, Seoul, Korea
[4]Department of Radiation Convergence Engineering, Yonsei University, Wonju, Gangwon-do, Korea

An alanine/ESR dosimetry is relevant to biological and physical dosimetry application. Recently, standard laboratories like National Physics Laboratory(NPL, UK), National Institute of Standard and Technology(NIST, US), Physikalisch-Techniche Bundesanstalt(PTB, Germany) are developing reference dosimetry based on alanine/ESR dosimetry[1]. An alanine is the most well-known substance as a free radical dosimeter and is widely used in various dosimetry fields. Especially, radiation transport characteristic of alanine is highly close to that of water, making this substance useful for dosimetry in radiation therapy. An alanine also has advantages that are less environmental factors and easier to handle than GD/TLD/OSL, which is traditionally used in the medical field. In this study, the feasibility of clinical application for the alanine/ESR dosimetry was evaluated. The evaluation method is based on ISO/ASTM 51607:2013 protocol described for dosimeter materials, instrumentation, and procedures for using the alanine-ESR dosimetry system for measuring the absorbed dose in the photon and electron[2].

In order to apply the Alanine/ESR dosimetry to radiation therapy, it is necessary to evaluate the properties of the alanine sample and validate the sample reference irradiation to improve the reliability of the measured signals. In this study, a clinical linear accelerator(CLINAC) installed in a domestic hospital was used to evaluate therapeutic radiation. In addition, Co-60 irradiation system was used to compare the absorbed dose to water with CLINAC. First of all, beam stability test was performed using farmer type ion-chamber. Prior to the beam stability test, the ion-chamber cross-calibration between KARA and hospital was performed to improve the reliability of the result. The beam stability test was conducted in two ways: dose response and dose rate. As an experimental result, %RSD for all results was obtained with less than 0.045%, it is confirmed that the beam was very stable. Secondly, the characteristics of the alanine such as the dose rate dependence and integrity of dose accumulation for alanine were evaluated to verify the reference irradiation for alanine sample. In case of alanine sample, two types of alanine sample, each 4.8 mm and 4.0 mm in diameter were used. From the results, both alanine samples were assessed to have a relative standard deviation(%RSD) of 0.71% or less, which confirmed the integrity of the dose accumulation of the alanine. In the case of dose rate dependence, %RSD for all results was obtained with less than 5%. Finally, the dose response curves for water absorption doses were derived using the Co-60 gamma-ray irradiation system and CLINAC to evaluate linearity of dose response and energy dependence. The dose response curves were analyzed by comparing the response curves for Co-60 gamma rays and 6MV, 10MV X-rays in the dose range of 1-100 Gy. As an experimental result, the R-square values of the dose response curves were more than 99.99%. And we confirmed that based on the Co-60 gamma-ray absorbed dose to water response curve, the slope of each response curve was assessed to be less than 1%. It is judged that the energy dependency

is insufficient based on the absorbed dose to water. We also verified the dose response curve by measuring an alanine sample with a high dose of 63.02 Gy. It was confirmed that the converted dose has a 0.1% difference from the reference dose.

In this study, we confirmed that alanine/ESR dosimetry fulfills many of the properties required for clinical applications. Based on the results, the alanine/ESR dosimetry is judged to be suitable for clinical application.

Acknowledgement

This work was supported by KOREA HYDRO & NUCLEAR POWER Co., LTD (No. 2018-Tech-02).

References

[1] J. Helt-hansen, F. Rosendal, I. Matilde Kofoed, C. Erik Andersen, Acta Oncol. 48, 216 (2009).

[2] International Organization for Standarization (ISO), ISO/ASTM 51607 (2013).

Magnetic Modulated Radiation Therapy, a simple new idea

정누리현[1*], 곽정원[2], 안소현[1], 주은빈[1], 신영섭[2], 김창환[2]
[1]강원대학교병원 방사선종양학과
[2]서울아산병원 방사선종양학과

방사선치료는 암세포를 제거함에 있어서는 효과가 뛰어나나, 치료 부위 주변의 정상조직이 손상되는 한계가 있다. 치료 부위 주변 정상조직의 손상이 방사선치료의 부작용으로 나타나며, 부작용에 대한 우려로 충분한 방사선치료가 이루어지지 못할 경우 암이 완전히 제거되지 못하며, 이는 치료 실패 혹은 재발로 귀결된다. 방사선치료 관련 기술의 고도화로 치료 부위에서 다소 떨어진 (>5-10mm) 정상조직에 미치는 방사선량은 상당히 감소시킬 수 있게 되었으며, 이로 인해 해당 정상조직의 손상을 최소화 할 수 있다. 하지만 치료 부위에 인접한 (<5mm) 정상조직의 손상은 현대 방사선치료에서도 여전히 해결되지 않은 문제이다. 치료 부위 인접한 정상조직의 손상은 방사선 단독 치료의 물리적 한계로, 방사선의 종류 (광자, 전자, 양성자)나 방사선 전달의 기술 (IGRT, IMRT)과 무관하게 모든 방사선 치료에서 나타난다.

한편, 방사선치료 시 에너지 (방사선량) 전달은 주로 광자와 인체 조직의 상호작용으로 발생한 2차 전자에 의해 이루어진다. 따라서 자기장으로 2차 전자의 운동 방향을 조절하면 방사선량 분포를 조절이 가능하다. 하지만 체내에서 유의미한 수준의 전자 분포 조절을 위해서는 3-5T 이상의 자기장이 필요한데, 이러한 고강도 자기장은 방사선 생성에 영향을 주어, 그 동안 자기장 장치와 방사선치료기의 융합이 어려웠다.

본 연구팀은 체내에 공기 주입함으로써 0.2-0.5T의 저강도 자기장으로 방사선 분포를 조절하는 개념을 제안한다. '자기 조절 방사선치료 (Magnetic Modulated Radiation Therapy)'를 통해 전립선암 환자에 대한 전산모사, 팬텀, 동물 실험 모델에서 전립선암에 인접한 직장 부위의 방사선량을 20-30% 감소시킬 수 있음을 확인했다.

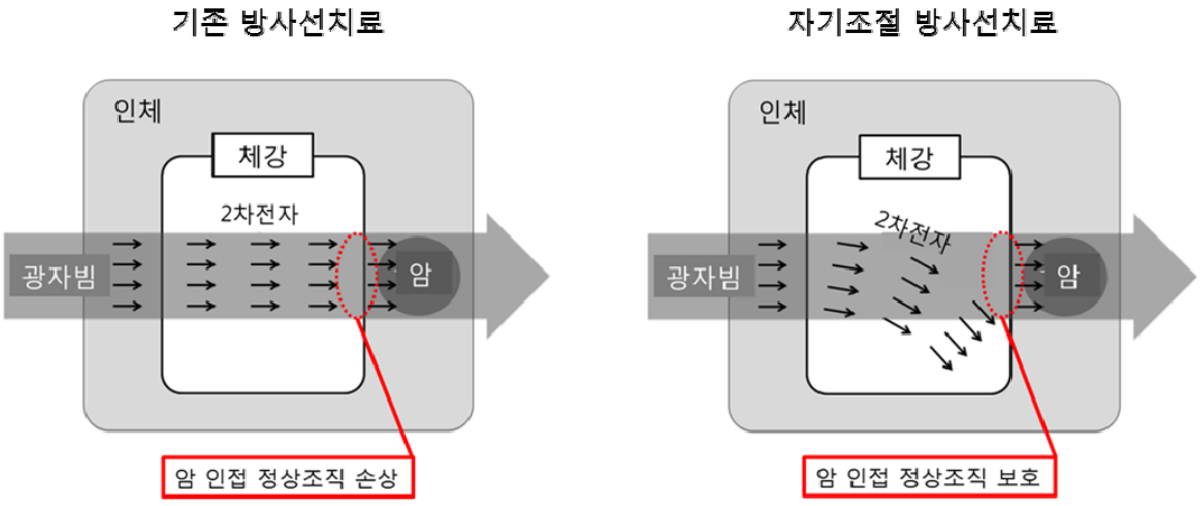

Interplay Effect in Proton Scanning Therapy by Magnetic Scanner

Jeongmin Seo*
Dept. of Radiological Science, Catholic University of Pusan, Korea

Proton therapy is cutting edge technology in clinical radiation oncology. Especially Proton pencil beam spot scanning is one of most advanced techniques in radiation therapy. Proton therapy have two types of shooting radiation. One is scattering type which performed by scatterers, other is scanning type performed by control magnetic scanner. Scanning type use pencil beams which do not consider the movements of organs and targets from breathing.

Radiation therapy planning systems do not properly reflect the interplay effect caused by the independent movement of the beam and the target in the patient. Thus, the interplay effect may cause the delivered radiation dose to deviate from the planned one.

This effect has emerged as a topic of significant interest in the field of proton therapy. Previous studies used 10 phases or less of 4D plan were used to represent the continuous respiratory motion, making these dose calculations questionable. It has never been confirmed if these discrete phases properly represent a patient's actual/continuous movement of respiratory motion.

In this study, the respiratory motion was simulated using phantoms and fast 4D dose calculation was performed using a kernel method for investigating proper temporal resolution of 4D calculation in spot scanning by magnetic scanner.

The results of this study suggest a paradigm to reason the appropriate temporal resolution, depending on factors such as amplitudes, for evaluation of interplay effect in spot scanning by magnetic scanner.

KMS 2020 Summer Conference

Special Session Ⅳ

‘산화물 자성체 세션’

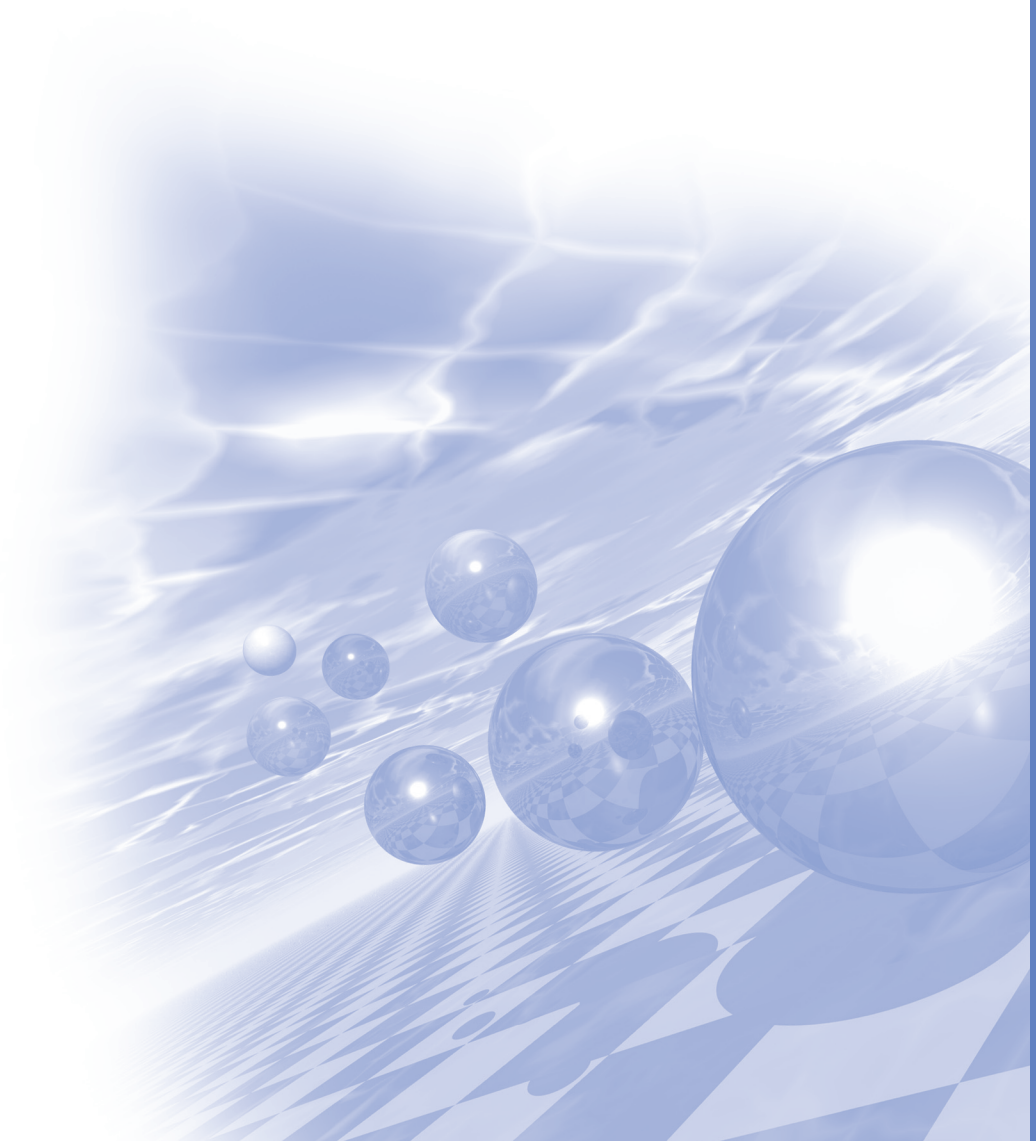

Magnetic skyrmions

Jung Hoon Han*
Department of Physics, Sungkyunkwan University, Suwon 16419, Korea

A full decade has passed since the initial discovery of magnetic skyrmion lattice in thin-film ferromagnets. Fundamental attributes responsible for their formation, namely the competing effects of asymmetric Dzyaloshinskii-Moriya spin exchange and the Zeeman interactions, on top of the ferromagnetic spin exchange, had been quickly identified. The dynamical equations governing the skyrmion motion and its interaction with the electron fluid were also immediately understood. A few years later, a solid foundation for the way in which magnons interact with the skyrmion spin texture was also laid out. Some interesting ideas for the nucleation of skyrmions by non-magnetic means, i.e. without involving the large external magnetic field, were proposed and realized in laboratories. Within a decade, skyrmions have evolved from a novelty to ubiquitous sightings in various non-centrosymmetric materials. In this review, I will cover several key themes in skyrmion physics from theoretical perspective and describe some recent developments in the field. Hall-like motion of magnons passing through skyrmions have been observed indirectly in the interesting “ratchet” experiment by Tokura's group some years ago. I will discuss the possibility of a more direct observation of the magnon thermal Hall effect in skyrmion matter.

Spin Liquid State and Topological Structural Defects in Hexagonal $TbInO_3$

Jaewook Kim[1,2*], Xueyuen Wang[1], Fei-Ting Huang[1], Yazhong Wang[1], Xiaochen Feng[1], Xuan Luo[3], Y. Li[1], Meixia Wu[1], S. Mori[4], D. Kwok[1], Eundeok Mun[5,6], Vivien Zapf[5] and Sang-Wook Cheong[1,3]

[1]RCEM and Dept. of Physics and Astronomy, Rutgers University, Piscataway, U.S.A.
[2]Korea Atomic Energy Research Institute, Daejeon, Republic of Korea
[3]Lab. For Pohang Emergent Materials and Max Plank POSTECH Center for Complex Phase Materials, Pohang, Republic of Korea
[4]Dept. of Materials Science, Osaka Prefecture University, Osaka, Japan
[5]National High Magnetic Field Laboratory, Los Alamos National Laboratory, Los Alamos, U.S.A.
[6]Dept. of Physics, Simon Fraser University, Burnaby, Canada
E-mail: jaewook@kaeri.re.kr, sangc@physics.rutgers.edu

The Kitaev model describes an exactly solvable quantum model in a two-dimensional honeycomb lattice which may host anyonic excitations, which can be implemented in topological quantum computing [1]. Here, we report the coexistence of ferroelectricity and a spin liquid state in hexagonal $TbInO_3$ with quasi two-dimensional triangular spin lattice. Geometrical ferroelectricity associated with In trimerization naturally accompanies topological ferroelectric structural defects. Magnetic susceptibility data show in-plane magnetic anisotropy of Tb spins without any long-range order above 1.8 K, and we also confirm no trace of any phase transition down to 0.15 K from a specific heat measurement, which indicates that this system is highly frustrated and may host a spin liquid ground state. By analyzing the Schottky anomaly in the specific heat results, we propose a model where crystal-field levels are different in each Tb sites, and only one of them has a magnetic ground state and forms a unique honeycomb spin lattice. These observations put forward an interesting possibility where spin liquid and ferroelectric behaviors coexist, and the atomically sharp ferroelectric domain walls may host new magnetic edge states or local spin excitations [2]. We also discuss the further tunability of this system by substituting rare-earth ions such as Sm, Eu, and Gd [3].

References

[1] A. Kitaev, Ann. Physics 321, 2 (2006).
[2] J. Kim *et al.* Phys. Rev. X **9**, 031005 (2019).
[3] J. Kim *et al.* in preparation.

Interplay between spin-orbit coupling and van Hove singularity in Sr_2RuO_4

Choong Hyun Kim*
Center for Correlated Electron Systems, Institute for Basic Science,
Seoul National University, Seoul 08826, Korea

We present a systematical theoretical study on the role of spin-orbit coupling and van Hove singularity in the dynamical properties of Sr_2RuO_4 by means of density functional theory plus dynamical mean-field theory with an exact diagonalization solver. We show the Fermi liquid to Hund's metal crossover through a phase diagram on the temperature-Hund's coupling plane. Doping dependence calculations suggest that the suppression of the Fermi liquid phase is driven not only by the well-known spin-freezing mechanism but also by van Hove singularity. The spin-orbit-coupling brings crucial changes to this effect, by amplifying van Vleck contribution of magnetic responses. Our results provide a new implication on how Hund's metal emerges in a realistic electronic structure.

Magnetic excitations in d^7 j_{eff}=1/2 Kitaev honeycomb materials, $Na_3Co_2SbO_6$ and $Na_2Co_2TeO_6$

Jaehong Jeong[1,2*], Chaebin Kim[1], Gaoting Lin[3], Shinichiro Asai[4], Takatsugu Masuda[4], Jie Ma[3] and Je-Geun Park[1]

[1]Center for Quantum Materials, Dept. of Physics & Astronomy, Seoul National University, Seoul 08826, Korea
[2]Center for Correlated Electron Systems, Institute for Basic Science, Seoul National University, Seoul 08826, Korea
[3]Department of Physics and Astronomy, Shanghai Jiaotong University, Shanghai 200240, China
[4]Institute for Solid State Physics, The University of Tokyo, Chiba 277-8581, Japan
E-mail: hoho4@snu.ac.kr

The materialization of the Kitaev spin liquid driven by bond-dependent anisotropic interactions has been of great interest over the last decade. Based on the Jackeli-Khaliullin mechanism, the candidates have been limited mostly to the 4*d* and 5*d* electron systems with the low-spin d^5 electron configuration, such as Ir^{4+} and Ru^{3+} compounds. Very recently, it has been highlighted that the j_{eff}=1/2 state is stabilized and the Kitaev interaction emerges in the high-spin d^7 systems, such as Co^{2+} and Ni^{3+} compounds, which goes beyond the J-K mechanism. Here, using inelastic neutron scattering, we report low-energy magnetic excitations for d^7 Kitaev honeycomb materials, $Na_3Co_2SbO_6$ and $Na_2Co_2TeO_6$. The j_{eff}=1/2 ground state is experimentally confirmed by the j_{eff}=1/2 to 3/2 excitons observed around 27 meV. By carefully examining magnon dispersions with the minimal model Hamiltonian including J_1-J_2-J_3 Heisenberg interactions, Kitaev interaction and symmetric off-diagonal interactions, we evidence a sizable Kitaev interaction in both compounds.

High-velocity spin waves in the $Sr_2IrO_4/Sr_3Ir_2O_7$ heterostructure

B. J. Kim*
Department of Physics, Pohang University of Science and Techonology, Pohang 790-784, Korea

Oxide heterestructures offer a fertile ground for novel phenomena not found in the bulk constituents such as interface superconductivity, magneto-elastic coupling, and the quantum Hall effect, through the reconstruction of the charge, spin, and orbital states at the interface on the nanometer scale. However, how the spin dynamics changes under the constraints set by interfaces remains largely unexplored. In this talk, I will discuss the effect of magnon velocity renormalization in a magnetic heterostructure composed of Sr_2IrO_4 and $Sr_3Ir_2O_7$, which are magnetic insulators with predominantly Heisenberg and Ising interactions, respectively. Using resonant inelastic x-ray scattering, we observe that the magnon velocity in the Sr_2IrO_4 layer near the magnetic zone center is enhanced by almost a factor of two relative to its bulk counterpart. I will discuss possible origins of this phenomenon, in particular in connection with the suppression in the heterostructure of the magnetoelastic coupling which is manifest in the bulk Sr_2IrO_4.

Special Session V

'Magnetization Dynamics'

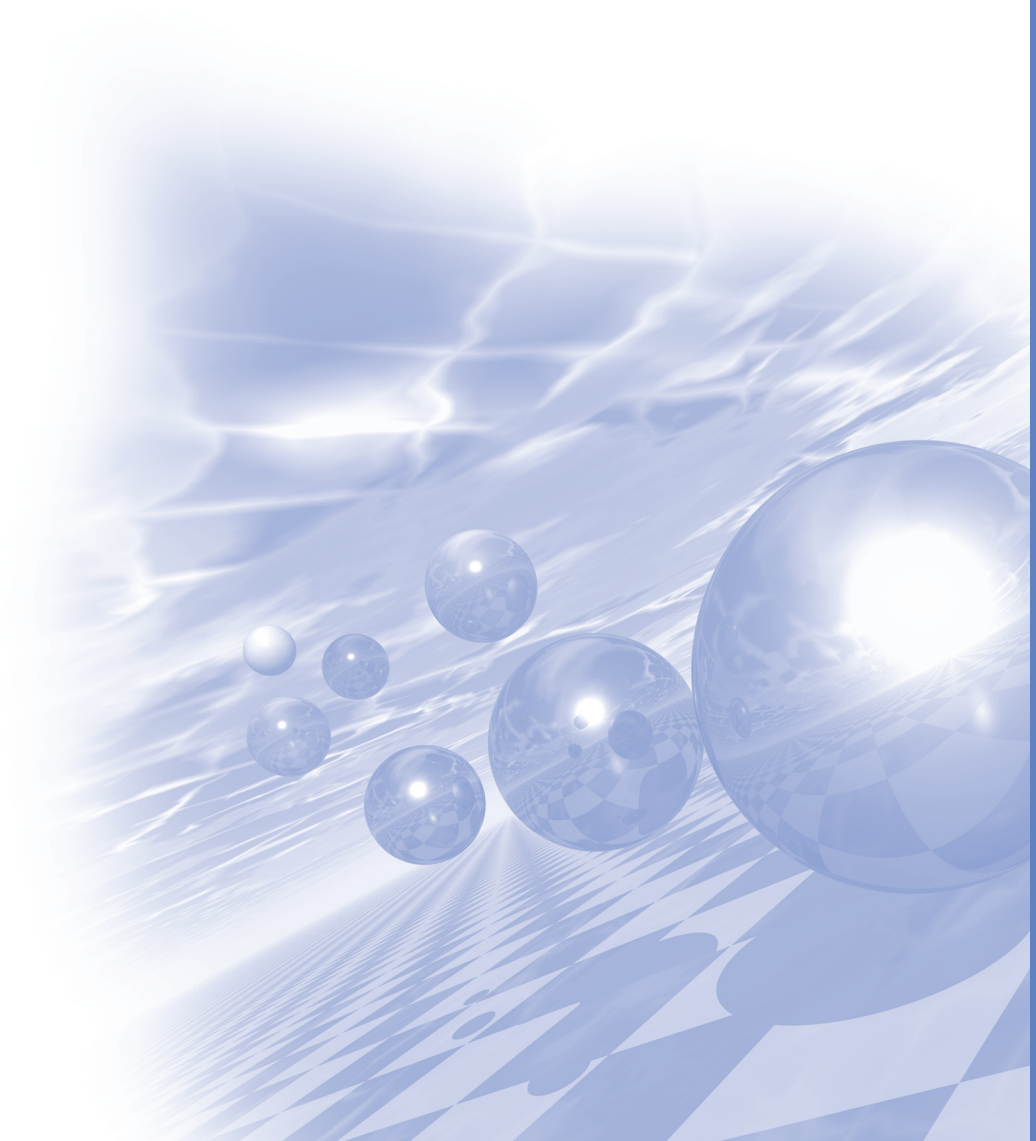

The Systematic Investigation of Dzyaloshinskii-Moriya Interaction by using Brillouin Light Scattering Spectroscopy

June-Seo Kim* and Jaehun Cho
Division of Nanotechnology, Daegu Gyeongbuk Institute of Science and Technology (DGIST),
Daegu 42988, Republic of Korea

The Brillouin light scattering (BLS) spectroscopy is a useful equipment to investigate propagating spin waves (SWs) directly with a range of wave-vector from 10^3 to 10^5 cm^{-1}. From the systematic measurements of two individual types of the propagating SWs such as Damon-Eshbach (surface) mode and perpendicular standing spin wave (PSSW, bulk) mode, various magnetic properties such as the saturation magnetization (M_S), the perpendicular magnetic anisotropy energy density, the exchange stiffness constant (A_{ex}), and the magnetic damping constant (a) in magnetic thin films can be determined. Recently, BLS spectroscopy shows the capability to measure the interfacial Dzyaloshinskii-Moriya interaction (iDMI), which is a non-collinear exchange interaction to nucleate magnetic skyrmion state or magnetic solitons (chiral magnetic domain walls). Especially, the combination of surface mode and bulk mode measurements can determine the exchange stiffness constant directly.

In this study, we review the iDMI energy density dependences as various functions of (i) thickness of ferromagnet (inverse proportionality), (ii) thickness of heavy metal layer, (iii) materials of top and bottom layers, and (iv) thin film properties such as amorphous or polycrystalline materials. Recently, we observe that the intensity of BLS signals and signal-to-noise ratios are dramatically increased over 450% by introducing the dielectric layer due to the anti-reflection coating effect. This fact can overcome the critical issue of BLS measurements that the errors of iDMI energy density measurements are reduced significantly. Lastly, the exchange stiffness constants and the saturation magnetizations with various buffer layers such as Pd, Pt, Ta, and no buffer are directly evaluated by using systematic BLS measurements as shown in Fig. 1. We obtain that Pt and Pd buffer layers lead to higher exchange stiffness constants more than 12% compared with the cases of the Ta buffer layer and no buffer layer. This observation reveals that the exchange stiffness constant and the saturation magnetization, which are one of basic magnetic properties show the same trend on various buffer layers.

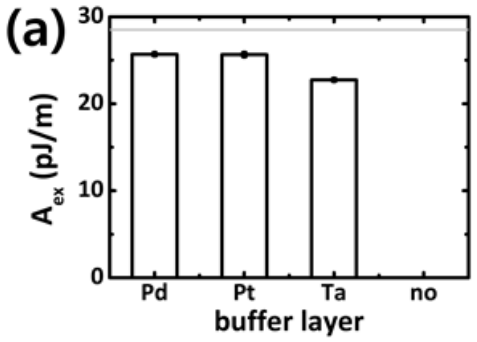

Fig. 1. The exchange stiffness constants of Co films with different buffer layer. The gray line is the literature value of Co (28.5 pJ/m).

Coupled Spin-Charge Transport in Doped-Graphene

Jungmin Park[1,2*], Jung-Woo Yoo[2]
[1]Center for Scientific Instrumentation, Korea Basic Science Institute, Daejeon, Korea
[2]School of Materials Science and Engineering, Ulsan National Institute of Science and Technology, Ulsan, Korea

Graphene, which is two-dimensional material and described with massless Dirac equation, is promising spin transporting channel because it has a long spin relaxation length with very weak spin-orbit coupling. In addition, the disordered graphene with vacancy, adatom, and proximity effect by substrate can have unique electronic characteristics, such as a strong localization, a magnetic ordering, a large spin-orbit coupling, and topological edge state. These properties can lead to unprecedented spin-dependent transport features. Therefore, to understand spin transport properties in disordered graphene is very important for the graphene spintronics. In this talk, we will present the spin and charge transport properties in graphene with Au and Fe adatoms. In Au-clustered graphene, we employ a nonlocal geometry to study the spin Hall effect induced nonlocal resistance. Our results show that the nonlocal resistance highly depends on the applied gate voltage due to various current channels. However, the spin Hall induced nonlocal resistance becomes dominant at a particular carrier concentration, which is further confirmed through Hanle curves. The obtained spin Hall angle is as high as ~ 0.09 at 2 K [1]. Also, we researched localization and quantum edge state of disordered graphene prepared with Fe clusters. The disordered graphene displayed Anderson localization and quantum spin edge state with splitting of Landau zeroth level. These phenomena could be understood with topological Anderson insulator state [2].

References

[1] J. Park et al., Gate-dependent spin Hall induced nonlocal resistance and the symmetry of spin-orbit scattering in Au-clustered graphene, Phys. Rev. B **95**, 245414 (2017).

[2] J. Park et al., Observation of spin-polarized Anderson state around charge neutral point in graphene with Fe-clusters, Sci. Rep. **10,** 4784 (2020).

Introduction to probabilistic computing based on random MTJs

Ouk Jae Lee* and Seokmin Hong
Center for Spintronics, Korea Institute of Science and Technology, Seoul, Korea

A new computing paradigm that fundamentally increases computational efficiency is required than ever before in order to overcome the energy consumption, miniaturization problems in the nanofabrication process, and computational limitations of current CMOS technology. In particular, non Von-Neumann computing technologies that go beyond existing logic circuit technology, such as Neuromorphic computing and quantum computing, are being studied with greater intention in academy and industry. In the meantime, a new computing method based on the randomness at the physical property level was proposed, which offers excellent possibilities for solving problems that are difficult with conventional computing. The proposed method, called as probabilistic computing (*p-computing*) [1,2], shows a promising candidate to provide novel non-Boolean computing schemes. More importantly, invertible logic functions, integer factorization, and emulation of quantum bits are unique possibilities where the *p-computing* might have advantages compared to conventional digital computing [1 and references therein].

In this presentation, we will introduce the basic concepts of *p-computing* and our initial works on random MTJs that can be used for recently proposed p-computing scheme. In addition we will discuss our primitive results from p-computing circuits with commercially available test-beds.

References

[1] K. Camsari et al., Applied Physics Reviews, 6, 011305 (2019).
[2] W. A. Borders et al., Nature, 573, 390 (2019)

Controlled Writing and Deleting of Magnetic Skyrmions in 2-Terminal Device

Soong-Geun Je[1,2,3*]
[1]Chonnam National University, Korea
[2]Lawrence Berkeley National Laboratory, USA
[3]DGIST, Korea

Magnetic skyrmions are fascinating magnetic pseudo-particles that promises future low-power electronics. Their nanoscale and ambient stability as well as efficient coupling to electric currents make the skyrmions potential information carriers in novel concepts of non-volatile memory, logic devices and, recently, neuromorphic devices. An indispensable requirement for developing such application is the controlled writing and deleting of skyrmions using robust and scalable techniques. Existing schemes utilizing current-induced spin-orbit torques need to implement associated symmetry breaking constraints within devices. In practice, this requires fabricating custom-designed top electrodes or geometric constrictions, positioning defects, or using current pulses of peculiar shapes. Most solutions have hard-coded write/delete locations with fabrication complexities limiting their scalability. Here we present a simple alternative approach for writing and deleting skyrmions with spatial and temporal selectivity using conventional current pulses within a two-terminal nanowire device. X-ray microscopy experiments and micromagnetic simulations establish the writing and deletion effects as arising from current-induced Joule heating and Oersted field effects, respectively. Consequently, the schemes target contrasting spatial and temporal regions at rates varying oppositely with external bias field. Further, our work outlines energetic considerations governing these schemes and their broader applicability to skyrmionic devices.

The Exchange Stiffness Constant and Its Applications

Jaehun Cho*, June-Seo Kim
Division of Nanotechnology, Daegu Gyeongbuk Institute of Science and Technology (DGIST)

In magnetic heterojunction systems, the strong competition among Heisenberg exchange interaction, Dzyaloshinskii-Moriya (DM) interaction, and magnetocrystalline anisotropy can exhibit complex spin textures such as Skyrmions [1, 2], chiral magnetic domain walls (DWs) [3, 4], Bloch lines [6, 7], and so on. The interfacial DMI based on an inversion symmetry breaking structure has been widely investigated because of its various physical roles in the dynamics of the non-colinear spin structure. The exchange interaction is a purely quantum mechanical phenomenon on the ferromagnetic materials that only occurs between an atom spin and its nearest neighbor magnetic atoms.

In this study, we introduce the determination of exchange stiffness constant on the ferromagnetic thin film and circular dots. The first method is using Brillouin light scattering (BLS). BLS is a versatile tool to investigate various magnetic properties such as the saturation magnetization, the perpendicular magnetic anisotropy energy, the exchange stiffness constant. The second way is using spin-wave eigenmode in the dish-shaped nanomagnet. Furthermore, we will discuss the magnetic skyrmion dynamics by applying gradient magnetic fields investigated by performing LLG simulations and Thiele approach. We described analytical and micromagnetic simulation studies of magnetic skyrmion dynamics in a 1-dimensional nanowire, force by magnetic field gradient along the z-direction while field gradient applied x-direction.

References

[1] T. H. R. Skyrme, Nucl. Phys. **31**, 556 (1962).
[2] U. K. Rössler, A. N. Bogdanov, and C. Pfleiderer, Nature **442** (7104), 797 (2006).
[3] Soong-Geun Je, Duck-Ho Kim, Sang-Cheol Yoo, Byoung-Chul Min, Kyung-Jin Lee, and Sug-Bong Choe, Phys. Rev. B **88**, 214401 (2013).
[4] A. Hrabec, N. A. Porter, A. Wells, M. J. Benitez, G. Burnell, S. McVitie, D. McGrouther, T. A. Moore, and C. H. Marrows, Phys. Rev. B **90**, 020402(R) (2014).
[5] Gong Chen, Alpha T. N'Diaye, Sang Pyo Kang, Hee Young Kwon, Changyeon Won, Yizheng Wu, Z.Q. Qiu and Andreas K. Schmid, Nat. Commun., **6**, 6598 (2015).
[6] Yoko Yoshimura, Kab-Jin Kim, Takuya Taniguchi, Takayuki Tono, Kohei Ueda, Ryo Hiramatsu, Takahiro Moriyama, Keisuke Yamada, Yoshinobu Nakatani and Teruo Ono, Nat. Phys., **12**, 157 (2016).

The dynamics of magnetic droplet soliton driven by spin transfer torque

Sunjae Chung*
Department of Physics Education, Korea National University of Education, Cheongju 28173, Korea

Spin-transfer torque (STT) driven magneto-dynamics have been received many attentions due to its fundamental physics as well as possible industrial applications. Particularly, STT can be utilized for the manipulation of different nano-scale spin-dynamics such as magnetic vortices, bubbles, skyrmions, droplet solitons, and spin-waves. Among these interesting magnetodynamics, I will introduce magnetic droplet solitons which can be nucleated and sustained underneath nano-contact (NC) in so-called spin torque nano-oscillators (STNOs). Magnetic droplet soliton was theoretically predicted in 2010 [1] in the magnetic free layer having a perpendicular magnetic anisotropy and then it was realized experimentally in 2013 [2]. During recent years, several studies have shown its interesting characteristics [3-7]. Here, I will show new experimental results about 1) coexisting and strongly interacting spin torque driven free and reference layer magnetic droplet solitons [8], 2) freezing and thawing magnetic droplet solitons near zero magnetic field [9].

References

[1] M. A. Hoefer , T. J. Silva, and M. W. Keller, Phys. Rev. B **82**, 054432 (2010).
[2] S. M. Mohseni *et al*., Science **339**, 1295 (2013).
[3] F. Macià, D. Backes, and A. D. Kent, Nat. Nanotechnol. **9**, 992 (2014).
[4] S. Chung *et al*., Nat. Commun. **7**, 11209 (2016).
[5] S. Chung *et al*., Phys. Rev. Lett. **120**, 217204 (2018).
[6] J. Hang *et al*., Sci. Rep. **8**, 6847 (2018).
[7] N. Statuto *et al*., Phys. Rev. B **99**, 174436 (2019).
[8] S. Chung *et al*., unpublished.
[9] S. Chung *et al*., unpublished.

Energy optimized switching condition for STT-MRAM

Eunchong Baek, Indra Purnama and Chun-Yeol You*
Department of Emerging Materials Science, Daegu Gyeongbuk Institute of Science and Technology, Daegu, Korea

The spin transfer torque magnetic random access memory (STT-MRAM) is one of the promising future memory technologies and it has been actively studied for a decade. One of the main requirements is reduce the switching current density. Since too strong switching current possibly damaged the ultra-thin MgO barrier, furthermore, writing energy must be minimized. The dilemma is lower current density requires longer pulse duration for the switching. We studied the switching (or non-switching) probabilities for a given pulse amplitude and duration time by solving Fokker-Planck equation (FPE). The analytical expressions for the optimized switching current density are obtained by solving the Fokker-Planck equation with a given specific non-switching probability value. Most importantly, by using the optimizing the current density together with the related pulse-duration time, we find the optimum combination of current amplitude and pulse duration, which may reduce the energy consumption of the STT MRAM by up to 75% [1].

Reference

[1] E. Baek, I. Purnama, and C.-Y. You, Phys. Rev. Appl. **12**, 064004 (2019)

KMS 2020 Summer Conference

Special Session VI

'Magnetism in reduced dimension'

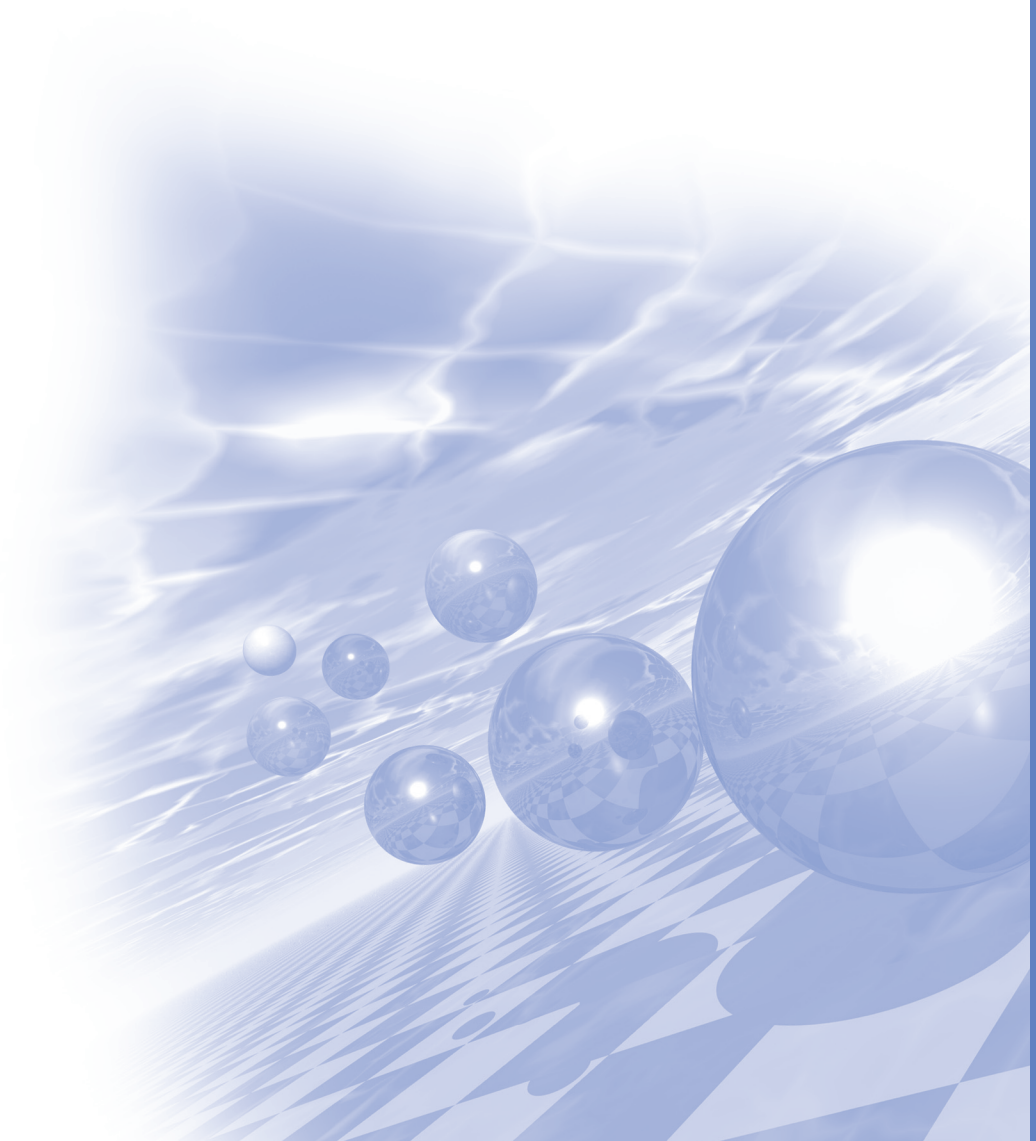

Time-dependent density functional theory calculations of spin-phonon dynamics and band topology of two-dimensional materials

Noejung Park*
Department of Physics, UNIST, UNIST-gil 50, Ulsan 44919, Republic of Korea

Topological states have commonly been cited as a new classification of materials, and global properties immune to local perturbations have been suggested in terms of topological invariants or associated quantities. For real materials, actual computations for them have been achieved through the theories of linear responses over the static ground electronic structure. In this talk, I first summarize our proposal for alternative ways of computation: calculating the real-time evolution of the Hamiltonian, letting the pumping parameter run periodically through the geometric space of the Hamiltonian. As test examples of this method, we present a trivial insulator, a spin-frozen valley-Hall system, a spin-frozen Haldane-Chern insulator, and a quantum spin-Hall insulators. In later part, we also demonstrate the spin precession dynamics of MoS2, in which the spin is strongly coupled to the optical phonon. This dynamical spin state can be resolved into discrete Floquet-phononic spectra, and once the phonon is pumped so as to break time-reversal symmetry, the resulting spin-Floquet structures induce net out-of-plane magnetizations in the otherwise non-magnetic 2D material.

First principles studies of two dimensional ferromagnetic materials

Brahim Marfoua, Imrna Khan and Jisang Hong*
Department of Physics, Pukyong National University, Busan 48513, Korea

Study on two dimensional materials is one of the most intriguing issues in condensed matter physics and materials sciences. So far, numerous types of 2D materials have been experimentally fabricated. Nonetheless, only few materials have ferromagnetic ground state such as CrI3, $FeGeTe_3$, $CrGeTe_3$. Recently, many first principles studies have claimed that new type of 2D ferromagnetic material can exist in stable form although such prediction has not been proved yet experimentally. We also have investigated fundamental magnetic properties of 2D materials such as Curie temperature, magnetic anisotropy, and spin valley polarization in 2D heterostructures. Along with these magnetic properties, we have proposed that 2D magnetic material can show very large spin Seebeck effect, and this feature can be utilized for potential device applications.

This research was supported by the Basic Science Research Program through the National Research Foundation of Korea (NRF) funded by the Ministry of Science, ICT and Future Planning (2019RA21B5 B01069807).

Electron Spin Resonance on Individual Atoms and Molecules on Surfaces

Xue Zhang[1,2], Yu Wang[1,2], Philip Willke[1,2], Aparajita Singa[1,2],
Minhee Choi[1,2] and Taeyoug Choi[1,2*]

[1]Department of Physics, Ewha Womans University, Seoul 03760, Republic of Korea
[2]Center for Quantum Nanoscience, Institute for Basic Science (IBS), Seoul 03760, Republic of Korea
[*]E-mail: tchoi@ewha.ac.kr

Scanning tunneling microscopy (STM) studies of spin properties arising from individual atoms and nanostructures on surfaces have demonstrated nanoscale memory bits and logic gates toward miniaturizing electronic and information devices. In recent years, understanding and controlling individual spins with maintaining quantum coherence become one of highly interesting research topics to utilize the coherent spins for quantum sensing and information processing.

Recently, we successfully combined a conventional electron spin resonance (ESR) technique with a spin-polarized STM and coherently drive spins of individual Fe and Ti atoms on ultrathin insulating MgO. Using this newly developed ESR-STM, we studied magnetic interaction of individual atoms that are coupled through magnetic dipolar and exchange interactions. Unique and advantageous aspects of ESR-STM compared to other quantum magnetic sensors (such as NV centers) are the atom manipulation and imaging capabilities, which allow us to build atomically precise nanostructures and examine their interactions. In addition, we found that both a spin-polarized tip and an external magnetic field play important role to drive the single-atom ESR. Utilizing stronger interaction between a spin-polarized tip and an atom on surface, we successfully drive the single-atom ESR without any external magnetic field which may be useful to study spin systems under low magnetic fields.

Lastly, we use the ESR-STM technique to investigate single atom-molecule complexes as well as Dy (4f elements) atoms to investigate spin distribution across the complexes and to lengthen the coherence time of the spins.

Coherent quantum control of individual atoms on surfaces combined with atom manipulation may promise the STM as a new and unique platform for a quantum sensor, investigating spin-labeled molecular structures and a quantum information processor, modeling quantum magnetism.

Molecule-based magnetic thin film for spin-thermoelectrics

Inseon Oh[1*], Jungmin Park[2], Daeseong Choe[1], Junhyeon Jo[1], Hyeonjung Jeong[1], Mi-Jin Jin[1], Younghun Jo[2], Joonki Suh[1], Byoung-Chul Min[3] and Jung-Woo Yoo[1†]

[1]Department of Materials Science and Engineering, Ulsan National Institute of Science and Technology, Ulsan, 44919, Korea

[2]Center for Scientific Instrumentation, Division of Scientific Instrumentation & Management, Korea Basic Science Institute, Deajeon, 34133, Korea

[3]Center for Spintronics, Korea Institute of Science and Technology, Seoul, 02792, Korea

Spin thermoelectrics (STE), an emerging thermoelectric technology, offers energy harvesting from waste heat with advantages of large-area capability and potential advance in energy conversion efficiency, thanks to orthogonal paths for heat and charge flow. However, magnetic insulators used for STE pose challenges for scale-up due to high temperature processing and difficulty in large-area deposition. Here, we introduce a molecule-based magnetic film for STE applications because it entails versatile synthetic routes in addition to weak spin-lattice interaction and low thermal conductivity. Thin film of CrII[CrIII(CN)6] grown on a Cr electrode via room temperature electrochemical deposition shows effective spin thermoelectricity associated with strong excitations of low energy spin waves. Moreover, the ferromagnetic resonance studies exhibit low Gilbert damping constant ~ (2.4±0.67)×10-4, indicating low loss of heat-generated magnons. The demonstrated STE applications of a new class of magnet will pave the way for versatile recycling of ubiquitous waste heat.

Coupled spin-charge transport in oxide interface

Jung-Woo Yoo*
Department of Materials Science and Engineering,
Ulsan National Institute of Science and Technology, Republic of Korea

A two-dimensional (2D) electron gas emerged at a $LaAlO_3/SrTiO_3$ (LAO/STO) interface is an interesting electronic platform as the structure itself has broken inversion symmetry. This noncentrosymmetric 2D conductor retains Rashba-type spin-orbit interaction, which ties spin and momentum of electrons in the band structure leading to coupled spin and charge transport. In this talk, I will present coupled spin-charge transport in LAO/STO interface evidenced in various experimental platforms. We demonstrated the non-local spin diffusion in conducting interface of LAO/STO using H-bar type structure, where the spin Hall and its inverse effect function as the spin injector and detector [1]. The inherent structural asymmetry in the conductive oxide interface can induce further intriguing transport properties. When the time-reversal symmetry is further broken, the system could exhibit directional propagation of itinerant electrons, i.e. the rightward and leftward currents differ from each other. In addition, the Rashba spin-orbit interaction can be further tuned by applying gate bias, so does the nonreciprocal charge transport [2].

References

[1] Nonlocal Spin Diffusion Driven by Giant Spin Hall Effect at Oxide Heterointerfaces, Nano Lett. **17**, 36-43 (2017)

[2] Gate-tunable giant nonreciprocal charge transport in noncentrosymmetric oxide interfaces, Nat. Comm. **10**, 1-8 (2019)

KMS 2020 Summer Conference

Special Session VII

'Mossbauer & Nano'

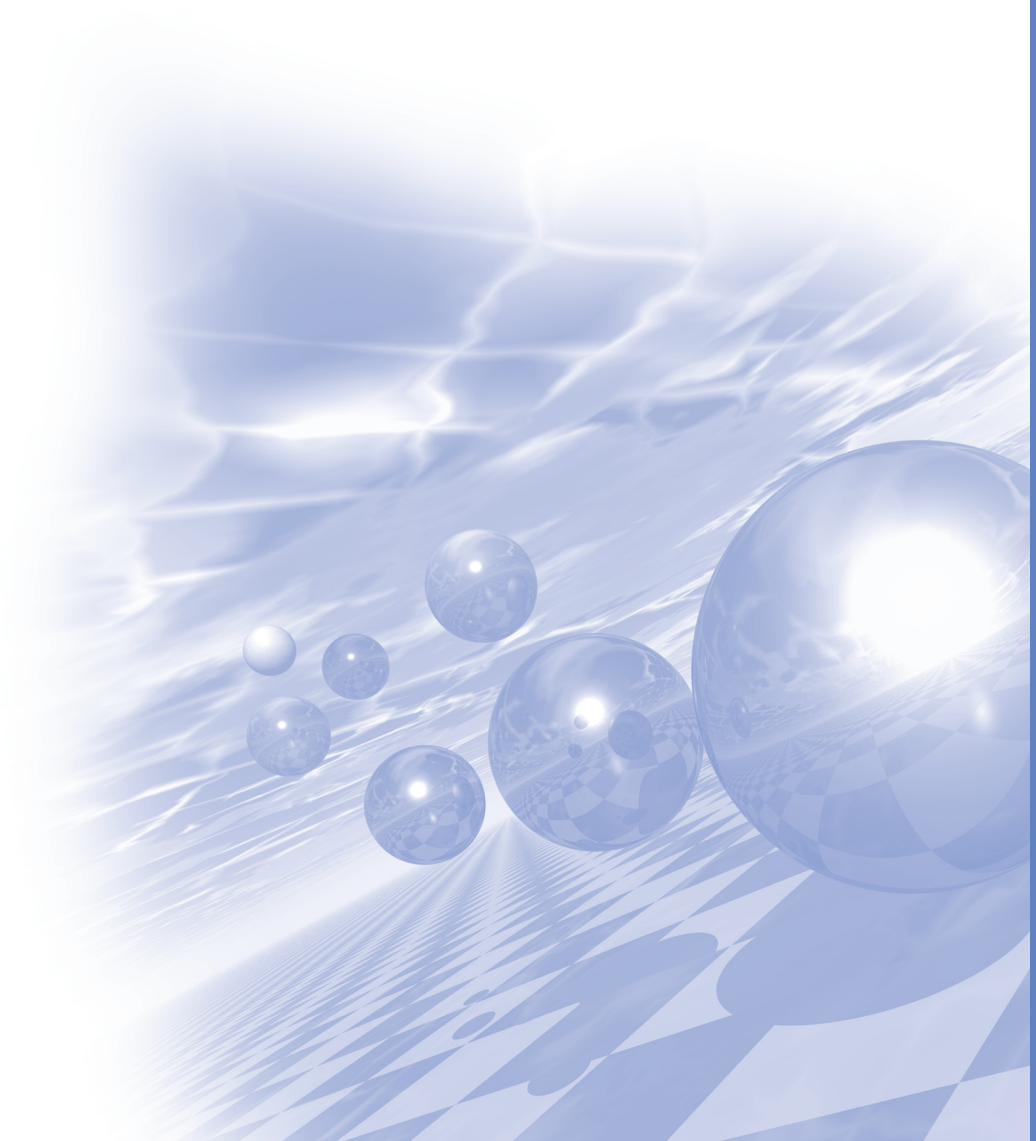

Mössbauer spectroscopic study about firing conditions and coloring mechanism of the ancient Baekje black burnished potteries

Dong Hyeok Moon[1,2*], Myeong Seong Lee[1], Sang Won Nam[1],
Hyen Goo Cho[2], Young Rang Uhm[3]

[1]National Research Institute of Cultural Heritage (NRICH), Daejeon 34122, Korea

[2]Department of Geology and Research Institute of Natural Science, Gyeongsang National University (GNU), Jinju 52828, Korea

[3]Affiliation A, Korea1Radioisotope Research Division, Korea Atomic Energy Research Institute (KAERI), Daejeon, 34057 Korea

Archaeological black burnished potteries collected from Pungnaptoseong, Seoul, South Korea have been subjected to Mössbauer spectroscopic studies, X-ray diffraction, SEM-EDS and organic elementary analysis in order to characterize the black coloring mechanism and firing condition. Two type of samples, BBP1 (black burnished pottery with blackish surface and blackish matrix) and BBP2 (black burnished pottery with blackish surface and ochreish matrix) were not observed difference in mineral and chemical composition between each surface and matrix. In the case of carbon content, a small amount of carbon was detected in the blackish surface in both samples, whereas not detected in each type of matrices. It suggested that the possibility of the existence of another black coloring material. Mössbauer spectra were allows the determination the relative amounts of iron oxide phase in both samples. As a result, BBP1 revealed that higher paramagnetic iron oxide ratio (especially Fe_3O_4 phase) than BBP2, which indicates that one of the black coloring factor. Meanwhile, the magnetic and organic characteristics of RES1 (restored black burnished pottery with traditional method) and PN29 (soot coated red-brownish pottery) were also estimated in order to compare the firing condition. In result, the blackish surface of RES1 examined the higher paramagnetic iron oxide ratio without carbon, while blackish part of PN29 examined lower paramagnetic iron oxide ratio (but higher α-Fe_2O_3) and abundant carbon. It indicates that RES1 might have been fired under reducing atmospheric condition than PN29. In conclusion, each type of black burnished potteries in this study were fired in reducing atmosphere, and it caused a Fe_3O_4 rich higher paramagnetic iron oxide ratio through progressive reduction reaction with iron oxide in soil material. The color of the potteries also reflects the above results.

Activation Study of Nanocrystalline Ferrihydrite-Based Catalysts for Fischer-Tropsch Synthesis using Mössbauer Spectroscopy

Dong Hyun Chun[1,2*]

[1]Carbon Conversion Research Laboratory, Korea Institute of Energy Research,
152 Gajeong-Ro, Yuseong-Gu, Daejeon 34129, Republic of Korea

[2]Advanced Energy and System Engineering, University of Science and Technology,
217 Gajeong-Ro, Yuseong-Gu, Daejeon 34113, Republic of Korea

FTS (Fischer-Tropsch synthesis) is a promising process to obtain low-pollutant liquid fuels and high value-added chemical from syngas (H_2 + CO). Precipitated iron-based catalysts are highly promising for the FTS due to their high activity, low cost, and ease of mass production. In general, the as-prepared precipitated iron-based catalysts should be subjected to a proper pre-activation treatment to change the as-prepared catalysts into active phases for FTS. Several oxide and carbide phases evolve in the precipitated iron-based catalysts during the pre-activation and subsequent FTS reaction. XRD (X-ray diffraction), the most commonly used technique for phase identification, can give only limited information in particular for nanocrystalline catalysts with multiple phases. Mössbauer spectroscopy has proven to be a useful technique for precision analyses on the phase structure of precipitated iron-based catalysts. Furthermore, the Mössbauer spectra can be deconvoluted based on the values of magnetic hyperfine field (H_{hf}), isomer shift (δ), and quadruple splitting (E_Q) for each iron-based species. This can offer detailed quantitative information of iron-based phases in the activated catalysts. In this presentation, we report the activation behavior of nanocrytalline ferrihydrite-based ($FeOOH \cdot nH_2O$, $0<n<1$) catalysts for FTS. The Mössbauer analysis revealed that the ferrihydrite-based catalysts exhibited reducibility and carburizability much higher than conventional hematite (α-Fe_2O_3) based catalysts, due to their unique structural properties.

Study on the hyperthermia and magnetic properties of MNPs using Mössbauer spectroscopy

Hyunkyung Choi*, Chul Sung Kim
Department of Physics, Kookmin University, Seoul, 02707 Korea

Magnetic nanoparticles (MNPs) are attracting considerable attention as materials that are widely applied in medical fields such as biosensors, drug delivery systems, MRI contrast media, and in hyperthermia, and fundamental studies on the change in magnetic properties of nanoparticles have been actively studied. Hyperthermia was first reported by Gilchrist in 1957 as a technique to kill heat-sensitive cells, such as tumors, by applying heat with a temperature of 42 – 43 °C to localized areas of the body. Ultrasonic waves, microwaves, RF induction heating, etc. are used to apply heat to the local site. However, their use is limited as they use a high frequency band that can damage normal cells. To solve this problem, hyperthermia that uses magnetic nanoparticles, a method of killing cancer cells by converting a magnetic loss occurring when an external magnetic field is applied in a frequency range harmless to the human body into heat, has been studied. Furthermore, these magnetic nanoparticles are mainly used as oxides, and metal ions such as nickel, zinc, and manganese have been added in some cases. In this study, MNPs were synthesized by high-temperature thermal decomposition method. The magnetic and thermal properties of MNPs were investigated by VSM, Mössbauer spectroscopy, and magneTherm device. Based on the obtained results, we established suitable magnetic nanoparticles that can be applied to hyperthermia applications.

Study of Archeological Heritages using Mössbauer Spectroscopy

Young Rang Uhm[1*], Gwang Min Sun[1], Hun-Kyung Choi[2] and Chul Sung Kim[2]
[1]Neutron& Radioisotope Application Research Division, Korea Atomic Energy Reasearch Institute(KAERI), Daejeon, Rep.of Korea
[2]Nano-Electro Physics, Koomin univercity, Seoul Rep.of Korea
[*]E-mail: uyrang@kaeri.re.kr

Mössbauer spectroscopy using ^{57}Co as a source is able to apply analyses of reproducing chromaticity of Celadon and Dancheong which is traditional multicolored paintwork on wooden buildings. The greenish colored celadon is determined by the condition of kiln and valence state of iron in glaze. The traditional multicolor of Dancheong is also restored using mineral pigment. Its reddish base color results in the ocher soil in Ulleong-do, Korea. The valence state of iron and its ratio can be accurately analyzed using Mössbauer spectrometer. Recently, development of the potable Mössbauer spectrometer is also focused in our research to apply in-situ detection of heritages.

KMS 2020 Summer Conference

Special Session VIII

'Electro-Magnetic Energy Convergence'

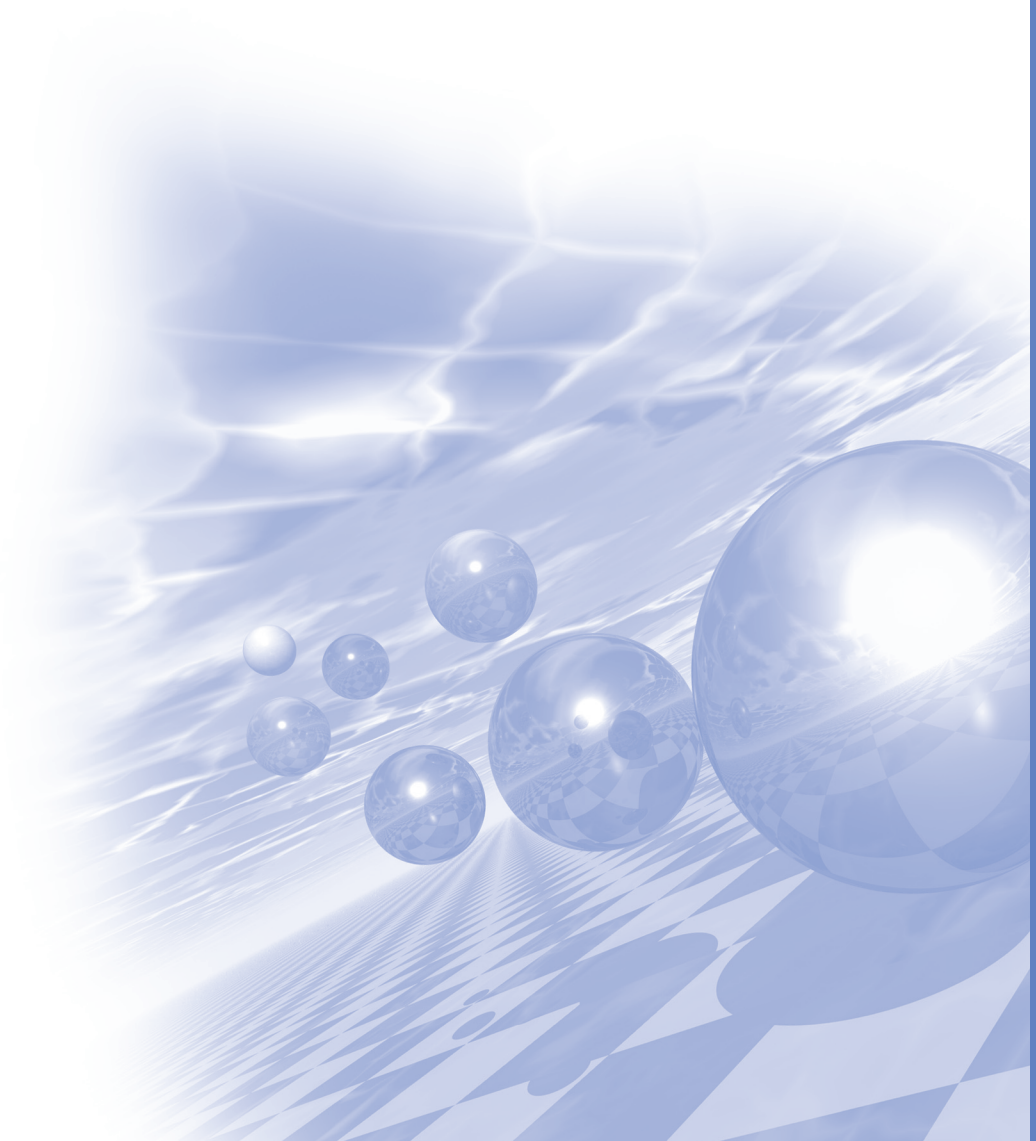

Electrical Parameter Comparison of 8-pole 6-slot and 8-pole 12-slot using Equivalent Magnetic Circuit for Servo motor

Jin-Cheol Park*, Soo-Hwan Park, Sung-Woo Hwang and Myung-Seop Lim
Department of Automotive Engineering, Hanyang University, Seoul, Korea

Since environmental regulations have been strengthened recently, the mechanical component is being replaced by an electric motor in the industrial or automotive application. Among the electric motor types, the PMSM (Permanent Magnet Synchronous Motor) using permanent magnets is adopted owing to a high power density. The types of PMSM can be divided into IPMSM (Interior Permanent Magnet Synchronous Motor) and SPMSM (Surface-mounted Permanent Magnet Synchronous Motor) based on the location of the permanent magnet. The servo motor mainly uses SPMSM because it is relatively simple to control and easier to manufacture than IPMSM. In particular, it is important to select a combination of the pole and slot number for design SPMSM. The cogging torque, power density, and vibration performance are different depending on the combination of poles and slots. Therefore, it is necessary to study the motor performance according to the combination of the pole and slot number.

This paper analyzes and compares the electrical parameters of 8-pole 6-slot and 12-slot motors. The electrical parameters are phase resistance, inductance, and back EMF. Also, the difference in parameters between 6-slot and 12-slot is analyzed using a magnetic equivalent circuit as shown in fig.1. As a result, the phase resistance and inductance of the 8-pole 12-slot are reduced compared to the 8-pole 6-slot under the same condition. Using inverter simulation for BLDC control as shown in fig.2, the torque-speed performance is confirmed from the voltage equation with the determined parameters. Therefore, it is verified that the power density of 8-pole 12-slot is higher than that of 8-pole 6-slot within the same size as shown in fig.3.

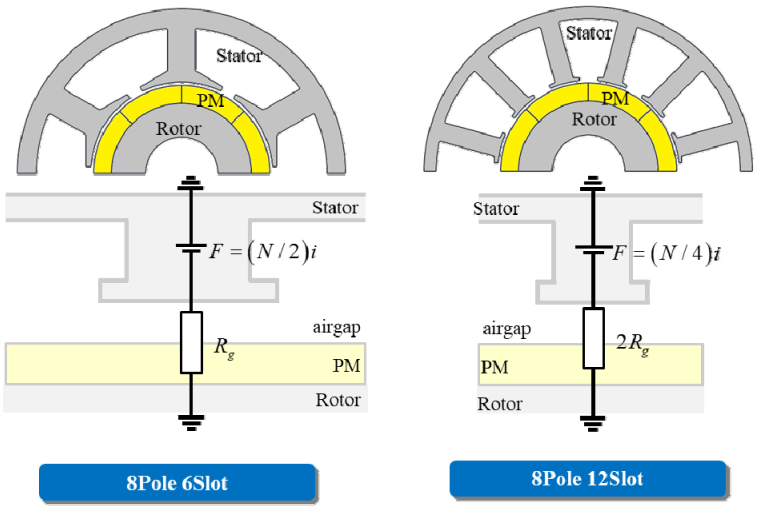

Fig. 1. 8-pole 6-slot and 8-pole 12-slot of magnetic equivalent circuit

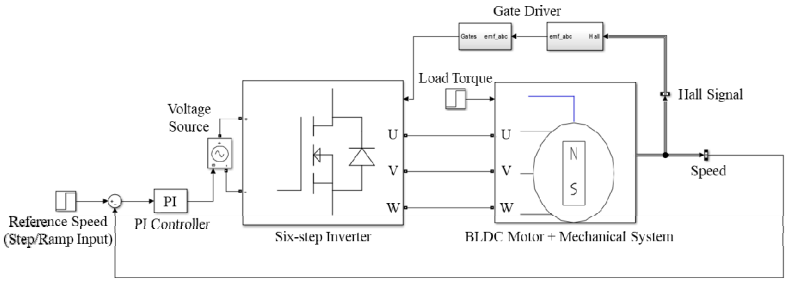

Fig. 2. Inverter simulation for BLDC control

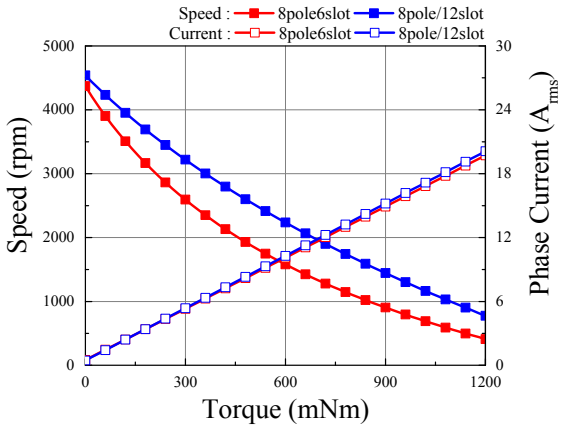

Fig. 3. Simulation result of 8-pole 6-slot and 12-slot

A Study on the Design Technology of Synchronous Motors Related to the Improvement of Permanent Magnet Material Properties

Dong-woo Kang*
Electrical Energy Engineering, Keimyung University, Daegu, Korea

Recently, the trends of conversion of the drive system to electrification has been spreading to various industries including the automobile industry. Hydraulic systems that require high power density are also gradually replacing their position by utilizing high-power gear-motor package technology. This trend could be accelerated by the advancement of technological advances in the high output of permanent magnet materials. Generally, electric motors are classified into DC motors, induction motors, and synchronous machines, and are applied to systems suitable for dynamic characteristics of each device. Systems with a high starting torque and easy speed and torque control has a relatively large share of the DC motors. And systems requiring environmental resistance and long life, the induction motors have a higher preference than other motors. On the other hand, the synchronous motors have relatively high price and difficult control characteristics compared to the two devices mentioned above, but they have been used in more expensive systems due to the advantages of high precision controllability, high power density and high efficiency.

However, in order to replace the mechanically implemented driving technology in the automobile industry market, the technical development of materials had to be supported, because the requirements of the system of light weight and small size must be satisfied. In this paper, the author would like to present the results of the analysis on the development of the introduction of permanent magnets and the technological development trends of synchronous motors. In addition, this paper describes how the market of motors is composed of various industries, and proposes a design guide for permanent magnet synchronous motors according to changes in automobile driving systems. In particular, the author analyzed the past case where a motor structure was developed to replace the shortage of supply and demand depending on the price of permanent magnets and weaponization of resources. Through this,the author will discuss the importance of correlation between material development and motor design to predict and prepare for this situation in the future.

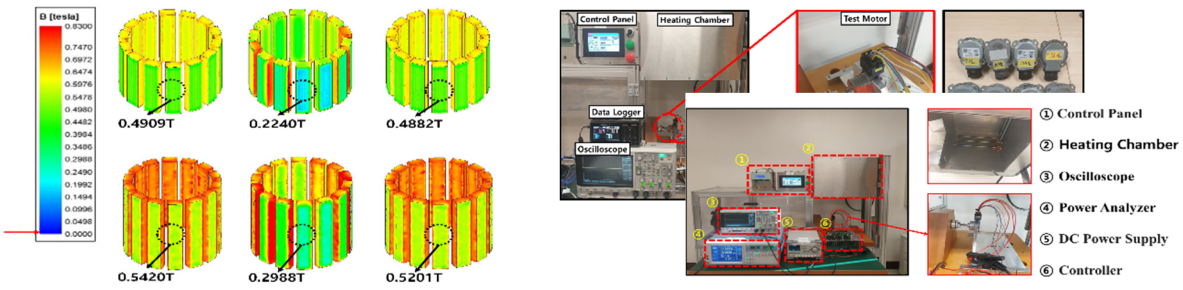

(a) (b)

Fig. 1. reliable analysis of synchronous motors with permanent magnets,
(a) demagnetization analysis based on 3D model (b) Experiment of demagnetization

The Simulation Process of Electromagnetic Field, Thermal and NVH for EV/HEV Traction Motor

Eun-sil Han*
Tae Sung S&E, Seoul, Korea

Currently, the automotive industry is rapidly changing to eco-friendly vehicles and various transportation types because of globally various environmental regulations. So, the importance of traction motors is more increasing, and motor design and analysis engineers need not only optimization of electromagnetic performances but also analysis processes in an integrated environment, including thermal and noise/vibration solutions. The reason is that the temperature characteristics of the magnetic materials and the coil heating affect the motor performance, and the imbalance of the electromagnetic force occurred for various reasons causes vibrations and noises. Today, I present about EV/HEV traction motor analysis process considering electromagnetic material properties in an Ansys-based integrated simulation environment.

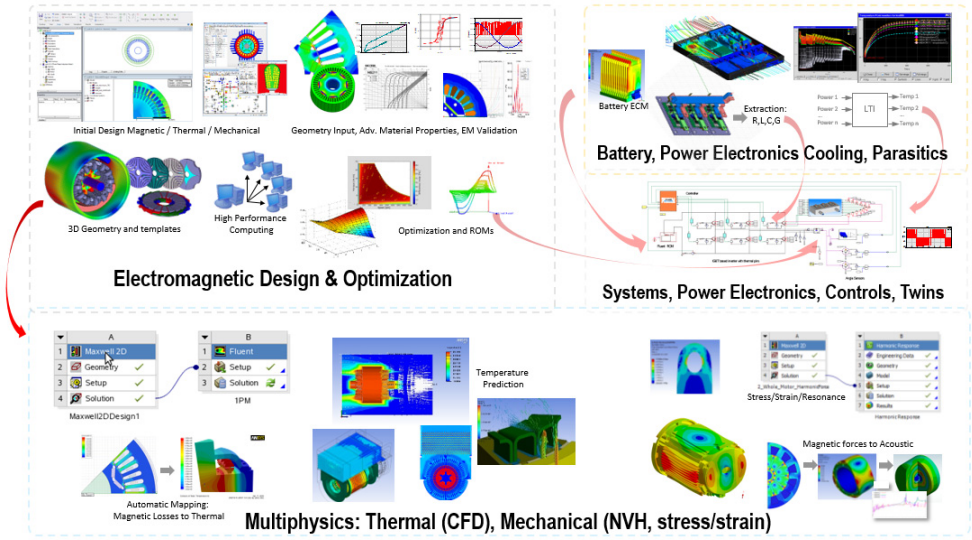

그림 1. Simulation Workflow : Motor and Drive system

[그림 2]와 [그림 3은] 모터의 Electro-Thermal 해석 과정과 NVH 해석 과정과 결과들을 보여준다.

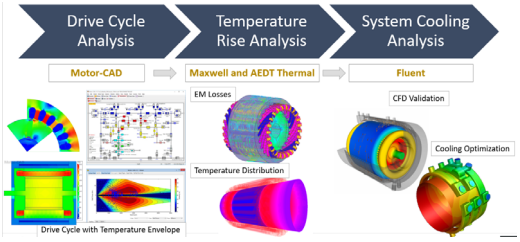

그림 2. Electro-Thermal Analysis Process

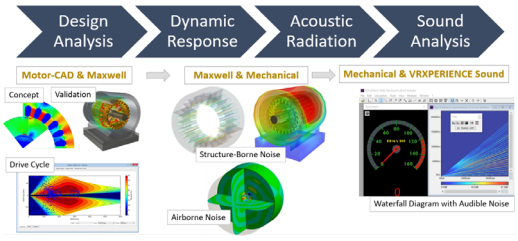

그림 3. NVH Analysis Process

Study on Reduction of Cogging Torque and Torque Ripple of Permanent Magnet Electric Motor Considering Magnetization Pattern Using Magnetization Yoke

Sung Gu Lee*
Department of Electrical Engineering, Dong-A University, Busan, Korea

The efficiency and output density of permanent magnet motors are continually improved by the development of magnetic materials such as high-performance permanent magnets and the development of motor technology. In addition, the standards for noise and vibration in various applications are continuously being strengthened. However, the inverse relationship between efficiency/power density and cogging torque/torque ripple serves as a factor that complicates cogging/torque ripple reduction. Currently, the design technique limited to the shape of the existing core and magnet has reached the technical limit for reducing cogging torque/torque ripple.

In order to effectively reduce cogging torque/torque ripple while minimizing the decrease in efficiency/power density, it is necessary to be able to accurately consider the correct magnetization pattern of the permanent magnet according to the magnetizing yoke shape and the exact physical property data of the permanent magnet. However, studies considering magnetization patterns of magnets using magnetization yokes at the design stage are difficult to find. This presentation intends to show that the efficiency/output density can be maximized while effectively reducing cogging torque/torque ripple through a motor design that considers the magnetization pattern of the magnet according to the magnet properties and magnetization yoke shape in the motor design stage.

A Study for motor requirement of electrical airplanes

Sungchan Kim*, Hyun-ki Kim
Korea Aerospace Research Institute, Korea

The development of transportation power in preparation for fossil fuel exhaustion has been strategically studied as a global concern from the past, and the main energy source to be replaced is estimated to be electric energy, and the development of transportation air vehicles using it is competitively promoted in each country. In Europe, the U.S. and other countries, the company is studying commercialization through a pilot project of small airplanes using various eco-friendly electric power devices(secondary battery, fuel cell, solar cell, etc) to enter the eco-friendly airplane market. Korea also believes that now is the right time for technology independence and technology guidance related to electric airplanes. Moreover, the development of electric airplanes using Siemens' electric propulsion system is actively promoted. In addition, Pipistel's Electrical plane was the first in the world to receive EASA certification. Korea also started developing 65kW propulsion motor and starting generator for General Aviation class aircraft electric propulsion system in 2018. This task is to develop high efficiency propulsion motors and starting generators suitable for aviation as core components, and KARI is responsible for system integration and component flight test evaluation.

This study is intended to examine foreign motor development cases and analyze the requirements of the systems necessary for the development of motor for electric propulsion aircraft and propose them as development requirements.

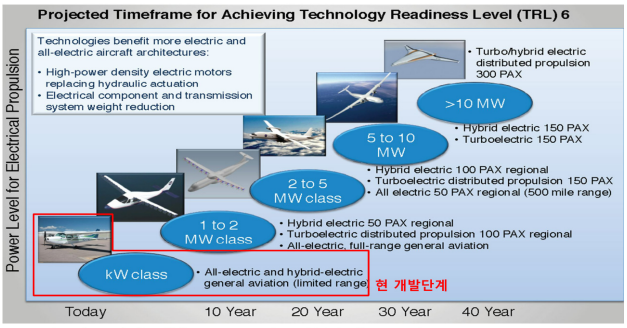

Fig. 1. Road map of Electrical Propulsion

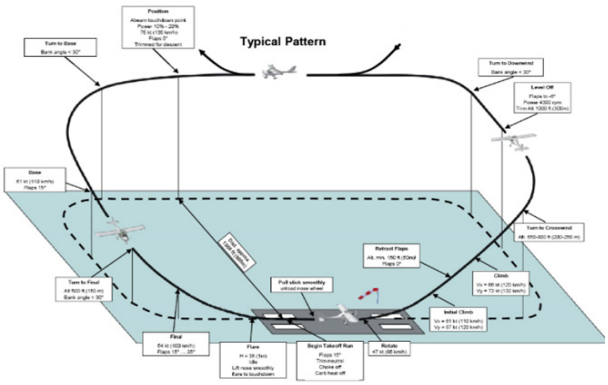

Fig. 2. Mission profile of flight test

Vibration Analysis on IPMSM Depending on Types of Eccentricity

Dae-Kee Kim*, Jae-Hyun Kim, Dong-Min Kim, Myung-Seop Lim
Department of Automotive Engineering, Hanyang University, Korea

The growing concerns of global scale of pollution and the depletion of conventional energy sources such as fossil fuel caused the interests in alternative energy source. Then, electric motor is applied to various industrial fields to solve these problems. Interior permanent magnet synchronous motor (IPMSM) is one of the motor types. Because the torque density of IPMSM is relatively high compared with other types of electric motor, it is widely used in various appliances. Researches on magnetic material and design technology improved the performance of motor. On the other hand, as the importance of quality of life grew higher, demand for lowering the noise and vibration has increased. Thus, it is important to analyze the vibration generated by electric motor.

The radial electromagnetic force generated by electric motor, acts as the excitation force. This force acts on the teeth of the stator inducing the vibration of whole stator core of motor. Thus, in order to analyze the motor vibration, it is necessary to analyze the radial electromagnetic force. The amplitude and vibration order of radial electromagnetic force mainly affect the aspect of motor vibration. The vibration order of radial force is the spatial harmonic component which indicates the spatial distribution. Because the deformation of stator is inversely proportional to the vibration order, lower vibration order cause the larger motor vibration.

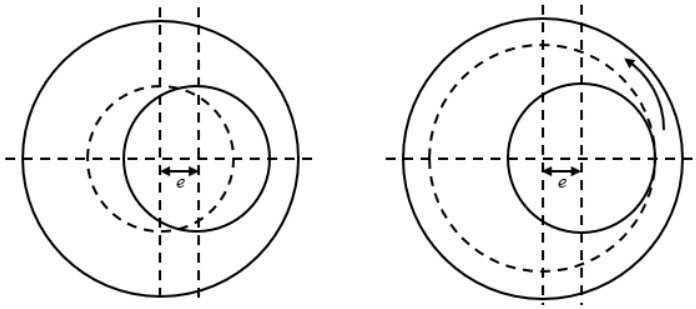

(a) (b)

Fig. 1. Types of eccentricity (a) static eccentricity (b) dynamic eccentricity

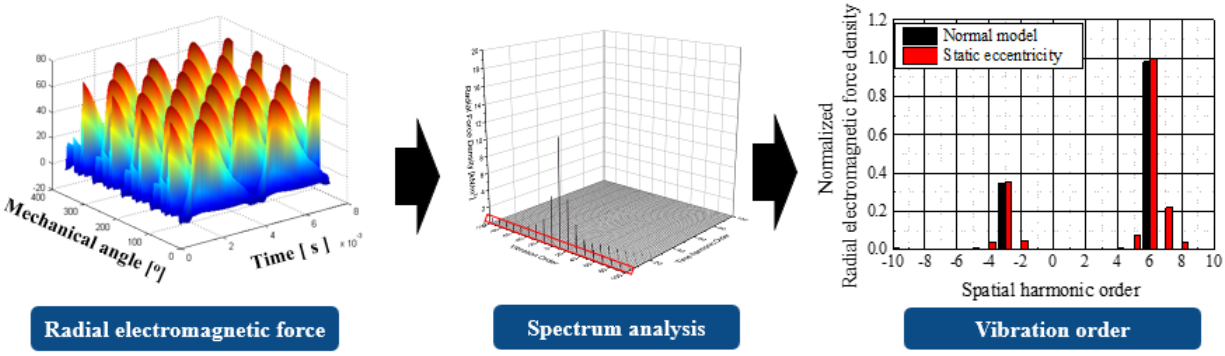

Fig. 2. Process of analyzing vibration order of radial electromagnetic force

When eccentricity occurs, the vibration order of motor can be changed causing unbalance of radial electromagnetic force. Fig. 1 shows the types of eccentricity. Static eccentricity in Fig. 1 (a) occurs when the rotating axis and the center of rotor are moved simultaneously and while dynamic eccentricity in Fig. 1 (b) occurs when the center of the rotor is moved. In this paper, the changes in vibration order of motor depending on type of eccentricity are discussed by using spectrum analysis shown in Fig. 2. The time and spatial harmonics of radial electromagnetic force is analyzed by spectrum analysis. After that, applying different radial electromagnetic force by different eccentricity type, the deformation of stator is calculated by finite element analysis verifying the effect of changed vibration order.

Design of Four-Layer Winding Method for the Vibration Reduction of Electrical Motor

Myung-Hwan Yoon*, Ki-Doek Lee, Se-Hyun Rhyu and Jeong-Jong Lee
Intelligent Mechatronics Research Center, Korea Electronics Technology Institute, Korea
yoonmh@keti.re.kr

Fractional slot concentrated winding synchronous motor has great electrical properties such as high torque density, low cogging torque, and low torque ripple. However severe vibration, for instance 12-slot/10-pole motor, is caused by sub-harmonics which are below the fundamental harmonic order in magnetomotive force (MMF). In this paper, four-layer winding is proposed to the motor design for sub-harmonics reduction instead of double-layer winding because sub-harmonics are affected by the ratio of armature winding and magnet field. To prevent the four-layer winding from lowering electromagnetic characteristics, design optimization is performed because vibration is coupled with MMF from result of electromagnetic analysis. Finally, optimized motors of four-layer winding and double-layer winding are manufactured and their performances are compared

Index Terms— Electromagnetic analysis, four-layer winding, motor, vibration

The electric power steering (EPS) is becoming an alternative to hydraulic power steering due to high power density and energy saving [1]. For EPS motor, fractional slot concentrated winding synchronous motor (FSSM) has been applied. 12-slot/10-pole motor topology of FSSM is widely employed in surface-mounted permanent magnet (SPM) motor due to non-overlapping winding, low cogging torque and high winding factor. However, 12-slot/10-pole motor has a disadvantage of vibration caused from sub harmonic. Sub-harmonics which are below fundamental harmonic order have harmful effects on the vibration. Four-layer winding is one of winding methods and proposed to reduce sub-harmonics of magnetomotive force (MMF) in this paper [2]-[3]. The effect of four layer winding for sub-harmonics reduction is affected by the ratio of armature winding and magnet field. However, winding factor of four layer winding is lower than that of double layer due to coil distribution. In other words, average torque or back- electromotive force (B-EMF) of four layer winding is smaller than two layer winding as the same current is excited. Thus, to satisfy the requirement of motor such as electromagnetic characteristics, an optimization technique is necessary to consider electromagnetic characteristics and structural characteristics at the same time. In this paper, design of electric motor considering electromagnetic characteristics and vibration reduction is presented.

1. Four Layer Winding

Layout of double layer winding and four layer winding are shown in Fig. 1.

MMF can be obtained by the layout of winding and MMF of 12-slot/10-pole motor can be expressed in (1

$$F_{total} = f_{1-phase} + f_{2-phase} + f_{3-phase}$$

$$f_{1-phase} = \sum_{\nu=1,3,5,\cdots}^{\infty} -\frac{8NI\cos(\omega t)}{\nu\pi} \cdot (\sin\nu \cdot \frac{\pi}{12})^2 \cdot \sin(\nu x - \frac{\pi}{12}\nu) \qquad (1)$$

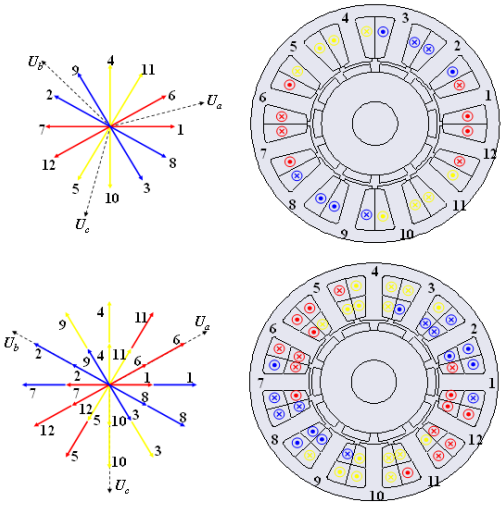

Fig. 1. Layout of winding; upper :12-slot/10-pole two-layer winding, lower: four-layer winding

where $f_{1-phase}$ is one of three-phase MMF and three phases are offset 120 electrical degree from each other, N is coil turns, I is current, ω is angular velocity and ν is harmonic order.

Flux density in air-gap can be obtained by multiplying permeance and MMF. The result of harmonic analysis is shown in Fig. 2. As winding factor of four layer is smaller than factor of double layer, magnitude of fundamental harmonic order in four layer winding is smaller than double layer. Therefore, increase of torque is necessary for designing four layer winding motor.

Normal force is calculated by (2)

$$Force = \frac{1}{2} \cdot \frac{B^2}{\mu_0} \tag{2}$$

Most of sub-harmonics which are below fundamental harmonic order are reduced by four layer winding as shown in Fig. 2. As normal force decreased by applying four layer winding, vibration of motor can be improved.

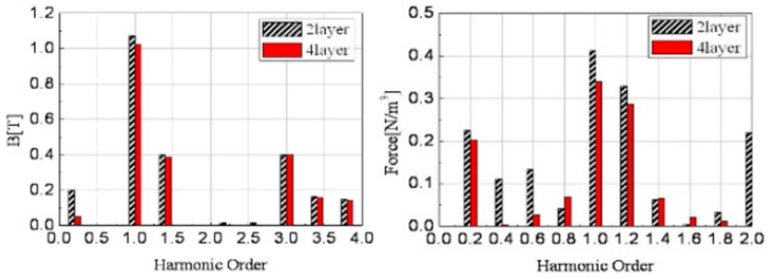

Fig. 2. Flux density and normal force in air-gap

2. Ratio of Armature Winding and Magnet Field

As reduction of harmonics in flux density and normal force affects average torque and vibration respectively, the appropriate ratio of armature winding and magnet field is necessary. In other words, four layer winding is effective for vibration as the ratio of armature winding to magnet field is greater. However, average torque which is one of electromagnetic characteristics decreases. Therefore, the ratio of armature winding and magnet field should be optimized in design of FSSM.

During the optimization, results of transient analysis are illustrated in Fig. 3. Reduction of deformation for four-layer winding is shown. The magnitude of phase back-emf for double-layer and four-layer winding are 2.32 [V] and 2.23 [V] respectively. Deformation reduced by 40% as four-layer is applied compared to double layer.

In order to verify the proposed method, experiment for measurement of vibration and electromagnetic characteristics will be conducted. Fig. 4 shows experimental set-up.

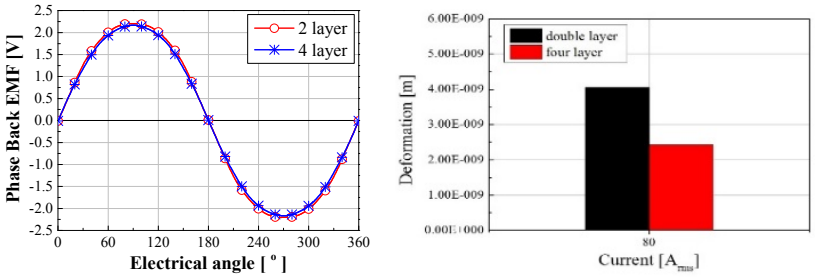

Fig. 3. Comparison between two different windings; left : back-EMF, right : deformation

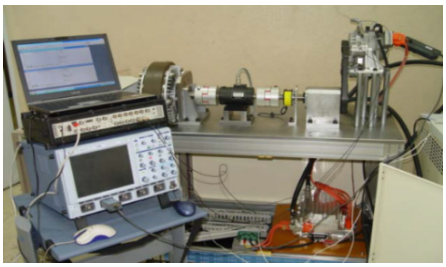

Fig. 4. Experimental set-up.

Acknowledgment

This work was supported by Korea Institute of Energy Technology Evaluation and Planning(KETEP) grant funded by the Korea government(MOTIE) (2018201010633A, The Development of Design Technology for IE4 Class Motors)

References

[1] Su-Jin Lee, Sung-Il Kim, and Jung-Pyo Hong, "Characteristics of PM Synchronous Motors According to Pole-Slot Combinations for EPS Application," *International Journal of Automotive Technology,* vol. 15, No. 7, pp. 1183-1187, 2014.

[2] Luigi Alberti, and Nicola Bianchi, "Theory and Design of Fractional-Slot Multilayer Windings," *IEEE Trans. Industry Application*, vol. 49, No. 2, pp. 841-849, March/April. 2013.

[3] Afang Sun, Jian Li, Ronghai Qu, and Dawei Li, "Effect of Multilayer Windings on Rotor Loss of Interior Permanent Magnet Generator With Fractional-Slot Concentrated-Windings," *IEEE Trans. Magnetics,* vol. 50, No. 11, 2014

KMS 2020 Summer Conference

Special Session IX

'Hard & Soft Magnetic Materials: Motor'

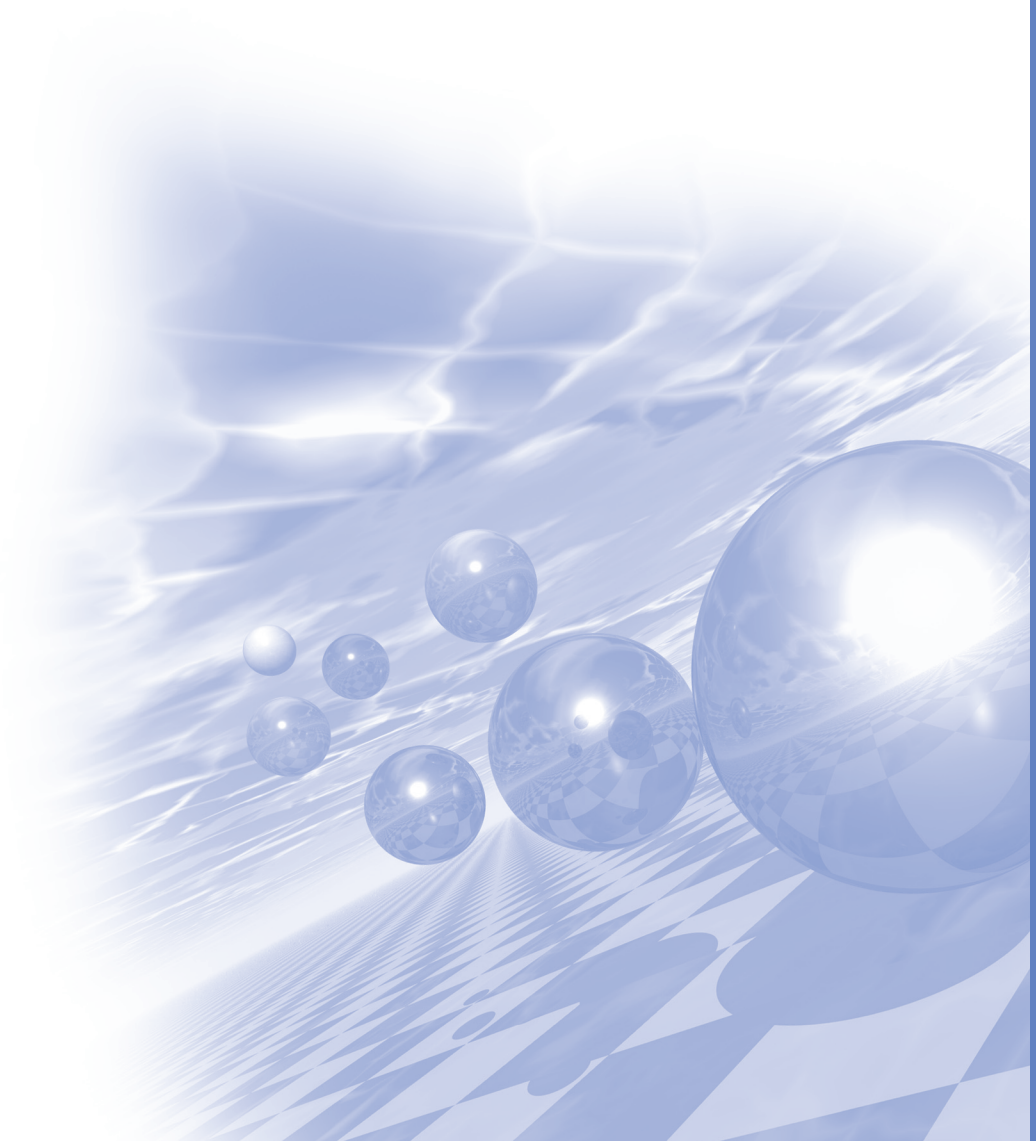

Development of High Performance (L)RE-Fe-B Permanent Magnets by Grain Boundary Engineering

Sumin Kim[1*], Donghwan Kim[2], Hyun-Sook Lee[1] and Wooyoung Lee[1†]
[1]Department of Materials Science and Engineering, Yonsei University, Seoul 03722, Republic of Korea
[2]R&D Center, Star Group, Daegu 42714, Republic of Korea

The most high-performance Nd-Fe-B magnets in existence have been widely used in many different applications, such as motors, generators, actuators, hard disk drives, and communication devices, since their discovery in 1894. In particular, as the demand for eco-friendly vehicles has increased in recent years due to environmental issues, developing high performance of Nd-Fe-B magnets at high temperature has received considerable attention. In order to improve the coercivity, heavy rare-earth element (HRE) such as Dy and/or Tb was partially substituted into the Nd sites in the base magnet in the usual way, because the magnetic anisotropy filed of $Dy_2Fe_{14}B$ (22 T) and $Tb_2Fe_{14}B$ (15 T) is higher than that of $Nd_2Fe_{14}B$ (7.3 T).

On the one hand, to reduce the consumption of critical (H)RE elements such as Nd, Pr, Dy, and Tb, new type of magnets using light-rare-earth(LRE) elements such as La and Ce, whose energy density is in-between ferrite and sintered Nd-Fe-B magnets, has been proposed.

In this study, in order to solve these two issues of 2:14:1 permanent magnets, we investigated the improvement of magnetic and thermal properties of 2:14:1 permanent magnets by grain boundary diffusion process. Firstly, we investigated the effect of low-melting-point Al aided TbH on the magnetic properties, thermal stability, and Tb content of the sintered Nd-Fe-B magnets. In order to improve the sufficient diffusion depth of Tb and the well-defined boundary structure, the fabrication temperature of GBDP and additional heat-treatment was adjusted and the dip-coating amount of diffusion source was tuned. Secondly, we will propose the Ce or La based 2:14:1 magnets and grain boundary diffusion process using RE-TM alloys for new type of magnets having energy density between ferrite and sintered Nd-Fe-B magnets.

Non-trivial Giant Magnetic Anisotropy in 3d Ferromagnetic Materials

Jae-Hoon Park*
Centre for Complex Phase Materials, MPK
Department of Physics, POSTECH

Governed by the spin-orbit (LS) coupling, the magnetic anisotropy in magnetic materials projects the magnetic spin axis in the internal coordinates to the real space coordinates, and determines the magnetization direction. In general, the orbital angular momentum L is mostly quenched in 3d transition metal compounds, and thus relatively small magnetic anisotropy is often observable in the 3d ferromagnetic systems. In spite of this general fact, giant magnetic anisotropy have occasionally been discovered in 3d ferromagnets. Here I will present ferromagnetic iron and chromium coumpounds with giant magnetic anisotropy, and discuss the origins and mechanisms, providing insights to design ferromagnets with enhanced magnetic anisotropy.

Magnetic Field-induced Linear Clustering of Spherical Particles for Thermally Conductive Polymer Composites

Young-Kuk Kim*
Dept. of Powders/Ceramics, Korea Institute of Materials Science (KIMS), Korea

Development of modern electronic devices has led to a rapid increase in power density as a result of miniaturization and integration of device elements operating at high frequencies. For efficient removal of heat dissipated from high power electronic devices, thermally conductive polymer composites with both high thermal conductivity and mechanical flexibility were extensively pursued. We developed a novel processing route for efficient formation of linear thermal networks which is essential to high thermal conductivity with low filler content. Here, linearly agglomerated clusters of spherical fillers based on spherical Al_2O_3 particles guided by magnetic field to form thermal networks for high thermal conductivity along plane normal direction which is essential for thermal interface materials (TIMs). The thermally conductive particles exhibiting ferromagnetic response by magnetic field were prepared by a simple precipitation method. The prepared hybrid particles were well aligned through direction of magnetic field as confirmed by microscopic observation. The polymer composites obtained with the hybrid particles possessed high thermal conductivity in a parallel magnetic alignment direction at low filler loading, which is more than 240% outperformed the composites with randomly dispersed fillers.

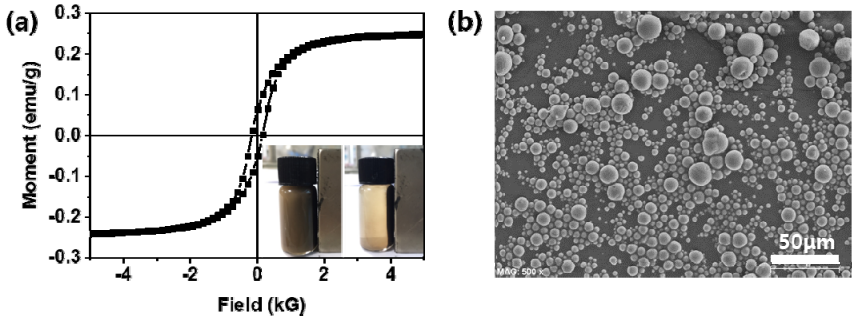

Fig. 1. (a) Magnetic property and (b) morphology of the thermally conductive spherical fillers

입계확산형 희토자석 기술개발 현황과 향후 과제

김동환*, 공군승
성림첨단산업(주) 연구소, 대구광역시 달서구 호림동 8

현대사회 산업구조가 점차 고도화되고 인간의 편이성을 추구하는 방향으로 발전이 가속화됨에 따라 자동차, 로봇, 에너지, 정보 분야 등 첨단산업 중심으로 모터의 사용량이 급격히 증가하는 추세이다. 동시에 모터 수요증가와 더불어 에너지의 사용량이 점차 증가함에 따라 지구상에 자원부족 문제 및 환경오염 문제가 가장 큰 화두가 되었고, 이를 극복하기 위해 정부에서는 국가 전체에너지의 11%를 소비하고 있는 모터의 효율등급을 현재 IE3급에서 2030년까지 IE5급으로 향상시키기 위한 법적 제도를 실행 중에 있다.

이와 같은 모터산업 발전 및 에너지 절감 추이에 대응하기 위해 이들 고효율 모터에 사용되는 핵심소재인 고성능 희토자석 역시 기술적인 진보가 필요하다. 2010년 이후 희토자석 분야는 “중희토저감 희토자석 개발”이라는 새로운 이슈가 시작되었고, 그 동안 중희토확산기술, 입자미세화기술, 열간변형자석 기술 등이 개발되고 있는데 이들 기술 중 중희토입계확산기술은 가장 먼저 안정적 기술을 확보함에 따라 친환경차용 고특성 모터 중심으로 상용화가 시작되고 있다.

중희토 입계확산기술은 Nd-Fe-B계 자석에서 보자력은 “자석에 반전자장이 인가될 경우 결정립 외측에 형성되는 역자구에 의해 지배된다(역자구 핵생성메카니즘)” 원리를 이용하여 개발되었는데, 보자력 향상에 효과적인 중희토(HRE=Dy, Tb)를 결정립계를 따라 자석 내부로 확산시키고 최종적으로 결정립 외측에 HRE rich 확산층을 형성함으로서 가장 효율적으로 보자력을 향상시키는 기술이다. 따라서, 자석 내/외부에 균일한 확산층을 형성하기 위해 입내확산을 최대한 억제하고 안정적인 입계확산이 진행되도록 확산을 진행해야 하는데 이와 같은 기술 개발을 위해 중희토 물질에 3d-천이금속을 첨가하여 융점을 낮춤으로서 확산온도를 최대한 낮추는 방향으로 개발이 진행 중에 있다.

당사 연구소에서는 지난 5년간 중희토입계확산형 희토자석 개발에 역량을 집중하여 연구를 수행하였고 최근에는 국내 H사, L사의 자동차용 모터에 사용되는 중희토저감형 희토자석을 국내 최초로 개발하여 공급하기 시작하였다. 본 발표에서는 중희토입계확산기술의 기술개발 현황을 리뷰하고 향후 완벽한 입계확산자석 구현하기 위한 기술적 발전방안에 대한 제언을 하고자 한다.

References

[1] H. Nakamura, K. Hirota, M. Shimao, T. Minowa and M. Honoshima, IEEE Trans. Magn. **41**, 3844 (2005).

[2] M. Sagawa: Proc. 21th Int. Workshop on REPM and their Applications (2010) 183.

Properties of soft and hard magnetic materials based on amorphous alloy system

Haein Choi-Yim*
Department of Physics, Sookmyung Women's University

Magnetic materials play an increasingly important role in modern industry as essential components of commercial products such as motors, sensors, actuators, and data storage devices.

In particular, nanocrystalline materials such as Finemet, Nanoperm and Hitperm are widely used in the soft-magnetics industry for management of electro-magnetic interference, magnetic heads, and magnetic shielding. Nanocrystalline are the best classes of soft magnetic materials because of their excellent soft magnetic properties including low coercivity, high saturation magnetization (M_s), high saturation magnetic flux density and high permeability.

Also, rare-earth-free hard magnet such as LTP-MnBi, $L1_0$-FePt, α″-FeN and $L1_0$-FeNi are being noticed as a new material in the field of permanent magnet. They show high magnetic M_s, a large uniaxial magnetic anisotropy, and a theoretically high BH_{max}.

These magnetic properties – soft and hard magnetic properties – can be implemented based on amorphous alloy system through various process method like melt spinning technique, annealing process. Therefore, the development of amorphous alloys with unique structures and superior magnetic properties has attracted considerable interest in physics, materials science, and engineering technology research.

Current status and prospect of ceramic permanent magnets

Sang-Im Yoo* and Kang-Hyuk Lee
Department of Materials Science and Engineering & Research Institute of Advanced Materials,
Seoul National University, Seoul 151-744, Korea

Hard ferrites, known as ceramic permanent magnets, constitute the major fraction of world tonnage in permanent magnets. Among various hexagonal ferrites, M-type hexaferrties which have the magnetoplumbite structure and the chemical formula of $MeFe_{12}O_{19}$ (Me = Ba, Sr, Pb). Their magnetic properties, including coercivity ($_BH_c$,), remanence (B_r) and the maximum energy product $(BH)_{max}$, have been improved in the order of BaM, SrM, $(La,Sr)(Fe,Co)_{12-x}O_{19}$, and $(La,Ca)(Fe,Co)_{12-x}O_{19}$, This improvement is basically due to the enhancement of the uniaxial magnetocrystalline anisotropy without degrading their saturation magnetization (M_s), leading to improved $_BH_c$, via cation substitutions for both Me^{2+} and Fe^{3+} sites in $MeFe_{12}O_{19}$. On the other hand, to achieve a squareness in their demagnetization curves which is essential for high B_r and $(BH)_{max}$, it is critical to optimize their microstructures by properly controlling processing conditions such as the forming process under the applied magnetic field for texturing along the c-axis, heat treatment schedules of calcination and sintering for grain size control and densification, and the compositions of additives for grain morphology and densification. In this talk, I will explain the progress in the improvement of intrinsic magnetic properties, including M_s and K_u (uniaxial anisotropy constant) via anisotropy field (H_a). Next, I will describe the important factors affecting the extrinsic properties, including $_BH_c$, B_r, and $(BH)_{max}$, for the system of $(La,Sr)(Fe,Co)_{12-x}O_{19}$. Finally, I will discuss the prospect of higher-performance ceramic permanent magnets.

Mass Production Technologies of Amorphous Fibers and Strips

Eonbyeong Park*, Yongchan Kim, Deok Kim
Research Institute of Industrial Science and Technology, Materials & Processing Research Laboratory, Korea

The amorphous materials have been considered as attractive materials due to their excellent mechanical and magnetic properties. These alloys have been widely used in the power and electronic industries. Among the developed amorphous alloys, Fe-based amorphous alloys have become very popular among researchers not only because of their good properties such as superior strength, high fracture toughness, and good soft magnetic properties but also because of the cost-effectiveness of iron element. Most of the amorphous materials have, up to date, been fabricated by using rapid solidification technologies with a cooling rate of about 1×10^6 K/s.

Rapid solidification processes have been developed from the rapid splat quenching to single roll casting. Of the various rapid solidification processes, planar flow casting method is widely used for the industrial production of Fe-based amorphous alloy, feeding melt from a narrow nozzle into a melting pool between the nozzle and the cooling roll. However, commercial applications of planar flow casting for amorphous alloy have been strictly limited because of the high production cost, and the low market demands. A critical production cost factor is the prices of raw materials since ferrous metallic glasses should be made of high purity electrolytic iron. An idea to reduce the production cost is to utilize molten iron and steel directly taken from steel plants.

Investigations have been performed to find whether metallic glasses made of molten iron and steel demonstrate appropriate mechanical and magnetic performances. Pilot scale equipment was designed to produce amorphous fibers and strips continuously under the atmospheric condition. Process conditions were optimized by controlling process variables such as composition adjustment and nozzle design, feeding temperature, wheel speed and so on. Possibilities of application for the Fe-based amorphous fibers to reinforced concrete were also investigated. It was confirmed that a small addition of amorphous fibers in concrete increased the mechanical performance compared to that of commercial concrete reinforced with steel wires. In addition, amorphous strips of 142mm width and 25㎛ were manufactured continuously with 1 ton of molten iron and steel. It has been demonstrated that the amorphous strips have superior properties such as low core loss compared to commercial electrical steel, therefore it can be widely applicable for the transformer core and the soft magnetic electric parts.

KMS 2020 Summer Conference

Special Session X

'Bio-Convergence Magnetics'

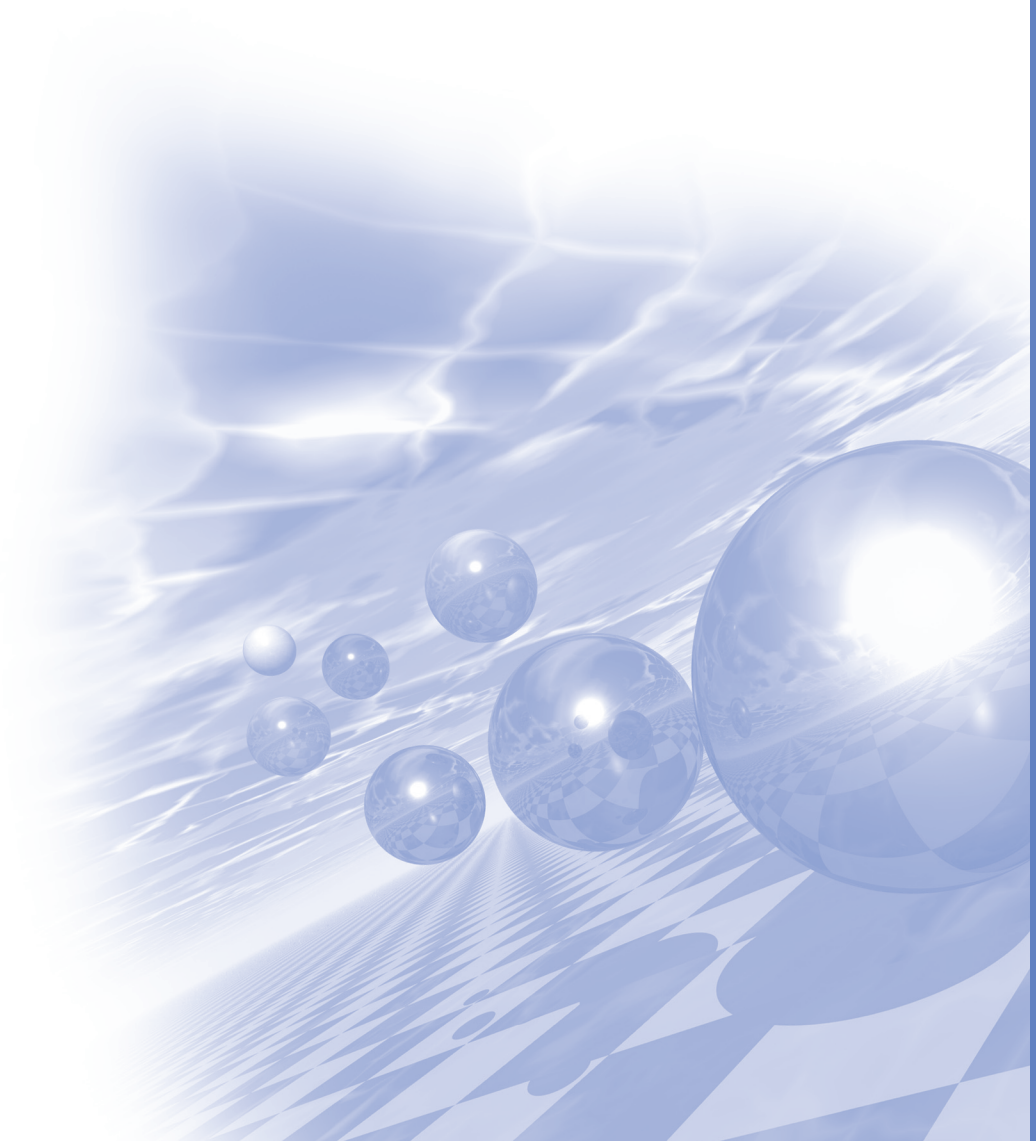

Is there any method to overcome conventional magnetic hyperthermia?

Jae-Hyeok Lee, Bosung Kim, Youngsub Kim and Sang-Koog Kim*

National Creative Research Initiative Center for Spin Dynamics and Spin-Wave Devices, Nanospinics Laboratory, Research Institute of Advanced Materials, Department of Materials Science and Engineering, Seoul National University, Seoul 151-744, South Korea

*Correspondence and requests for materials should be addressed to S.-K. K. (sangkoog@snu.ac.kr)

Hyperthermia therapy is a therapeutic treatment to kill targeted cancer cells in a body. However, the realization of its full clinical potential has been limited by an insufficient amount of intrinsic specific loss power. To overcome this obstacle for conventional hyperthermia methods, we have studied the resonant magnetization dynamics of magnetic particles of different sizes, including uniform magnetization precession and vortex-core precession[1,2]. Since such magnetization dynamics are followed by energy dissipation owing to the intrinsic damping of spin precession, low-power-driven heat generation can be achievable.[3,4] In this talk, we introduce the relevant characteristic spin dynamics of nanoparticles and show how such novel dynamic behaviors can be used for heat generation; additionally, we present an amazing result of heat generation rates, the values of which have yet to be recorded for conventional magnetic hyperthermia. This work may offer a precisely controllable and highly efficient means of heat generation for full realization of clinical cancer treatments using FDA-approved magnetic particles.

References

[1] S.-K. Kim et al., Sci. Rep. 5, 11370 (2015)

[2] S.-K. Kim et al., Sci. Rep. 6, 31513 (2016)

[3] M.-K. Kim and S.-K. Kim et al., Phys. Rev. Applied 9, 054037 (2018)

[4] M.-K. Kim and S.-K. Kim et al., J. Appl. Phys. 125, 063901 (2019)

Role of lactate in metabolism of skeletal muscle

Kyung-Oh Doh*
Department of Physiology, College of Medicine, Yeungnam University, Daegu, Korea

Lactate that is the last metabolite of glycolysis is induced by muscle contraction was recognized as signal molecular for various tissue including adipose tissue and brain. Lactate can be resynthesized to energy substrate for muscle during exercise, and also be molecular to signals for the muscle cell and adipocyte to regulate energy metabolism via autocrine and paracrine, respective. However, how this role is regulated has not been defined. To identify how the lactate regulates energy metabolism in muscle and adipose tissue, lactate was daily administered to intraperitoneal in chow and high fat diet (HFD) mouse, respectively, for 8 weeks. We found that glucose disposal rate and metabolic rate were higher in lactate mice, whereas RER is lower in lactate mice when compared with saline mice regardless chow and high-fat diet. We observed that the running endurance was lower in lactate mice than saline, thus, we studied the bioenergetic characteristics of muscle and adipose tissue mitochondria to understand the potential link to increased metabolic rate and attenuated running endurance. We could not find any difference of mitochondrial respiration when using glucose and malate as substrate in muscle mitochondria, whereas state III respiration in lactate muscle mitochondria were significantly lower than saline when using palmitate and malate as substrate. We also found lactate with high fat diet had significantly lower respiratory control ratio (RCR) when using palmitate and malate as substrate. Different phenomena were observed in adipose tissue, lactate with HFD had higher state III respiration and RCR when using glucose and malate as substrate, whereas RCR was lower in lactate with HFD when using palmitate and malate as substrate. Overall, these results indicate that lactate mice exhibit marked shifts in skeletal muscle and adipose tissue mitochondrial bioenergetics and the shift might induce higher metabolic rate and glucose disposal rate as well as lower running endurance capacity in lactate with HFD mice.

Single molecular dynamics of Plasmalemmal Vesicle Associated Protein-1 (PV-1) in live vascular cell

Daeha Seo*
Department of Emerging Materials Science, DGIST, Daegu, Korea

Monitoring the dynamics of membrane proteins in live cell on appropriate spatiotemporal scales may provide key information on long-standing questions in cellular and organelle regulatory mechanisms. However, tools capable of imaging the conformational changes over time have been elusive. Here, we present a single-molecule imaging technique by developing plasmonic nanoparticles and optical microscope techniques, allowing for replication of protein-protein interactions and the association dynamics based on lateral diffusivities. This study is the first to monitor the diffusion coefficient of Plasmalemmal Vesicle Associated Protein-1 (PV-1), that is a key component for the formation of the fenestral diaphragms, to decipher undiscovered association dynamics in live cells without any molecular perturbations. Such a method not only offers a strategy to visualize assemblies and conformational changes, but also provides unique insights into the clinical understanding underlying the material transport related vascular disease.

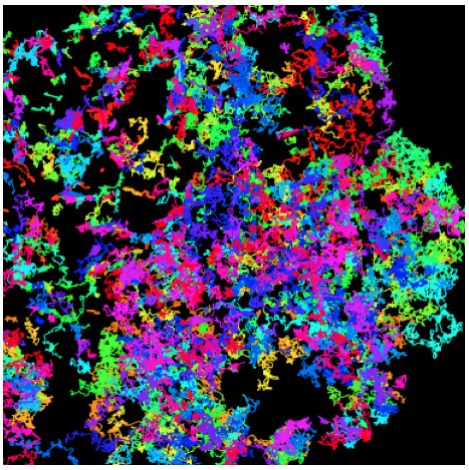

Fig. 1. Single protein trajectories in live cell

References

[1] Sangwon Shin, Jisu Choe, Youngchan Park, Donghyun Jeong, Hyunjoon Song, Youngmin You, Daeha Seo, Jaeheung Cho "Artificial Control of Cell Signaling Using a Photocleavable Co-balt(III)–Nitrosyl Complex" *Angew. Chem. Int. Ed*. **2019**, 58, 10126

[2] Youngchan Park, Sangwon Shin, Hyeonggyu Jin, Jiseong Park, Yeonki, Hong, Jaemin Choi, Byunghyuck Jung, Hyunjoon Song, Daeha Seo "Single-Molecule Rotation for EGFR Conformational Dynamics in Live Cells" *J. Am. Chem. Soc*. **2018**, 140, 15161

[3] Daeha Seo, Kaden M. Southard, Ji-wook Kim, Hyunjung Lee, Justin Farlow, Jung-uk Lee, David Litt, Thomas Haas, Jinwoo Cheon, A. Paul Alivisatos, Zev J. Gartner, Young-wook Jun "A Mechanogenetic Toolkit for Interrogating Cell Signaling in Space and Time" *Cell*, **2016**, 165, 1507

High resolution magnetic sensor to analyze physical properties of blood vessels through pulse wave pattern detection technology

Cheol Gi Kim[1*], Sunjong Oh[2], Mijin Kim[1]
[1]Department of Emerging Materials Science, DGIST, Korea
[2]Department of Nature-Inspired Nanoconvergence Systems, Korea Institute of Machinery and Materials, Korea

A high-resolution magnetic-based sensor platform works on a pulse wave measurement system was developed to measure and analyze the physical properties of blood vessels through pulse wave pattern detection technology that accurately detects pulse patterns while varying the externally applied pressure (absolute pressure) applied to the measurement object.

We constructed a blood vessel simulator that generates pulse patterns using elastic polymer-based model blood vessels and pulse wave generators, and combined magnetic-based signal measurement sensors in an array to confirm the possibility of pulse wave transmission rate measurement through parallax measurement of output signals.

In this study, a planar hall magnetoresistance (PHR) sensor is manufactured to accurately monitor the pulse pattern (dynamic pressure) while changing the external static pressure (applied pressure) applied to the measurement object to monitor the exact physical blood vessel characteristics according to the health condition of the patient. We are developing portable electronic circuits for precision measurement, and based on this static/dynamic pressure sensing element technology, we developed a single pulse measurement system through the pulse pattern sensing unit and signal processing and non-invasively responds to absolute pressure. We will develop a single system that analyzes the pattern of pulse patterns and infers the stiffness of blood vessels.

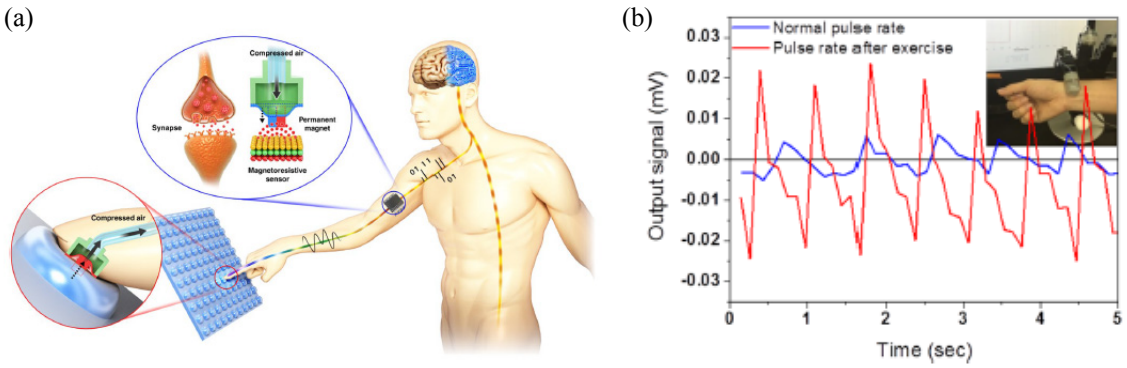

S.Oh, Y.Jung, S.Kim, SJ.Kim, X.H, H.L, CG.Kim, "Remote tactile sensing system integrated with magnetic synapse", Scientific Reports, 2017

Fig. 1. (a) A schematic of a method for measuring pulse wave detection, (b) Measurement results of heart rate and relative blood pressure using the developed remote tactile sensing system under two different conditions: at rest and after exercise. The inset shows the remote tactile sensing system attached to a robot hand (Allegro Hand) to measure the pulse signal automatically in real time.

자성기반 압력센서를 이용한 맥박 패턴 측정 기술

오선종[1*], 정영도[1], 이보연[1], 김성기[1], 신상훈[2]
[1]한국기계연구원, 자연모사응용연구실
[2]상지대학교, 한방의료공학과

동맥 혈관의 탄력조직(elastin)이 신체노화, 당뇨 및 심혈관 질환 등 질병, 흡연, 비만 등으로 감소 또는 파괴됨에 따라 혈관의 경직도(stiffness)는 상승하게 되고 맥파전달 속도가 빨라지게 된다. 맥박패턴은 심장의 수축/이완기 때 발생하는 진행파와 반사파의 중첩으로 나타나는데, 맥파전달 속도의 증가로 반사파 속도가 상승하게 되면 진행파와 중첩된 수축기때 최대 혈압이 상승하게 된다. 수축기 최대 혈압 상승은 심혈관, 뇌혈관, 관상동맥, 말초혈관 등에 영향을 주어 혈관건강에 문제가 발생하게 된다.

개발된 자성기반 압력센서를 이용한 맥박 패턴 측정 기술은 맥박을 감지하고자 하는 혈관에 가해지는 인가압력(정적압력)을 달리하면서 맥박 패턴(동적압력)을 정밀하게 감지할 수 있으며 서로 다른 위치에서 동시에 맥박 패턴 측정이 가능한 어레이로 구현되어 맥파속도의 측정이 가능하여 진단환자의 건강상태에 따른 정확한 물리적 혈관특성을 모니터링 할 수 있는 측정시스템이다. 또한, 자성기반 맥박 패턴 측정시스템은 기존 의료진단/모니터링용 전자소자 및 센서 시장에 적용이 가능하며, 혈관의 물리적 특성을 비침습적 방법으로 측정할 수 있는 새로운 소재 및 소자 시장의 창출과 차세대 의료장비 및 센서분야, 유연디스플레이, 로봇분야 시장에서의 응용이 가능할 것으로 기대된다.

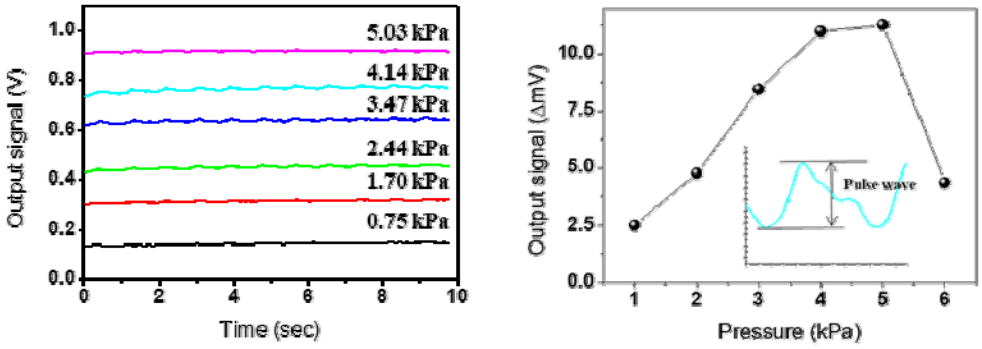

그림 1. 모형 혈관 인가 압력에 따른 출력신호 및 맥박패턴 크기

Highly soluble magnetic nanoclusters for biomedical applications

Hak-Jong Choi, Junhyoung Ahn, Soongeon Kwon, Hyungjun Lim,
Geehong Kim, Kee-Bong Choi, Jaejong Lee*
Korea Institute of Machinery and Materials, Korea

Iron oxide nanoparticles have been well known as superparmagnetic material with unique magnetic properties and studied for biomedical applications such as drug delivery, therapeutic application, and detection of biomolecules, and so on.[1] Especially, the superparamagnetic iron oxide nanoparticles can freely move according to the induction of an external magnetic field and overcome the aggregation in the blood.[2]

In this study, we successfully prepared the magnetic nanoclusters to possess unique magnetic properties. Especially, Poly(acrylic acid) (PAA) was covered on the synthesized magnetic nanocluster as shell ligand by surface modification method in order to increase the stability in aqueous solution. The synthesized magnetic nanoclusters were investigated the shape, size and structural information using electron microscopy, dynamic light scattering, powder X-ray diffraction, vibrating sample magnetometer and so on. The magnetic nanocluster was observed about 100 nm of average diameter with narrow size distribution and revealed the spinel structure when it compared with only iron oxide nanoparticles. Furthermore, the magnetic nanoclusters indicated strong magnetic properties. These magnetic nanoclusters with higher solution stability and magnetism will be effectively utilized to the biomedical application as a specific conjugation material to detect biomolecule such as protein, gene and exosome as well as therapeutic application using a drug and gene delivery.

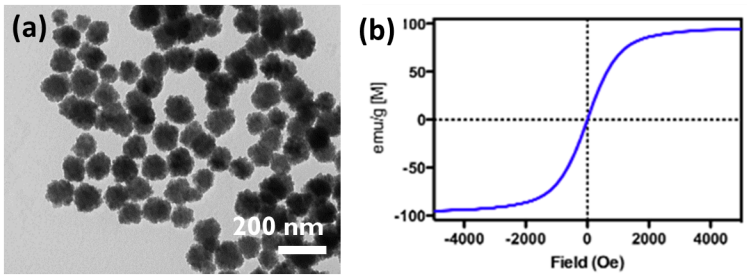

Fig. 1. (a) TEM image and (b) vibrating sample magnetometer (VSM) of superparamagnetic iron oxide nanoparticles

References

[1] J. M. Cha, Y.S. Kwon, T. J. Yoon and J. K. Lee, *J. ChemComm.* 49 (5), 457 **(2013).**

[2] Y. S. Kwon, K. J. Sim, T. Y. Seo, J. K. Lee, Y. W. Kwon, T. J. Yoon, *J. RSC Adv,* 6 (109), 107298 **(2016).**

KMS 2020 Summer Conference

Special Session XI

'Spintronics'

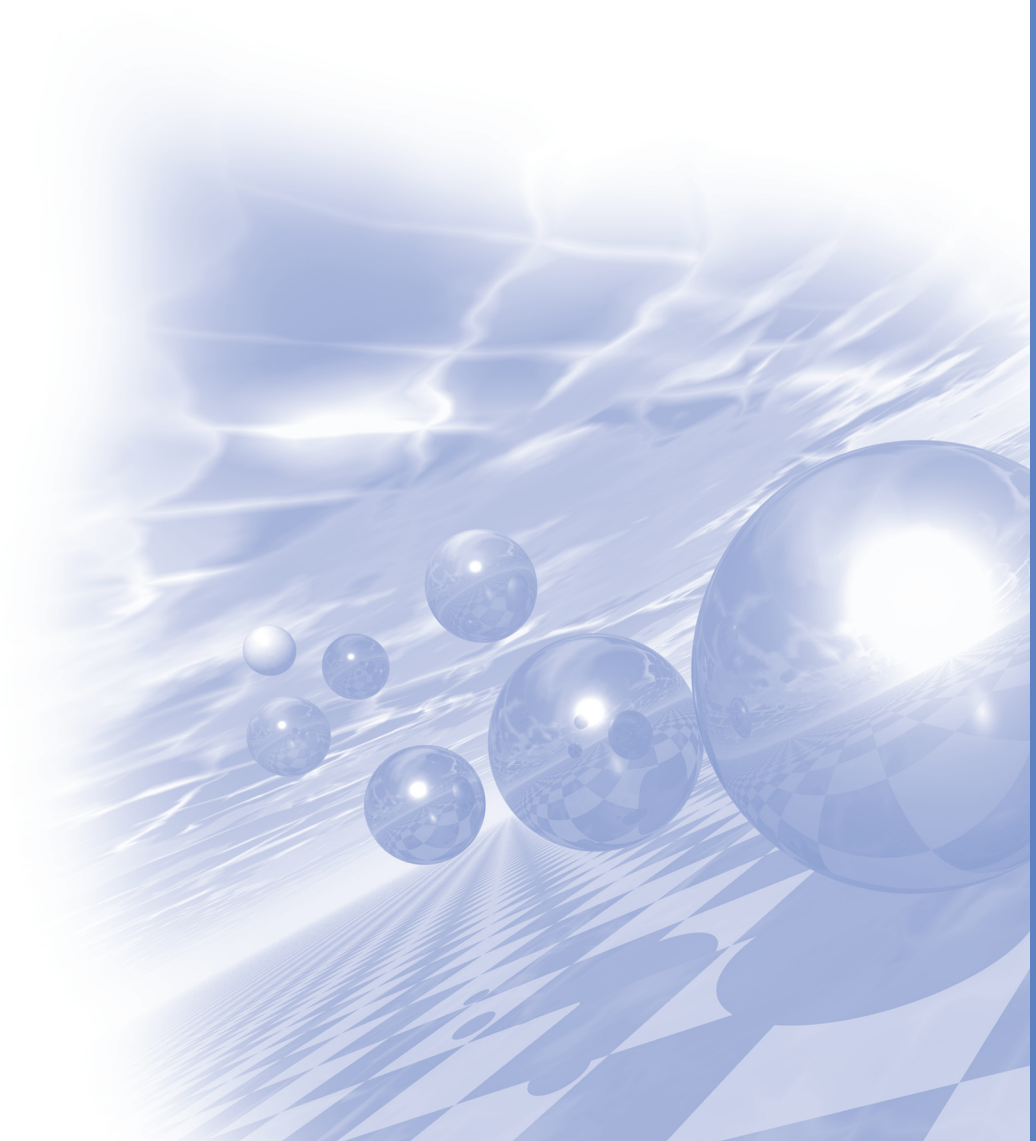

Spin-orbit torque engineering by orbital current in Cr-based magnetic heterostructures

Soogil Lee[1*], Min-Gu Kang[1], Dongwook Go[2,3], Taekhyeon Lee[4], Dohyoung Kim[1], Geun-Hee Lee[4], Jun-Ho Kang[4], Jong-Ryul Jeong[5], Kyung-Jin Lee[6,7], Hyun-Woo Lee[8], Kab-Jin Kim[4], Sanghoon Kim[9] and Byong-Guk Park[1]

[1]Department of Materials Science and Engineering, KAIST, Daejeon 34141, Korea
[2]Peter Grünberg Institut and Institute for Advanced Simulation, Forschungszentrum Jülich and JARA, Jülich 52425, Germany
[3]Institute of Physics, Johannes Gutenberg-University Mainz, Mainz 55128, Germany
[4]Department of Physics, KAIST, Daejeon 34141, Korea
[5]Department of Materials Science and Engineering, Chungnam National University, Daejeon, 34134, Korea
[6]Department of Materials Science and Engineering, Korea University, Seoul 02841, Korea
[7]KU-KIST Graduate School of Converging Science and Technology, Korea University, Seoul 02841, Korea
[8]Department of Physics, Pohang University of Science and Technology, Pohang 37673, Korea
[9]Department of Physics, University of Ulsan, Ulsan 44610, Korea

Spin-orbit torque (SOT) in nonmagnet/ferromagnet (FM) heterostructures has been intensively studied to realize energy efficient spintronic devices. In particular, there have been strong desire for finding nonmagnetic materials with large SOT efficiency. Though 5*d* transition metals such as Ta, W and Pt have been exhibited relatively large SOT efficiency as a result of the spin Hall effect (SHE) due to strong spin-orbit coupling (SOC), much enhancement of the SOT efficiency is still demanded to achieve low power operation. Recently proposed orbital torque (OT) [1] would be considered for an excellent way to enhance the SOT efficiency because the orbital Hall effect (OHE) is usually quite larger than the SHE in most transition metals [2-5]. For example, the orbital Hall conductivity of weakly spin-orbit-coupled Cr is gigantic, $\sim 10^4$ $(\hbar/e)(\Omega \cdot \mathrm{cm})^{-1}$, which is an order of magnitude larger than the spin Hall conductivities of 5*d* transition metals. Such large OHE can give rise to the torque on a magnetization of FMs by the orbital-to-spin conversion via SOC. Therefore, orbital-to-spin conversion engineering is a crucial key to bring the large OT from the OHE. In this presentation, we show the sizable OT and resultant magnetization switching in various Cr-based magnetic heterostructures. Effect of different FMs or insertion layers at the Cr/FM interface with varying SOC strength on the OT will be discussed, which proves that the orbital current from Cr can exert the torque on the adjacent FM. Our systematic study suggests that the OT can provide a great opportunity to accomplish energy efficient spintronic devices.

References

[1] Dongwook Go and Hyun-Woo Lee, Phys. Rev. Research 2, 013177 (2020)
[2] T. Tananka et al, Phys. Rev. B 77, 165117 (2008)
[3] H. Kontani, et al, Phys. Rev. Lett. 102, 016601 (2009)
[4] Dongwook Go, et al, Phys. Rev. Lett. 121, 086602 (2018)
[5] Daegeun Jo, et al, Phys. Rev. B 98, 214405 (2018)

준 강자성체에서 전류에 의한 위상 스핀 구조체 운동

김덕호*
한국과학기술연구원

자성물질에서 위상 스핀 구조체(Topological spin object)의 동역학 현상은 학문적으로 흥미로울 뿐 아니라 차세대 메모리 소자 응용가능성으로 활발히 연구가 되어왔다[1-4]. 대표적인 위상 스핀 구조체는 나선형 자구벽(Chiral magnetic domain wall)[1,2]과 자기 스커미온(Magnetic skyrmion)[3,4]이다. 전류를 이용해 위상 스핀 구조체를 움직일 수 있는데, 그 기본 매커니즘은 전자의 스핀이 자성체의 위상 스핀 구조체를 지나갈 때, 전자의 스핀과 위상 구조체의 스핀 사이에 상호작용이 발생으로 발생하는 각운동량 보존이다[5,6]. 이 상호작용을 스핀 토크라고 불리며, 전달 매개체에 따라 스핀 전달 토크(spin-transfer torque), 스핀 궤도 토크(spin-orbit torque)로 나눌 수 있다. 최근, 이론 논문에 의해 반 강자성체(Antiferromagnet, 총 자화=0)에서 초고속 위상 스핀 구조체 운동이 예측되었는데[7], 불행히도 반 강자성체는 측정하기 어렵고(총 자화=0), 컨트롤 하기도 어려워(매우 강한 커플링 에너지) 이론을 실험으로 규명하기가 어려웠다. 그러나 준 강자성체(Ferrimagnet)의 경우 각운동량이 0인 각운동량 보상점에서 유한한 자화 값을 가지고 있어 반 강자성 스핀 동역학 연구가 가능하였다. 이러한 가능성으로 자기장으로 위상 스핀 구조체가 움직일 때, 각운동량 보상점에서 초고속 운동 관측이 보고되었다[8]. 본 발표에서는 준 강자성체 물질에서 전류로 위상 스핀 구조체 움직일 때, 각운동량 보상점에서 스핀 전달 토크 현상[9]과 스커미온 홀 현상[10]에 대해 논의하고자 한다.

References

[1] S. S. P. Parkin, M. Hayashi and L. Thomas, Science **320**, 190 (2008).
[2] S. P. Parkin, Sci. Am. **300**, 76 (2009).
[3] A. Fert, V. Cros and J. Sampaio, Nat. Nanotechnol. **8**, 152 (2013).
[4] J. Sampaio, V. Cros, S. Rohart, A. Thiaville and A. Fert, Nat. Nanotechnol. **8**, 839 (2013).
[5] G. Tatara and H. Kohno, Phys. Rev. Lett. **92**, 086601 (2004).
[6] S. Zhang and Z. Li, Phys. Rev. Lett. **93**, 127204 (2004).
[7] T. Shiino et al. Phys. Rev. Lett. **117**, 087203 (2016)
[8] K.-J. Kim et al., Nat. Mater. **16**, 1187 (2017).
[9] T. Okuno et al., Nat. Electron. **2**, 389 (2019).
[10] Y. Hirata et al., Nat. Nanotechnol. **14**, 232 (2019).

Nontrivial Topology induced by Magnon-Phonon Hybridization

Gyungchoon Go[1*], Se Kwon Kim[2] and Kyung-Jin Lee[1,3]
[1]Department of Materials Science and Engineering, Korea University, Seoul 02841, Korea
[2]Department of Physics, KAIST, Daejeon 34141, Korea
[3]KU-KIST Graduate School of Converging Science and Technology, Korea University, Seoul 02841, Korea

We present the topological aspects of the magnon-phonon hybrid excitation in a simple two-dimensional (2D) square-lattice ferromagnet with perpendicular magnetic anisotropy. Several distinguishing features of our model are as follows. Our model is optimized for atomically thin magnetic crystals, i.e., 2D magnets. The recent discovery of magnetism in 2D van der Waals materials opens huge opportunities for investigating unexplored rich physics and future spintronic devices in reduced dimensions. Because we consider the 2D model, we ignore the nonlocal dipolar interaction, which is not a precondition for a finite Berry curvature in 2D magnets. Moreover, the Berry curvature we find does not require a special spin asymmetry such as the DM interaction nor a special lattice symmetry: Our 2D model description is applicable for general thin-film ferromagnets. Therefore, we show in this work that even without such long-range dipolar interaction, DM interaction, or special lattice symmetry, the nontrivial topology of a magnon-phonon hybrid can emerge by taking account of the well-known magnetoelastic interaction driven by Kittel. As Kittel's magnetoelastic interaction originates from the magnetic anisotropy, which is ubiquitous in ferromagnetic thin-film structures, our result does not rely on specific preconditions but is quite generic. Furthermore, we show that the topological structures of the magnon-polaron bands can be manipulated by effective magnetic fields via topological phase transition. We uncover the origin of the nontrivial topological bands by mapping our model to the well-known two-band model for topological insulators, where the Chern numbers are read by counting the number of topological textures, called skyrmions, of a certain vector in momentum space. In this picture, the magnon-phonon hybridization induces the chiral texture of the momentum space vector. As an experimental probe for our theory, we propose the thermal Hall conductivity.

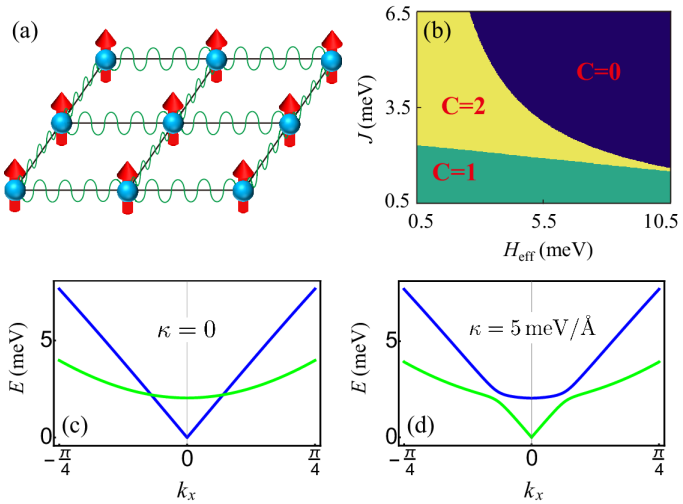

Fig. 1. (a) The schematic illustration of the magnon and phonon system. (b) The Chren number of the magnon-phonon system. $H_{\rm eff}$ represents the effective magnetic field including the anisotropy field and the external magnetic field. Band dispersion (c) without magnon-phonon interaction and (d) with the magnon-phonon interaction

Effect of broken inversion symmetry in magnetic multilayers

Dong-Soo Han*
Center for Spintronics, Korea Institute of Science and Technology, Seoul, Republic of Korea

Spin-orbit coupling combined with a broken inversion symmetry in space gives rise to intriguing phenomena in condensed matters [1-4]. Particularly, in magnetic materials, it is responsible for many extraordinary behaviors from spin transports [1,2] to dynamic and static properties of magnetic entities [5,6]. Rashba effect [1] and Dzyaloshinskii-Moriya interaction [3,4] are the most representative phenomena in magnetic multilayers, both of which arise from an inversion symmetry breaking to the surface normal direction. For the last decade, they have gained particular interest in the spintronics community, as they provide non-trivial fundamentals and show potential for the application in fast and energy-efficient spintronic devices [8-10]. In addition to the inversion asymmetry at the interfaces, the inversion symmetry breaking in the plane of the magnetic multilayers further generates hitherto undiscovered effects [11-13]. In this talk, I would like to discuss the new phenomena from the broken inversion symmetry, particularly, from the symmetry breaking in the plane of magnetic multilayers.

References

[1] E. Rashba, Sov. Phys. Solid State 2, 1224 (1960).
[2] G. Dresselhaus, Phys. Rev. 100, 580 (1955).
[3] I. Dzyaloshinsky, J. Phys. Chem. Solids 4, 241 (1958).
[4] T. Moriya, Phys. Rev. 120, 91 (1960).
[5] S. Emori et al., Nat. Mater. 12, 611 (2013).
[6] K.-S. Ryu, L. Thomas, S.-H. Yang, and S. Parkin, Nat. Nanotechnol. 8, 527 (2013).
[7] A. Fert, V. Cros, and J. Sampaio, Nat. Nanotechnol. 8, 523 (2013).
[8] I. Miron et al., Natture, 476, 189 (2011).
[9] L. Liu et al., Science, 336, 555 (2012).
[10] S. Woo et al., Nat. Mater. 15, 501 (2016).
[11] D.-S. Han et al., Nat. Mater. 18, 703 (2019).
[12] A. Fernández-Pacheco et al., Nat. Mater. 18, 679 (2019).
[13] D. MacNeill et al., Nat. Phys., 13, 300 (2017).

Spin transport in ferrimagnet

Jae-Hyun Park, Jun-Ho Kang, Soogil Lee, Kab-Jin Kim*
Department of Physics, Korea Advanced Institute of Science and Technology, Daejeon, Korea

The rare earth (RE)–transition metal (TM) ferrimagnets, which are a class of magnets where the spins of two inequivalent sublattices are coupled antiferromagnetically, is receiving great interest because they can serve as convenient platforms to study antiferromagnetic spin dynamics. Indeed, several recent reports have shown that antiferromagnetic spin dynamics can be observed in RE-TM ferrimagnets through the motion of topological solitons such as domain walls and skyrmions [Nat. Mater. 16, 1187 (2017); Nat. Nano. 14, 232 (2019)]. However, the transport properties of RE-TM ferrimagnets, which is another fundamental element of spintronics research, have remained largely unexplored so far.

In this talk, we will present our recent studies on the transport properties of RE-TM ferrimagnets. First, we will discuss effects of oxidation on the transport properties of RE-TM ferrimagnets. To elucidate the oxidation effect, we directly visualized the oxygen ion migration in single Gd layer while monitoring the resistance. We found that the electrical resistance as well as the magnetoresistance was largely affected by the oxygen ion migration. Second, we will discuss the contribution of RE and TM sub-moments to the transport of ferrimagnet. To this end, we measured the longitudinal and transverse resistivity of ferrimagnet at various temperatures and magnetic fields. We found that the unconventional magnetoresistance emerged in RE-TM ferrimagnet due to the sperimagnetic nature. This result unveils that, contrary to the common belief that the TM dominates transport of RE-TM ferrimagnets, the RE contribution to magnetoresistance is comparable to the TM contribution, showing that the antiferromagnetic nature of GdFeCo is important for understanding its transport. If time is allowed, we will further discuss our recent results on the unidirectional magnetoresistance in ferrimagnet/heavy metal hetero-structures.

Topological Spin Transport in 2D Quantum Magnets

Se Kwon Kim*
KAIST

Recent advancements in spintronic techniques originally developed for spin-based devices now enable us to study fundamental spin physics of various quantum materials with unprecedented spin-current control and measurement, opening a new area of theoretical and experimental investigation of quantum systems. In this talk, we will introduce this emerging research area of spin transport in quantum materials which is fueled by the global interest in quantum information science. As concrete examples, we will discuss our research on new types of topological phases referred to as magnonic topological insulators hosted by various magnets [1-4], which include 2D honeycomb ferromagnets such as CrI3 [1] and ferrimagnets in skyrmion crystal phase [2]. We will conclude the talk by offering a future outlook on quantum spintronics.

References

[1] S. K. Kim, H. Ochoa, R. Zarzuela, and Y. Tserkovnyak, “Realization of the Haldane-Kane-Mele Model in a System of Localized Spins,” Phys. Rev. Lett. 117, 227201 (2016)

[2] S. K. Kim, K. Nakata, D. Loss, and Y. Tserkovnyak, “Tunable Magnonic Thermal Hall Effect in Skyrmion Crystal Phases of Ferrimagnets,” Phys. Rev. Lett. 122, 057204 (2019)

[3] G. Go, S. K. Kim, and K.-J. Lee, “Magnon-Phonon Hybrid Excitations in Square-Lattice Ferromagnets with tunable Chern numbers,” Phys. Rev. Lett. 123, 237207 (2019)

[4] S. Zhang, G. Go, K.-J. Lee, S. K. Kim, “SU(3) Topology of Magnon-Phonon Hybridization in 2D Antiferromagnets,” Phys. Rev. Lett. 124, 147204 (2020)

Contorl of Half-skyrmion Hall Effect and its Neuromorphic Computing Application

Seungmo Yang[1*], Jeonghun Shin[2], Taeyoon Kim[3], Kyung-woong Moon[1], Jaewook Kim[3], Gabriel Jang[2], Da Seul Hyeon[2], Jung Yup Yang[4], Chanyong Hwang[1], YeonJoo Jeong[3] and Jinpyo Hong[2]

[1]Quantum Spin Team, Korea Research Institute of Standards and Science, Daejeon, Korea
[2]Research Institute of Natural Science, Nanoscale Semiconductor Engineering and Department of Physics, Hanyang University, Seoul, Korea
[3]Electronic Materials Research Center, Korea Institute of Science and Technology, Seoul, Korea
[4]Department of Physics, Kunsan University, Gunsan, 54150, South Korea

Skyrmions have attracted a great attention in spintronics because of their potential use as robust information carriers with distinctive protection. Though the realization of skyrmion-based devices requires flexible control of a skyrmion motion, achieving such a skyrmion motion has been hampered by the skyrmion Hall effect (SkHE), which refers to the presence of a finite angle between a current and the skyrmion trajectory. Here, we present a new insight for precise control of a half-skyrmion motion including complete suppression of the SkHE by deforming the internal structure of skyrmions, which is experimentally achieved by external magnetic field to steer current-driven half-skyrmions in the desired direction. Furthermore, based on the unique advantages in half-skyrmions, the potential of half-skyrmions application beyond skyrmion-based electronics is also demonstrated by presenting half-skyrmion-based synapse devices, along with extremely linear and symmetric synaptic response. Lastly, the half-skyrmion-based neural network is simulated using the extracted device characteristics, demonstrating high classification accuracy over 93% without particular assistance of additional software or circuit. These experimental studies provide a new step for establishing more compact and efficient neural network systems with the optimized multi-functional half-skyrmion devices.

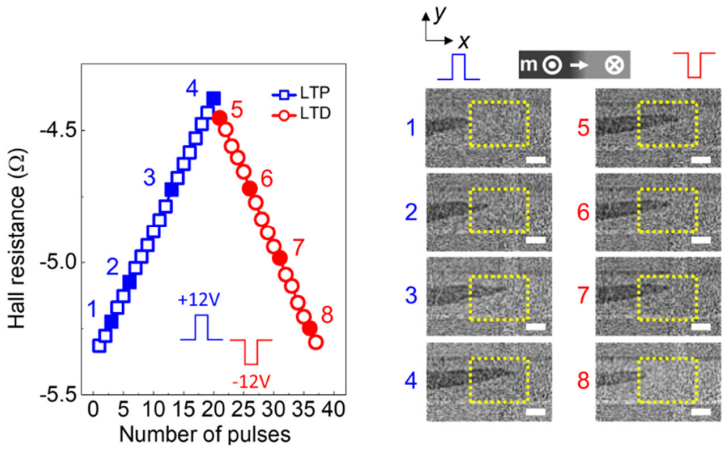

Fig. 1. Representative spin synapse functions and its corresponding magnetic images of half-skyrmion motion.

Author Index

Digests of the KMS 2020 Summer Conference

The Korean Magnetics Society

사단법인 한국자기학회

2020년도 하계학술연구발표회 논문개요집 제 30권 1호

(06130) 서울특별시 강남구 테헤란로 7길 22(역삼동635-4) 한국과학기술회관 신관 905호

TEL. (02)3452-7363, **FAX.** (02)3452-7364

E-mail. komag@unitel.co.kr, **Home-page.** www.komag.org